



Università della Calabria

**Dottorato di Ricerca in Ingegneria Chimica e dei Materiali**  
*SCUOLA DI DOTTORATO " PITAGORA " IN SCIENZE INGEGNERISTICHE*

**Tesi**

**Membrane emulsification for the development of  
particulate systems for drug encapsulation**

**Settore Scientifico Disciplinare CHIM/07 – Fondamenti chimici delle tecnologie**

*Supervisori*

*Candidato*

Dr. Lidietta GIORNO  
*Lidietta Gior*  
Ch.mo Prof. Enrico DRIOLI

Alessandra Imbrogno  
*Alessandra Imbrogno*

*Enrico Drioli* Ciclo XXVII

*Il Coordinatore del Corso di Dottorato*

Ch.mo Prof. Raffaele MOLINARI

*Raffaele Molinari*

---

A.A. 2013-2014

*“Cogito ergo sum”*

*Cartesio*

## **Acknowledgments**

*I desire to express my thankfulness firstly to my supervisors, Dr. Lidietta Giorno and Prof. Enrico Drioli for giving me the opportunity to be part of the “membrane family” at their Institute. Their experience has been an important source that gave me the basis in the research field allowing me to get higher and higher. A special thanks is for Dr. Emma Piacentini, who perfectly knows how one feels going through a PhD, and nevertheless, she was always there to help me and support me throughout these years. I would like to mention also my family and Fabio, you were all by my side to relieve me from falling day-by-day. Great thanks are also for all my colleagues and friends of “the third floor” for being always ready to laugh at the right moment, for sharing with me every moment of joy and difficulty of these years. Finally, I would also like to thank Prof. Holdich, Dr. Dragosavac and Dr. Vladislavljević for giving me the opportunity to carry out part of my project at Loughborough University (UK). Working with them was a fruitful experience not only for my career but also for my life.*

# INDEX

|   |           |
|---|-----------|
| LIST OF FIGURES .....   | 8         |
| LIST OF TABLES .....  | 13        |
| <b>SOMMARIO .....</b>   | <b>15</b> |
| Obiettivi della ricerca .....   | 17        |
| Contenuti della tesi .....  | 20        |
| <b>SUMMARY .....</b>  | <b>22</b> |
| Research objectives .....   | 24        |
| Dissertation outline.....   | 27        |
| <b>CHAPTER 1.....</b>   | <b>28</b> |
| <b>Membrane emulsification: principles and applications for particle production ....</b>                | <b>28</b> |
| 1. Introduction.....  | 28        |
| 2. Emulsions and conventional emulsification methods.....   | 28        |
| 3. Membrane emulsification .....  | 30        |
| 4. Forces on a spherical droplet .....  | 31        |
| 5. Basic parameters .....   | 33        |
| 5.1. Membrane parameters .....  | 34        |
| 5.2. Phase parameters .....   | 35        |
| 5.3. Process parameters in dynamic membrane emulsification .....  | 36        |
| 6. Dynamic membrane emulsifications devices .....   | 37        |
| 7. Static membrane emulsification principles and devices .....  | 39        |
| 8. Membrane emulsification applications in the pharmaceutical field .....                               | 40        |
| 8.1. Emulsions.....   | 41        |
| 8.2. Solid particles: spheres, capsules and beads .....   | 41        |
| 8.3. Liposomes and solid lipid particles.....   | 44        |
| 8.4. Sensing stimuli-responsive particles .....   | 44        |
| 9. Conclusions.....   | 46        |
| <b>CHAPTER 2.....</b>   | <b>54</b> |
| <b>Membrane with tailored wettability property to improve emulsion productivity and efficiency.....</b> | <b>54</b> |
| 1. Introduction.....  | 54        |
| 2. Experimental section.....  | 56        |
| 2.1. Chemicals.....   | 56        |
| 2.2. Membranes and Membrane Cleaning Procedure .....  | 56        |
| 2.3. Experiments carried out and operative conditions .....   | 57        |
| 2.4. Protein adsorption .....   | 57        |
| 2.5. Membrane emulsification equipment and W/O emulsion preparation .....                               | 59        |
| 2.6. Membrane surface analysis .....  | 59        |
| 2.7. Particle size analysis .....   | 60        |

|   |           |
|---|-----------|
| 3. Results and Discussion .....   | 60        |
| 3.1. Effect of protein adsorption on membrane functionalities and surface properties.....   | 60        |
| 3.2. Effect of the membrane surface properties on W/O emulsion preparation by membrane emulsification .....                               | 63        |
| 4. Conclusions.....   | 67        |
| <br>  |           |
| <b>CHAPTER 3.....</b>   | <b>70</b> |
| <b>Microsieve nickel and stainless steel membrane: a comparative study on the influence of membrane fouling by polymer solution .....</b> | <b>70</b> |
| 1. Introduction.....  | 70        |
| 2. Experimental section.....  | 71        |
| 2.1. Chemicals .....  | 71        |
| 2.2. Stirrer membrane emulsification equipment .....  | 71        |
| 2.3. Particle characterization .....  | 72        |
| 3. Results and discussion .....   | 73        |
| 4. Conclusions.....   | 75        |
| <br>  |           |
| <b>CHAPTER 4.....</b>   | <b>78</b> |
| <b>Production of poly-caprolactone microparticles from O/W emulsion by membrane emulsification/solvent diffusion process.....</b>         | <b>78</b> |
| 1. Introduction.....  | 78        |
| 2. Experimental section.....  | 80        |
| 2.1. Chemicals .....  | 80        |
| 2.2. O/W emulsion preparation: membrane emulsification equipment .....  | 81        |
| 2.3. Microparticle preparation.....   | 81        |
| 2.4. Particle characterization .....  | 82        |
| 3. Results and discussion .....   | 82        |
| 3.1. Effect of polymer concentration.....   | 82        |
| 3.2. Effect of the fluid-dynamic conditions .....   | 83        |
| 3.3. Microparticle preparation: influence of the volume of dilution medium on shape, surface morphology and size.....                     | 85        |
| 4. Conclusions.....   | 89        |
| <br>  |           |
| <b>CHAPTER 5.....</b>   | <b>93</b> |
| <b>Production of multi-core matrix particles from double W/O/W emulsion by membrane emulsification/solvent diffusion process .....</b>    | <b>93</b> |
| 1. Introduction.....  | 93        |
| 2. Experimental section.....  | 94        |
| 2.1. Chemicals .....  | 94        |
| 2.2. W/O/W emulsion preparation: membrane emulsification equipment .....  | 95        |
| 2.3. Droplet size modeling .....  | 96        |
| 2.4. Microparticle preparation.....   | 97        |
| 2.5. Particle characterization .....  | 97        |
| 3. Results and discussion .....   | 98        |
| 3.1 Influence of process parameters on simple particle production: dispersed injection flux and shear stress .....                        | 98        |

|   |     |
|---|-----|
| 3.2. Influence of the chemical composition on the stability of the primary W/O emulsion .....                                       | 102 |
| 3.3. Influence of the chemical composition on the stability of the double W/O/W emulsion .....                                      | 105 |
| 3.4. Influence of the chemical composition of the double emulsion on particle size and particle shape of PCL matrix particles ..... | 106 |
| 3.5. Effect of the polymer concentration on particle size and size distribution of PLGA matrix particles .....                      | 108 |
| 4. Conclusion .....   | 109 |

## **CHAPTER 6..... 113**

### **Pulsed back-and-forward membrane emulsification for the production of micro and nanoparticles for pharmaceutical application ..... 113**

|  |     |
|--|-----|
| 1. Introduction.....   | 113 |
| 2. Experimental section.....   | 114 |
| 2.1. Chemicals .....   | 114 |
| 2.2. O/W emulsion preparation: membrane emulsification equipment .....           | 115 |
| 2.3. Particle preparation .....  | 117 |
| 2.4. Particles characterization: size, morphology and surface charge.....        | 117 |
| 3. Results and discussion .....  | 117 |
| 3.1. Effect of dispersed phase flux on particle size and size distribution ..... | 117 |
| 3.2. Effect of the shear stress on particle size and size distribution.....      | 118 |
| 3.3. Effect of the membrane pore size: particle size from micro to nanoscale ... | 120 |
| 3.4. From emulsion droplets to solidified PCL particles .....                    | 121 |
| 3.5. Particles Morphology .....  | 122 |
| 3.6. Particles stability .....   | 123 |
| 4. Conclusions.....  | 124 |

## **CHAPTER 7..... 127**

### **Study of micro-sieve stainless steel membrane in torsional motion for large scale production of simple O/W and double W/O/W emulsion ..... 127**

|   |     |
|---|-----|
| 1. Introduction.....  | 127 |
| 2. Experimental section.....  | 128 |
| 2.1. Chemicals .....  | 128 |
| 2.2. Membrane emulsification equipment.....   | 128 |
| 2.3. Droplet size modelling .....   | 130 |
| 2.4. Microparticle preparation.....   | 131 |
| 2.5. Particle characterization .....  | 131 |
| 2.6. Encapsulation efficiency of copper into the double W/O/W emulsion.....   | 131 |
| 3. Results and discussion .....   | 132 |
| 3.1. Influence of the frequency and amplitude of the torsion on simple O/W emulsion and solid particle size and size distribution .....   | 132 |
| 3.2. Influence of the frequency and amplitude of the torsion on double W/O/W emulsion and solid particle size and size distribution ..... | 134 |
| 3.3. Influence of dispersed phase injection flux on emulsion (O/W and W/O/W) and particle production.....                                 | 135 |
| 3.4. From batch-scale to large scale production by torsional membrane emulsification .....  | 137 |

|  |            |
|--|------------|
| 4. Conclusions.....  | 139        |
| <b>CHAPTER 8.....</b>  | <b>141</b> |
| <b>Micro-structured particles for the encapsulation of hydrophilic and hydrophobic compounds: influence of process and chemical parameters .....</b> | <b>141</b> |
| 1. Introduction.....   | 141        |
| 2. Experimental section.....   | 142        |
| 2.1. Chemicals.....  | 142        |
| 2.2. Multi-core matrix particle preparation.....   | 142        |
| 2.3. Copper extraction, encapsulation efficiency and drug loading.....   | 142        |
| 2.4. Vitamin extraction and encapsulation efficiency.....  | 143        |
| 2.5. Particle morphology.....  | 144        |
| 3. Results and discussion.....   | 144        |
| 3.1. Influence of the chemical composition on particle morphology and encapsulation efficiency.....  | 144        |
| 3.2. Influence of the volume of dilution medium and the kind of stabilizer used in the solidification step.....                                      | 147        |
| 3.3. Influence of the inner aqueous phase volume fraction ( $W_1$ ) on the encapsulation efficiency.....   | 150        |
| 3.4. Comparison between PLGA and PCL for the encapsulation of hydrophilic molecules.....   | 152        |
| 4. Conclusion.....   | 154        |
| <b>OVERALL CONCLUSIONS .....</b>   | <b>156</b> |
| <b>APPENDIX 1.....</b>   | <b>158</b> |
| A.I Malvern Mastersizer.....   | 158        |
| A.II Scion Image analysis.....   | 159        |
| A.III Zetasizer NanoZS.....  | 159        |
| A.IV Tensiometer- Du Noüy ring method.....   | 161        |
| A.V UV/Vis Spectrophotometer.....  | 161        |
| A.VI BCA test.....   | 162        |
| A.VII Atomic Absorbance Spectrophotometer (AAS).....   | 163        |
| <b>APPENDIX 2.....</b>   | <b>165</b> |
| Award.....   | 165        |
| Education and training from 2011 to 2014.....  | 165        |
| Publications from 2011 to 2014.....  | 166        |
| Proceedings.....   | 167        |

# List of Figures

- Figure 1.1** Schematic representation of direct and premix membrane emulsification
- Figure 2.1** Forces acting on a droplet at the pore level
- Figure 3.1.** Parameters influencing membrane emulsification process
- Figure 1.2** Schematic representation of the equipment used for protein adsorption: (1) bulk protein solution; (2) peristaltic pump; (3) purge valve; (4) membrane module
- Figure 2.2** Cross-flow membrane emulsification equipment: (1) disperse phase graduated vessel; (2) micropump; (3) purge valve; (4) membrane module; (5) peristaltic pump; (6) continuous phase container
- Figure 3.2** Proteins adsorption on the membrane surface over time
- Figure 4.2** SEM/EDX analysis carried out on fragments of (A) unmodified and (B) lipase-loaded ceramic membrane
- Figure 5.2** Water permeability reduction of PES membrane after lipase adsorption and the values of contact angle ( $\theta$ ) measured between water drop and unmodified and lipase-loaded membrane
- Figure 6.2** (A) Mean droplets size and droplet size distribution of W/O emulsions prepared by cross-flow membrane emulsification using un-modified and lipase-loaded membrane. (B) Microscope images of W/O emulsions prepared using (A) un-modified ceramic membrane (emulsifier: Span 80 2 wt%); (B) lipase-loaded ceramic membrane (emulsifier: Span 80 2 wt%); (C) BSA-loaded ceramic membrane (emulsifier: Span 80 2 wt%); (D) lipase-loaded ceramic membrane (emulsifier: SY-Glyster PO-5S 4 wt%). Experimental conditions: emulsifier: Span 80 2 wt%; dispersed phase flux:  $30 \pm 0.67 \text{ L h}^{-1} \text{ m}^{-2}$ ; continuous phase axial velocity:  $0.05 \text{ ms}^{-1}$ ; dispersed phase content 9 % (v/v)
- Figure 7.2** Mean droplets size and particle size distribution for quadruplicate tests conducted using the same lipase-loaded membrane for the preparation of W/O emulsions. Experimental conditions: emulsifier: Span 80 2 wt%; dispersed phase flux:  $30 \pm 0.67 \text{ L h}^{-1} \text{ m}^{-2}$ ; continuous phase axial velocity:  $0.05 \text{ ms}^{-1}$ ; dispersed phase content 9 % (v/v)
- Figure 1.3** Photographs of the surface of the membrane: A) stainless steel membrane; B) nickel membrane



- Figure 2.3** *Stirred membrane emulsification equipment scheme. 1: syringe pump; 2: injection chamber; 3: glass cylinder; 4: Stainless steel stirrer with a blade at the bottom ending; 5: voltage regulator;*
- Figure 3.3** *O/W emulsion produced with: A) 1% PVA, nickel membrane; B) 1% PVA, stainless steel membrane; C) 2% SDS nickel membrane; D) 2% SDS, stainless steel membrane. ( $J= 9 \text{ L h}^{-1} \text{ m}^{-2}$ ,  $\tau= 11 \text{ Pa}$ ).*
- Figure 4.3** *O/W emulsion produced with: A) 1% PVA, nickel membrane; B) 1% PVA, stainless steel membrane; C) 2% SDS nickel membrane; D) 2% SDS, stainless steel membrane ( $J= 216 \text{ L h}^{-1} \text{ m}^{-2}$ ,  $\tau= 11 \text{ Pa}$ )*
- Figure 1.4** *Effect of the polymeric concentration on particle size and size distribution of the emulsion prepared with a dispersed phase flux of  $9 \text{ L h}^{-1} \text{ m}^{-2}$  and a shear stress of  $8.6 \text{ Pa}$*
- Figure 2.4** *Optical microscopy pictures of: A) O/W emulsion; B) solidified microparticles*
- Figure 3.4** *Effect of increasing shear stress on particle size and size distribution of particles prepared with 16% of PCL and a dispersed phase flux of  $9 \text{ L h}^{-1} \text{ m}^{-2}$*
- Figure 4.4** *Effect of the dispersed phase flux on particle size and size distribution of particles prepared with 16% of PCL and a shear stress of  $8.6 \text{ Pa}$*
- Figure 5.4** *Optical microscope pictures of microparticles produced by membrane emulsification/solvent diffusion at decreased  $V_{sd}/V_{theoretic}$ : A)  $V_{sd}/V_{theoretic} = 6$ , B)  $V_{sd}/V_{theoretic}=3$ , C)  $V_{sd}/V_{theoretic}= 1.4$ , D)  $V_{sd}/V_{theoretic}= 1$ , E)  $V_{sd}/V_{theoretic}=0.5$ . Microparticles are suspended in aqueous phase with SDS 0,5 %.*
- Figure 6.4** *Particle size and size distribution of solidified particles at different volume of water*
- Figure 7.4** *SEM pictures of microparticles prepared :A) unsaturated condition ( $V_{sd}/V_{theoretic}$  ratio = 6); B) saturated condition ( $V_{sd}/V_{theoretic}$  ratio = 1); C) oversaturated condition ( $V_{sd}/V_{theoretic}$  ratio = 0.5) of continuous phase*
- Figure 1.5** *Schematic representation of the capillary force and drag force acting on a growing droplet*
- Figure 2.5** *Effect of injection flux on particle and droplet size and size distribution of O/W emulsion and solid particles containing: A) PCL (16 and 30% ) in the dispersed phase; B) PLGA ( 10 and 30% ) in the dispersed phase*
- Figure 3.5** *Effect of the shear stress on particle and droplets size and size distribution of O/W emulsion and solid particles containing: A) PCL (16*

and 30%) in the dispersed phase; B) PLGA ( 10 and 30%) in the dispersed phase

- Figure 4.5** Droplet size and the predicted model against the shear stress: A) PCL (16 and 30%) in the dispersed phase; B) PLGA ( 10 and 30%) in the dispersed phase
- Figure 5.5** Influence of cold water-fish gelatin on the interfacial tension at water/oil interface containing PCL in the organic phase
- Figure 6.5** Influence of PGPR and Abil em-90 on the interfacial tension at water/oil interface containing PCL in the organic phase
- Figure 7.5** Photographs of double  $W_1/O/W_2$  emulsion with different concentration of polymer in the organic phase: A) 16% PCL in DCM; B) 20% PCL in DCM; C)30% PCL in DCM
- Figure 8.5** Particle size and size distribution of W/O/W emulsion and matrix particles produced with different concentration of PCL (16-30%) and different stabilizer (5% fish gelatin or 4% of PGPR)
- Figure 9.5** Photographs of matrix particles produced with different concentration of polymer and different stabilizer. A-B-C (4% PGPR), 16-20-30% of PCL in DCM; D-E-F (5% fish gelatin):16-20-30% of PCL in DCM. Solidification conditions:  $V_{sd} = 3V_{th}$  and SDS as stabilizer
- Figure 10.5** Particle size and size distribution of W/O/W emulsion droplets and matrix particles produced with different concentration of PLGA (10-30%) and 5% of fish gelatin in the inner aqueous phase.
- Figure 11.5** Photographs of matrix particles produced with fish gelatin and PLGA 10% (A) and 30% (B). Solidification conditions:  $V_{sd} = 3V_{th}$  and PVA as stabilizer
- Figure 1.6** Pulsed back and forward membrane emulsification system. 1: membrane module; 2: purge valve; 3: dispersed phase graduated tank; 4: pressure regulator; 5: nitrogen gas cylinder; 6: peristaltic pump; 7: continuous phase tank; 8: emulsion tank
- Figure 2.6** Effect of the dispersed phase flux on particle size and size distribution of microparticles prepared with SPG membrane with 1  $\mu\text{m}$  pore size and a shear stress of 2.1 Pa
- Figure 3.6** Malvern Mastersizer particle size distribution of microparticles prepared at different value of shear stress and constant dispersed phase flux (2.2  $\text{L h}^{-1}\text{m}^{-2}$ ).

- Figure 4.6** *Effect of shear stress on: A) particle size and B) size distribution at lower ( $0.9 \text{ L h}^{-1} \text{ m}^{-2}$ ) and higher ( $2.2 \text{ L h}^{-1} \text{ m}^{-2}$ ) dispersed phase flux.*
- Figure 5.6** *Effect of membrane pore size on Z-average of emulsion droplets and solidified particles measured by Zetasizer NanoZS*
- Figure 6.6** *SEM pictures of polycaprolactone micro and nanoparticles prepared by pulsed back and forward membrane emulsification. A-B: microparticles prepared with SPG membrane with  $1 \mu\text{m}$  pore size; C-D: nanoparticles prepared with SPG membrane with  $0.1 \mu\text{m}$  pore size.*
- Figure 1.7** *Torsional system equipment scheme. 1-syringe pump containing the dispersed phase; 2- continuous phase tank; 3- membrane module; 4- servo motor; 5- emulsion tank; 6- control panel.*
- Figure 2.7** *Oil droplet and solid particle size and size distribution as a function of frequency (15-50 Hz,  $a = 1.5 \text{ mm}$ ) and amplitude (1-3.5 mm,  $f = 25 \text{ Hz}$ );  $Q_{dp} = 1 \text{ mlmin}^{-1}$ ;  $4 \text{ mlmin}^{-1}$ .*
- Figure 3.7** *Photographs of O/W emulsion produced with  $a = 1.5 \text{ mm}$ ,  $Q_{dp} = 1 \text{ mlmin}^{-1}$  and  $f = 15 \text{ Hz}$  (A),  $30 \text{ Hz}$  (B) and  $50 \text{ Hz}$  (C).*
- Figure 4.7** *Droplet size of W/O/W emulsion and solid particle size and size distribution as a function of frequency (15-50 Hz,  $a = 1.5 \text{ mm}$ ) and amplitude (1-3.5 mm,  $f = 25 \text{ Hz}$ );  $Q_{dp} = 4 \text{ mlmin}^{-1}$ .*
- Figure 5.7** *Photographs of O/W emulsion (A-D) and W/O/W emulsion (1A-4D) produced at constant shear stress of  $5 \text{ Pa}$  ( $45 \text{ Hz}$ ,  $1.5 \text{ mm}$ ) and different injection flux: A- $23 \text{ Lh}^{-1} \text{ m}^{-2}$ ; B- $125 \text{ Lh}^{-1} \text{ m}^{-2}$ ; C- $288 \text{ Lh}^{-1} \text{ m}^{-2}$ ; 1D- $216 \text{ Lh}^{-1} \text{ m}^{-2}$ .*
- Figure 1.8** *Encapsulation efficiency of Cu(II) of the double emulsion and solidified particles produced with 30% of PCL and fish gelatin (F1), PGPR (F2).*
- Figure 2.8** *SEM photographs of multi-core matrix particles containing: 5% of fish gelatin (A and B), 4% of PGPR (C and D).*
- Figure 3.8** *Encapsulation efficiency of Cu(II) and  $\alpha$ -tocopherol of multi-core matrix particles solidified in different volume of water and with different stabilizer.*
- Figure 4.8** *SEM photographs of PCL matrix particles produced with different ratio between the volume used ( $V_{sd}$ ) and the theoretic volume ( $V_{th}$ ) and SDS*

2% as stabilizer. A)  $V_{sd}/V_{th}=1$ ; B)  $V_{sd}/V_{th}=2.5$ ; C)  $V_{sd}/V_{th}=5$ ; D)  $V_{sd}/V_{th}=8$ .

**Figure 5.8** SEM photographs of PCL matrix particles produced with different ratio between the volume used ( $V_{sd}$ ) and the theoretic volume ( $V_{th}$ ) and PVA 1% as stabilizer. A)  $V_{sd}/V_{th}=1$ ; B)  $V_{sd}/V_{th}=2.5$ ; C)  $V_{sd}/V_{th}=5$ .

**Figure 6.8** SEM photographs of PCL multi-core matrix particles produced with different volume fraction of inner aqueous phase ( $\phi_{wo}$ ). A (1-2):  $\phi_{wo}=0.1$ ; B(1-2):  $\phi_{wo}=0.15$ ; C(1-2):  $\phi_{wo}=0.3$ . Solidification conditions:  $V_{sd}/V_{th}=5$  and 2% SDS.

**Figure 7.8** SEM photographs of: A) multi-core matrix particles with PLGA, 30%; B) multi-core matrix particles with PCL, 30%.

**Figure A.1** Image of the capillary cells and electrophoresis of charged particle in presence of an electric field ([www.atascientific.com.au](http://www.atascientific.com.au)).

**Figure A.2** Schematic representation of the Du Noüy ring method (<http://www.mastrad.com/tsd1.htm>).

**Figure A.3** Calibration curve of  $\alpha$ -tocopherol determined by UV/VIS spectrophotometer.

**Figure A.4** Calibration curve of BSA determined by BCA assay and UV/VIS spectrophotometer.

**Figure A.5** Calibration of copper ions using SpectrAA in a range of concentration 0.5-3 ppm.

# List of tables

|                  |  |
|------------------|--|
| <b>Tabella 1</b> | <i>Avanzamenti proposti</i>  |
| <b>Table 1</b>   | <i>Advances promoted.</i>  |
| <b>Table 1.1</b> | <i>Common methodologies used for the preparation of particles from emulsions.</i>  |
| <b>Table 1.2</b> | <i>Typical dispersed phase flux membrane obtained during membrane emulsification method.</i>   |
| <b>Table 2.2</b> | <i>The type of experiments and the related surface carried for the tubular ceramic and flat sheet membrane used in the present work.</i>   |
| <b>Table 3.2</b> | <i>Water permeability reduction and protein adsorbed amount on tubular ceramic and flat sheet membrane and experimental conditions used for protein adsorption experiments.</i>                |
| <b>Table 1.3</b> | <i>Particle size and size distribution of particles produced O/W emulsion: O-16% PCL in DCM; W-water with SDS or PVA.</i>  |
| <b>Table 1.4</b> | <i>Experimental conditions used to carry out the solvent diffusion process at decreased <math>V_{sd}/V_{theoretic}</math> ratio and the effect on the solidification time of the droplets.</i> |
| <b>Table 1.5</b> | <i>Chemical composition of the double W/O/W emulsion used for the preparation of the solid particles.</i>  |
| <b>Table 2.5</b> | <i>Effect of polymer kind and polymer concentration on the interfacial tension at organic/water interface.</i>   |
| <b>Table 3.5</b> | <i>Chemical composition of W/O emulsion and chemical structure of the emulsifiers tested.</i>  |
| <b>Table 1.6</b> | <i>Experimental conditions used to increase the shear stress by increasing the amplitude or the frequency of pulsation of the continuous phase.</i>  |
| <b>Table 1.7</b> | <i>Amplitude and frequency used to control the shear stress in the torsional system.</i>   |
| <b>Table 2.7</b> | <i>Effect of dispersed phase flux on mean droplet size, solid particle size and size distribution and experimental conditions.</i>   |

- Table 3.7** *Comparison of process and membrane parameters, particle size, uniformity and encapsulation efficiency achieved at bath scale and large scale production. DP-dispersed phase emulsified.*
- Table 1.8** *Experimental conditions to carry out the solvent diffusion process at increased  $V_{sd}/V_{theoretic}$  ratio and the effect on the solidification time of the droplets.*
- Table 2.8** *Experimental conditions, encapsulation efficiency (EE) and drug loading (DL) of solid particles produced at different volume fraction of  $W_1$  ( $\Phi_{wo}$ ). FG-fish gelatin; PCL-polycaprolactone; PVA-poly-vinyl alcol;  $V_{sd}$ -Volume used;  $V_{th}$ - theoretic volume;  $\Phi$ -volume fraction.*
- Table 3.8** *Encapsulation efficiency (EE%) and drug loading (DL%) of copper into PLGA and PCL particles.*

## Sommario

Il micro-incapsulamento è una tecnica ampiamente utilizzata per incapsulare sostanze nutraceutiche, farmaci, proteine, cellule ecc. Oggigiorno, la ricerca nel campo farmaceutico viene sempre più indirizzata allo sviluppo di forme farmaceutiche a rilascio modificato (ad esempio emulsioni multiple, sfere e capsule mono/ polinucleate) in grado di migliorare la biodisponibilità di principi attivi scarsamente solubili.

La maggior parte delle metodologie utilizzate per la preparazione di particelle micro e nano-strutturate prevedono un processo iniziale di emulsificazione. In questo caso, il controllo della dimensione e dell'uniformità delle gocce è di fondamentale importanza per produrre particelle solide di dimensione controllata, da cui dipende la via di somministrazione, la distribuzione nei tessuti e l'interazione con le cellule.

Negli ultimi 25 anni, enormi progressi sono stati realizzati nella preparazione di emulsioni con una dimensione controllata delle gocce grazie a un sempre più vasto utilizzo dell'emulsificazione a membrana, un processo vantaggioso rispetto alle tecniche convenzionali in termini di semplicità operativa, basso consumo energetico, alta riproducibilità e facile scale-up. L'aspetto innovativo di questo processo è la produzione delle gocce di emulsione singolarmente, ottenuta mediante permeazione della fase dispersa attraverso i pori della membrana, mentre il distacco della goccia avviene all'uscita del poro per effetto di uno sforzo di taglio esercitato dal fluire della fase continua. Un grande potenziale dell'emulsificazione a membrana per la preparazione di formulazioni farmaceutiche è la possibilità di combinare le proprietà chimiche della formulazione con le proprietà strutturali della particella (quali dimensione e dispersione) in modo da realizzare prodotti con caratteristiche funzionali idonee a specifiche applicazioni.

Nella realizzazione di sistemi micro e nano-strutturati per l'incapsulamento di molecole bioattive, le proprietà chimico-fisiche del materiale sono anche di fondamentale importanza. Tra i materiali organici, i polimeri biodegradabili (in particolare il policaprolattone e il copolimero dell'acido lattico e glicolico) sono quelli di maggiore impiego in quanto offrono la possibilità di realizzare particelle che, una volta introdotte nell'organismo, vengono degradate in sottoprodotti metabolizzati dalle cellule. Questa proprietà conferisce a questi materiali un'eccellente biocompatibilità e il rilascio del farmaco incapsulato nelle particelle può essere modulato dalla velocità di degradazione del polimero. Inoltre questi polimeri sono idrofobi e quindi ideali per l'incapsulamento di farmaci insolubili in acqua, una procedura necessaria per poter essere somministrati nella circolazione sanguigna. Nonostante questi polimeri siano ampiamente utilizzati per la preparazione di sistemi micro e nano-strutturati, numerose problematiche sono state riscontrate nel controllo della dimensione e dispersione delle particelle e la loro morfologia.

Lo scopo del presente lavoro di tesi è quello di utilizzare l'emulsificazione a membrana per la preparazione di sistemi micro e nano-strutturati utilizzabili per l'incapsulamento di farmaci idrofili e lipofili e realizzati con i polimeri biodegradabili precedentemente

menzionati. Dall'analisi dello stato dell'arte sono stati individuati una serie di requisiti importanti per la preparazione di sistemi particellari: i) produrre particelle con dimensione e dispersione controllata utilizzando un processo ad alta produttività; ii) mantenere un basso stress meccanico per preservare l'attività delle sostanze incapsulate; iii) utilizzare un processo che può essere applicato su larga scala a livello industriale. La produzione di particelle altamente uniformi e con dimensione controllata mediante l'utilizzo dell'emulsificazione a membrana è già stato pienamente riportato in letteratura. Tuttavia, la possibilità di poter ottenere una produzione controllata dell'emulsione mantenendo allo stesso tempo un'alta produttività e un basso stress meccanico nell'impianto è tutt'ora oggetto di studio. Sulla base di queste osservazioni, gli avanzamenti proposti dal presente lavoro di tesi sono:

- migliorare la produttività e l'efficienza del processo di emulsificazione a membrana mediante: i) l'utilizzo di una membrana con bagnabilità asimmetrica lungo la sezione al fine di mantenere allo stesso tempo una produzione controllata dell'emulsione ad un alto flusso di fase dispersa; ii) l'utilizzo di membrane di tipo "setaccio" in acciaio inox in modo da combinare i vantaggi delle caratteristiche strutturali della membrana setaccio (bassa porosità, basso spessore, pori rettilinei e uniformemente distribuiti) con l'elevata resistenza chimica dell'acciaio inossidabile, che è meno soggetto allo "sporco" per interazione con i componenti dell'emulsione;
- indagare, inizialmente su piccola scala e poi con processi adatti per la produzione su larga scala, la preparazione di sistemi micro e nano particellari combinando la emulsificazione a membrana con il processo di diffusione del solvente per ottenere un controllo della dimensione e morfologia delle particelle in modo preciso e riproducibile rispetto all' evaporazione del solvente comunemente utilizzata;
- investigare l'utilizzo di processi di emulsificazione a membrana recentemente introdotti per applicazioni su larga scala, quali emulsificazione a membrana con flusso pulsato e invertito della fase continua ed emulsificazione a membrana con movimento torsionale della membrana, per la produzione di particelle micro e nano-strutturate in condizioni di basso stress meccanico e alta produttività del processo.



## Obiettivi della ricerca

Lo sviluppo di metodologie che permettono l'incapsulamento di molecole bioattive preservandone l'attività terapeutica e mantenendo allo stesso tempo un controllo preciso della dimensione e dispersione delle particelle sono tutt'ora oggetto di studio per la preparazione di forme farmaceutiche a rilascio modificato. Sulla base di questa osservazione, gli avanzamenti proposti nel presente lavoro di tesi mirano al raggiungimento dei seguenti obiettivi:

- migliorare la produttività e l'efficienza del processo di emulsificazione a membrana;
- indagare la preparazione di sistemi particellari utilizzando i polimeri biodegradabili e associando l'emulsificazione a membrana con il processo di diffusione del solvente per ottenere un controllo preciso e riproducibile della dimensione e morfologia delle particelle;
- indagare la produzione di nanoparticelle in condizioni di basso stress meccanico utilizzando l'emulsificazione a membrane a flusso pulsato e invertito, un processo idoneo per una produzione su larga scala;
- indagare la produzione su larga scala di formulazioni micro-strutturate utilizzando membrane di tipo setaccio in acciaio inossidabile in un impianto di emulsificazione con movimento torsionale della membrana, in modo da ottenere un'alta produttività mantenendo uno stress meccanico ridotto nell'impianto;
- indagare l'uso dei sistemi particellari micro-strutturati per l'incapsulamento simultaneo di composti idrofili e lipofili;

In Tabella 1 sono riassunti gli avanzamenti proposti nel presente lavoro di tesi rispetto allo stato dell'arte e i capitoli nei quali sono specificatamente discussi.

Tabella 1. Avanzamenti proposti

| Stato dell'arte  | Avanzamenti proposti  | Capitolo |
|--|---|----------|
| La principale limitazione dell'avanzamento del processo di emulsificazione a membrana a livello industriale è il basso flusso di permeazione della fase dispersa con conseguente rallentamento del processo. Il flusso della fase dispersa può essere migliorato | La produttività e l'efficienza del processo sono state migliorate mediante l'utilizzo di una membrana con un profilo di bagnabilità asimmetrica lungo la sezione. La struttura esterna idrofila ha permesso di mantenere un alto flusso di permeazione della fase | 2        |

|   |  |     |
|---|--|-----|
| <p>mediante lo sviluppo di membrane con specifiche proprietà strutturali e chimiche del materiale.</p>  | <p>dispersa, mentre, la superficie idrofoba dello strato attivo ha permesso di preservare l'uniformità delle gocce di acqua in uscita dal poro nella preparazione di emulsioni acqua/olio.</p>   |     |
| <p>Lo sporcamento della membrana è uno dei principali ostacoli per l'uso sostenibile di quest'ultima. L'interazione tra la superficie della membrana e i componenti dell'emulsione modificano le sue proprietà superficiali influenzando il controllo della dimensione e uniformità delle gocce in uscita dal poro.</p>   | <p>E' stata studiata l'influenza dello sporcamento delle membrane piane di tipo setaccio in acciaio inossidabile e nickel sull'uniformità di emulsioni contenenti una soluzione polimerica come fase dispersa. La maggiore resistenza chimica dell'acciaio inossidabile ha permesso un migliore controllo della dispersione delle gocce di emulsione rispetto alla membrana in nickel, che è comunemente utilizzata con l'impianto della "Celletta agitata", idoneo per lo studio di formulazioni su piccola scala</p>   | 3   |
| <p>Una serie di problematiche sono riscontrate nelle metodologie comunemente utilizzate per la preparazione di microparticelle in policaprolattone (PCL), quali il controllo della dimensione, dispersione e morfologia delle particelle. In letteratura, sono riportati alcuni studi sulla preparazione di microcapsule utilizzando il copolimero dell'acido lattico e glicolico (PLGA) e l'emulsificazione a membrana combinata con l'evaporazione o estrazione del solvente. Non sono stati trovati, invece, studi sulla preparazione di microcapsule polinucleate in PCL partendo dalla preparazione di un'emulsione multipla acqua/olio/acqua e utilizzando il processo di</p> | <p>Il processo di emulsificazione a membrana combinato con la diffusione del solvente è stato indagato per la produzione di microsfeere e microcapsule polinucleate in PCL e PLGA. L'utilizzo della membrana microporosa ha permesso un controllo preciso e simultaneo della dimensione e uniformità delle gocce di emulsione, precursori delle particelle solide. Il processo di diffusione del solvente ha permesso di controllare la morfologia delle particelle nella fase di solidificazione del polimero, preservando la dimensione e uniformità delle goccioline di emulsione iniziali.</p> | 4-5 |

|  |   |   |
|--|---|---|
| emulsificazione a membrana.  |   |   |
| La produzione di nanoparticelle con tecniche adatte per una produzione su larga scala sono attualmente oggetto di studio. Pochi studi sono stati trovati in letteratura sulla produzione di nanoparticelle utilizzando processi di emulsificazione a membrana per applicazioni a livello industriale, quali l'emulsificazione a flusso tangenziale. Tuttavia, una problematica di questo processo è l'elevato stress meccanico a cui è soggetta l'emulsione che può essere facilmente danneggiata. | L'emulsificazione a membrana a flusso pulsato e invertito è stata indagata per la preparazione di sistemi micro e nano particellari con dimensione controllata (2-0.2 $\mu\text{m}$ ). Questo processo innovativo può essere usato per una produzione su larga scala e ha permesso un controllo preciso della dimensione delle gocce utilizzando una velocità assiale ( $0.5 \text{ m s}^{-1}$ ) molto più bassa rispetto ai valori riportati in letteratura per il processo di emulsificazione a flusso tangenziale ( $1-4.5 \text{ m s}^{-1}$ ) | 6 |
| Per promuovere l'avanzamento dell'emulsificazione a membrana a livello industriale è necessario migliorare le condizioni del processo al fine di ottenere un'alta produttività, mantenendo una buona qualità dell'emulsione in condizioni di basso stress meccanico.   | L'utilizzo di un'impianto di emulsificazione basato sul movimento torsionale di una membrana "setaccio" in acciaio inossidabile ha permesso di ottenere un'alta produttività, in termini di flusso di fase dispersa e concentrazione dell'emulsione prodotta, preservando l'uniformità delle gocce di emulsione e mantenendo condizioni di basso stress meccanico. Questo processo è stato utilizzato per trasferire su larga scala la produzione di emulsioni con dimensioni nell'intervallo micro.  | 7 |
| La co-somministrazione di più farmaci è una strategia comunemente utilizzata nell'ambito clinico per migliorare l'efficienza terapeutica. L'incapsulamento di farmaci di natura diversa in un singolo sistema particellare è tutt'ora oggetto di studio e pochi esempi sono riportati in letteratura.  | Le particelle micro-strutturate preparate mediante l'emulsificazione a membrana e diffusione del solvente sono state investigate per l'incapsulamento simultaneo di molecole di natura idrofilica e idrofobica. Un'alta efficienza di incapsulamento maggiore del 90% è stata ottenuta ottimizzando la composizione chimica e i parametri del processo.   | 8 |

---

|  |  |  |
|--|--|--|
|  | Una potenziale applicazione di queste particelle può essere come forme farmaceutiche a rilascio modificato per la multi-terapia. |  |
|--|--|--|

---

### Contenuti della tesi

La tesi è organizzata in due sezioni principali, la prima incentrata sull'analisi dello stato dell'arte e la seconda sull'attività sperimentale. L'analisi dello stato dell'arte è stata finalizzata al consolidamento delle conoscenze generali raggiunte nel campo oggetto di studio. In particolare, sono stati studiati i principi di base del processo di emulsificazione a membrana e le applicazioni nella preparazione di forme farmaceutiche a rilascio modificato (emulsioni multiple, particelle polimeriche micro e nano strutturate, liposomi) (**Capitolo 1**). L'attività sperimentale è stata suddivisa in diversi capitoli come riportato di seguito:

- nel **Capitolo 2** è riportato lo studio finalizzato al miglioramento della produttività dell'emulsificazione a membrana tramite l'utilizzo di una membrana con una bagnabilità asimmetrica lungo la sezione. La membrana è stata modificata mediante adsorbimento di una molecola modello lipofila sullo strato attivo interno della membrana;
- nel **Capitolo 3** è riportato lo studio dell'influenza dello sporco delle membrane piane di tipo setaccio in nickel e acciaio inossidabile sull'uniformità di emulsioni prodotte utilizzando una soluzione polimerica come fase dispersa. Il materiale con cui è realizzata la membrana influisce sulla proprietà superficiale e quindi sulla qualità dell'emulsione;
- nei **Capitoli 4 e 5** è riportato lo studio dell'emulsificazione a membrana associata alla diffusione del solvente come metodologia innovativa per la preparazione di microsfele e microcapsule polinucleate in PCL e PLGA da emulsioni semplici olio/acqua e multiple acqua/olio/acqua rispettivamente. Questo studio è stato condotto inizialmente su piccola scala utilizzando la "Celletta agitata";
- nel **Capitolo 6** è riportato lo studio della preparazione di particelle con dimensione controllata su scala micro e nano mediante il processo di emulsificazione a membrana con flusso pulsato e invertito utilizzando condizioni di stress meccanico ridotte rispetto ai processi di emulsificazione a membrana adatti per una produzione su larga scala;

- nel **Capitolo 7** è riportato lo studio dell'emulsificazione con movimento torsionale della membrana per trasferire la produzione di sistemi particellari semplici e micro-strutturati su larga scala. In questo studio sono state applicate membrane tubolari di tipo setaccio in acciaio inossidabile;
- nel **Capitolo 8** è riportato lo studio dell'incapsulamento simultaneo di composti idrofili e lipofili nelle microcapsule polinucleate in PCL e PLGA. Particolare attenzione è stata rivolta allo studio dell'influenza della composizione chimica e del processo di solidificazione delle particelle sull'efficienza di incapsulamento.

## Summary

Microencapsulation is an extensively used technique to encapsulate food compounds, cosmetics, drugs, protein, cells etc. Nowadays, there is an increasing interest in the pharmaceutical field to develop specifically designed micro and nanostructures (such as double emulsions, spheres, beads and core-shell structures) able to improve the bioavailability of poorly soluble therapeutic substances.

Most of the methods used for the preparation of micro and nano particles are based on emulsification processes. In this case, the control of particle-size is necessary to preserve the stability and produce emulsions and particles with new functional roles. Small and uniform size of the particle are also important requirements to control the distribution in the body and the interaction with living cells. In the last twenty five years, the process of membrane emulsification demonstrated to offer numerous advantages over conventional emulsification techniques in terms of operational flexibility, reproducibility and straightforward up-scaling. This process is based on the production of target droplets size by “drop-by-drop” mechanism obtained by feeding the dispersed liquid phase into the continuous phase through a high throughput microporous membrane. The microporous membrane works as emulsifying device to micro-manufacture droplets with regular dimensions and controlled size distribution. Particles produced by membrane emulsification are able to combine the chemical composition and the structural properties (such as size, size distribution) with the functional activity properly designed for specific applications. This great potentiality may lead to novel process intensification in particles production.

The successful development of a drug carrier is also related to the physical-chemical properties of the material used for the drug encapsulation. Biodegradable polyesters (such as poly-caprolactone, PCL, or poly-lactide-co-glycolide, PLGA) received great interest because they offer possibilities to produce drug delivery systems where the matrix material can be decomposed into non-toxic and low molecular-weight species with the concomitant release of drug. The hydrophobic property of these polymers make them suitable for the encapsulation of poorly water soluble compounds. However, the methodologies commonly used for the preparation of particles with these polymers are associated with many problems regarding the control of particle size and size distribution and particle morphology.

The aim of the present work is to investigate the use of membrane emulsification for the production of uniform micro and nano-structured particles suitable for drug encapsulation using biodegradable polyesters as matrix material. The important requirements that emerged from the analysis of the state-of-the-art to design a micro and nano-manufacturing process include i) the possibility to produce particles with tailored size and uniformity at high-throughput, ii) low shear conditions and, iii) in an easily scalable way. Membrane emulsification demonstrated to be successful to prepare uniform particles with the required average size. However, the possibility to achieve high productivity and high emulsion quality at low shear condition is still under

investigation. On the basis of these observations, the advances promoted in the present PhD thesis are:

- improvement of membrane emulsification productivity and efficiency, i) using membrane with asymmetric wettability property between thickness and surface in order to keep at the same time the controlled production of uniform droplets and high dispersed phase flux at low transmembrane pressure; ii) using stainless steel micro-sieve membrane in order to combine the advantageous properties of the micro-sieve membrane (high potential flux at low transmembrane pressure, low porosity and rectilinear pore structure) with the high chemical resistance of stainless steel which is less prone to get fouled by the ingredients of the emulsion;
- investigating firstly at batch scale and then with processes suitable for large scale production the combination of membrane emulsification with the solvent diffusion process to achieve a control of PCL and PLGA particle size and particle morphology in a precise and easily scalable way compared to the commonly used solvent evaporation;
- investigating recently introduced membrane emulsification processes (pulsed-back-and-forward membrane emulsification and torsional membrane emulsification) suitable for large scale production for the preparation of micro and nano-structured particles at low shear conditions and high throughput;

## Research objectives

The development of methodologies that allow at the same time the incorporation of biomolecules without affecting their activity as well as a precise control of particle size and uniformity is a challenge for the production of drug delivery systems. The present work aimed at facing this challenge by pursuing the following objectives:

- improve membrane emulsification efficiency in terms of productivity and droplet size distribution;
- investigate at batch scale the combination of membrane emulsification and solvent diffusion process for an innovative PCL and PLGA particle preparation methodology able to achieve a controlled particle size and particle morphology in a precise and reproducible way;
- investigate the production of nanoparticles at low shear conditions using pulsed back-and-forward membrane emulsification which is suitable for the encapsulation of shear sensitive compounds and large scale production;
- use of micro-sieve stainless steel membrane in torsional motion for the production of simple and micro-structured particles at high throughput and in continuous mode for industrial outlook;
- investigate the use of micro-structured particles with an hydrophilic core and hydrophobic matrix for the simultaneous encapsulation of hydrophilic and hydrophobic compounds;

In Table 1 are summarized the advances promoted in the present work compared with the state of the art and the chapter where each advance is specifically discussed.

Table 1. Advances promoted

| State of the art  | Advances promoted   | Chapter |
|---|---|---------|
| The main obstacle of membrane emulsification advancing to an industrial scale is the low dispersed phase flux that is related with long production time. The dispersed phase flux can be modulated by an appropriate choice of membrane structure and membrane material | Emulsion productivity and efficiency are improved using a membrane with asymmetric wetting property. The hydrophilic shell allowed to keep high flux at low transmembrane pressure and the hydrophobic surface of the lumen allowed to improve the uniformity of the aqueous droplets of water-in-oil emulsion. | 2       |



|   |   |     |
|---|---|-----|
|   |   |     |
| <p>Membrane fouling is still a significant hindrance for its sustainable use. The interaction between membrane surface and the ingredients used in the emulsion preparation modify the surface properties of the membrane and influence the controlled particle production and the productivity of the process.</p>   | <p>The influence of micro-sieve stainless steel and nickel membranes on membrane fouling by polymer solution is investigated. The higher chemical resistance of stainless steel allowed the production of highly uniform emulsion compared with nickel membrane which is commonly used with the stirrer Dispersion Cell.</p>  | 3   |
| <p>The methodologies commonly used for the preparation of polycaprolactone (PCL) microparticles are associated with many problems regarding the control of particle size and size distribution and particles morphology. There are some examples in literature regarding the preparation of microstructured poly(lactide-co-glycolide) (PLGA) particles using membrane emulsification process combined with solvent extraction/evaporation. On the contrary, no works are reported in literature regarding the preparation of PCL micro-structured particles from double water-in-oil-in-water (W/O/W) emulsion using membrane based processes.</p> | <p>Membrane emulsification/solvent diffusion process was investigated at batch scale for the production of simple PCL and microstructured PCL and PLGA particles. The use of microporous membrane allows the simultaneous control of particle size and size distribution during the emulsification step. The solvent diffusion compared to the solvent evaporation allows precise control of size, uniformity and morphology of the particles during the solidification step.</p> | 4-5 |
| <p>The production of nanoparticles with methods suitable for large scale is still a challenge. There are few example in literature about the</p>  | <p>Pulsed back-and-forward membrane emulsification was investigated for the preparation of uniform micro and nanoparticles.</p>   | 6   |

|   |   |   |
|---|---|---|
| <p>preparation of nanoparticles using membrane emulsification methods suitable for large scale production (cross-flow and premix). However, in these processes damage of the emulsion can occurred because of the high mechanical stress</p>  | <p>(size range 2-0.2 <math>\mu\text{m}</math>). This innovative process suitable for large scale production allowed to achieve a controlled particle size and size distribution with an axial velocity (<math>0.5 \text{ m s}^{-1}</math>) that is much lower than the range of cross flow velocity reported in literature (<math>1-4.5 \text{ m s}^{-1}</math>)</p>                                      |   |
| <p>Advances on innovative process conditions able to achieve maximum productivity and high emulsion quality at low shear stress conditions are necessary to promote membrane emulsification technology for an industrial outlook.</p>   | <p>The use of micro-sieve stainless steel membrane in torsional motion allowed to achieve high-throughput in terms of dispersed phase flux and concentration of the emulsion per unit time keeping the uniformity of the emulsions and low shear conditions in the bulk of the product stream. This process was used to shift from a batch to a large scale production of particles in a micron-range</p> | 7 |
| <p>Co-administration of two or more drugs in clinical practice is a common strategy for the improvement of the therapeutic efficacy. So far, combining drugs into a single carrier is still a challenge for encapsulation technologies and very few studies have reported the simultaneous encapsulation and delivery of hydrophilic and hydrophobic compounds.</p> | <p>Micro-structured particles were investigated for the simultaneous encapsulation of hydrophilic and hydrophobic compounds. Encapsulation efficiency higher than 90% was achieved combining membrane emulsification with the solvent diffusion process. These particles could be potentially used as drug delivery system for multi-therapy.</p>   | 8 |

### Dissertation outline

The flow chart of the dissertation outline is reported in Figure 1. The thesis is organized in two main sections, the first one covering the analysis of the state-of-the-art and the second one covering the research activity. The analysis of the state of the art aimed at consolidating the knowledge achieved in the field present in the open literature. In particular, membrane emulsification basic principles and its applications for the preparation of drug delivery systems (multiple emulsions, micro/nano solid and polymer particles, liposomes) have been highlighted (**Chapter 1**). The research activity is organized in several chapters as reported below:

- investigation of a modified membrane with tailored wettability property for the improvement of membrane emulsification productivity keeping a narrow size distribution of the emulsion. The membrane was modified by adsorption of hydrophobic macromolecules on the lumen side of hydrophilic membrane (**Chapter 2**);
- study of the influence of membrane fouling of nickel and stainless steel flat sheet micro-sieve membranes on the production of emulsions containing polymer solution in the formulation. The membrane material influences the surface property and so the uniformity of the emulsion (**Chapter 3**);
- study of the combination of membrane emulsification and the solvent diffusion process as innovative particle preparation methodology for the production of simple PCL particles by oil-water emulsion and micro-structured PCL and PLGA particles by multiple oil-water-oil emulsion. This study was carried out using the stirrer Dispersion Cell which is suitable to work at laboratory scale (**Chapter 4-5**);
- investigation of pulsed-back-and-forward membrane emulsification as innovative process for the production of uniform PCL micro and nanoparticles at lower shear conditions compared to other membrane emulsification processes suitable for large scale production (**Chapter 6**);
- transition from a batch scale to a large scale production of simple and micro-structured PCL particles using micro-sieve stainless steel membrane in torsional motion (**Chapter 7**);
- study of PCL and PLGA micro-structured particles for the simultaneous encapsulation of hydrophilic and hydrophobic compounds. The influence of process and chemical parameters on the encapsulation efficiency is investigated (**Chapter 8**);

# CHAPTER 1

## **Membrane emulsification: principles and applications for particle production**

### **1. Introduction**

So far, emulsions are an expanding area of research as the creation of controlled size and shape particles to achieve specific properties is investigated. The idea that the microstructure of an emulsion can be designed specifically to enhance the designed function of the emulsion has many potential applications. There is an increasing interest in developing specifically designed micro and nanostructure (such as double emulsions, spheres, beads and core-shell structures) using emulsification processes. In this case, the control of particle-size is necessary to preserve the stability and giving emulsions new functional roles. The conventional emulsification processes are based on the use of turbulent forces to reduce pre-existing droplets to the size range required. However, these turbulent flows cannot be controlled or generated uniformly. The consequences are that the control of droplet size is difficult and wide size distributions are commonly obtained, therefore the energy is used inefficiently in these technologies. Moreover, for the preparation of formulations containing labile molecules (such as bioactive compounds) low shear conditions are required in order to prevent their degradation. Nakashima et al. [1] introduced an innovative concept at the 2nd International Conference on Inorganic Membranes (1991). This is based on the production of each droplet already at the desired size by forcing the dispersed phase liquid through a microporous membrane into the continuous phase. The microporous membrane works as emulsifying device to produce droplets with regular dimensions and controlled size distribution; from this concept “membrane emulsification” derived. Technology for preparing monodispersed particles with a definite size has not been available until the membrane emulsification technique was developed. In this chapter, an overview of the basic principles and applications of membrane emulsification for the production of micro and nano-structured particles is given. In the first part of the chapter, the conventional methods and membrane emulsification principles and devices will be described while, in the second part, a summary of different particulate systems prepared by membrane emulsification for pharmaceutical applications is given.

### **2. Emulsions and conventional emulsification methods**

According to P. Becher [2] an emulsion is “a heterogeneous system”, consisting of at least one immiscible liquid intimately dispersed in another in the form of droplets, whose diameters, in general, exceed 0.1  $\mu\text{m}$ . The type of simple emulsion (water-in-oil or oil-in-water, commonly abbreviated as W/O or O/W) is decided mainly by the

volume ratio of the two liquids, their order of addition and the nature of the emulsifier (the emulsifier should be soluble in the continuous phase). An emulsion may also be an emulsion of an emulsion e.g. water-in-oil-in-water (W/O/W) and oil-in-water-in-oil (O/W/O) emulsions, also termed multiple or double emulsions. Due to their large interfacial area, emulsions are thermodynamically unstable and have a tendency to undergo coalescence, a process in which two droplets merge into a bigger one, minimizing the surface energy. Certain molecules or materials, such as surfactants, amphiphilic polymers or proteins, can be added to prevent coalescence, making emulsions kinetically stable. These emulsion stabilizers usually provide electrostatic repulsion, steric repulsion, and/or strength to the interfacial layer of the droplets, according to widely accepted theories. Except in special cases where spontaneous emulsification can occur, energy must be supplied to produce such metastable mixtures. From a thermodynamic point of view, surfactants reduce the surface free energy required to increase any interfacial area by lowering the interfacial tension, and allow finely media to be created easily. In fact, a much higher amount of energy is necessary, since breaking of large droplets into smaller ones involves additional shear forces, so that the viscous resistance during agitation absorbs most of the energy [3]. Conventional mechanical methods used to provide the required energy to produce an emulsion are: a) Rotor-stator system; b) High-pressure system; c) ultrasonic system.

a) *Rotor-stator systems*

Rotor-stator systems can be operated in continuous or discontinuous mode. For the discontinuous or quasi-continuous production agitators, different geometry or gear-rim dispersion machine are usually used. In this system the dispersed phase droplets are broken-up to a large extent by forces of inertia and shearing in turbulent flow. The produced stress can be classified as medium to high, depending on the number of revolutions and the geometry of the rotor-stator systems. Mean droplet diameter below 2  $\mu\text{m}$  cannot be obtained with this system [4].

b) *High-pressure homogenizer*

In a high-pressure homogenizer, the oil and water mixture is passed through a narrow orifice, or inject dispersion in which two jets of different components are made to collide head-on; pressures in the range of  $5.0 \times 10^6$ - $3.5 \times 10^7$  Pa are commonly used. In this system emulsion is subjected to intense turbulent and shear flow fields. Turbulence, the predominant mechanism, leads to the break-up of the dispersed phase into small droplets and laminar shear and cavitation can assist the process. Mean droplet diameter below 0.2  $\mu\text{m}$  can be obtained with this system and high product yields. However, the stress on the product is very high due to the high pressure gradients and flow rate [5].

c) *Ultrasonication*

In ultrasound emulsification, reported for the first time by Wood and Loomis, high frequency - vibrations applied to a diphasic liquid system provide a different breaking

and dispersing of a bulk phase: large drops produced by the instability of interfacial waves are broken into smaller ones by acoustic cavitation. Due to the small product throughput this process is mainly applied in laboratories when mean droplets diameter of approximately  $0.4\ \mu\text{m}$  can be obtained [6].

### 3. Membrane emulsification

Membrane emulsification has received increasing attention over the last 20 years as successful method of emulsification to produce emulsions and particles with narrow size distribution. The use of membrane to manufacture emulsion follows two innovative approaches respect to conventional methods:

- 1) reduction of turbulent perturbations in the mixing processes that rupture the liquids;
- 2) manufacture of droplets individually (drop-by-drop) using micro-engineered structured systems;

The conventional direct ME involves the permeation of the dispersed phase through a porous membrane in order to form droplets at the opening pore successively detached from the membrane surface by the shear stress of the moving continuous phase (Figure 1.1).

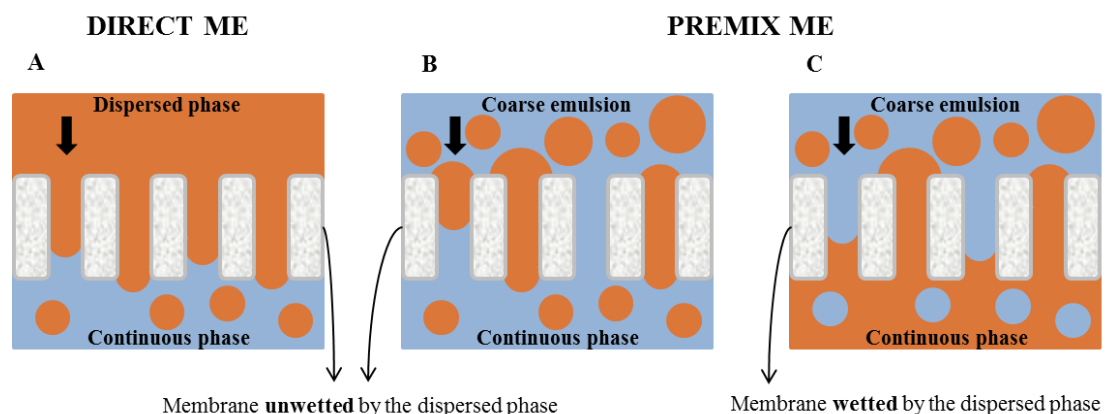


Figure 1.1 Schematic representation of direct and premix membrane emulsification

Suzuki et al. [7] introduced a modified form of the classic emulsification system, in which a coarse emulsion (prepared using a conventional stirrer mixer) is refined upon passage through a microporous membrane. The method is referred as premix ME (Figure 1.1, B-C). Usually, in premix ME method, the membrane is wetted by the continuous phase of the coarse emulsion and the emulsion is broken up into smaller droplets (Figure 1.1, B). Sometimes the membrane is wetted by the dispersed phase of the coarse emulsion, and in this case phase inversion can take place, leading to very high disperse phase volume fractions (Figure 1.1, C). The energy costs for premix

emulsification are relatively low, since no cross-flow is needed, the process is easier to control and operate than direct ME but the droplet polydispersity is higher [8].

#### 4. Forces on a spherical droplet

In membrane dispersion process, droplet formation mainly consists of the following three processes: (I) droplet across the pore; (II) droplet growth; (III) droplet detachment. The main forces that act on the forming droplets are [9]:

- (1) the *interfacial tension force* or capillary force,  $F_\gamma$ , which is the effect of dispersed phase adhesion around the edge of the opening pore;

$$F_\gamma = \pi d_p \gamma \quad (1)$$

- (2) the *static pressure difference force*,  $F_{sp}$ , due to the pressure difference between the dispersed phase and the continuous phase at the membrane surface;

$$F_{sp} = \frac{\gamma}{d_p} \pi d_d^2 \quad (2)$$

- (3) the *drag force*,  $F_d$ , created by moving the continuous phase or using moving membranes;

$$F_d = \frac{3}{2} k_x \pi \tau_{c,s} d_d^2 \quad (3)$$

- (4) the *dynamic lift force*,  $F_L$ , which results from the asymmetric velocity profile of the continuous phase near the droplet;

$$F_L = 0.761 \frac{\tau_{c,s}^{1.5} \rho_c^{0.5}}{\mu_c} d_d^3 \quad (4)$$

- (5) the *buoyancy force*,  $F_B$ , due to the density difference between the continuous phase and the dispersed phase;

$$F_B = \frac{1}{6} \pi g \Delta \rho d_d^3 \quad (5)$$

- (6) the *inertial force*,  $F_i$ , caused by the dispersed phase flow moving through the capillary as it inflates the droplet;

$$F_i = \rho_d \left( \frac{J_d}{\varepsilon} \right) A_N \quad (6)$$

with:

$d_d$ : droplet diameter

$A_N$ : cross-sectional area of the droplet neck,

$k_x$ : equal to 1.7 and takes into account the wall correction factor for a single sphere touching an impermeable wall,

$\varepsilon$ : membrane porosity,

$\tau_{c,s}$ : wall shear stress,

$\gamma$ : dynamic interfacial tension,

$\rho_c$ : density of the continuous phase,

$\rho_d$ : density of the dispersed phase,

$\mu_c$ : viscosity of the continuous phase,

$\Delta\rho$ : the difference between continuous and dispersed phase density.

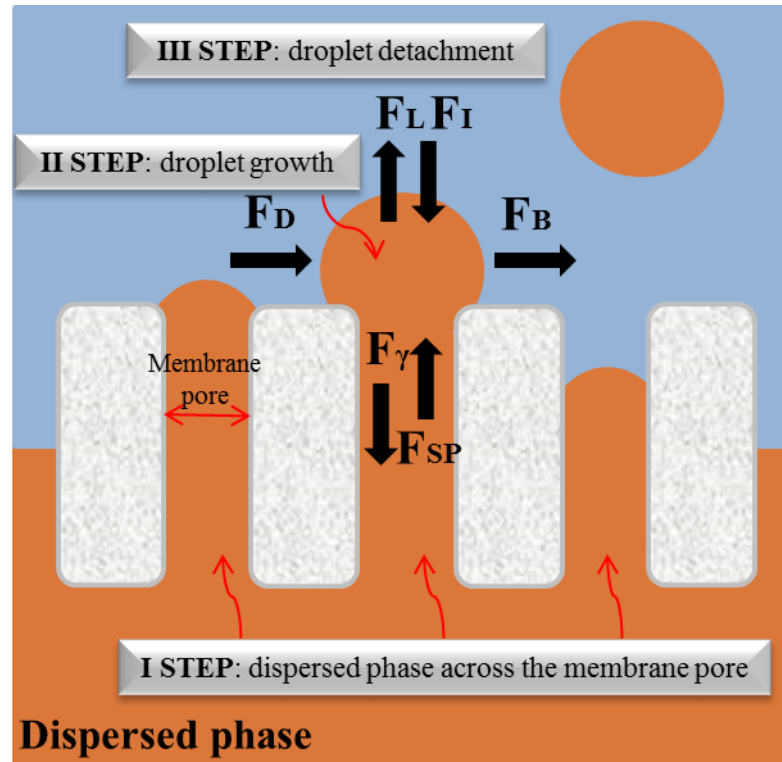


Figure 2.1 Forces acting on a droplet at the pore level

These forces can be divided into holding and detaching forces, which hold the droplet on the sieve-like structure surface and detach the droplet from the surface, respectively (Figure 2.1). Drag force, inertial force, static pressure force tend to detach the droplets whereas interfacial tension forces the drop to remain attached to the pore; when the detaching forces become higher than the holding forces, the formed droplet begins to go away from the surface [9,10].

The drag force can be generated by the continuous phase flowing parallel to the membrane surface (cross flow ME) or pumped in a pulsed way (pulsed ME) or stirring up (stirred ME) the membrane surface. Alternatively, vibrating or rotating membranes can be also used.

In the absence of any drag force, droplets can be spontaneously detached from the pore outlets. ME processes carried out in quiescent condition are referred as *static ME* while those carried out in moving conditions are referred as *dynamic ME*.

In *dynamic ME*, the droplet formation and breakup process can be correlated with a *dripping* or *jetting* behavior depending on the relative strength of different forces acting on the process. The inertial force imparted by the dispersed flow acts as detaching force during the drop formation, and acts against the attaching force of surface tension. If the inertial force of the dispersed phase is too small compared to the drag force of the



continuous phase or unable to overcome the surface tension force, the droplet forms and breakups at the pore level forming the dripping mode. After the first droplet has been detached and carried away from the pore by continuous phase flow, droplets with constant volume have been periodically detached at a constant frequency. This is called “dripping region”. The droplet size in the dripping region is affected by two main forces: drag force imparted by the continuous phase flow and the surface tension force. The inertial force of dispersed phase has negligible effect in drop detachment during dripping region. At high dispersed phase flow rates, the inertial force exceeds the surface tension force, leading to a transition to jetting behavior. In this case, an extension of the droplet neck and filament occurs. Thus, the detachment point of the droplets moves further downstream from the pore typically to a distance greater than five times of the pore diameter. This is called “jetting region”. From an industrial perspective, the flux should be maximized to increase productivity without jetting occurring which is a less controlled process. [11,12]

## 5. Basic parameters

The main factors influencing membrane emulsification (Figure 3.1) include:

- *membrane parameters*, including porosity, mean pore size, pore geometry, pore distance, wettability;
- *phase parameters*, including interfacial tension, emulsifier type and concentration, viscosity and density of dispersed and continuous phases, phase composition, pH and ionic strength;
- *process parameters*, including wall shear stress, trans-membrane pressure, membrane module configuration, temperature;

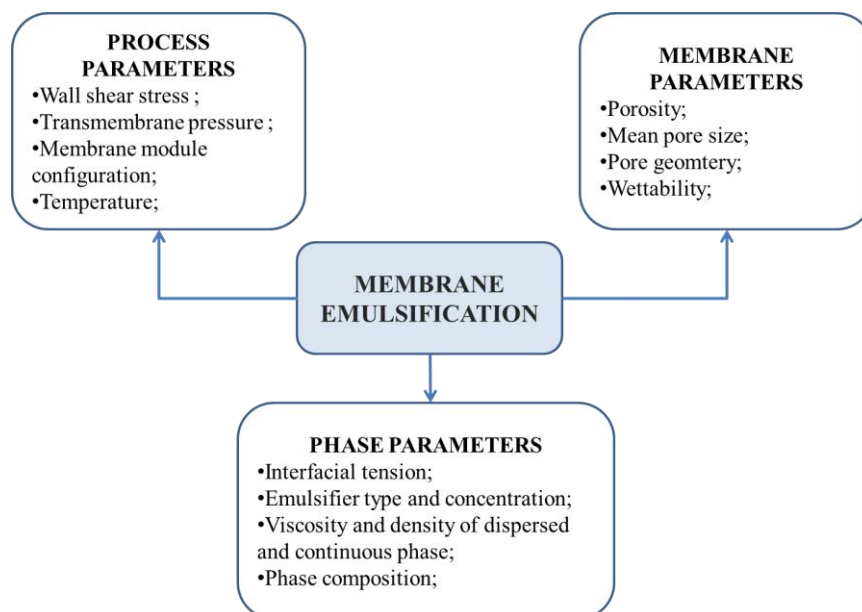


Figure 3.1. Parameters influencing membrane emulsification process

### 5.1. Membrane parameters

Shirasu porous glassy (SPG) membranes are among the first membranes specifically developed for emulsion preparation. They are synthesized from  $\text{CaO-Al}_2\text{O}_3\text{-B}_2\text{O}_3\text{-SiO}_2$  type glass which is made from “Shirasu”, a Japanese volcanic ash. SPG membranes are characterized by interconnected micro-pores, a wide spectrum of available mean pore size (0.05-30  $\mu\text{m}$ ) and high porosity (50-60%). The surface wettability can be changed by reaction with organic silanes [13]. Other commercial microfiltration membranes are attractive because of their availability in very large surface area, and their high flux through the membrane pores: ceramic aluminium oxide ( $\alpha\text{-Al}_2\text{O}_3$ ) membranes (Membrflow, Germany) [14],  $\alpha$ -alumina and zirconia coated membranes (SCT, France) and polytetrafluoroethylene (PTFE) membranes. W/O emulsions were also successfully prepared using microporous polypropylene hollow fibres (Mycrodyn module, Germany), macroporous silica glass membranes and polyamide hollow fibres membrane [15]. Micropore Technologies (United Kingdom) developed flat-sheet or tubular micro pore sieve type metal membranes characterized by cylindrical pores, uniform and in a regular array with a distance between each pore of 200  $\mu\text{m}$  [16]. Silicon and silicon nitride microsieves membranes (Aquamarijn Microfiltration BV, The Netherlands) are also successfully applied for the preparation of O/W emulsions [17].

It has been generally observed that droplet size ( $d_d$ ) of an emulsion can be related to the pore size ( $d_p$ ) of the membrane by a linear relationship for given operating condition:

$$d_d = x d_p \quad (7)$$

where  $x$  can range typically from 2-10 for SPG membranes. For membranes other than SPG the values reported for  $x$  are typically from 3-50 [18].

To allow optimal production of mono-dispersed emulsions, the affinity between membrane surface, dispersed and continuous phase and electrical charge of the emulsifier, must be considered. For a preparation of O/W emulsions, hydrophilic membranes must be used in order to avoid the wetting and spreading of the oil on the membrane surface; on the contrary hydrophobic membrane must be used for the preparation of W/O emulsion. Similar principles may also apply to the choice of the emulsifiers; in fact, its functional groups must not carry opposite charge respect to the membrane surface in order to preserve hydrophilicity of the membrane. For example, an untreated SPG membrane has a negative surface charge within the pH range of 2 to 8, due to the dissociation of acid silanol groups, therefore cationic emulsifier must be avoided for the preparation of O/W emulsion [1].

Membrane purchased in a hydrophilic form can be made hydrophobic by chemical surface modification or by pre-soaking it in the oil phase. Pre-sonication in solutions of surfactants has also been shown to improve dispersed phase flux and the decreased interfacial tension in the pores leads to better filling [19]. The porosity of a membrane is also an important parameter because it determines the distance between adjacent pores, this distance increases as the porosity decreases. Monodispersed emulsions can be produced if the membrane pore-size distribution is sufficiently narrow. The porosity is

critical to ensure that two adjacent droplets do not come sufficiently close to allow contact with each other and to coalesce. Therefore, the pores are preferred to be uniformly located on the surface to ensure maximum distance between any two adjacent pores for a given porosity [13]. Abrahamse et al. [18] calculated the maximum membrane porosity of 1.5% to prevent coalescence of droplets growing on neighboring pores of 5  $\mu\text{m}$  diameter. However, low porosity has the negative effect of low dispersed phase flux.

### *5.2. Phase parameters*

The type of emulsion (O/W or W/O emulsion) is dictated by the emulsifier and the latter should be more soluble in the continuous phase. The HLB number (that is the ratio of the hydrophilic and lipophilic groups of the surfactant molecules) can be used to select the surfactant for a given emulsion. Non-ionic surfactants have HLB numbers ranging from 0 to 20. Surfactant with  $\text{HLB} > 10$  have an affinity for water (hydrophilic) while surfactant with  $\text{HLB} < 10$  have an affinity for oil (lipophilic). Therefore, a water continuous phase system benefits from a surfactant with a high HLB value and an oil continuous phase system from a surfactant with low HLB value [10]. The interfacial tension force, which represents the effects of dispersed phase adhesion around the edge of the opening pore, forces the drop to remain attached to the pore; therefore, the drop grows until a diameter is reached at which the shear force is higher than the interfacial tension force. Emulsifiers have two main roles in the formation of an emulsion. Firstly, it lowers the interfacial tension between oil and water; secondly, it stabilizes the droplets against coalescence and /or aggregation. Shröder et al. [21] studied the effect of dynamic interfacial tension on droplet formation. They found that the adsorption kinetics of the emulsifier determine the time needed to stabilize the droplets against coalescence in all stages of formation. Faster an emulsifier adsorbs at the newly formed interfaces, smaller droplets are produced. Fast adsorbing emulsifiers reduce the influence of coalescence and allow smaller droplet to detach from the pore because of faster decrease of retaining forces [22]. Geerken et al. [23] found that using fast emulsifier, like SDS, the lag time, which is the period of inactivity of the pore after the detachment of a drop, is negligible; after droplet detachment, a sufficient amount of emulsifier have to adsorb at the hemispherical interface before the critical Laplace pressure is reached again. For faster adsorbing emulsifiers the lag time reduces because the required critical interfacial tension is reached at earlier time.

The viscosities of dispersed and continuous phase have also an important effect on the membrane emulsification process. According to Darcy's law, the dispersed flux is inversely proportional to the dispersed phase viscosity, therefore, if it is high the dispersed flux will be low, and as a consequence the droplet diameter will be small compared to the mean pore diameter [13].

### 5.3. Process parameters in dynamic membrane emulsification

The transmembrane pressure,  $\Delta P_{tm}$ , is defined as the difference between the pressure of the dispersed phase,  $P_d$ , (feed in dead-end mode) and the mean pressure of the continuous phase:

$$\Delta P_{tm} = P_d - \frac{(P_{c,in} + P_{c,out})}{2} \quad (8)$$

where  $P_{c,in}$  and  $P_{c,out}$  are the pressure of the flowing continuous phase at the inlet and outlet of the membrane module respectively. The minimum emulsification pressure required to allow the dispersed phase to pass through the pores into the other side of the membrane can be estimated by the capillary pressure,  $P_{ca}$ :

$$P_{ca} = \frac{4\gamma \cos\delta}{d_p} \quad (9)$$

where  $\gamma$  is the interfacial tension,  $\delta$  is the contact angle of the droplets against the membrane surface wetted with the continuous phase and  $d_p$  is the average pore diameter [18].

The flux of the dispersed phase ( $J_d$ ) is correlated with the transmembrane pressure ( $\Delta P_{tm}$ ) by the Darcy's law:

$$J_d = \frac{K\Delta P_{tm}}{\mu L} \quad (10)$$

where  $K$  is the membrane permeability,  $L$  the membrane thickness, and  $\mu$  the dispersed phase viscosity. Vladisavljevic and Shubert [24] focused especially on the production of emulsions with very narrow droplet size distributions at a transmembrane pressure near the capillary pressure. Increasing the transmembrane pressure increases the dispersed phase flux through the membrane. Actually, the porosity of the membrane changes as a function of pressure with some membrane materials such as SPG and ceramics. Increasing the applied pressure leads to the opening or 'activation' of tortuous pore channels within the structure. An increase in both porosity and pressure driving force affects the flux which increases in a non-linear way. The mean droplet size decreases initially with the increasing of the transmembrane pressure, due to gradual activation of smaller pores, and then increases with further pressure increase because of increased droplet coalescence at the membrane surface [13]. Schröder et al.[21] demonstrated that the increase of droplet size with the increase of flux depends also on the adsorption kinetics of the emulsifier and the formation time of the droplets. If the formation time is longer compared to the time necessary to decrease the interfacial tension, then the interfacial tension have not significant influence on the droplets size and the size remain unchanged on increasing flux. The effect of the dispersed-phase flux on the droplet formation behavior was investigated also by Nakajima et al [25]. They observed that the formation of uniform droplets is only possible within the "size-stable zone", in which

the mean droplet size is almost independent on the disperse phase flux and wall shear stress. The dispersed phase that grew at the opening pore was spontaneously cut off into spherical droplets in the size-stable zone, on the contrary, a drastic increase in the diameter of the formed droplets was observed in the “continuous out-flow zone”. In the direct ME, it is very low the dispersed phase flux through the membrane ( $0.01\text{--}0.1\text{ m}^3/(\text{m}^2\text{ h})$ ), to restrain the transition from the size stable zone to the out-flow stable zone [26].

The generation of a surface shear is the most conventional way to control droplet detachment in membrane emulsification. In general, the mean droplets size decreases exponentially (Figure 4.1) with increasing the wall shear stress until it reaches a size where it becomes more or less independent of the applied shear. Thus, the largest change in droplet size occurs at small shear stress. In membrane emulsification this result is achieved by increasing:

- the continuous phase velocity in cross-flow and stirred ME
- the frequency or amplitude of continuous phase pulsed flow in pulsed ME
- the rotation speed of the membrane in rotating ME
- the frequency vibration of the membrane in vibrating ME

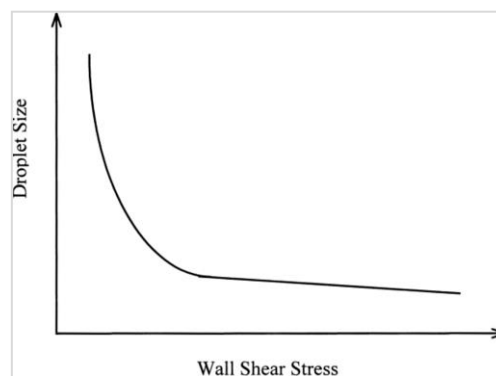


Figure 4.1 Schematic effect of wall shear stress on droplet size produced using membrane emulsification. This figure was published in *Journal of Membrane Science* by S.M. Joscelyne and G. Trägårdh [18]

## 6. Dynamic membrane emulsifications devices

The **stirred ME** device (Figure 5.1) is a dispersion emulsifying system in which the inside of tube-shaped membrane is filled with dispersed phase liquid and the outside with continuous phase liquid; then pressure (internal pressure) is given to the inside of the membrane by using nitrogen gas while stirring the continuous phase with a rotator. Another configuration could be used in which the outside of tube-shaped is filled with dispersed phase liquid, and the inside, with continuous phase liquid; then pressure (external pressure) is given from outside to inside of SPG membrane by using nitrogen gas while stirring the continuous phase liquid with a rotator. Alternatively, a flat-sheet membrane can be used and the dispersed phase is pressed through the membrane from the bottom to the top while a paddle blade stirrer, positioned on the top of the membrane, is used to stirrer the continuous phase. Micropore Technologies Ltd. (UK)

developed the “Dispersion Cell”, which is a stirred ME system useful for laboratory test to study the effect of different experimental conditions on the preparation characteristics but suitable for small scale production [16].

A typical **cross-flow ME** apparatus (Figure 5.1) includes a tubular or flat-sheet microfiltration membrane, a pump for the recirculation of the continuous phase along the lumen side of the membrane, a feed vessel, and a pressured ( $N_2$ ) container for the disperse phase [27]. The dispersed phase, under a gas pressure, is forced through the pores of the membrane while the continuous phase flows along the membrane surface in order to detach the droplets at the opening pore after they reached a certain size. Cross-flow ME is suitable for large scale production and continuous or semi-continuous operation, however there are still problems in obtain narrow droplet size distribution at high dispersed flux and droplets break-up can occurs using high cross-flow velocities.

**Pulsed flow ME** (Figure 5.1) is an alternative method of producing emulsions with a high dispersed to continuous phase ratio continuously in a single- pass operation of the continuous phase [29,30]. The dispersed and the continuous phase are injected using a pump while the pulsed flow is generated by a frequency generator or in alternative, with a programmable peristaltic pump with a reverse flow direction function to produce a pulsed cyclic flow of the continuous phase tangentially to the membrane surface. The potential benefits of the system are that it does not require a special module design, it is suitable for large scale production and it can be connected in series with a baffled reactor, to achieve simultaneous drop generation and chemical/physicochemical reaction in the produced emulsion. This method is suitable for the preparation of emulsions containing shear sensitive material (such as polymer solution or biomolecules) because low shear conditions are maintained in the circuit.

In **rotating ME** (Figure 5.1) the dispersed phase is introduced into the center of a rotating tubular porous membrane, and dispatched through the pores in the membrane wall in radial direction into the stationary continuous phase. The pressure is given to the inside of the membrane using nitrogen gas or a pump while the membrane was rotated and the continuous phase was stirred with a overhead stirrer. In this system the tangential drag force is the major detaching force produced by the rotating membrane. Moreover, additional forces such as the centrifugal force to promote droplet detachment and the tangential velocity differences between the droplet and the continuous phase have also to be considered. The droplet diameter is a function of the membrane pore size and rotational speed, interfacial tension, continuous phase viscosity and radial distance of the membrane central axis to the center of the droplet. Increasing the membrane rotation speed and the continuous phase viscosity, or decreasing the interface tension through the addition of surfactants will all favor the production of smaller droplets in the system [28]

In **vibrating ME** (Figure 5.1) the membrane is immersed into a beaker containing the continuous phase and filled inside with the dispersed phase [29]. The pressure is given to the inside of the membrane by using a pump while frequency and amplitude of the oscillation of the membrane was generated by an electrically driven vertical oscillator.

The membrane oscillates in a direction normal to the flow of the injection phase through the membrane. Rotating and vibrating ME methods are suitable for fragile and structured particles, in which the droplets and/or particles could be subject to breakage during the pump circulation or continuous phase stirring. They can be potentially used for large scale production and continuous operation, however they have a complicated and more expensive design and the energy consumption is high when the membrane area is increased.

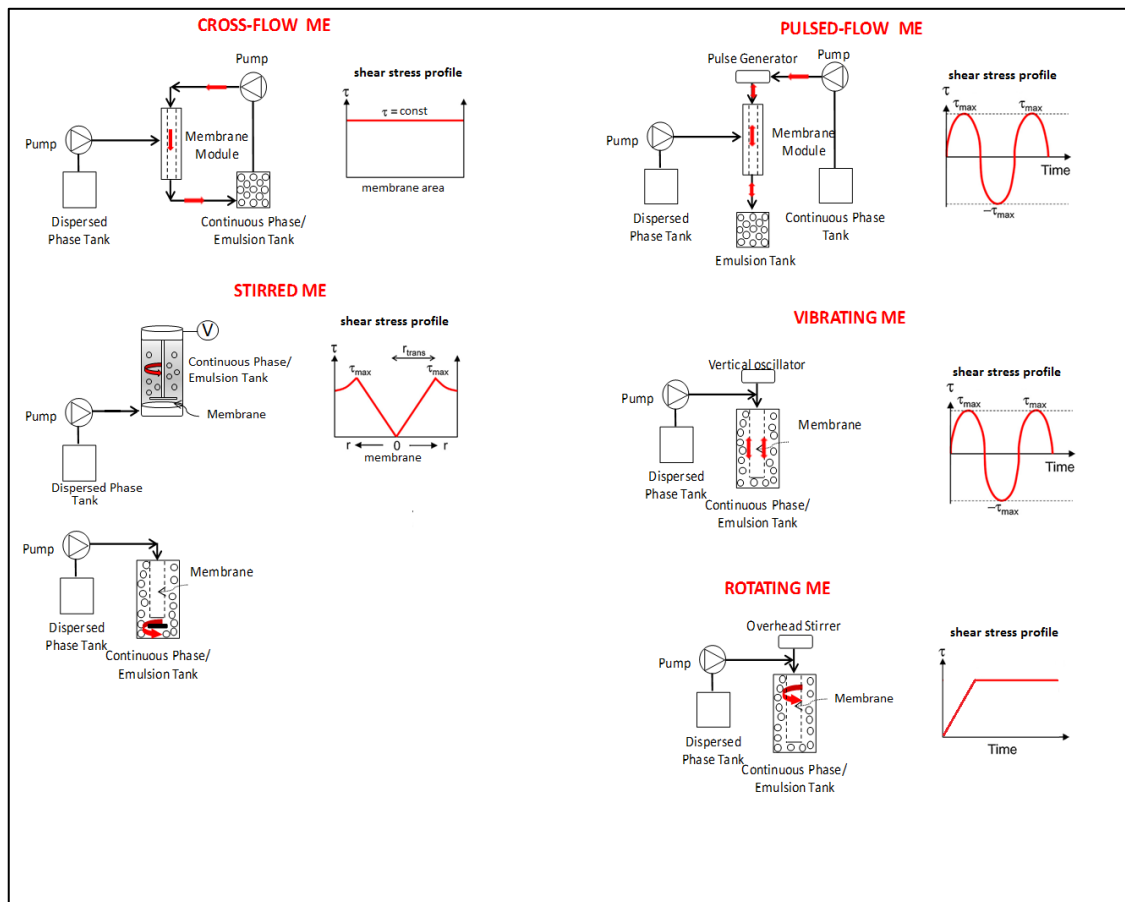


Figure 5.1. Membrane emulsification devices. (This figure was published in *Smart Membranes and Sensors: Synthesis, Characterization, and Applications*, John Wiley & Sons, 2014).

## 7. Static membrane emulsification principles and devices

The generation of a surface shear is the most conventional way to control droplet detachment in membrane emulsification. However, a regular and uniform droplet formation can be achieved even without any surface shear, by selecting appropriate parameters. It may happen if there is a large number of drops at the membrane surface and the drop diameter is bigger than the distance between the pores, so that the drops push each other at the membrane surface. This droplet formation mechanism is known as “push-to-detach”, and it occurs when a critical injection rate is exceeded and all of the membrane pores become active. In this condition, droplet formation at one pore is affected by the presence of other droplets forming at adjacent pores and uniform droplets can be produced. The push-off force is connected with some collective motion

of the drops when, ideally, all the pores on the membrane surface are working. In one limiting case, when only few pores are active and the distance between those pores is bigger than the size of the drops, the push-off force is zero and final drop size is defined only by an equilibrium of buoyancy and capillary forces. At increasing injection rate, more and more pores will be activated and the push-off force becomes significant [30]. Another example of ME carried out also in quiescent condition is **premix ME** in which droplets of a coarse pre-emulsion are disrupted by the flow of the emulsion through the porous structure of the membrane. The device used for this process is composed by a vessel above the membrane for the coarse emulsion which is pressed through the pores of the membrane under applied pressure. The fine emulsion is collected in a vessel below the membrane [31]. The dispersed phase droplets start accumulating before the membrane and inside the channels. These accumulating droplets can influence each other and thus induces break-up. Break-up in this case is strongly dependent on the interfacial properties: a stable emulsion will resist coalescence, and yield net steric break-up; a less stable emulsion may well coalesce. Repeated or multi-stage premix emulsification improves the uniformity and the permeate flux increases with increasing number of passes, most probably as a result of the decreased viscosity related to droplet size reduction. If the droplet size is similar to the pore size, it is expected to pass unhindered, and less pressure is required. The largest increase in flux takes place in the second pass as the largest droplet size reduction occurs in the first pass. However, the fouling of the membrane can occurred during pre-mix operation and the frequent membrane cleaning requirements may undermine the production rate from an industrial perspective [32].

## 8. Membrane emulsification applications in the pharmaceutical field

Drug delivery systems (DDSs) are one of the most rapidly advancing area of pharmaceutical science and technology. DDSs, such as multiple emulsions, micro/nano solid and polymer particles (sphere or capsules) can entrap drugs or biomolecules into their interior structures and/or absorb drugs or biomolecules onto their exterior surfaces. Small and uniform size are important requirements to control the distribution in the body and the interaction with living cells [33].

Membrane emulsification is an attractive process in this field because it is possible to prepare uniform particles with the required average size. This provides the possibility to investigate single property of the particles without interference from polydispersity of the particles [34]. Moreover, the low energy density of the process (energy input per cubic meter of emulsion produced, in the range of  $10^4$ - $10^6$  Jm<sup>-3</sup>) compared to the conventional mechanical methods ( $10^6$ - $10^8$  Jm<sup>-3</sup>) allows to preserve the quality and functionality of labile emulsions ingredients, such as biomolecules.[9] Indeed, in the conventional methods the high mechanical shear or the increase of the temperature have negative effects on the shear or temperature sensitive compounds. In this paragraph an overview of emulsions and particulate systems produced by membrane emulsification for pharmaceutical applications is given.



### 8.1. Emulsions

Multiple emulsions and micro/ nanoemulsions are of particular interest in the pharmaceutical field. The mild operating conditions of membrane emulsification are especially useful to prevent the rupture of the double emulsion during the second emulsification step. Among the first applications reported in literature there is the preparation of multiple emulsion for the treatment of liver cancer. Clinical studies showed that the multiple emulsions were effective in contracting the liver cancer when injected directly into the liver via the epatic artery.[35]

Nakajima et al.[36] presented a novel E/O/W (ethanol-oil-water) multiple emulsions prepared by membrane emulsification for the encapsulation of drugs that have low solubility in water and oil but are soluble in ethanol (such as polyphenols, taxol and validamycin).

Toorisaka et al. [37] proposed an S/O/W (solid-oil-water) dispersion for the oral administration of insulin prepared by premix ME. This formulation consists in a S/O (solid-in-oil) suspension containing surfactant coated insulin dispersed in soybean oil and then this suspension was mixed with water containing an hydrophilic surfactant. The coarse emulsion was then pressed through an SPG membrane to produce a monodispersed emulsion with mean droplet size of 1  $\mu\text{m}$ . The S/O/W dispersions showed an hypoglycemic activity for a long period after oral administration in rats, owing to the conversion of insulin into a lipophilic complex and the uniformity of the emulsion.

Vladisajevic et al. [38] prepared multiple W/O/W emulsions for drug delivery using repeated premix membrane emulsification. Uniform emulsion droplets were produced after 5 passages of the coarse emulsion through the membrane and the encapsulation efficiency of a drug model into the emulsion droplets was 84 %. The work demonstrated the high operation flexibility and suitability of repeated SPG membrane homogenization for controlled production of W/O/W emulsions with a high encapsulation efficiency at high production scales.

### 8.2. Solid particles: spheres, capsules and beads

Most of methods used for the preparation of solid particles (spheres, capsules, beads) include two main steps. The preparation of an emulsified system in the first step whereas the solidified particles are formed during the second step of the process. The first step is crucial to design particles with controlled size. During the last decade, progresses were mainly focused on the improvement of existing methods thanks to innovation of the emulsification methods. In this field, membrane emulsification received a great interest because it offers the possibility to manufacture size-controllable particles in mild conditions on a variety of scales . A variety of particulate products such as spheres, beads, capsules have been prepared in a micron range [10,13,34,39,40] by using membrane emulsification technology whereas few works are reported for the

preparation of particles in submicron range. The latters are obtained using membrane contactors or premix ME for the production of the emulsion and the formation of the solid particles is achieved by solvent extraction/evaporation, interfacial polymerization or cross-linking reaction [41–44]. Despite the numerous methods available to produce nanoparticles on a small scale, there are still problems to the establishment of large scale production methods. This is considered one of the reasons preventing the successful introduction of the nanoparticles to the clinic and the pharmaceutical market [45]. The main techniques used for the preparation of particulate systems using emulsification methods are summarized in Table 1.1

Table1.1 Common methodologies used for the preparation of particles from emulsions

| <b>Technique</b>                                     | <b>Procedure</b>  | <b>Particles produced using membrane emulsification</b>  |
|--|---|--|
| <b>emulsification-solvent extraction/evaporation</b> | <p>In this technique the polymer solution is emulsified in an aqueous phase to produce a simple O/W emulsion. Alternatively, it can also be used as oil phase for the preparation of simple W/O emulsion, which is emulsified again in an aqueous phase to produce a multiple W/O/W emulsion. The solvent is removed by extraction/evaporation where two mass flows took place: the solvent diffuses from the droplets into the external phase (solvent diffusion) and the solvent diffuses into the continuous phase and evaporates at the external phase/air interface (solvent evaporation). These two processes are correlated and the evaporation of the solvent cannot occur without a previous diffusion into the continuous phase. Volatile solvents, such as dichloromethane, chloroform, toluene were evaporated and the polymer solidified to form microspheres (from simple emulsion) or capsules (from double emulsion).</p> | <p>Poly-lactide (PLA) spheres and capsules [43, 46-48]</p> <p>Poly(lactide-co-glycolide) (PLGA) spheres and capsules [49,50]</p> |
| <b>emulsification-</b>                               | <p>This process is suitable for the production of spheres or capsules. In the first case, the dispersed phase (containing monomer, solvent and initiator) is emulsified into the</p>  | <p>Poly-N-isopropyl-</p>   |

|   |  |  |
|---|--|--|
| <b>direct polymerization</b>  | aqueous phase containing the emulsifier and stabilizing agent to form O/W emulsions. The polymerization is carried out in a second step by the activation of the initiator within the droplets. In the second case, a monomer is added in both the continuous and the dispersed phase and the polymerization occurs at the interface after the addition of the initiator into the emulsion. In this last case the process is also called “interfacial polymerization”  | acrylamide (PNIPAM) spheres and capsules<br>[50–52]  |
| <b>emulsification-droplet swelling</b>  | This process is particularly used for the preparation of particle with acrylate monomers using membrane emulsification process. The seed emulsion containing uniform droplets is prepared by membrane emulsification while the secondary small emulsion composed of hydrophilic monomers was obtained by conventional homogenization. Then, the two emulsions were mixed in order to absorb the hydrophilic monomers from the secondary emulsion on the seed emulsion droplets resulting in monodispersed swollen droplets. Solidified particles are obtained with a polymerization process of the swollen droplets. | Poly-styrene-co-divinyl-benzene (PS-DVB) particles [53]<br>polyimide prepolymer (PIP) particles [54]                                     |
| <b>emulsification-phase separation (coacervation, salting out, addition of non solvent)</b> | This process can be used for the preparation of spheres (from simple O/W or W/O emulsion) or capsules (from multiple emulsions). The term phase separation describes a process in which a polymer solution separates in two immiscible phases (a polymer rich phase and a polymer poor phase) after a perturbation of the equilibrium of the system. The latter can be carried out by: i) addition of a salt (salting out) into the polymer solution in order to induce a desolvation of the polymer that precipitates; ii) variation of pH to induce the phase separation of polymer solution                       | PLA microspheres [55]<br>Gelatin capsules with oil core [56]<br>Poly-ether-sulphone (PES) microspheres [57]<br>PCL and PLGA nanocapsules |

---

that have a water solubility pH dependent [44,58,59]  
or for ternary system to induce the  
electrostatic interaction between polymers  
with opposite charge (coacervation); iii)  
addition of third component (non solvent)  
into a polymer solution to induce the  
demixing of the polymer solution.

---

### 8.3. Liposomes and solid lipid particles

Liposomes are vesicular particles in a micro or submicro range composed of one or several bilayer membranes formed by polar lipids. Because of their structure, liposomes can entrap hydrophilic drugs in their internal aqueous compartment or lipophilic drugs within the lipid membrane. Due to their biocompatibility, biodegradability and low toxicity, potential applications of liposomes as pharmaceutical carriers for efficacy enhancement and toxicity reduction are well recognized [60].

Laouini et al. [61] produced multilamellar phospholipid vesicles with a mean size of 85 nm by injection of ethanolic phase (ethanol, phospholipid and cholesterol) through a microengineered membrane into aqueous phase using different membrane devices. Stirred cell was used at batch scale and cross-flow and oscillating system were tested to scale-up the production. The process developed in a stirred cell device was scaled-up by a factor of 8 with both systems. However, the oscillating membrane system, which avoids recirculation of the liposomes, was fully capable of maintaining the size and polydispersity of the liposomal nanoparticles during scale-up.

Solid lipid particles were prepared using high melting point lipid as the encapsulating material, followed by cooling of the preparation at room temperature. Solid lipid microparticles were produced by D'oria et al [62]. The lipid phase was pressed, at a temperature above the melting point of the lipid, through SPG membrane allowing the formation of small droplets. The aqueous phase circulates inside the membrane device, and sweeps away the droplets forming at the opening pore. The influence of the lipid phase, the pores size of SPG membranes and the lipid flux were investigated. The use of membrane emulsification allowed the production of uniform particles with a mean size between 50 and 750 nm and the high flux suggest the scaling-up of this process could be possible for industrial applications.

### 8.4. Sensing stimuli-responsive particles

Sensing particles are a rapidly developing class of stimuli-responsive systems that find applications in drug delivery system, catalysis, and sensor. They include micro-nano-emulsions, capsules or spheres and micelles able to sense and respond directly to environmental conditions. They are of considerable interest in applications such as bioactive compounds preservation, fragrance release and drug delivery. Micro- and nanostructure sensing systems can maximize the efficacy of therapeutic treatments because they have the ability to detect and respond to disease states directly at the site,

without compromise physiologically healthy cells and tissues and thereby reducing the side effects. pH-sensitive quaternized chitosan microspheres were prepared by combining membrane emulsification technique and thermal-gelation method [63]. The influence of process conditions on the property of prepared microspheres was investigated and the optimized preparation condition was obtained. The microspheres had porous structure and showed apparent pH-sensitivity by dissolving rapidly in acid solution (pH 5) and kept stable in neutral solution (pH 7.4). The pH-sensitivity of microspheres was demonstrated to influence the release of bovine serum albumin (BSA) used as a model drug and BSA was released rapidly in acid solution and slowly in neutral medium. Chitosan has been also used by Vladislavljević et al.[64] in the electrostatic deposition method to modify interfacial characteristics of uniformly sized droplets produced by premix membrane emulsification. The interfacial properties of emulsion droplets can be changed by using surfactant-displacement and/or electrostatic deposition methods. The surfactant-displacement method simply involves mixing a preformed emulsion with an emulsifier solution so that the original emulsifier is partially or fully displaced from the droplet surfaces by the new emulsifier. The electrostatic deposition technique involves depositing polyelectrolytes onto oppositely charged droplet surfaces. This technique offers a promising way to improve the stability of emulsions against environmental stresses such as pH, ionic strength, freezing, and heating. Lipophilic active components can be encapsulated within the oil droplets, whereas charged hydrophilic components can be incorporated within the interfacial layers. Potentially, active ingredients can be released at the site of action in response to a specific environmental stimulus.

Laouini et al.[65] produced pH-sensitive micelles for targeted drug delivery using a novel membrane contactor method. In this work the organic phase containing a copolymer composed of hydrophilic poly(ethylene)glycol (PEG) and hydrophobic polycaprolactone (PCL) and a volatile solvent was split into numerous microscopic sub streams by injection through the membrane and mixed with an agitated aqueous phase. A precise control over the micelle size in a range of 92 and 165 nm and size distribution of 0.09 was achieved by controlling the pore size and interpore distance of the membrane. The responsive pH property of the micelles was due to the hydrolysis of the ester bonds in the PCL block at acidic pH. Since vitamin E (the hydrophobic drug model) was predominantly encapsulated within the hydrophobic core, hydrolytic degradation of hydrophobic PCL segments allowed the release of vitamin E. A proportional decrease in the drug encapsulation efficiency with the decrease of the medium acidity was observed. Another kind of pH sensitive particles produced with membrane contactor method was proposed by Sheibat-Othman et al. [66]. A polymer with a solubility pH dependent (Eudragit) was dissolved in water at a set pH and then injected through the pores of a membrane into a continuous phase of a different pH in order to induce the precipitation of the polymer within the droplet at the pore level. In this way the use of organic solvent was avoided. This method can be useful in order to predict and control the particle size by manipulating the viscosity of the dispersed phase (by controlling the temperature or the concentration of polymer) and the velocity of the

tangential flow rate. These particles could be potentially used for the encapsulation of active compounds.

Another interesting application of membrane emulsification was the realization of a glucose-sensitive multiple emulsion W1/O/W2 proposed by Piacentini et al. [67] to delivery insulin in diabetic patients. The system is able to control the release of insulin depending on the glucose concentration present in the external environment. Concavalin A, a glucose-binding protein, was selected as biomolecule-sensor and was used as surfactant that promotes the release of bioactive molecule added in the W1 dispersed phase when glucose is added in the W2 aqueous phase. J. Ma et al.[68], used membrane emulsification coupled with internal gelation for the preparation of Ca-alginate gel beads with small and uniform size. Alginate has several unique properties that have enabled it to be used as a matrix for the entrapment and /or delivery of a variety of biological agents. Thanks to its bioadhesive properties and non-immunogenicity it can be advantageous for the site specific delivery to mucosal tissues and as protein delivery system. Fluorescent chitosan microspheres were produce combining membrane emulsification method and cross-linking reaction [69]. Chitosan microspheres were found to exhibit fluorescent properties without conjugation to any fluorescent agent. The fluorescence color varied with different crosslinkers and can be modulated by further chemical reduction, whereas the fluorescence intensity can be controlled by tuning the particle size and degree of crosslinking. The chitosan microspheres were studied as photo stable tracers to study the phagocytosis of Human hepatocellular carcinoma cells (HepG2).

## 9. Conclusions

There is an increasing use of membrane emulsification technology in the preparation of particles for pharmaceutical applications as demonstrated by literature data during the last years. Results demonstrated that particles produced by membrane emulsification are able to combine the structural properties such as size, size distribution and chemical compositions with the functional activity properly designed for specific applications. The operational flexibility, reproducibility, straightforward up-scaling of membrane based methods may lead to novel process intensification in particles production. A robust research was focused on the production of emulsions and particles in a micron range (10-100  $\mu\text{m}$ ) while the production of particles and emulsions in a submicron range ( $< 1\mu\text{m}$ ) is still at exploratory level.

Comparing to the conventional emulsification processes, membrane emulsification allowed to obtain a better control of particle size and size distribution at low energy material and consumption but the productivity is still low, so further studies are necessary to maximize the process throughput in order to promote its applicability at an industrial level. Challenges in this direction include the design of innovative intensified manufacturing processes and developing membrane with specific properties in terms of structure for the application in emulsification process. Cross-flow ME and premix ME are the membrane-based processes generally used for particle preparation at large scale,

however the droplet breakage or damage of shear sensitive materials still needs to be solved. The development of preparation methodologies that allow the incorporation of biomolecules without affecting their activity is of crucial importance in order to preserve their bioactivity.

### *References*

1. Nakashima T, Shimizu M, Kukizaki M. Particle control of emulsion by membrane emulsification and its applications. *Adv Drug Deliv Rev.* 2000;45(1):47–56.
2. Paul Becher. *Emulsions: Theory and Practice* 2nd Ed. 1965.
3. Pieter Walstra. Principles of emulsion formation. *Chem Eng Sci.* 1993;48(2):333–49.
4. Maa Y, Hsu C. controlled release Liquid-liquid emulsification by rotor / stator homogenization. 1996;38:219–28.
5. Schultz S, Wagner G, Urban K, Ulrich J. High-Pressure Homogenization as a Process for Emulsion Formation. *Chem Eng Technol.* 2004;27(4):361–8.
6. Abismail B, Canselier JP, Wilhelm a M, Delmas H, Gourdon C. Emulsification by ultrasound: drop size distribution and stability. *Ultrason Sonochem.* 1999;6(1-2):75–83.
7. Susuki K., Fujiki I ., Hagura Y. Characteristics of the Membrane Emulsification Method Combined with Preliminary Emulsification for Preparing Corn Oil-in-Water Emulsions. *Food Sci Technol.* 1996;2(1):43–7.
8. Nazir A, Schroën K, Boom R. Premix emulsification: A review. *J Memb Sci;* 2010;362(1-2):1–11.
9. Giorno L, Luca G De, Figoli A, Piacentini E, Drioli E. *Membrane Emulsification : Principles and Applications.* Wiley. 2009;463–94.
10. Charcosset C. *Membrane Processes in Biotechnologies and Pharmaceutics.* Elsevier, 2012.
11. Spyropoulos F, Lloyd DM, Hancocks RD, Pawlik AK. Advances in membrane emulsification. Part B: recent developments in modelling and scale-up approaches. *J Sci Food Agric.* 2014;94(4):628–38.

12. Pathak M. Numerical simulation of membrane emulsification: Effect of flow properties in the transition from dripping to jetting. *J Memb Sci.* 2011;382(1-2):166–76.
13. Charcosset C. Preparation of emulsions and particles by membrane emulsification for the food processing industry. *J Food Eng.* 2009 ;92(3):241–9.
14. Schro V. Production of emulsions using microporous , ceramic membranes. 1999;152:103–9.
15. Susuki K., Fujiki I ., Hagura Y. Departmen. Preparation of Corn Oil/Water and Water/CornOil Emulsions Using PTFE. *Food Sci Technol.* 1998;4(2):164–7.
16. Stillwell MT, Holdich RG, Kosvintsev SR, Gasparini G, Cumming IW. Stirred Cell Membrane Emulsification and Factors Influencing Dispersion Drop Size and Uniformity. *Ind Eng Chem Res.* 2007 ;46(3):965–72.
17. Geerken MJ, Lammertink RGH, Wessling M. Interfacial aspects of water drop formation at micro-engineered orifices. *J Colloid Interface Sci.* 2007;312(2):460–9.
18. Joscelyne SM, Trägårdh G. Membrane emulsification: a literature review. 2000;169(1999):107–17.
19. Katoh R, Asano Y, Furuya A, Sotoyama K, Tomita M. Preparation of food emulsions using a membrane emulsification system. *J Memb Sci.* 1996;113:131–5.
20. Abrahamse a. J, van Lierop R, van der Sman RGM, van der Padt A, Boom RM. Analysis of droplet formation and interactions during cross-flow membrane emulsification. *J Memb Sci.* 2002 ;204(1-2):125–37.
21. Schro V. Effect of Dynamic Interfacial Tension on the Emulsification Process Using Microporous , Ceramic Membranes. 1998;340(202):334–40.
22. Vladislavljevic G. Influence of process parameters on droplet size distribution in SPG membrane emulsification and stability of prepared emulsion droplets. *J Memb Sci.* 2003;225(1-2):15–23.
23. Geerken MJ, Lammertink RGH, Wessling M. Interfacial aspects of water drop formation at micro-engineered orifices. *J Colloid Interface Sci.* 2007;312(2):460–9.



- 
24. Vladisavljević GT, Schubert H. Preparation of Emulsions with a Narrow Particle Size Distribution Using Microporous  $\alpha$ -Alumina Membranes. *J Dispers Sci Technol.* 2003;24(6):811–9.
  25. Kobayashi I, Nakajima M, Mukataka S. Preparation characteristics of oil-in-water emulsions using differently charged surfactants in straight-through microchannel emulsification. *Colloids Surfaces A Physicochem Eng Asp.* 2000;229(1-3):33–41.
  26. Kobayashi I, Nakajima M, Mukataka S. Preparation characteristics of oil-in-water emulsions using differently charged surfactants in straight-through microchannel emulsification. *Colloids Surfaces A Physicochem Eng Asp.* 2003;229(1-3):33–41.
  27. Peng SJ, Fellow RAW. Controlled production of emulsion using a crossflow membrane. Part I: Droplet Formation from a Single Pore. *Inst Chem Eng.* 1998;76.
  28. Vladisavljević GT, Williams R a. Manufacture of large uniform droplets using rotating membrane emulsification. *J Colloid Interface Sci.* 2006;299(1):396–402.
  29. Holdich RG, Dragosavac MM, Vladisavljevic GT. Membrane Emulsification with Oscillating and Stationary Membranes. *Ind Eng Chem Res.* 2010;3810–7.
  30. Kosvintsev SR, Gasparini G, Holdich RG. Membrane emulsification: Droplet size and uniformity in the absence of surface shear. *J Memb Sci.* 2008;313(1-2):182–9.
  31. Lambrich U, Schubert H. Emulsification using microporous systems. *J Memb Sci.* 2005;257(1-2):76–84.
  32. Nazir A, Schroën K, Boom R. Premix emulsification: A review. *J Memb Sci.* 2010;362(1-2):1–11.
  33. Koo OM, Rubinstein I, Onyuksel H. Role of nanotechnology in targeted drug delivery and imaging: a concise review. *Nanomedicine.* 2005;1(3):193–212.
  34. Wu J, Fan Q, Xia Y, Ma G. Uniform-sized particles in biomedical field prepared by membrane emulsification technique. *Chem Eng Sci.* 2014;
  35. Higashi S, Tabata N, Kondo KH, Maeda Y, Shimizu M, Nakashima T, et al. Size of lipid microdroplets effects results of hepatic arterial chemotherapy with an anticancer agent in water-in-oil-in-water emulsion to hepatocellular carcinoma. *J Pharmacol Exp Ther.* 1999;289(2):816–9.

36. Nakajima M. ( 12 ) United States Patent U . S . Patent. 2003;1(12):0–6.
37. Toorisaka E. Hypoglycemic effect of surfactant-coated insulin solubilized in a novel solid-in-oil-in-water (S/O/W) emulsion. *Int J Pharm* . 2003;252(1-2):271–4.
38. Vladislavljević GT, Shimizu M, Nakashima T. Production of multiple emulsions for drug delivery systems by repeated SPG membrane homogenization: Influence of mean pore size, interfacial tension and continuous phase viscosity. *J Memb Sci*. 2006;284(1-2):373–83.
39. Vladislavljević GT, Williams R a. Recent developments in manufacturing emulsions and particulate products using membranes. *Adv Colloid Interface Sci*. 2005;113(1):1–20.
40. Liu W, Yang X-L, Ho WSW. Preparation of uniform-sized multiple emulsions and micro/nano particulates for drug delivery by membrane emulsification. *J Pharm Sci*. 2011;100(1):75–93.
41. Lv P, Wei W, Gong F, Zhang Y, Zhao H, Lei J, et al. Preparation of Uniformly Sized Chitosan Nanospheres by a Premix Membrane. *Ind. Eng. Che. Res.*2009;8819–28.
42. Charcosset C, El-Harati A, Fessi H. Preparation of solid lipid nanoparticles using a membrane contactor. *J Control Release* . 2005;108(1):112–20.
43. Wei Q, Wei W, Lai B, Wang L-Y, Wang Y-X, Su Z-G, et al. Uniform-sized PLA nanoparticles: preparation by premix membrane emulsification. *Int J Pharm* . 2008;359(1-2):294–7.
44. Charcosset C, Fessi H. Preparation of nanoparticles with a membrane contactor. *J Memb Sci*. 2005;266(1-2):115–20.
45. Vauthier C, Bouchemal K. Methods for the preparation and manufacture of polymeric nanoparticles. *Pharm Res*. 2009;26(5):1025–58.
46. Liu R, Ma G, Meng F-T, Su Z-G. Preparation of uniform-sized PLA microcapsules by combining Shirasu porous glass membrane emulsification technique and multiple emulsion-solvent evaporation method. *J Control Release* . 2005 ;103(1):31–43.
47. Gasparini G, Kosvintsev SR, Stillwell MT, Holdich RG. Preparation and characterization of PLGA particles for subcutaneous controlled drug release by membrane emulsification. *Colloids Surf B Biointerfaces*. 2008;61(2):199–207.

48. Ito F, Makino K. Preparation and properties of monodispersed rifampicin-loaded poly(lactide-co-glycolide) microspheres. *Colloids Surf B Biointerfaces*. 2004;39(1-2):17–21.
49. Liu R, Huang S-S, Wan Y-H, Ma G-H, Su Z-G. Preparation of insulin-loaded PLA/PLGA microcapsules by a novel membrane emulsification method and its release in vitro. *Colloids Surf B Biointerfaces*. 2006;51(1):30–8.
50. Cheng C-J, Chu L-Y, Zhang J, Zhou M-Y, Xie R. Preparation of monodisperse poly(N-isopropylacrylamide) microspheres and microcapsules via Shirasuporous-glass membrane emulsification. *Desalination*. 2008 ;234(1-3):184–94.
51. Cheng C-J, Chu L-Y, Zhang J, Zhou M-Y, Xie R. Preparation of monodisperse poly(N-isopropylacrylamide) microspheres and microcapsules via Shirasuporous-glass membrane emulsification. *Desalination*. 2008;234(1-3):184–94.
52. Ma G, Sone H, Omi S. Preparation of Uniform-Sized Polystyrene - Polyacrylamide Composite Microspheres from a W / O / W Emulsion by Membrane Emulsification Technique and Subsequent Suspension Polymerization. *Macromolecules*.2004;2954–64.
53. Omi S, Taguchi T, Nagai M, Ma G. Synthesis of 100 nm Uniform Porous Spheres by SPG Emulsification with Subsequent Swelling of the Droplets. *J Polym Sci*.1996;63:931-942
54. U So, Matsuda A, Imamura K, Nagai M, Ma G. Synthesis of monodisperse polymeric microspheres including polyimide prepolymer by using SPG emulsification technique. *Colloids Surfaces A Physicochem Eng Asp*. 1999;153:373–381.
55. Sawalha H, Purwanti N, Rinzema A, Schroën K, Boom R. Polylactide microspheres prepared by premix membrane emulsification—Effects of solvent removal rate. *J Memb Sci*. 2008;310(1-2):484–93.
56. Piacentini E, Giorno L, Dragosavac MM, Vladislavljević GT, Holdich RG. Microencapsulation of oil droplets using cold water fish gelatine/gum arabic complex coacervation by membrane emulsification. *Food Res Int*. 2013;53(1):362–72.
57. Piacentini E, Lakshmi DS, Figoli A, Drioli E, Giorno L. Polymeric microspheres preparation by membrane emulsification-phase separation induced process Open pores. 2013;448:190–7.
58. Khayata N, Abdelwahed W, Chehna MF, Charcosset C, Fessi H. Preparation of vitamin E loaded nanocapsules by the nanoprecipitation method: from laboratory

- scale to large scale using a membrane contactor. *Int J Pharm*; 2012;423(2):419–27.
59. Limayem Blouza I, Charcosset C, Sfar S, Fessi H. Preparation and characterization of spironolactone-loaded nanocapsules for paediatric use. *Int J Pharm*. 2006;325(1-2):124–31.
  60. Lian T, Ho RJ. Trends and developments in liposome drug delivery systems. *J Pharm Sci*. 2001;90(6):667–80.
  61. Laouini A, Charcosset C, Fessi H, Holdich RG. Preparation of liposomes: A novel application of microengineered membranes – From laboratory scale to large scale. *Colloids Surf B Biointerfaces*. 2013;112:272–8.
  62. D'oria C, Charcosset C, Barresi A a., Fessi H. Preparation of solid lipid particles by membrane emulsification—Influence of process parameters. *Colloids Surfaces A Physicochem Eng Asp*. 2009;338(1-3):114–8.
  63. Wu J, Wei W, Wang L-Y, Su Z-G, Ma G-H. Preparation of uniform-sized pH-sensitive quaternized chitosan microsphere by combining membrane emulsification technique and thermal-gelation method. *Colloids Surf B Biointerfaces*. 2008;63(2):164–75.
  64. Vladislavljević GT, McClements DJ. Modification of interfacial characteristics of monodisperse droplets produced using membrane emulsification by surfactant displacement and/or polyelectrolyte electrostatic deposition. *Colloids Surfaces A Physicochem Eng Asp*. 2010;364(1-3):123–31.
  65. Laouini A, Koutroumanis KP, Charcosset C, Georgiadou S, Fessi H, Holdich RG, et al. pH-sensitive micelles for targeted drug delivery prepared using a novel membrane contactor method. *ACS Appl Mater Interfaces*. 2013;5(18):8939–47.
  66. Sheibat-Othman N, Burne T, Charcosset C, Fessi H. Preparation of pH-sensitive particles by membrane contactor. *Colloids Surfaces A Physicochem Eng Asp*. 2008;315(1-3):13–22.
  67. Piacentini E, Drioli E, Giorno L. Preparation of stimulus responsive multiple emulsions by membrane emulsification using con a as biochemical sensor. *Biotechnol Bioeng*. 2011;108(4):913–23.
  68. Liu XD, Bao DC, Xue WM, Xiong Y, Yu WT, Yu XJ, et al. Preparation of Uniform Calcium Alginate Gel Beads by Membrane Emulsification Coupled with Internal Gelation. *J Appl Polymer Sci* 2003;87:848-852.

69. Wei W, Wang L-Y, Yuan L, Wei Q, Yang X-D, Su Z-G, et al. Preparation and Application of Novel Microspheres Possessing Autofluorescent Properties. *Adv Funct Mater.* 2007;17(16):3153–8.

## CHAPTER 2

### **Membrane with tailored wettability property to improve emulsion productivity and efficiency**

#### **1. Introduction**

Emulsions with tailored microstructure in terms of droplet size and size distribution are required for the high quality of the product respect to the stability and functionality. Membrane emulsification has attracted academic and industrial interests as alternative method to produce emulsion-based products in mild conditions by a drop-by-drop mechanism [1–3]. However, the production of emulsions with narrow droplet size distribution at high productivity is still a challenge in membrane emulsification. The interaction between the dispersed phase and the membrane pore wall is a significant factor for the productivity enhancement. The membrane pore wall with good wettability to the dispersed phase allows a fast permeation of the phase in the pores, and hence results in significant higher productivity. However, membranes with high interfacial tension are necessary to avoid the wetting of the membrane by the phase to be dispersed and as a consequence to obtain emulsion with controlled size and size distribution. This means that low dispersed phase flux values are usually obtained resulting in low productivity. Kawakatsu et al. [4] demonstrated that monodispersed droplets were produced when the contact angle of water droplet on microchannel plate in an oil phase was greater than  $120^\circ$ , whereas Kobayashi et al [5] obtained monodispersed O/W emulsions when the contact angle of oil droplet on microchannel plate in water phase was greater than  $138^\circ$ . The contact angle measured between the dispersed phase and the membrane wetted by the continuous phase is strictly connected to the properties of emulsifier used in emulsion preparation. The affinity of the emulsifier for the membrane surface further influenced droplet formation because the contact angle could be decreased by the interaction between emulsifier and membrane (such as charged emulsifier and oppositely charged membrane) resulting in a failed droplet size control. Low dispersed phase flux was usually achieved when membranes unwetted by the dispersed phase are used. Typical values of dispersed phase flux are reported in Table 1. So far, the problem to obtain controlled droplets size at high dispersed phase flux has not been overcome. Katoh et al. [6] suggested to pre-treat a hydrophilic membrane by soaking in the oil phase to render it hydrophobic and to increase the dispersed phase flux. However, the membrane surface wettability modification was not permanent and the dispersed phase could wet the membrane pores during the emulsification process. Some additional strategies have been studied to increase the productivity in membrane emulsification such as the use of membranes with: i) thin active layer to decrease the flow resistance [7]; ii) different pore shape and orientation to promote the unbalanced interfacial tension [8,9]. Q. Yuan et al.[10] demonstrated that hybrid hydrophilic

membranes were suitable for the preparation of O/W emulsion when the pore wall affinity for the dispersed phase was increased. The use of one miscible alcohol combined with viscous oil increased the dispersed phase flux as a consequence of the increased wettability of the dispersed phase on the pore wall.

Table 1.2. Typical dispersed phase flux membrane obtained during membrane emulsification method

| Membrane                | Wettability | Membrane pore [ $\mu\text{m}$ ] | Emulsion Type | Disperse phase flux [ $\text{L h}^{-1} \text{m}^{-2}$ ] | References |
|-------------------------|-------------|---------------------------------|---------------|---|------------|
| SPG                     | Hydrophilic | 0.2                             | o/w           | 5 - 15  | [11]       |
| SPG                     | Hydrophilic | 0.5                             | o/w           | 10 - 45   | [11]       |
| $\text{Al}_2\text{O}_3$ | Hydrophilic | 0.2                             | o/w           | 1.5 - 21  | [12]       |
| $\text{Al}_2\text{O}_3$ | Hydrophilic | 0.5                             | o/w           | 4.7 - 47  | [12]       |
| SPG                     | Hydrophilic | 0.5                             | w/o           | 200   | [13]       |
|                         | pretreated  |                                 |               |   |            |
| SPG                     | Hydrophilic | 1.0                             | w/o           | 2300  | [13]       |
|                         | pretreated  |                                 |               |   |            |
| SPG                     | Hydrophobic | 0.4                             | w/o           | 1.5   | [14]       |
| Propylene               | Hydrophobic | 0.4                             | w/o           | 0.05 - 0.2  | [15]       |

In this study, the use of a membrane with asymmetric properties in terms of wettability between external and internal side was tested in the preparation of W/O emulsions as a method to increase dispersed phase flux and process productivity. W/O emulsions were prepared using hydrophilic SPG membranes immersed or pre-soaked in the continuous phase in order to render the membrane non-wetted by the dispersed phase [6]. Comparing with the preparation of W/O emulsions using a hydrophobic membrane, the dispersed phase flux was 100 time higher using an hydrophilic membrane pre-treated by immersion in the oil phase. The wettability of the membrane surface to the water phase was decreased and the interfacial tension between the dispersed phase and the membrane wetted with the continuous phase was increased in order to promote the controlled droplets production. However, the membrane wettability properties are expected to be not permanent but they can be modified over time as soon as the dispersed phase was extruded through the membrane pores. An alternative strategy was proposed by Jing et al.[16] to obtain W/O emulsions by using hydrophilic ceramic membrane. A cationic surfactant was introduced in the dispersed phase and the interaction between hydroxyl groups of the membrane and the charged head of the surfactant led to a decrease of hydrophilicity of the membrane. In the present work, the membrane wettability modification was obtained by hydrophobic protein adsorption on the lumen side of the hydrophilic membrane where droplets are generated. The final aim was to obtain a membrane with hydrophobic surface at the opening pore and hydrophilic properties at the membrane pore wall. The hydrophilic pore allowed a faster permeation of water resulting in higher dispersed phase flux. The hydrophobic part is introduced by the adsorbed protein layer that avoided the spread of water phase over the

membrane resulting in a better control of the emulsion quality. The method is expected to significantly improve the emulsification productivity maintaining the control of droplet size and uniformity.

## 2. Experimental section

### 2.1. Chemicals

Lipase from *Candida Rugosa*, type VII, containing 1 g protein/5.88 g powder and 1.180 units  $\text{mg}^{-1}$  of solid (purchased from Sigma–Aldrich) and Bovine Serum Albumin (BSA, purchased from Sigma–Aldrich) were used to functionalize the lumen side of the ceramic membrane. Since Lipase solution was not pure, a preliminary centrifugation at 3000 rpm for 15 min of the initial protein solution was made and the supernatant recovered was used. After centrifugation, the protein concentration was  $1 \text{ g l}^{-1}$  as estimated by BCA protein assay. Sodium dihydrogen phosphate anhydrous ( $\text{NaH}_2\text{PO}_4$ ) and disodium hydrogen phosphate anhydrous ( $\text{Na}_2\text{HPO}_4$ ) were used to prepare phosphate buffer solution at pH 7.0. Isooctane containing 2 wt% of sorbitan mono-oleate (Span 80) or 4 wt% of hexaglycerol penta-oleate (SY-Glyster PO-5S) was used as the continuous phase. Ultrapure water (USF Elsa, model Purelab Classic PL5221) with a resistivity of 18.2 MVcm was used as dispersed phase and for the preparation of all the aqueous solutions. NaOH, NaOCl (purchased from Carlo Erba) were used for the preparation of the cleaning solutions. BCA protein assay (Sigma Aldrich) was used to evaluate protein solutions concentration (see Appendix 1).

### 2.2. Membranes and Membrane Cleaning Procedure

A flat-sheet polyethersulphone (PES) membrane (NADIR, Germany) with a molecular cut-off of 150 kDa (~60 nm), a thickness between 210-250  $\mu\text{m}$  and a membrane area of 17.3  $\text{cm}^2$  was selected to evaluate the effect of lipase adsorption on membrane wetting properties. Lipase was then adsorbed on tubular ceramic membrane (Membrflow, Germany) which was used for the preparation of W/O emulsions. The membrane is a ceramic zirconia oxide ( $\text{ZrO}_2$ ) membrane with mean pore sizes of 50 nm, inner diameter of 7 mm, outer diameter of 10 mm and length of 100 mm. A multiple ceramic layer could be identified: i) a first layer with  $\alpha$ -alumina, pore size about 1 micron, layer thickness about 50 micron; ii) a second layer with  $\alpha$ -alumina, pore size about 200 micron, layer thickness about 50  $\mu\text{m}$  and iii) the active layer with  $\text{ZrO}_2$ , with layer thickness of 1-2 micron. The effective membrane area was 22  $\text{cm}^2$ .

After each experiment, the ceramic membrane was cleaned using a detergent solution obtained with 20 wt% of NaOH, 2.5 wt% of NaOCl and 77,5 wt% of water. In the first step, 3% wt of detergent solution was recirculated along the lumen side of the membrane for 30 min at 80°C. Subsequently, the detergent solution was permeated through the membrane pores and the trans-membrane pressure was increased from 0.2 to 0.6 bar. The membrane was then cleaned with the previous detergent solution for 30



min at 70°C in an ultrasonic bath and rinsed with distilled water. This procedure allowed a complete recovery of the initial water permeability of the ceramic membrane.

### 2.3. Experiments carried out and operative conditions

A preliminary study to evaluate protein adsorption on the membrane surface was carried out. Proteins with different structural properties, such as Lipase and BSA, were selected to evaluate protein adsorption effect on membrane permeability of polymeric and inorganic hydrophilic membranes. Ceramic membranes are suitable membranes to be used in membrane emulsification. They are very resistant to heat, pressure and solvents. Polymeric membranes in flat-sheet configuration was also used to study the adsorption and the subsequent surface modifications effects because a flat surface made up of the same ceramic material was not available. Physical-chemical analysis (such as contact angle) and functional studies (such as water permeability) have been carried out on poly-ethersulfone (PES) membrane. Tubular ceramic membrane un-modified and modified by protein adsorption were characterized by energy dispersive X-ray (EDX) and functional properties (such as water permeability) and then it was used for emulsion preparation. The type of experiments carried out for each membrane and the related surface analysis were summarized in Table 2.

Table 2.2 The type of experiments and the related surface carried for the tubular ceramic and flat sheet membrane used in the present work

| Membrane        | Experiment Type   |                |                      | Membrane surface analysis |               |
|-----------------|-------------------|----------------|----------------------|---------------------------|---------------|
|                 | Lipase Adsorption | BSA Adsorption | Emulsion preparation | EDX                       | Contact Angle |
| Tubular Ceramic | V                 | V              | V                    | V                         | -             |
| Flat-sheet PES  | V                 | -              | -                    | -                         | V             |

### 2.4. Protein adsorption

The membrane plant used for the experiments of protein adsorption is showed in Figure 1.2.

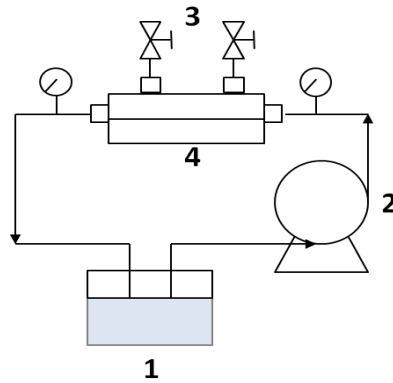


Figure 1.2 Schematic representation of the equipment used for protein adsorption: (1) bulk protein solution; (2) peristaltic pump; (3) purge valve; (4) membrane module

The protein solution was circulated along the lumen side of the membrane by using a peristaltic pump (Masterflex, Model 77310-01). Samples were collected from the protein solution after 5, 15, 30 and 45 minutes and analyzed by BCA protein assay in order to evaluate the protein content. After protein adsorption experiments, 30 ml of phosphate buffer solution were circulated at low flow rate for 5 min to remove the protein not stably adsorbed on the membrane. This procedure was repeated 3 times and a sample from each solution was also collected for further BCA protein assay. Two different protein types at a concentration of  $1 \text{ g l}^{-1}$  were used: Lipase from *Candida Rugosa* and Bovine Serum Albumin (BSA). The adsorbed protein amount ( $m_{ads}$ ) was calculated by mass balance according to Equation 1:

$$m_{ads} = m_i - (m_r + m_b) \quad (1)$$

where  $m_i$  is the initial mass of protein,  $m_r$  is the mass measured in the samples took from protein solution vessel (retentate) at different time and  $m_b$  is the mass of protein recovered in the buffer solution circulated after the protein adsorption experiments. The protein adsorbed percentage was calculated according to Equation 2:

$$m_{ads}\% = \frac{m_{ads}}{m_i} * 100 \quad (2)$$

The permeability reduction percentage ( $P_{red}$ ) was calculated according to Equation 3:

$$P_{red}\% = \frac{P_i - P_f}{P_i} * 100 \quad (3)$$

where  $P_i$  is the initial pure water permeability of the membrane and  $P_f$  is the pure water permeability measured after protein adsorption. Water permeability of unmodified and modified (by protein adsorption) ceramic membrane was measured in the pressure range of 0.2 and 0.6 bar. In all tests, water was fed to the membrane module in the lumen side and the permeation at 0.6 bar of water through the membrane was performed for a

period of 15 min before to start measurements of water flux in order to wet the membrane.

### 2.5. Membrane emulsification equipment and W/O emulsion preparation

Unmodified and modified (by protein adsorption) ceramic membrane were used to prepare W/O emulsions using cross-flow membrane emulsification method. The schematic representation of the emulsification plant is illustrated in Figure 2.2.

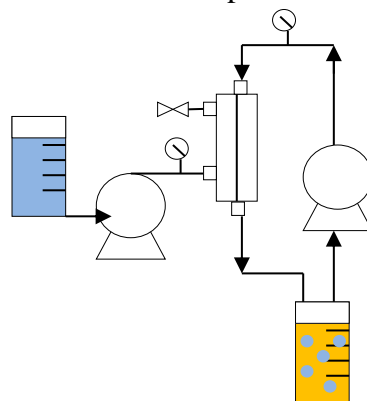


Figure 2.2 Cross-flow membrane emulsification equipment: (1) disperse phase graduated vessel; (2) micropump; (3) purge valve; (4) membrane module; (5) peristaltic pump; (6) continuous phase container

The dispersed phase was permeated through the membrane using a micropump (Ismatec, model C.P. 78016-30) with a flow rate of  $1.1 \text{ ml min}^{-1}$  that correspond to a dispersed phase flux of  $30 \pm 0.67 \text{ L h}^{-1} \text{ m}^{-2}$ . The continuous phase was circulated in the lumen side of the membrane using a peristaltic pump (Masterflex, Model 77310-01) with a flow rate of  $115.5 \text{ ml min}^{-1}$  that correspond to an axial velocity of  $0.05 \text{ m s}^{-1}$  and a shear stress of  $0.03 \text{ Pa}$ . The emulsification experiment was stopped when the dispersed phase content in the emulsion was 9% v/v.

### 2.6. Membrane surface analysis

PES membranes were characterized by contact angle measurement. The contact angle was measured by using a CAM 200 device (KSV Instruments, Ltd). The sessile drop of water was formed using a micro-syringe with automatic dispenser on the surface of PES membrane un-modified and modified by Lipase adsorption. The measurement was repeated three times with a precision of  $\pm 4^\circ$  and the respective mean value was calculated. The tubular configuration of ceramic membranes made unfeasible an accurate evaluation of water contact angle on modified and unmodified ceramic membranes. Ceramic membranes were fragmented, coated with gold and analyzed in a field emission scanning electron microscope (SEM) (Quanta FENG 200, FEI company) by using energy dispersive X-ray spectrometry (EDX) to evaluate membrane surface composition before and after Lipase adsorption.

### 2.7. Particle size analysis

Emulsion droplets were observed by optical microscopy and the image of the emulsions were analyzed with Scion Image software. The mean particle size was expressed as the surface weighted mean diameter (or Sauter diameter),  $D[3,2]$  and as the volume weighted mean diameter, (or De Brouckere diameter),  $D[4,3]$  Size distribution is expressed as Span number. The equations used to calculate the diameters and span are reported in the Appendix 1 of the thesis.

## 3. Results and Discussion

### 3.1. Effect of protein adsorption on membrane functionalities and surface properties

Two models of protein (Lipase from *Candida Rugosa* and BSA) were used to modify membrane surface properties. One of the most important characteristics of lipases is the activation at oil–water interface (interfacial activation) [17]. Data on 3D structure of lipases indicated that they are fairly hydrophilic and expose uncharged polar residues in aqueous solution. Their main hydrophobic area is located in the catalytic site that is activated in the presence of emulsion interface [18]. BSA chemical structure is basically composed of a low content of apolar aminoacids and a high content of charged aminoacids [19] and the most outstanding properties of BSA is the ability to interact with different type of ligands. In Figure 3.2 is illustrated the time profile of Lipase and BSA adsorption on ceramic and PES membranes, using an initial protein concentration of  $1 \text{ g L}^{-1}$ .

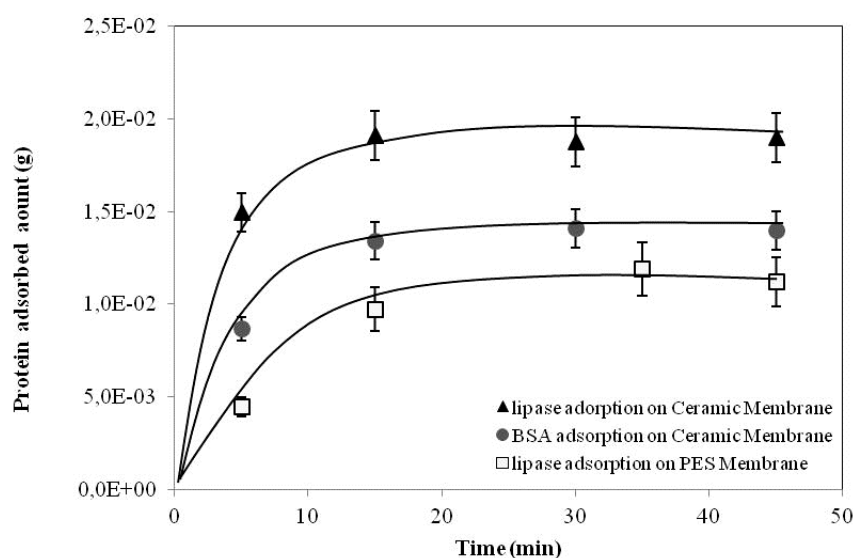


Figure 3.2 Proteins adsorption on the membrane surface over time

The adsorption equilibrium is reached after 30 min at this concentration value, as showed by the behaviour of isotherm adsorption. The behaviour of protein adsorption as

a function of time was monitored in order to obtain a membrane surface saturated with protein. The resulting time profiles were similar for both proteins (Lipase and BSA) and membranes (Ceramic and PES) studied. Water permeability reduction and protein adsorbed amount on ceramic membrane were reported in Table 3.2.

Table 3.2 Water permeability reduction and protein adsorbed amount on tubular ceramic and flat sheet membrane and experimental conditions used for protein adsorption experiments

| Membrane        | Protein | Experimental Conditions  | $m_{ads}$ (%) | Permeability reduction (%) |
|-----------------|---------|--|---------------|----------------------------|
| Tubular Ceramic | Lipase  | $V_{axial} = 0.58 \text{ m s}^{-1}$<br>Flow rate = 1340 ml<br>$\text{min}^{-1}$  | 0.79          | 83                         |
|                 | BSA     | Adsorption time: 45 min<br>No pressure applied   | 0.56          | 18                         |
| Flat-sheet PES  | Lipase  | $V_{axial} = 0.02 \text{ m s}^{-1}$<br>Flow rate = 300 ml<br>$\text{min}^{-1}$<br>Adsorption time: 45 min<br>No pressure applied | 0.65          | 58                         |

The difference in terms of total protein amount between Lipase and BSA was not significantly high and the protein adsorbed amount was 17.4 % and 12.4 % for Lipase and BSA, respectively. However, water permeability was significantly reduced after lipase adsorption. The permeability reduction was 83 % and 18 % for Lipase and BSA, respectively. Results indicated that physical-chemical properties of protein influenced also water permeability. Specific analysis were carried out in order to analyze the surface properties of lipase-loaded membrane. Figure 4.2 reported SEM/EDX analysis carried out on fragments of unmodified and lipase-loaded inorganic membrane.

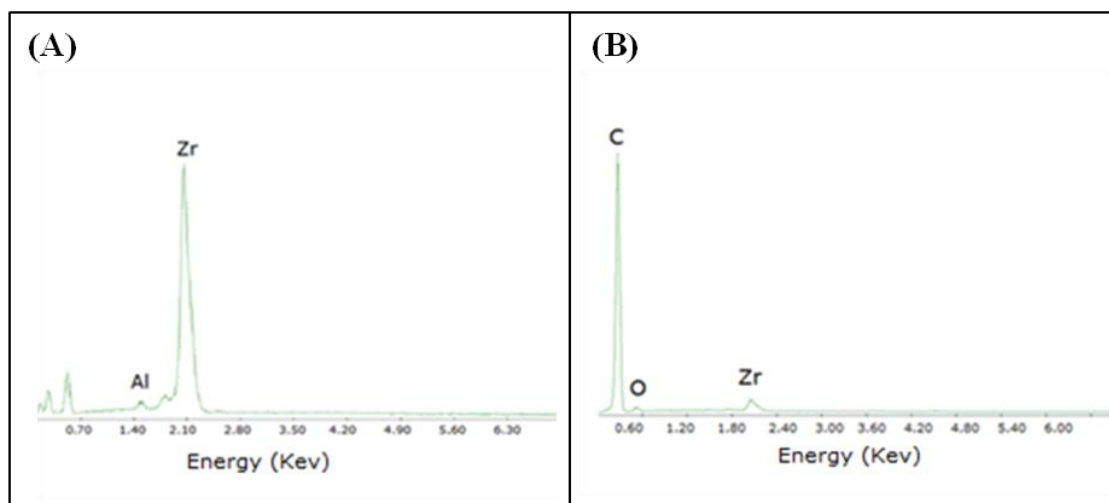


Figure 4.2 SEM/EDX analysis carried out on fragments of (A) unmodified and (B) lipase-loaded ceramic membrane

In the spectrum of lipase-loaded membrane, the peak of carbon, the most abundant element of peptide chains, had the major energy while the peak of zirconia was reduced at 4% indicating that most of the hydrophilic surface of the membrane was hidden by protein layers. Since the impossibility to have a flat surface composed of the same ceramic material, a flat-sheet PES membrane was used to evaluate the wettability properties of the membrane before and after lipase adsorption. PES membrane was selected considering that the measured contact angle was  $69^\circ \pm 4^\circ$  that was very similar to the value reported in literature for zirconia oxide membranes ( $71.8^\circ \pm 2^\circ$ ) [20]. Water permeability reduction of PES membrane after protein adsorption and the values of contact angle measured between water drop and membrane (unmodified and modified) were reported in Figure 5.2.

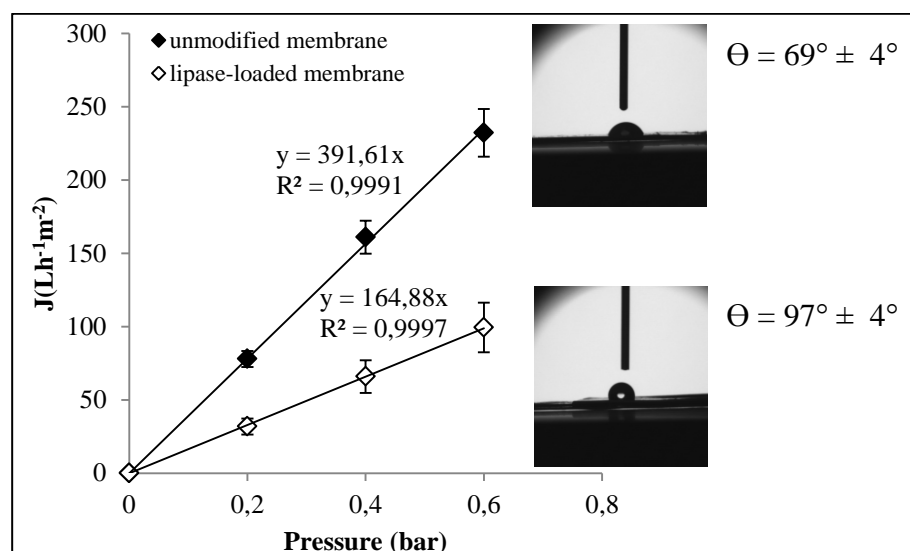


Figure 5.2 Water permeability reduction of PES membrane after lipase adsorption and the values of contact angle ( $\theta$ ) measured between water drop and unmodified and lipase-loaded membrane.

The permeability reduction was 58 % after lipase adsorption whereas the contact angle measured was  $97^\circ \pm 4^\circ$ . Results indicated that physical-chemical properties of protein influenced also water permeability. Although some reduction in pore size may occur, the significant influence on permeability reduction was due to hydrophobization, resulting in incomplete water penetration/air entrapment that determined a lower number of active pores. Indeed, the hydrophilic properties of the membrane pore wall allowed the easy penetration of water through the pores wall (compared with an hydrophobic membrane) even though the hydrophobic properties of the membrane lumen surface determined the incomplete water penetration. This determined that some pores were still non-active while the remaining pores were activated. The increased contact angle value could be explained considering the chemical structure of lipase characterized by uncharged polar and apolar residues that reduced the interaction with water molecules. The contact angle measurements confirmed that Lipase adsorption changed the surface wettability properties of the membrane by reducing its hydrophilicity. The higher permeability reduction of lipase-loaded inorganic membrane (83 %) compared with BSA-loaded inorganic membrane (18 %) could be correlated with the reduced hydrophilic properties of the ceramic membrane observed after Lipase adsorption in addition to the hydraulic resistance itself. Data suggested the possibility to use lipase as modifying agent to design a new membrane with asymmetric wettability profile: a hydrophilic thickness and hydrophobic surface suitable for the production of W/O emulsion by membrane emulsification where the membrane surface must not be wetted by the aqueous disperse phase.

### *3.2. Effect of the membrane surface properties on W/O emulsion preparation by membrane emulsification*

The use of membrane with asymmetric properties in terms of wettability between shell and lumen side was tested for the preparation of W/O emulsion as a method to increase dispersed phase flux (and process productivity). After lipase adsorption, the modified membrane was used to produce a W/O emulsion using Isooctane and Span 80 as continuous phase and ultrapure water as dispersed phase. Mean droplets size and size distribution and the photographs of W/O emulsions prepared by cross-flow membrane emulsification with un-modified and lipase-loaded membrane are shown in Figure 6.2.

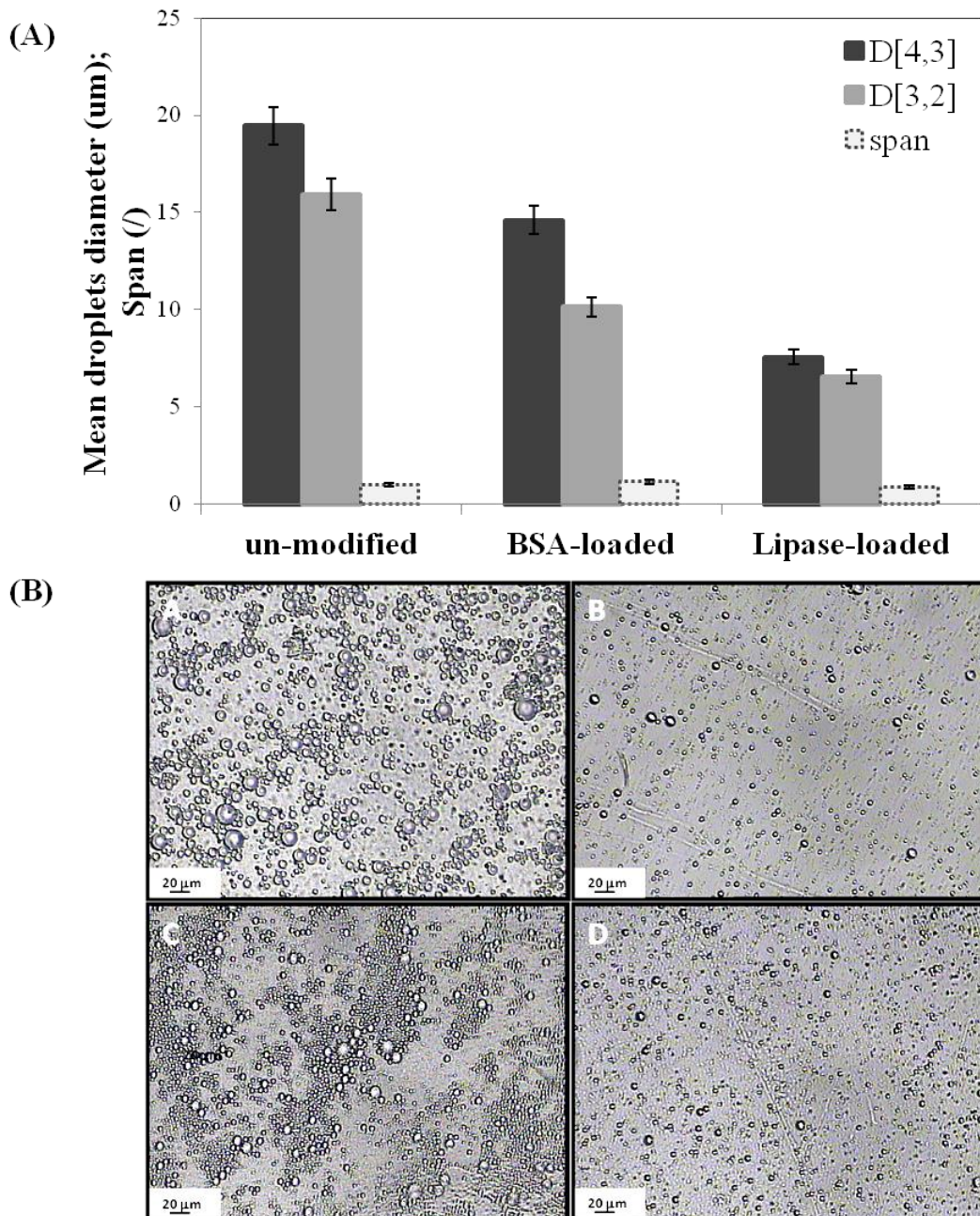


Figure 6.2 (A) Mean droplets size and droplet size distribution of W/O emulsions prepared by cross-flow membrane emulsification using un-modified and lipase-loaded membrane. (B) Microscope images of W/O emulsions prepared using (A) un-modified ceramic membrane (emulsifier: Span 80 2 wt%); (B) lipase-loaded ceramic membrane (emulsifier: Span 80 2 wt%); (C) BSA-loaded ceramic membrane (emulsifier: Span 80 2 wt%); (D) lipase-loaded ceramic membrane (emulsifier: SY-Glyster PO-5S 4 wt%). Experimental conditions: emulsifier: Span 80 2 wt%; dispersed phase flux:  $30 \pm 0.67 \text{ L h}^{-1} \text{ m}^{-2}$ ; continuous phase axial velocity:  $0.05 \text{ ms}^{-1}$ ; dispersed phase content 9 % (v/v)

The distinguishing feature of membrane emulsification is that droplets size is primarily controlled by membrane parameters. Membrane wettability must be carefully considered in order to avoid that membrane surface is wetted by the dispersed phase. The dispersed phase wetted the membrane surface and spread on the surface when the



un-modified membrane was used because of the hydrophilic properties. Coalescence of the aqueous droplets at the opening pore cannot be prevented resulting in an emulsion with a mean particle diameter of  $17.7 \pm 0.54 \mu\text{m}$ . The span value was 1 however the measurement did not take into account the water droplets coalesced resulting in phases separation observed at the end of the experiment (Figure 6.2 A and photograph A). On the contrary, when the lipase-loaded membrane was used, an emulsion with a mean particle diameter of  $7.1 \pm 0.35 \mu\text{m}$  and span of 0.89 was produced (Figure 6.2A and photograph B). The particle size obtained with lipase-loaded membrane was 60 % lower than the emulsion produced with the unmodified hydrophilic membrane. Lipase adsorption is supposed to modify the wettability properties of the membrane as indicated by the measurement of contact angle. The increased hydrophobicity of the membrane determined an increase in terms of interfacial tension between the dispersed phase and the membrane surface reducing the spreading on the membrane surface and keeping a small span value. The same emulsion was prepared using BSA modified membrane, in order to have an additional evidence that the structural properties of lipase was strictly responsible of the emulsion properties obtained with the modified membrane. The composition of the phases and the fluid dynamic conditions were kept constants. Droplets produced using BSA-loaded membrane were only 30 % smaller than droplets produced with unmodified membrane and the span of the distribution was 1.16 (Figure 6.2A, photograph C). The spreading of the dispersed phase at the opening pore cannot be reduced as much as it was observed with lipase-loaded membrane. Results indicated that BSA did not significantly modify the wettability properties of the membrane and fail to control the droplets formation at the pore level. The differences observed in terms of permeability reduction and emulsion droplets generation between BSA and lipase-loaded membranes suggested that the structural properties of lipase significantly influenced the gained membrane surface properties. An important aspect to consider is that the use of lipase-loaded membrane allowed the production of emulsion droplets to be controlled in terms of size and size distribution maintaining high disperse phase flux. The latter was obtained because the wettability change was not extended to all the membrane structure but it was related only to the lumen side maintaining unchanged the hydrophilicity of pore thickness and internal porous structure. The chemical modifications of the membrane surface are usually carried out by using silanes and the wettability change affected both surface and thickness of the membrane. The value of the dispersed phase flux obtained in the present study was significantly higher (more than 100 times higher), considering the pore size of the membrane, than the value obtained usually using hydrophobic membranes (see Table 1.2) [14,15]. In particular, the dispersed phase flux, normalized for the pore size of the membrane, obtained with the lipase-loaded membrane ( $600 \text{ L h}^{-1} \text{ m}^{-2} \mu\text{m}^{-1}$ ) resulted more than 100 times higher compared with the value obtained with the hydrophobic SPG membrane ( $3.75 \text{ L h}^{-1} \text{ m}^{-2} \mu\text{m}^{-1}$ ) that are the most used membranes in membrane emulsification [14]. In order to prove that lipase interaction with the membrane surface was stable, lipase-loaded membrane was used to prepare the same emulsion several times (Figure 7.2).

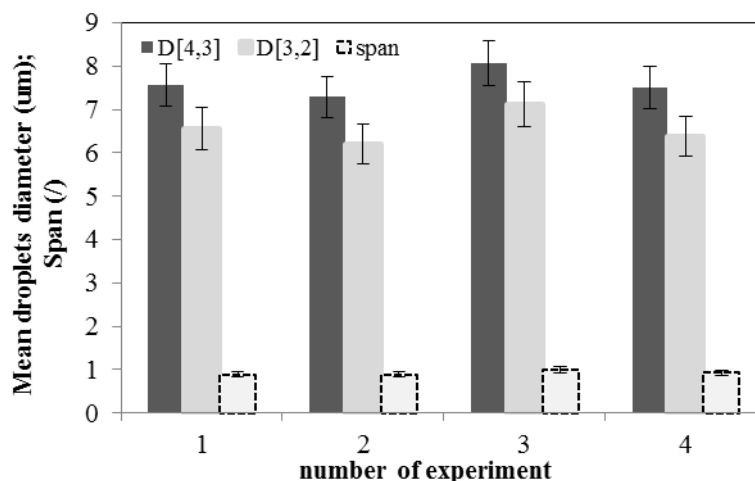


Figure 7.2 Mean droplets size and particle size distribution for quadruplicate tests conducted using the same lipase-loaded membrane for the preparation of W/O emulsions. Experimental conditions: emulsifier: Span 80 2 wt%; dispersed phase flux:  $30 \pm 0.67 \text{ L h}^{-1} \text{ m}^{-2}$ ; continuous phase axial velocity:  $0.05 \text{ ms}^{-1}$ ; dispersed phase content 9 % (v/v)

After emulsion preparation, the membrane surface was cleaned just by circulating the clean isoctane along the continuous phase circuit at low flow rate in order to remove the traces of the emulsion still in the plant after the emulsion collection at the end of the experiment. Particle size and particle size distribution were not significantly modified after the re-use of the membrane. Data indicated that lipase strongly adsorbed on the membrane surface, allowing the production of emulsions for several times without modifying its performance. Indeed, further stabilization of the lipase functionalization can be easily achieved by cross-linking and covalent bond.

Further experiments were carried out to modify the compositions of the continuous phase by using SY-Glyster PO-5S as emulsifier for the production of W/O emulsions with lipase-loaded membrane and unmodified membrane. The dynamic interfacial tension plays an important role to determine the final droplet size. When droplets are formed at the opening pore the newly formed interfaces are occupied by emulsifier molecules. The adsorption kinetics of the emulsifier influenced the time needed to stabilize the droplets against coalescence at membrane level. Therefore, the effect of emulsifier in relationship to the membrane surface properties was an important aspect to investigate. SY-Glyster PO-5S was a slower adsorbing emulsifier comparing with Span 80 [21]. The different diffusion rate of emulsifier molecules to the expanding interface influenced droplets formation time and droplets volume. Phases separation occurred very fast when SY-Glyster PO-5S and the unmodified membrane were used. This could be explained considering that when slow adsorbing emulsifier was used, the emulsifier diffusion toward the new formed interface was too slow resulting in longer droplets formation time and higher droplets volume comparing with fast adsorbing emulsifier such as Span 80 [22]. When lipase-loaded membrane was used, the dispersed phase grew at the membrane pore level as a form of droplets as a consequence of the increased interfacial tension between hydrophobic membrane surface and water phase. In these conditions, the high interfacial tension was able to balance the time needed for SY-Glyster PO-5S to adsorb at the interface. Emulsions with droplet size quite similar of

emulsion produced with Span 80 ( $D[3,2] = 6.2 \mu\text{m}$ ) were produced as illustrated in Figure 6.2 (photograph D).

#### 4. Conclusions

Hydrophobic proteins-loaded membranes have been used to obtain surface hydrophobicity control of the pore wall and detachment surface for the production of W/O emulsions by membrane emulsification. The particle size obtained with lipase-loaded membrane was 60 % lower than the emulsion produced with the unmodified hydrophilic membrane whereas the particle size distribution was 0.89. Emulsions productivity was significantly increased compared with the use of unmodified membrane. The membrane surface modification by hydrophobic proteins adsorption (such as lipase) introduces innovative strategies to generate membrane with tailored wettability properties for membrane emulsification. Hydrophilic pore wall and hydrophobic detachment surface were demonstrated to be useful for the controlled production of emulsions with an enhanced productivity.

#### References

1. Vladislavljević GT, Williams R a. Recent developments in manufacturing emulsions and particulate products using membranes. *Adv Colloid Interface Sci.* 2005;113(1):1–20.
2. Charcosset C. Preparation of emulsions and particles by membrane emulsification for the food processing industry. *J Food Eng.* 2009 ;92(3):241–9.
3. Giorno L, Luca G De, Figoli A, Piacentini E, Drioli E. *Membrane Emulsification : Principles and Applications.* 2009,Wiley. 2009;463–94.
4. Kawakatsu T, Tra G. The effect of the hydrophobicity of microchannels and components in water and oil phases on droplet formation in microchannel water-in-oil emulsification. 2001;179:29–37.
5. Kobayashi I, Nakajima M, Mukataka S. Preparation characteristics of oil-in-water emulsions using differently charged surfactants in straight-through microchannel emulsification. *Colloids Surfaces A Physicochem Eng Asp.* 2003;229(1-3):33–41.
6. Katoh R, Asano Y, Furuya A, Sotoyama K, Tomita M. Preparation of food emulsions using a membrane emulsification system. *J Memb Sci.* 1996;113(1):131–5.

7. Geerken MJ, Lammertink RGH, Wessling M. Interfacial aspects of water drop formation at micro-engineered orifices. *J Colloid Interface Sci.* 2007;312(2):460–9.
8. Yuan Q, Aryanti N, Hou R, Williams R a. Performance of slotted pores in particle manufacture using rotating membrane emulsification. *Particuology.* 2009;7(2):114–20.
9. Kobayashi I, Nakajima M, Chun K, Kikuchi Y, Fujita H. Silicon array of elongated through-holes for monodisperse emulsion droplets. *AIChE J.* 2002 ;48(8):1639–44.
10. Yuan Q, Aryanti N, Gutie G, Williams RA. Enhancing the Throughput of Membrane Emulsification Techniques To Manufacture Functional Particles. 2009;8:872–80.
11. Scherze I, Marzilger K, Muschiolik G. Emulsification using micro porous glass (MPG): surface behaviour of milk proteins. *Colloids Surfaces B Biointerfaces.* 1999;12(3-6):213–21.
12. Volker Schroder, Olaf Behrend and HS. Effect of Dynamic Interfacial Tension on the Emulsification Process Using Microporous , Ceramic Membranes. *J Colloid Interface Sci.* 1998;340(202):334–40.
13. Katoh R, Asano Y, Furuya A, Sotoyama K, Tomita M. Preparation of food emulsions using a membrane emulsification system. *J Memb Sci.* 1996;113:131–5.
14. Piacentini E, Drioli E, Giorno L. Preparation of stimulus responsive multiple emulsions by membrane emulsification using con a as biochemical sensor. *Biotechnol Bioeng.* 2011;108(4):913–23.
15. Vladislavljevic GT, , Sabine Tesch HS. Preparation of water-in-oil emulsions using microporous polypropylene hollow fibers : influence of some operating parameters on droplet size distribution. *Chem Eng Process.* 2002;41:231–8.
16. Jing W, Wu J, Jin W, Xing W, Xu N. Monodispersed W/O emulsion prepared by hydrophilic ceramic membrane emulsification. *Desalination.* 2006;191(1-3):219–22.
17. Reis P, Holmberg K, Watzke H, Leser ME, Miller R. Lipases at interfaces: a review. *Adv Colloid Interface Sci.* 2009;147-148:237–50.
18. Grochulskisq P, Schrags JD, Bouthilliers F, Smithll P, Harrisonll D. Insights into Interfacial Activation from an Open Structure of Lipase. 1993;268(17):12843–7.

19. Santos O, Nylander T, Paulsson M, Trägårdh C. Whey protein adsorption onto steel surfaces—effect of temperature, flow rate, residence time and aggregation. *J Food Eng.* 2006 ;74(4):468–83.
20. González-Martín ML. Wettability and surface free energy of zirconia. *J Material Sci.*1999;4:5923–6.
21. Wu J, Wei W, Wang L-Y, Su Z-G, Ma G-H. Preparation of uniform-sized pH-sensitive quaternized chitosan microsphere by combining membrane emulsification technique and thermal-gelation method. *Colloids Surf B Biointerfaces.* 2008;63(2):164–75.
22. Van der Graaf S, Schroën CGPH, van der Sman RGM, Boom RM. Influence of dynamic interfacial tension on droplet formation during membrane emulsification. *J Colloid Interface Sci.* 2004;277(2):456–63.

# CHAPTER 3

## **Microsieve nickel and stainless steel membrane: a comparative study on the influence of membrane fouling by polymer solution**

### **1. Introduction**

In the membrane emulsification process fouling phenomena consists of the interaction between the membrane surface and the components of the emulsions (such as dispersed phase and emulsifier) resulting in modification of membrane wetting properties which influences the controlled particle production, reduces the flux and the emulsion quality [1]. For example, oxidized silicon surface or untreated SPG membrane has a negative potential within a pH range of 2–8. For these membranes, cationic or zwitterionic surfactants must be avoided otherwise they adsorb on the membrane surface and the membrane get fouled by the surfactant molecules resulting in a spreading of the dispersed phase over the membrane surface [2]. Nowadays, future developments in membrane emulsification are focused on the production of membrane with more precise structure or alternative material which will improve the accuracy of the process [1]. Membranes used for emulsification may have different geometries (flat or tubular) and manufactured with several material: ceramic [3,4], microporous glass (Shirasu Porous Glass, SPG) [5–8], organic polymer [9] and metallic [10–14]. SPG and ceramic membranes are characterized by a tortuous structure of the pores which are prone to get fouled by the emulsion ingredients. Nickel microsieves manufactured using UV-LIGA process by Stork Veco BV [12] and Micropore Technologies Ltd [15], laser drilled aluminium and stainless steel foils fabricated by pulsed laser drilling [16,17] received great interest in the last years for the production of emulsions with high throughput. Micro-sieve membranes are ultra-thin foils with rectilinear pores and very low internal pore area so they are less prone to get fouled by emulsion ingredients than highly tortuous SPG membranes [2]. Moreover the metallic micro-sieve membrane offers also the advantage to have mechanical strength and long operating life compared to the more fragile ceramic and glassy membrane [18,19]. In this study, nickel and stainless steel flat sheet micrometer pore sized sieve type membranes (provided by Micropore Technologies, UK) were tested for the production of O/W emulsions using a polycaprolactone solution as dispersed phase and the stirrer membrane emulsification (Dispersion Cell). Most of the methods used for the preparation of polymeric particles involved an emulsification step in which sticky material (such as polymer solution) and aggressive chemicals (such as organic solvents) are used as dispersed or continuous phase. Nickel and stainless steel differs in terms of chemical resistance. Nickel membrane has a shorter operating life than stainless steel membrane because can be subjected to oxidative reaction in presence of water solutions and organic solvents or acid solutions which can be responsible of modification of the surface property of the

membrane over time [20,21]. In membrane emulsification the wetting property of the membrane is an important parameter to take into account. Indeed, the membrane surface must not be wetted by the dispersed phase to achieve a controlled particle production of uniform droplets. The influence of the membrane material on the uniformity of the emulsion was investigated at different injection flow rates of the dispersed phase and using emulsifiers with different interfacial adsorption kinetics in the continuous phase.

## 2. Experimental section

### 2.1. Chemicals

A polymer solution of poly-caprolactone (PCL, Sigma-Aldrich, Mw 14KDa) in dichloromethane (DCM, Sigma-Aldrich) was used as dispersed phase for the preparation of O/W emulsion. Poly-vinyl alcohol (PVA, 1%wt) and Sodium Dodecyl Sulphate (SDS, 2%wt) were all purchased from Sigma Aldrich and used as emulsifiers in the aqueous phase. Ultrapure water (USF Elsa, model Purelab Classic PL5221) with a resistivity of 18.2 M $\Omega$ -cm was used for the preparation of all the aqueous solutions. Sodium hydroxide (NaOH, 4M) was used for the cleaning of the membrane.

### 2.2. Stirrer membrane emulsification equipment

The study of the effect of membrane properties on the uniformity of O/W emulsion was carried out using the stirrer Dispersion Cell (provided by Micropore Technologies, UK) and two different flat sheet metallic membranes:

- hydrophilic nickel membrane with 10  $\mu$ m circular pore size distributed in a regular way in a membrane area of 8.55 cm<sup>2</sup> and with a porosity of 0.19% (Figure 1.3B);
- stainless steel membrane with 10  $\mu$ m circular pore size distributed in a ringed area of 1.85 cm<sup>2</sup> and a porosity of 0.19% (Figure 1.3A);

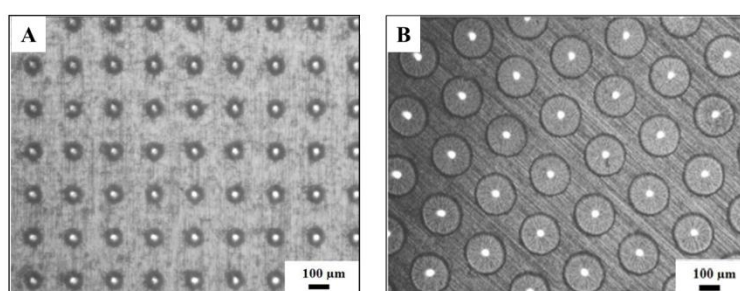


Figure 1.3 Photographs of the surface of the membrane: A) stainless steel membrane; B) nickel membrane

The system as well as the membranes were provided by Micropore Technologies Ltd (Leicestershire, UK). The system provides the ability to control droplets size and size distribution by changing operating conditions and the chemical properties of the phases

and it is suitable to work at laboratory scale [11,13]. A schematic representation of the system is shown in Figure 2.3.

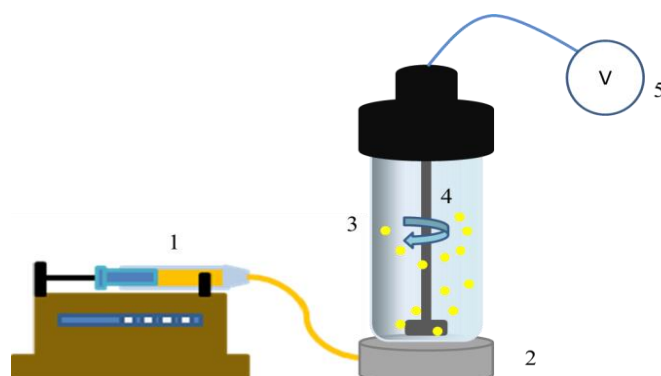


Figure 2.3 Stirred membrane emulsification equipment scheme. 1: syringe pump; 2: injection chamber; 3: glass cylinder; 4: Stainless steel stirrer with a blade at the bottom ending; 5: voltage regulator.

The stirred cell system consists of a PTFE base (named injection chamber) that hosts a flat membrane coupled with a dismantable threaded glass cylinder. A stainless steel stirrer is placed over the glass cylinder and regulated by a voltage regulator connected to the electricity. The angular velocity of the stirrer, from which depends the shear stress at the surface of the membrane, is regulated by selecting the appropriate voltage of the voltage regulator. The dispersed phase was injected through the porous structure by using a syringe pump.

Before each experiment the membrane was pre-wetted with the continuous phase by sonication in an ultrasonic bath for 1 min to remove air from the pores and fill them with the continuous phase. After each experiment, the membrane used for the production of the emulsion with the polymer solution was cleaned in an ultrasonic bath for few seconds in dichloromethane to remove residual polymer on its surface and inside the pores. Subsequently, it was rinsed with sodium hydroxide 4 M and distilled water in an ultrasonic bath for few seconds min and clean water.

### 2.3. Particle characterization

O/W emulsions were observed by optical microscopy. Particle size and size distribution were measured using Scion Image software. Droplet size distribution was expressed as Span number (see Appendix 1 for the calculation).



### 3. Results and discussion

The uniformity of emulsion drops detached at the surface of a micro-porous membrane can be influenced by both the adsorption rate of the emulsifier at oil-water interface and the surface property of the membrane. A polymeric stabilizer (PVA, MW 13000-23000 Da) and an anionic emulsifier (SDS, MW 288 Da) with different molecular weight (which influenced the interfacial adsorption kinetic) were selected for the preparation of the emulsion with both kind of membranes in order to evaluate the influence of the membrane surface property in different conditions of droplet interface stabilization. Water saturated with DCM was used as continuous phase and PCL 16 % w/v in DCM was used as dispersed phase. The emulsions contained 3% of organic phase were produced. The influence of the surface membrane property was evaluated at constant shear stress (11 Pa) and at low ( $9 \text{ L h}^{-1} \text{ m}^{-2}$ ) and high ( $216 \text{ L h}^{-1} \text{ m}^{-2}$ ) dispersed phase flux which influences the expansion rate of the droplet at the edge of the pore. In Figure 3.3 are compared the photographs of the emulsions produced with nickel and stainless steel membranes keeping the same process parameters ( $J= 9 \text{ L h}^{-1} \text{ m}^{-2}$ ,  $\tau= 11 \text{ Pa}$ ) and using PVA (A-B) and SDS (C-D) as emulsifier.

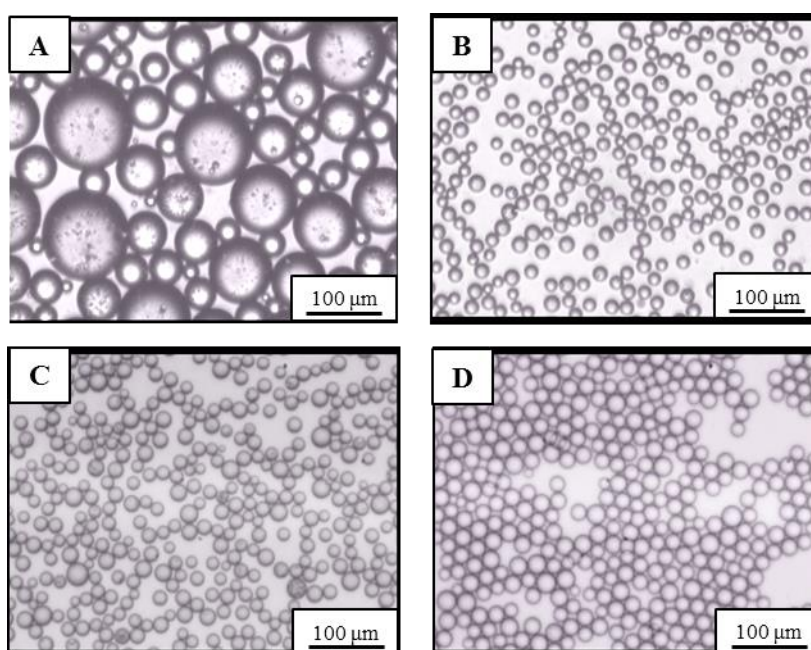


Figure 3.3 O/W emulsion produced with: A) 1% PVA, nickel membrane; B) 1% PVA, stainless steel membrane; C) 2% SDS nickel membrane; D) 2% SDS, stainless steel membrane. ( $J= 9 \text{ L h}^{-1} \text{ m}^{-2}$ ,  $\tau= 11 \text{ Pa}$ )

Non-uniform emulsion with big droplets was produced (photograph A) when nickel membrane was used in combination with PVA. In the membrane emulsification process, the interfacial tension is the main retaining force at the pore level and it is dependent on the expansion rate of the droplet at the opening pore and the concentration and type of emulsifier [22]. In this case the droplets grow slowly at the pore level because a low dispersed phase flux was applied. Nickel membrane can be subjected to oxidative reaction in presence of organic solvent and aqueous solution with a consequent

modification of the surface membrane property. Therefore, fouling of the membrane can occur in low flux conditions because of a spreading of the dispersed phase on the membrane surface. A consequence of this phenomena was the formation of very big droplets as showed in the photograph A. This effect is more significant when stabilizer with high molecular weight (such as PVA) are used because the low interfacial adsorption kinetic prolonged the permanence of the droplet at the pore level (and so the contact between the dispersed phase and the membrane surface) before the detachment. On the contrary, the stainless steel membrane is chemical resistant and the spreading of the dispersed phase did not occurred when low injection flux was applied and emulsifier with low adsorption kinetic was used in the continuous phase. The use of this membrane resulted in a good control of the uniformity of the emulsion independently from the kind of emulsifier used in the continuous phase as demonstrated in the photographs B and D. In the case of nickel membrane, a significant improvement of the uniformity of the emulsion was obtained when SDS was used as emulsifier in the continuous phase as observed in the photograph C. SDS is known to be a fast adsorption emulsifier for its low molecular weight, therefore it rapidly adsorbed at the interface of the droplet during the growing at the pore level. In this way the spreading of the dispersed phase on the surface of nickel membrane could be avoided because the droplets are stabilized sooner resulting in shorter permanence of the droplet at the edge of the pore [23]. In Table 1.3 are compared the mean droplet size and span value of the emulsion produced with nickel and stainless steel membrane and different emulsifiers. The emulsions were produced at higher injection flux ( $216 \text{ L h}^{-1} \text{ m}^{-2}$ ) and the same shear stress (11 Pa). The images of the emulsions produced are reported in Figure 4.3 (A-D).

Table 1.3. Particle size and size distribution of particles produced O/W emulsion: **O**-16% PCL in DCM; **W**-water with SDS or PVA

| <b>Emulsifier</b> | <b>Membrane</b> | <b>mean droplet size<br/>(<math>\pm 1</math>) [<math>\mu\text{m}</math>]</b> | <b>Span (<math>\pm 0.02</math>)</b> |
|-------------------|-----------------|--|-------------------------------------|
| SDS               | nickel          | 30   | 0.6                                 |
|                   | stainless steel | 26   | 0.35                                |
| PVA               | nickel          | 38   | 0.72                                |
|                   | stainless steel | 32   | 0.3                                 |

The use of stainless steel membrane allowed the production of highly uniform emulsions with a span value between 0.3 and 0.35 when both kind of emulsifiers were used (photographs B-D). Results demonstrated the potentiality of this membrane to keep a precise control of droplet uniformity also when the dispersed phase is injected at higher flux. The emulsions produced with nickel membrane and higher dispersed phase flux were less uniform compared to the emulsion produced with stainless steel membrane as demonstrated by the span values reported in the table and the photographs A and C. However, a reduction of the formation of very big droplet was observed increasing the dispersed phase flux when PVA was used as emulsifier (photograph A). This is because the droplets grew faster at higher flux and more pores are activated reducing the fouling of the membrane surface that was responsible of the formation of

very big droplets in low flux condition. However, a better control of droplet production could be achieved using SDS as emulsifier as demonstrated by the lower span value reported in the table and the photograph C.

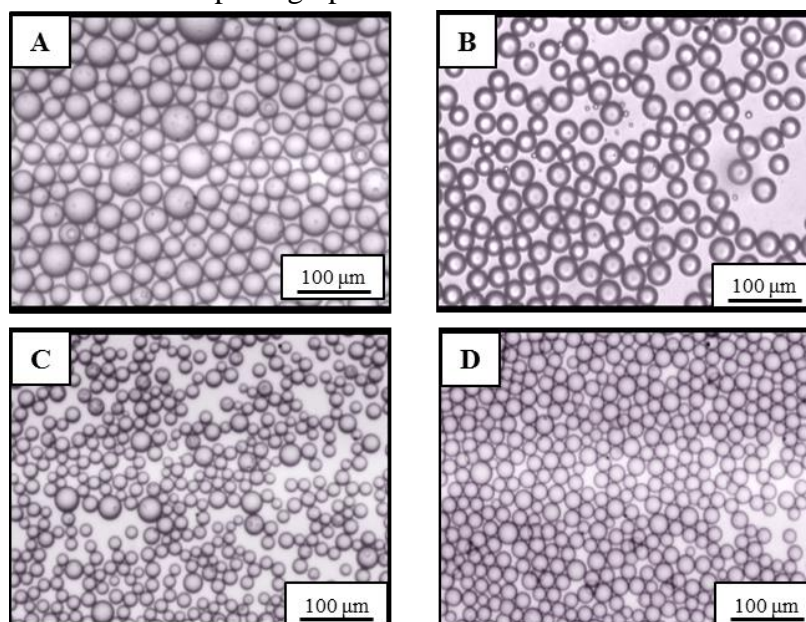


Figure 4.3 O/W emulsion produced with: A) 1% PVA, nickel membrane; B) 1% PVA, stainless steel membrane; C) 2% SDS nickel membrane; D) 2% SDS, stainless steel membrane ( $J= 216 \text{ L h}^{-1} \text{ m}^{-2}$ ,  $\tau= 11 \text{ Pa}$ )

#### 4. Conclusions

Results demonstrated the potentiality of stainless steel micro-sieve membrane to avoid fouling phenomena during the emulsification process compared with nickel membrane. Since the higher chemical resistance of stainless steel, the membrane surface is less prone to get fouled by the ingredients of the emulsions and this property is of great importance when sticky material (such as polymer solution) and organic solvents are used in the formulation. The use of stainless steel membrane allowed the production of highly uniform emulsions with a span value between 0.3 and 0.35 independently from the dispersed phase flux or the kind of emulsifier used in the continuous phase. Nickel membrane was more subjected to be fouled by the polymer solution especially when emulsifier that adsorbs slowly at the interface are used (such as PVA). A reduction of fouling with a consequent improvement of the uniformity of the emulsion can be achieved using emulsifier with fast adsorption kinetic (such as SDS) in such a way to stabilize the interface sooner reducing the permanence of the droplet at the edge of the pore.

---

*References*

1. Piacentini E, Drioli E, Giorno L. Membrane emulsification technology: Twenty-five years of inventions and research through patent survey. *Jof Memb Sci.* 2014;468:410–22.
2. Vladisavljević GT, Kobayashi I, Nakajima M. Production of uniform droplets using membrane, microchannel and microfluidic emulsification devices. *Microfluid Nanofluidics.* 2012;13(1):151–78.
3. Vladisavljević GT, Schubert H. Preparation of Emulsions with a Narrow Particle Size Distribution Using Microporous  $\alpha$ -Alumina Membranes. *J Dispers Sci Technol.* 2003;24(6):811–9.
4. Schro V. Production of emulsions using microporous, ceramic membranes. *Colloids Surfaces A Physicochem Eng Asp.* 1999;152:103–9.
5. Vladisavljevic G. Influence of process parameters on droplet size distribution in SPG membrane emulsification and stability of prepared emulsion droplets. *J Memb Sci.* 2003;225(1-2):15–23.
6. Cheng C-J, Chu L-Y, Xie R. Preparation of highly monodisperse W/O emulsions with hydrophobically modified SPG membranes. *J Colloid Interface Sci.* 2006;300(1):375–82.
7. Vladisavljevic G, Shimizu M, Nakashima T. Permeability of hydrophilic and hydrophobic Shirasu-porous-glass (SPG) membranes to pure liquids and its microstructure. *J Memb Sci.* 2005;250(1-2):69–77.
8. Yuyama H, Watanabe T, Ma G-H, Nagai M, Omi S. Preparation and analysis of uniform emulsion droplets using SPG membrane emulsification technique. *Colloids Surfaces A Physicochem Eng Asp.* 2000;168(2):159–74.
9. Vladisavljevic GT, , Sabine Tesch HS. Preparation of water-in-oil emulsions using microporous polypropylene hollow fibers : influence of some operating parameters on droplet size distribution. *Chem Eng Process.* 2002;41:231–8.
10. Yuan Q, Aryanti N, Hou R, Williams R a. Performance of slotted pores in particle manufacture using rotating membrane emulsification. *Particuology.* 2009;7(2):114–20.
11. Stillwell MT, Holdich RG, Kosvintsev SR, Gasparini G, Cumming IW. Stirred Cell Membrane Emulsification and Factors Influencing Dispersion Drop Size and Uniformity. *Ind Eng Chem Res.* 2007;46(3):965–72.
12. Nazir A, Schroën K, Boom R. High-throughput premix membrane emulsification using nickel sieves having straight-through pores. *J Memb Sci.* 2011;383(1-2):116–23.

13. Kosvintsev SR, Gasparini G, Holdich RG, Cumming IW, Stillwell MT. Liquid - Liquid Membrane Dispersion in a Stirred Cell with and without Controlled Shear. 2005;9323–30.
14. Kosvintsev SR, Gasparini G, Holdich RG. Membrane emulsification: Droplet size and uniformity in the absence of surface shear. *J Memb Sci.* 2008;313(1-2):182–9.
15. Egidi E, Gasparini G, Holdich RG, Vladisavljević GT, Kosvintsev SR. Membrane emulsification using membranes of regular pore spacing: Droplet size and uniformity in the presence of surface shear. *J Memb Sci.* 2008;323(2):414–20.
16. Dowding PJ, Goodwin JW, Vincent B. Production of porous suspension polymer beads with a narrow size distribution using a cross-flow membrane and a continuous tubular reactor. *Colloids Surfaces A Physicochem Eng Asp.* 2001;180(3):301–9.
17. Vladisavljević GT, Williams R a. Manufacture of large uniform droplets using rotating membrane emulsification. *J Colloid Interface Sci.* 2006;299(1):396–402.
18. Schadler V, Windhab EJ. Continuous membrane emulsification by using a membrane system with controlled pore distance. *Desalination .* 2006;189(1-3):130–5.
19. Suárez MA, Gutiérrez G, Matos M, Coca J, Pazos C. Chemical Engineering and Processing: Process Intensification Emulsification using tubular metallic membranes. *Chem Eng Processes.* 2014;81:24–34.
20. Prutton CF, Frey DR, Turnbull D, Dlouhy G. Corrosion of Metals by Organic Acids in Hydrocarbon Solvents. *Ind Eng Chem Res.* 1945;37:90–100.
21. LG Borisova. Corrosive effect of dichloromethane on metals. *Chem Petroleum Eng.* 1969;(9):700–1.
22. Spyropoulos F, Lloyd DM, Hancocks RD, Pawlik AK. Advances in membrane emulsification. Part A: recent developments in processing aspects and microstructural design approaches. *J Sci Food Agric.* 2014;94(4):613–27.
23. Van der Graaf S, Schroën CGPH, van der Sman RGM, Boom RM. Influence of dynamic interfacial tension on droplet formation during membrane emulsification. *J Colloid Interface Sci.* 277(2):456–63.

# CHAPTER 4

## Production of poly-caprolactone microparticles from O/W emulsion by membrane emulsification/solvent diffusion process

### 1. Introduction

Biodegradable microparticles are widely investigated drug delivery systems for bioactive compounds such as low molecular weight and macromolecular therapeutics. This is because they offer possibilities to produce drug delivery systems where the matrix material can be decomposed into non-toxic and low molecular-weight species with the concomitant release of drug. During the last two decades, among common biodegradable polyesters derived from lactic acid and glycolic acid (poly-lactic acid, poly-glycolic acid, poly-lactic-co-glycolic acid), there has been an increasing interest in the use of poly-caprolactone (PCL) in drug delivery. Reasons for this include its excellent biocompatibility, ability to be fully excreted from the body once bio-reabsorbed, relatively inexpensive production routes and superior rheological and visco-elastic properties when compared with other aliphatic polyesters [1].

Owing to its low glass transition temperature ( $T_g \sim -60^\circ\text{C}$ ), PCL is in a rubbery state at body temperature, giving it a highly flexible structure that permits easier diffusion of drugs than in glassy or crystalline structure. It is thus a good candidate for developing diffusion-controlled drug delivery systems [2-4].

PCL is an advantageous material also for its high permeability to small drug molecules and its negligible tendency to generate an acidic environment during the degradation process as compared to polylactids and polyglycolids, a problem that contributes to the generation of inflammatory reactions. The degradation of PCL is very slow compared to the other polyesters making it more suitable for long-term delivery systems with the advantage of less frequent administrations, increase of patient compliance and reduction of discomfort. Delivery of PCL particles can also be easily modulated with appropriate blending and copolymerization. Functional groups could also be added to design the desired mechanical and chemical properties or degradation kinetics [1].

Microspheres based on the use of PCL have been used to encapsulate many drugs such as antigens [5], antihypertensive [6], contraceptives [7], taxol [8], and were found resistant to simulated gastric fluid allowing the entrapped drugs to pass intact into the intestine [9]. Within the last decades, PCL polymers have been also successfully used to develop controlled delivery systems especially for peptides and proteins. Jameela et al. [5] showed that PCL has a good permeability to proteins unlike polylactids and polyglycolids and is a good carrier for vaccine delivery because it does not generate the acidic environment that affects antigenicity of vaccines .

PCL microparticles have been typically prepared by two kinds of processes: spray drying and emulsion solvent evaporation or diffusion. In the spray drying method,

particles are formed directly by atomization of the organic solvent containing the polymer and the treatment with hot air to remove the solvent. However, this process is not suitable when highly temperature-sensitive compounds have to be encapsulated and the control of particle size is difficult [10]. In the emulsification step of the emulsion/solvent evaporation process, a polymeric solution (obtained by dissolving the preformed polymer in the organic phase) can be emulsified in an aqueous phase to produce a simple O/W emulsion. The polymeric solution can also be used as oil phase for the preparation of simple water-in-oil (W/O) emulsion, which is emulsified again in an aqueous phase to produce a multiple water-in-oil-in-water (W/O/W) emulsion. In the solvent evaporation step, the organic solvent is removed after the emulsification step by evaporation. Solvent evaporation depends mostly on temperature and the concentration of solvent in the air. The process could be accelerated either by increasing the temperature of the continuous phase or by reducing the pressure. However, larger size, decreased drug encapsulation efficiency and coarser morphology have been reported in literature [11].

The preparation of particles using polyesters as polymeric material and emulsion solvent diffusion was proposed for the first time by Quintanar-Guerrero [12]. In this work, the emulsification of the partly water soluble solvent containing the polymer in an aqueous phase is followed by the addition of water into the system. This causes the diffusion of solvent into the external phase, resulting in the solidification of polymer within the droplets. This technique presents advantages such as the use of pharmaceutically acceptable organic solvents, high reproducibility and better control of particle size.

Moreover the use of preformed polymers is preferable compared to polymerization processes as the latter is associated with the presence of residual substances and cross reactions with the drug which produce potentially-toxic effects [12,13].

The conventional emulsification processes (homogenization, sonication or stirring) do not offer the possibility to easily control droplet size and size distribution simultaneously. Therefore, a significant quantity of microparticle product would be recycled as off-spec, thus potentially incurring a substantial increase in processing cost. Particle size is an important parameter that influences almost every aspect of particle function including degradation, flow properties, clearance and uptake mechanisms. It can be controlled through physical properties of the materials, such as polymer and surfactant concentration, or through the experimental parameters of the fabrication method [14]. Relatively newer emulsification techniques, such as membrane emulsification, offer great potentials in manufacturing “made-to-measure” emulsions and other solid particulates [15]. A distinguishing feature of membrane emulsification is the possibility to control the resulting droplet size primarily by the choice of the membrane and not by the generation of turbulent droplet break-up which characterizes conventional methods [16].

Membrane emulsification has been applied for the preparation of microspheres and microcapsules using mainly polyesters derived from lactic acid [17-20] and copolymers with glycolic acid [21,22]. In these works, the organic solvent was removed by evaporation or in some cases by extraction with alcohols.

PCL particles have been prepared by combining the use of membrane contactors and nanoprecipitation by Charcosset et al. [23]. In this case, an organic solvent completely soluble in water, containing dissolved PCL, was used as dispersed phase to form solidified particles directly at the opening pore. The solidification of the particles occurs after the droplets are in contact with the aqueous continuous phase. Charcosset and coworkers mainly focused on evaluating the effects of operating parameters (such as membrane pore size, dispersed phase flux and cross-flow velocity of the continuous phase) on particle size. They observed that the particles size was mainly controlled by the nanoprecipitation due to the interfacial deposition of the polymer followed by the displacement of the solvent and the effect of dispersed phase flux, continuous phase cross-flow velocity and membrane pore size was not as significant as expected by the use of the membrane process. To our knowledge, no other work is reported in literature about the preparation of PCL particles using membrane-based processes.

In this work, the preparation of PCL microparticles was carried out in a two-step process: a) the pre-emulsification step, where the membrane was used to prepare an O/W emulsion with an organic solvent partly soluble in water as dispersed phase; b) the post emulsification step, where the solidification of particles was carried out by the solvent diffusion process. The membrane was used to disperse the droplets of organic phase in the water phase saturated with the organic solvent, without promoting the direct exchange of the solvent and non-solvent at pore level. In this case, the pre-emulsification step is expected to finely control the production of particles in terms of size and size distribution by selecting the appropriate process parameters and membrane pore size. The effect of phase composition (polymer concentration in the dispersed phase) and fluid-dynamic parameters (dispersed phase flux and shear stress) on particle size and size distribution have been investigated in the pre-emulsification step. In the post emulsification step, the effect of the volume of water used to carry out the solvent diffusion on particle size and size distribution, particle shape and surface morphology has also been studied.

## 2. Experimental section

### 2.1. Chemicals

A polymeric solution of polycaprolactone (PCL, Sigma-Aldrich, MW 14 kDa) in dichloromethane (DCM, Sigma-Aldrich) was used as dispersed phase for the preparation of O/W emulsions and particles. Polycaprolactone is a hydrophobic polyester approved by Food and Drug Administration for human use. Ultrapure water (USF Elsa, model Purelab Classic PL5221) with a resistivity of 18.2 M $\Omega$ -cm was used as continuous phase for the preparation of the emulsions and as dilution medium for the preparation of particles by the solvent diffusion process. The continuous phase was saturated with solvent in order to avoid its diffusion during the emulsification process. Sodium Dodecyl Sulphate (SDS, 2% wt) was used as emulsifier.



## 2.2. O/W emulsion preparation: membrane emulsification equipment

The preparation of the emulsions with the Dispersion Cell was carried out with a hydrophilic flat-sheet micro-sieve nickel membrane with 10  $\mu\text{m}$  circular pore size distributed in a membrane area of 8.55  $\text{cm}^2$  and with a porosity of 0.19% (Micropore Technologies Ltd., Leicestershire, UK). This system, provides the ability to control droplets size and size distribution by changing operating conditions and the chemical properties of the phases, therefore it is suitable to work at laboratory scale. The shear stress ( $\tau$ )[Pa] at the surface of the membrane depends on the angular velocity ( $\omega$ ) [ $\text{s}^{-1}$ ] of the continuous phase, which can be regulated by selecting the appropriate voltage via a voltage regulator. The maximal shear over the whole membrane area was calculated with the Equation 1[15]:

$$\tau = 0.825\mu_c\omega r_{trans} \frac{1}{\delta} \quad (1)$$

where  $\mu_c$  [Pa s] is the continuous phase viscosity,  $r_{trans}$  is the transitional radius and  $\delta$  is the boundary layer thickness calculated from the Landau-Lifshitz equation ( $\delta = \sqrt{\mu/\omega\rho}$ ). Before each experiment the membrane was pre-wetted with the continuous phase by sonication in an ultrasonic bath for 1 min to remove air from the pores and fill them with the continuous phase. The dispersed phase was injected through the porous membrane using a peristaltic pump. After each experiment, the membrane was cleaned in an ultrasonic bath for few seconds in dichloromethane to remove residual polymer on its surface and inside the pores. Subsequently, it was rinsed with distilled water in an ultrasonic bath for few seconds.

## 2.3. Microparticle preparation

The resulting oil droplets were solidified by the solvent diffusion process. It consists in the addition of the emulsion into a known volume of fresh aqueous phase with SDS (0,5% wt) under gentle stirring to induce the diffusion of the solvent from the droplets into the external phase. This leads to the deposition of the polymer around the droplets and a consequent formation of particles. The resulting samples were decanted in a first step and subsequently recovered by centrifugation at 3000 rpm for 5 min. Afterwards, particles were washed for three times with deionized water and dried in a stove at 40  $^{\circ}\text{C}$  over-night to remove residual organic solvent. Microparticles shape and the solidification time of the droplets were evaluated by optical microscopy observation of the sample taken from the continuous phase at different times, and the surface morphology was evaluated by Scanning Electron Microscopy (SEM Zeiss EVO MA and LS Series) observation of the dried samples.

## 2.4. Particle characterization

O/W emulsions and solidified particles were observed by optical microscopy. Oil droplet size was analyzed using an image analysis system running Scion Image software. Microparticle size and size distribution were measured by laser diffraction (Mastersizer 2000, Malvern Instruments). The mean particle size is expressed as D[3,2] and D[4,3]. Droplet size distribution is expressed as Span number (see Appendix 1). Three samples were analyzed for each experiment and the reported results are the average of three different experiments.

## 3. Results and discussion

### 3.1. Effect of polymer concentration

The effect of polymer concentration (8-30% wt/v) on particle size and size distribution of solidified particles is reported in Figure 1.4. It was evaluated keeping constant the dispersed phase flux at  $9 \text{ L h}^{-1} \text{ m}^{-2}$  and shear stress at 8.6 Pa.

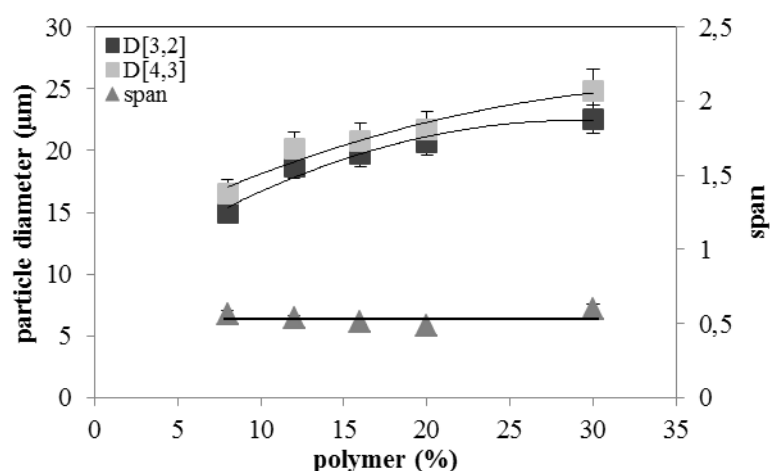


Figure 1.4 Effect of the polymeric concentration on particle size and size distribution of the emulsion prepared with a dispersed phase flux of  $9 \text{ L h}^{-1} \text{ m}^{-2}$  and a shear stress of 8.6 Pa

The increase of polymer concentration resulted in a progressive increase of particle size from 15  $\mu\text{m}$  to 24  $\mu\text{m}$  maintaining a good monodispersity of the emulsion with a span value in the range between 0.51 and 0.60. Considering that the other forces acting on the droplets growing at the membrane pore level are constant, only the physico-chemical parameters, such as viscosity and interfacial tension of organic polymer solution can affect particle size. The interfacial tension is the key retaining force during droplet formation and determines the adhesion of the dispersed phase around the edge of the opening pore. The polymer concentration has been demonstrated to have an effect on the interfacial tension when the polymeric solution was emulsified in the aqueous phase containing the emulsifier [16]. The concentration of the emulsifier (SDS) in the

aqueous phase was maintained constant at 2% while the concentration of the polymer in the dispersed phase was increased. This is in agreement with the results of previous work, e.g. V Baback et al who found that PCL has very poor interfacial activity when the polymer solution was kept in contact with water, whereas, the interfacial adsorption of a charged emulsifier agent was reduced when the PCL concentration was increased. Moreover, the increase of the polymer concentration is associated with an increase of the hydrophobic property of the dispersed phase and this influenced the interfacial adsorption of SDS with a consequent increase of the interfacial tension. Span was not significantly affected by the variation of polymer concentration because the interfacial tension influenced particle size more than size distribution, especially when a fast emulsifier, such as SDS, was used.

Particle shrinkage has been observed during the post emulsification step: 24% of shrinkage of the initial oil droplets compared to the solidified particles was measured as observed in Figure 2.4. This occurs as a result of the removal of the solvent from the droplets.

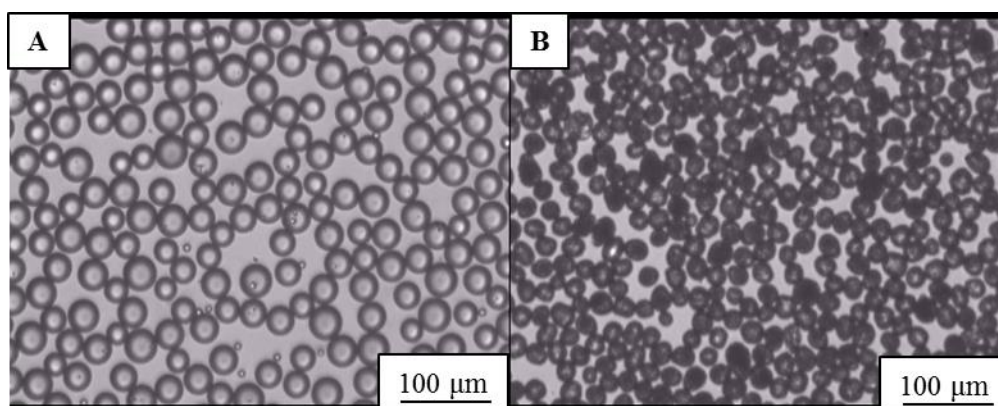


Figure 2.4 Optical microscopy pictures of: A) O/W emulsion; B) solidified microparticles

### 3.2. *Effect of the fluid-dynamic conditions*

In membrane emulsification, the dispersed phase flux and the shear stress are important parameters to control particle size and size distribution of emulsion. In this work, emulsions containing 3% of dispersed phase composed of a polymer concentration of 16% wt/v were prepared by increasing separately the dispersed phase flux and shear stress. The effects of shear stress on particles size and size distribution is reported in Figure 3.4.

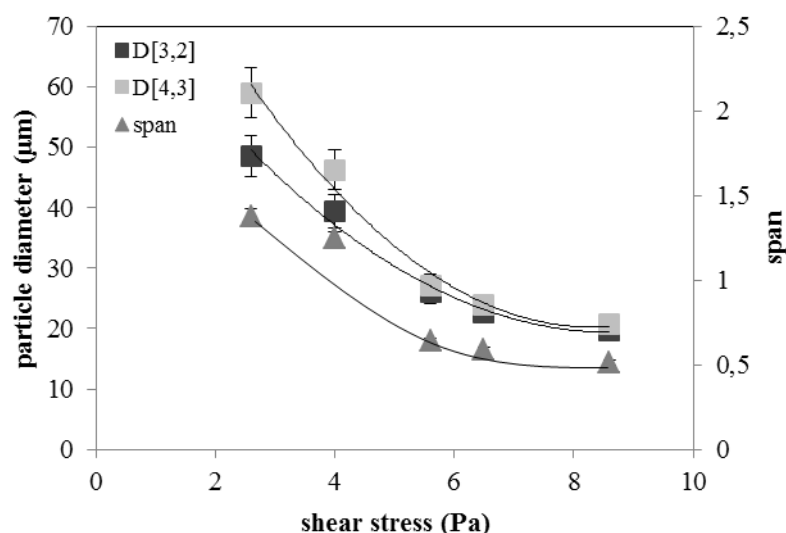


Figure 3.4 Effect of increasing shear stress on particle size and size distribution of particles prepared with 16% of PCL and a dispersed phase flux of  $9 \text{ Lh}^{-1}\text{m}^{-2}$

Particle diameters decreased exponentially with the increase of shear stress (in agreement with [17]), because droplets were detached sooner at the opening pore with a consequent reduction of droplet growing. The increase of shear stress allows also the production of more uniform particles. Particles with mean size of  $19.94 \pm 1.58 \mu\text{m}$ , corresponding 2 times the pore size of the membrane, and a span value of  $0.51 \pm 0.01$  can be obtained by using a shear stress of 8.6 Pa, which was selected as optimal value.

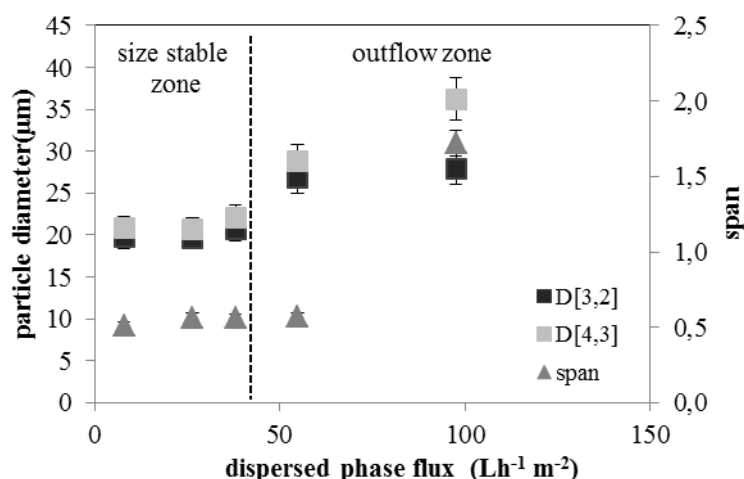


Figure 4.4 Effect of the dispersed phase flux on particle size and size distribution of particles prepared with 16% of PCL and a shear stress of 8.6 Pa

In Figure 4.4 is reported the effect of the dispersed phase flux on particle size and size distribution. The effect of this parameter was evaluated increasing the flow rate of the peristaltic pump in a range of  $0.13$  and  $1.5 \text{ ml min}^{-1}$ , keeping constant the shear stress at 8.6 Pa. A variation of the mean particle size and size distribution was not observed when the dispersed phase flux was progressively increased from 9 to almost  $40 \text{ Lh}^{-1}\text{m}^{-2}$ . This range has been defined in literature as “size stable zone”, where droplets diameter is almost independent of the applied flux and the interfacial tension is the dominant driving

force allowing the production of monodispersed emulsion [18]. On the contrary, when the flux was further increased from  $38 \text{ L h}^{-1}\text{m}^{-2}$  to  $100 \text{ L h}^{-1}\text{m}^{-2}$  the increase of particle diameter from  $20 \mu\text{m}$  to  $32 \mu\text{m}$  was observed because of a faster increase of drop size at the opening pore before the detachment. Moreover, when a flux of  $100 \text{ L h}^{-1}\text{m}^{-2}$  was used, a widening of size distribution was also observed because of the increase of  $D(90)$  from  $24 \mu\text{m}$  to  $67 \mu\text{m}$ . This range was defined as “outflow zone”, where the interfacial tension was not dominant and the dispersed phase flows out continuously forming larger droplets.

### *3.3. Microparticle preparation: influence of the volume of dilution medium on shape, surface morphology and size*

The formation of solidified particles is correlated with the solvent removal from the drop that causes the polymer accumulation and solidification at droplet interface forming a polymeric crust. The solvent removal is associated with the diffusion of the solvent from the droplets into the external phase (solvent diffusion) and the evaporation of the solvent at the external phase/air interface (solvent evaporation). These two processes are correlated and the evaporation of the solvent cannot occur without a previous diffusion into the continuous phase. The solvent diffusion was induced by the dilution of the emulsion in a large volume of continuous phase, therefore, changing the volume of water it is possible to control the solidification rate of droplets and the morphology of solidified particles. Since the solubility of dichloromethane in water is known (2%, w/v), the theoretic minimum volume of water required to ensure the complete diffusion of solvent contained in the dispersed phase ( $V_{\text{theoretic}}$ ) was calculated. Considering the percentage of the dispersed phase used for emulsion preparation (12 % v/v) and the polymer concentration (16% w/v), DCM volume ( $V_{\text{DCM}}$ ) was 10.5 ml. The volume of water used to control the solvent diffusion rate ( $V_{\text{sd}}$ ) was progressively reduced respect to the theoretic minimum volume,  $V_{\text{theoretic}}$ , in order to evaluate the effect on microparticles shape, size and morphology. The solidification of the droplets was carried out in three different thermodynamic conditions by changing  $V_{\text{sd}}/V_{\text{theoretic}}$  ratio: a) unsaturated condition ( $V_{\text{sd}} > V_{\text{theoretic}}$ ), where the volume of water was in excess respect to the theoretic volume, therefore a fast solidification of polymer was expected; b) saturated condition ( $V_{\text{sd}} = V_{\text{theoretic}}$ ), where the continuous phase was saturated by the solvent diffused out of droplets and a slower solidification of polymer was expected because the continuous phase was richer in solvent and the solvent evaporation was also involved in the removal of the solvent from the continuous phase; c) oversaturated conditions ( $V_{\text{sd}} < V_{\text{theoretic}}$ ), where the volume of water was below the theoretic volume therefore the organic solvent exceeded its solubility limit and the quantity of solvent diffused into the continuous phase is compensated with the quantity of solvent evaporated at air interface. In this case a slow formation of a polymer crust at the interface was expected because the solvent diffusion rate and the solvent evaporation rate were both involved in the solvent removal. The volume of the continuous phase used for the emulsification process was not considered in the volume used for the

solvent diffusion because it was saturated with solvent. Thus, it did not contribute to the solvent extraction in the post emulsification step. The experimental conditions used and the solidification time of droplets are summarized in Table 1.4.

Table 1.4 Experimental conditions used to carry out the solvent diffusion process at decreased  $V_{sd}/V_{theoretic}$  ratio and the effect on the solidification time of the droplets

| $V_{sd}(L)$ | $V_{sd}/V_{theoretic}$ | Diffusion condition | Droplets solidification time |
|-------------|------------------------|---------------------|------------------------------|
| 4.2         | 6                      | unsaturated         | instantaneous                |
| 2.1         | 3                      | unsaturated         | instantaneous                |
| 1           | 1.4                    | unsaturated         | 0.25 hour                    |
| 0.7         | 1                      | saturated           | 1.5 hours                    |
| 0.35        | 0.5                    | oversaturated       | 2 hours                      |

Results demonstrated that reducing the volume of water available for the solvent diffusion respect to the theoretic volume allowed a prolonged formation time of a polymer solidified crust at the interface because of a slower diffusion of solvent through the droplet. An instantaneous solidification of droplets was observed when the volume of water used was 6 and 3 times the theoretic volume, corresponding to the unsaturated conditions. A slight slowdown of the solidification time of droplets was observed when a volume of water 1.4 times the theoretic volume was used, even though the solvent diffusion was carried out in unsaturated condition. In this case, the volume of water was slightly higher than the theoretic volume (almost saturated condition) therefore the continuous phase used for the solvent diffusion was richer in solvent than the use of highly excess of water retarding the solidification of the polymer at the interface. As expected, a significant increase of the solidification time was observed when the solidification of droplets was carried out in saturated and oversaturated conditions. The process took 1.5 and 2 hours, respectively when the volume of water used was 0.7 and 0.35 L. The solidification time is an important aspect to consider when the drug encapsulation efficiency has to be evaluated. The molecule of interest could be more efficiently retained in microparticles when the rapid formation of a solidified crust occurred because the loss of drug into the continuous phase is reduced [19]. This aspect is significant when the encapsulated drug is soluble in the aqueous phase such as vaccines, proteins, antibiotics and other hydrophilic drugs. In this case the drug is encapsulated in the aqueous core of microcapsules and the rapid formation of the polymeric shell reduced the drug diffusion before the particle solidification.

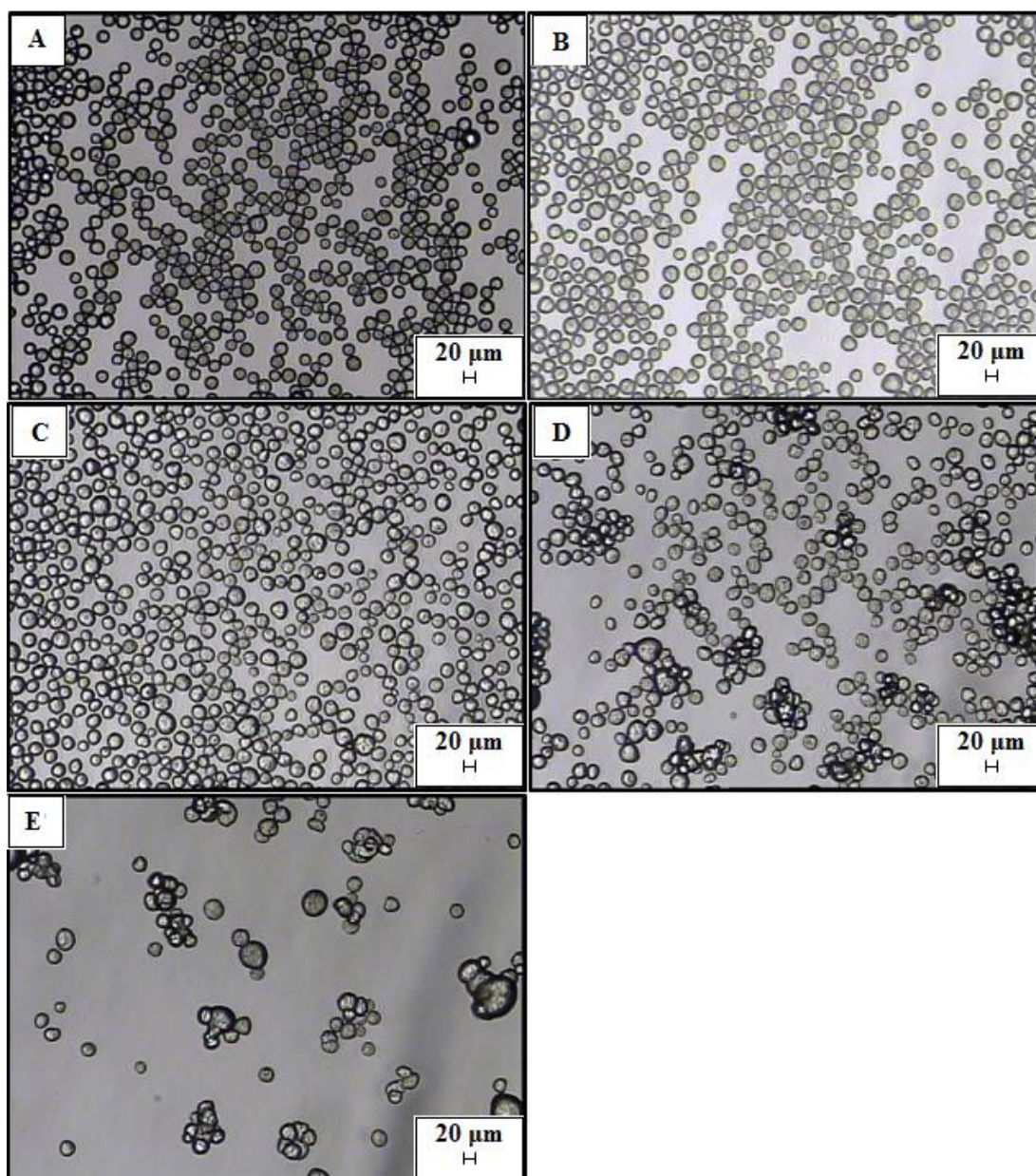


Figure 5.4 Optical microscope pictures of microparticles produced by membrane emulsification/solvent diffusion at decreased  $V_{sd}/V_{theoretic}$ : A)  $V_{sd}/V_{theoretic} = 6$ , B)  $V_{sd}/V_{theoretic} = 3$ , C)  $V_{sd}/V_{theoretic} = 1.4$ , D)  $V_{sd}/V_{theoretic} = 1$ , E)  $V_{sd}/V_{theoretic} = 0.5$ . Microparticles are suspended in aqueous phase with SDS 0,5 %.

In Figure 5.4 is shown the effect of the volume of water used for the solvent diffusion on microparticles shape. The rate of solvent diffusion influenced the shape of particles. Prolonging the solidification time of polymer, the formation of particles that did not keep the spherical shape of the initial oil droplets was observed (photograph C). When the solidification of the polymer was carried out in saturated and oversaturated conditions, droplets coalescence occurred, in addition to the formation of particles with irregular shape. This resulted in the formation of polymeric aggregates (photograph D-E). The long time required to obtain the solidification of polymer at the interface of droplets was responsible of coalescence because it prolonged the unstable condition of droplets owing to the instability of the emulsion during the solidification step.

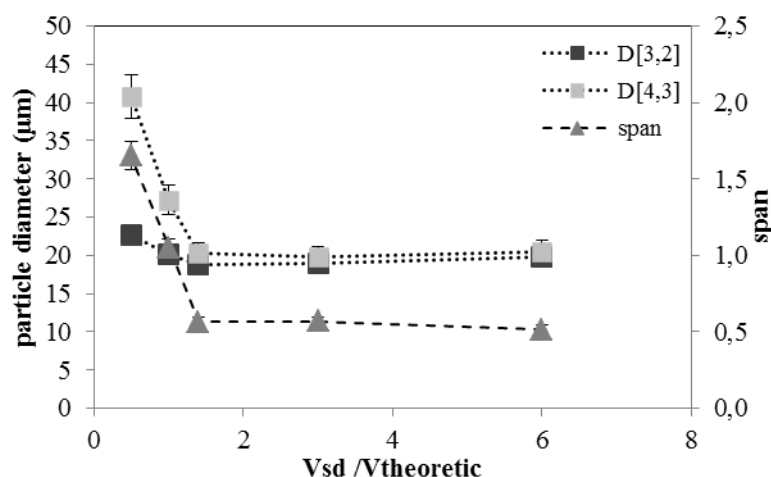


Figure 6.4 Particle size and size distribution of solidified particles at different volume of water

In Figure 6.4 are summarized particle size and size distribution of microparticles obtained with different volumes of water (expressed as  $V_{sd}/V_{theoretic}$  ratio). The particle size and size distribution is controlled at the emulsification step while the volume of water used for the solidification of the droplets (expressed as  $V_{sd}/V_{theoretic}$  ratio) during the post emulsification step affected droplets aggregation and particles shape. In unsaturated conditions ( $V_{sd} > V_{theoretic}$ ), no coalescence occurred and the solidified particles maintained the uniformity of the initial emulsion as demonstrated by a span value of  $0.51 \pm 0.03$ . In saturated ( $V_{sd} = V_{theoretic}$ ) and over-saturated ( $V_{sd} < V_{theoretic}$ ) conditions, the uniformity of the emulsion could not be maintained because coalescence of the droplets occurred before the complete solidification of the polymers. A consequence of the formation of polymeric aggregates was the increase of D[4,3] from 20  $\mu\text{m}$  to 41  $\mu\text{m}$  and span from 0.5 to 1.6. However, the uniformity of shape and size of the oil droplets during the post-emulsification step could be preserved when the solidification of the droplets was carried out in a volume of water capable to ensure a fast solidification of polymer at the interface. Considering the conditions studied in the present work, the minimum volume of water that allowed the control of particle shape and solvent diffusion rate, was 3 times the theoretic volume (photograph A, B). The solidification time of microparticles influenced also the surface morphology as shown in SEM pictures (Figure 7.4).



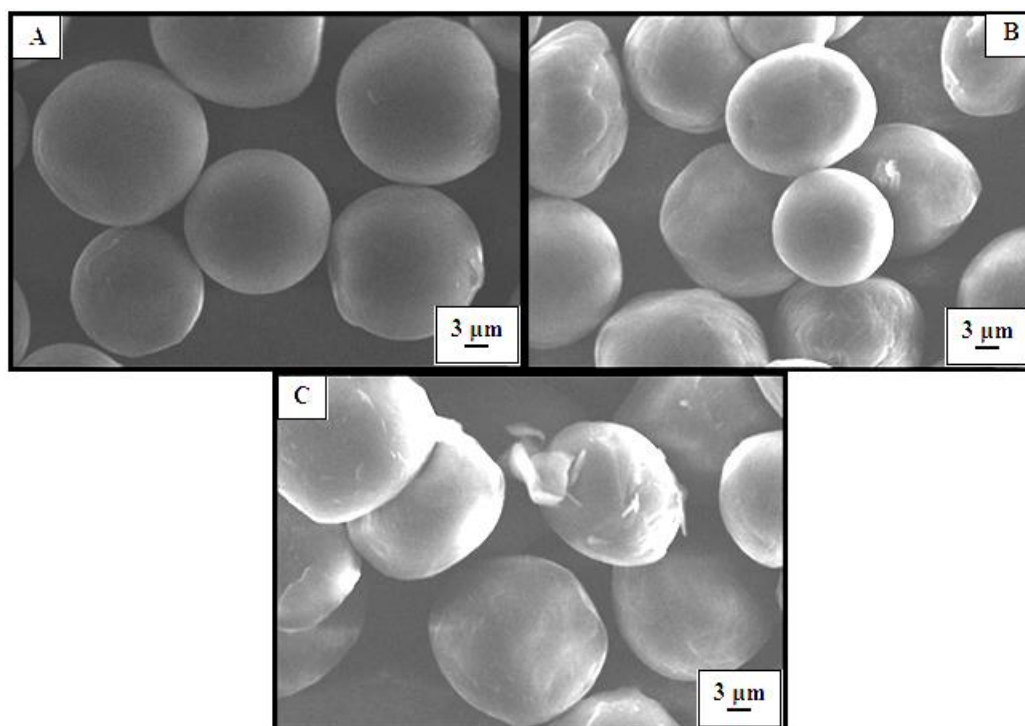


Figure 7.4 SEM pictures of microparticles prepared :A) unsaturated condition ( $V_{sd}/V_{theoretic}$  ratio = 6); B) saturated condition ( $V_{sd}/V_{theoretic}$  ratio = 1); C) oversaturated condition ( $V_{sd}/V_{theoretic}$  ratio = 0.5) of continuous phase

When the solidification process was carried out in saturation and over-saturation conditions, microparticles with a rough and inhomogeneous surface were obtained owing to the slow solvent diffusion rate. When a fast solidification of the polymer occurred by working in unsaturated conditions, microparticles with a smooth and regular surface could be produced.

#### 4. Conclusions

Membrane emulsification combined with solvent diffusion process was successfully applied to prepare uniform polycaprolactone microparticles. The optimization of process and chemical parameters was carried out and uniform microparticles with mean particle size of 20  $\mu\text{m}$  (2 times the pore size of the membrane) and a span value of 0.5 could be produced when the polymeric concentration was maintained in the range 16% - 20%, shear stress of 8.6 Pa and a dispersed phase flux lower than 40  $\text{L h}^{-1}\text{m}^{-2}$ . A shrinkage of 24% of the initial oil droplets compared to the solidified particles was also observed because of the removal of the solvent from the droplets during the post-emulsification step. The solidification time of polymer at droplet interface significantly influenced the spherical shape and surface morphology of microparticles. Microparticles with a spherical shape and smooth surface were produced when a fast solidification of polymer was carried out by using a volume of water that allowed a fast solvent diffusion. Considering the conditions studied in the present work, the minimum

volume of water that allowed the control of the particle shape and surface morphology was 3 times the theoretic volume. The use of smaller volume of water phase should be avoided during the solidification step because of the loss of the initial spherical shape of oil droplets and the formation of polymeric aggregates due to droplet coalescence. The use of membrane emulsification method in combination with the solvent diffusion process makes possible the production of PCL spherical particles with controlled size and size distribution and spherical regular shape.

### *References*

1. Woodruff MA., Hutmacher DW. The return of a forgotten polymer: Polycaprolactone in the 21st century. *Progr. Polym. Sci.* 2010; 35:1217-1256
2. Makadia HK., Hirenkumar K., Siegel SJ. Poly lactic-co-glycolic acid (PLGA) as biodegradable controlled drug delivery carrier. *Polymers.* 2011; 3: 1377-1397
3. Pitt CG., Marks TA., Schindler A. Biodegradable drug delivery systems based on aliphatic polyesters: application to contraceptives and narcotic antagonists. Academic Press: New York.1980; 19-43.
4. Hancock BC., ZOGRAFI GJ. Characteristics and significance of the amorphous state in pharmaceutical systems. *J. Pharm. Sci.* .1997; 86: 1-12.
5. Jameela SR., Suma N., Misra A., Raghuvanshi R., Ganga S., Jayakrishnan A. Poly ( $\epsilon$ -Caprolactone) micropsheres as a vaccine carrier. *Curr. Sci.* 1996; 70:669-671
6. Hombreiro Pérez M., Zinutti C., Lamprecht A., Ubrich N., Astier A., Hoffman M., Maincent P. The preparation and evaluation of poly ( $\epsilon$ -caprolactone) microparticles containing both a lipophilic and a hydrophilic drug. *J. Control. Release.* 2000; 65: 429-438.
7. Dhanaraju MD., Gopinath D., Ahmed MR., Jayakumar R., Vamsadhara CJ. Characterization of polymeric poly (epsilon-caprolactone) injectable implant delivery system for the controlled delivery of contraceptive steroids. *J. Biomedical Mater. Res. Part A* . 2006; 76, 63.
8. Dordunoo SK., Jackson JK., Arsenault LA., Oktaba AM., Hunter WL., Burt HM. Taxol encapsulation in poly(epsilon-caprolactone) microspheres. *Cancer. Chemother. Pharmacol.* 1995; 36:279-282
9. Sinha VR., Bansal K., Kaushik R., Kumria R., Trehan A. Poly- $\epsilon$ -caprolactone microspheres and nanospheres: an overview. *Int. J. Pharm.* 2000; 278: 1-23.

10. Dash TK., Konkimalla V., Badireenath. J. Poly- $\epsilon$ -caprolactone based formulations for drug delivery and tissue engineering: A review. *J. Controll. Release.* 2012; 15:, 15-33.
11. Li M., Rouaud O., Poncelet D. Microencapsulation by solvent evaporation: State of the art for process engineering approaches. *Int. J. Pharm.* 2008; 363: 26-39.
12. Quintanar-Guerrero D., Alléman E., Doelker E., Fessi H. Preparation and characterization of nanocapsules from preformed polymers by a new process based on emulsification-diffusion technique. *Pharm. Res.* 1998; 15: 1056-1062.
13. Quintanar-Guerrero D., Allémann E., Doelker E., Fessi HA mechanistic study of the formation of polymer nanoparticles by the emulsification-diffusion technique. *Colloid Polym. Sci.* 1997; 275: 640-647
14. Champion JA., Katare YK., Mitragotri S. Particle shape: a new design parameter for micro-and nanoscale drug delivery carriers. *J. Control. Release.* 2007; 121: 3-9.
15. Vladisavljević GT., Williams RA. Recent developments in manufacturing emulsions and particulate products using membranes. *Adv. Colloid Interface Sci.* 2005; 113: 1-20
16. Laouini A., Charcosset C., Fessi H., Holdich RG., Vladisavljevic' GT. Preparation of liposomes: A novel application of microengineered membranes from laboratory scale to large scale. *Colloids Surf. B: Biointerfaces.* 2013; 112: 272-278.
17. Liu R., Ma G., Meng, FT., Su ZG. Preparation of uniform-sized PLA microcapsules by combining Shirasu Porous Glass membrane emulsification technique and multiple emulsion-solvent evaporation method. *J. Controll. Release.* 2005; 103: 31-43.
18. Ma G., Nagai M., Omi S. Preparation of uniform poly (lactide) microspheres by employing the Shirasu Porous Glass (SPG) emulsification technique. *Colloids. Surf. A: Physicochem. Eng. Aspects.* 1999; 153: 383-394
19. Wei Q., Wei W., Lai B., Wang LY., Wang YX., Su ZG., Ma GH. Uniform-sized PLA nanoparticles: Preparation by premix membrane emulsification. *International journal of pharmaceuticals.* *Int. J. Pharm.* 2008;359: 294-297.
20. Sawalha H., Purwanti N., Rinzema A., Schroën K., Boom R. Polylactide microspheres prepared by premix membrane emulsification: Effects of solvent removal rate. *J. Membr. Sci.* 2008;310: 484-493.

21. Gasparini G., Kosvintsev SR., Stillwell MT., Holdich RG. Preparation and characterization of PLGA particles for subcutaneous controlled drug release by membrane emulsification. *Colloids Surf. B: Biointerfaces*. 2008; 61: 199-207.
22. Ito F., Honnami H., Kawakami H., Kanamura K., Makino K. Preparation and properties of PLGA microspheres containing hydrophilic drugs by the SPG (shirasu porous glass) membrane emulsification technique. *Colloids Surf. B: Biointerfaces*. 2008; 67: 20-25.
23. Charcosset C., Fessi H. Preparation of nanoparticles with a membrane contactor. *J. Membr. Sci.* 2005; 266: 115-120.
24. Stillwell MT., Holdich RG., Kosvintsev SR., Gasparini G., Cumming IW. Stirred cell membrane emulsification and factors influencing dispersion drop size and uniformity. *Ind. Eng. Chem. Res.* 2007; 46: 965-972.
25. Babak VG., Baros F., Boulanouar O., Boury F., Fromm M., Kildeeva NR. Impact of bulk and surface properties of some biocompatible hydrophobic polymers on the stability of methylene chloride-in-water mini-emulsions used to prepare nanoparticles by emulsification–solvent evaporation. *Colloids Surf. B: Biointerfaces*. 2007; 59: 194-207.
26. Kosvintsev SR., Gasparini G., Holdich RG., Cumming IW., Stillwell MT. Liquid-liquid membrane dispersion in a stirred cell with and without controlled shear. *Ind. Eng. Chem. Res.* 2005; 44: 9323-9330.
27. Kobayashi I., Nakajima M., Mukataka S. Preparation characteristics of oil-in-water emulsions using differently charged surfactants in straight-through microchannel emulsification. *Coll. Surf. A: Physicochem. Eng. Aspects*. 2003; 229:33-41
28. Hassou M., Couenne F., Le Gorrec Y., Tayakout M. Modeling and simulation of polymeric nanocapsule formation by emulsion diffusion method. *AIChE Journal*. 2009; 55: 2094-2105.

# CHAPTER 5

## **Production of multi-core matrix particles from double W/O/W emulsion by membrane emulsification/solvent diffusion process**

### **1. Introduction**

Particle design is a critical determinant of the efficacy of particle-based products in food, chemical, medical and pharmaceutical applications. Many new molecules that are synthesized have poor solubility in aqueous media, and some of them have also poor solubility in lipidic media [1]. Micro and nano-structured systems, such as multiple emulsions, micro/nano solid lipid particles and polymer particles (sphere or capsules) can entrap drugs or biomolecules into their interior structures and/or absorb drugs or biomolecules onto their exterior surfaces improving their bioavailability.

Microcapsules (particles size in the range between 3  $\mu\text{m}$  and 800  $\mu\text{m}$ ) consist of an inner core (in which the active molecule is entrapped) and a shell that covers and protects the core. Capsules can be classified on the basis of the morphology as: i) *reservoir* type (capsule or core-shell) which is composed of a single core with the active agent surrounded by a continuous shell; ii) *matrix* type (poly or multiple core particle) which is characterized by the presence of several reservoir chamber dispersed in one particle. In general hydrophilic material is protected by an hydrophobic shell and hydrophobic material is protected by an hydrophilic shell [2]. The majority of the methods achieved for the preparation of microcapsules are based on the preparation of an emulsified system in the first step, and the solidification of the shell is carried out in a second step. The emulsified system can be a simple O/W or W/O emulsions on the basis of the nature of the core material and the kind of polymer. O/W emulsion is used for the encapsulation of hydrophobic compounds in the core material. Simple W/O emulsion or double W/O/W emulsion are used for the encapsulation of hydrophilic compounds in the core material. In the latter case an aqueous solution of drug is firstly emulsified in an organic phase containing the polymer to form a W/O emulsion. This emulsion is subsequently emulsified in an external continuous phase containing a stabilizer to produce a double W/O/W emulsion. In the post emulsification step, the formation of the shell can be obtained: i) by precipitation or gelation of a polymer around the core (phase separation or coacervation), ii) by polymerization of monomers at the interface of two immiscible phases (interfacial polymerization), iii) by diffusion or evaporation of the solvent with the concomitant solidification of the polymeric shell around the core (solvent diffusion or evaporation) [3]. Important requirements to take into account in designing a microencapsulation process are: i) the possibility to preserve the stability and biological activity of the drug; ii) to produce particle with tailored size and uniformity; iii) to achieve high drug encapsulation efficiency; iiiii) easy scale-up of the process. However, the commonly used techniques are not always suitable in their

original forms for these requirements. Therefore, modifications of existing methods or the development of new techniques is necessary [1].

In this work, membrane emulsification was applied in the emulsification step for the production of uniform W/O/W emulsion to achieve a precise control of the dispersion of the oil droplets which are directly correlated with the size and uniformity of the solidified particles. Subsequently, the solidification of the polymer within the droplet was carried out by the solvent diffusion process, which is easily scalable and allows a good control of particle size and particle morphology. In the emulsification step it was evaluated: i) the influence of the process parameters (dispersed phase flux and shear stress) for the production of simple O/W emulsion using stainless steel membrane with the Dispersion Cell; ii) the influence of phase composition (kind of stabilizer and polymer concentration) on the stability of the primary W/O emulsion and double W/O/W emulsion. In the post emulsification step the influence of the chemical composition of the double emulsion (kind of stabilizer and polymer concentration) on particle uniformity and morphology was evaluated. Two biodegradable polyesters, polycaprolactone (PCL) and poly(lactide-co-glycolide) (PLGA 75:25) were used as matrix material and dissolved into the organic phase of the double emulsion. Biodegradable polymers have been frequently used to encapsulate drugs for controlled and sustained release. This is because a degradation in biocompatible monomers occurred once they are administered into the body due to the environmental conditions [4]. PLGA is the commonest polyesters used for the preparation of spheres and capsules and there are some works in literature regarding the preparation of micro-structured PLGA particles using membrane emulsification process combined with the solvent extraction/evaporation in the post-emulsification step [5–10]. However, decreased drug encapsulation efficiency and coarser morphology have been reported in literature when the solvent is removed by evaporation [11]. Moreover, if the drug molecules are volatile they can be removed at the same time. No works are reported in literature regarding the preparation of poly-caprolactone multi-core matrix particles from W/O/W emulsion using membrane based processes.

## 2. Experimental section

### 2.1. Chemicals

Polycaprolactone (PCL, Sigma-Aldrich, MW 14 kDa) and poly(lactide-co-glycolide) (PLGA 75:25, Lakeshore Biomaterials, MW 29 kDa) were used as hydrophobic polymer and dissolved in the organic phase (O) of the double emulsion using dichloromethane (DCM, Sigma-Aldrich) as organic solvent. Poly-vinyl alcohol (PVA, MW 13-23kDa) was used as emulsifier in the external ( $W_2$ ) aqueous phase previously saturated with DCM to avoid the diffusion of the solvent during the emulsification process. Cold water-fish gelatin (MW 60 kDa) was used as stabilizer in the inner ( $W_1$ ) aqueous phase of the double emulsion. Polyglycerol polyricinoleate (PGPR) and

modified polyether-polysiloxane/dimethicone copolyol (ABIL EM-90) were tested as emulsifier in the organic phase (O). Three different formulations of W/O/W emulsion were tested for the preparation of micro-structured particles and the chemical composition of the phases is reported in Table 1.5. All the aqueous solutions were prepared using ultrapure water with a resistivity of 18.2 M $\Omega$ ·cm.

Table 1.5 Chemical composition of the double W/O/W emulsion used for the preparation of the solid particles

| Inner water phase<br>(W <sub>1</sub> ) | Organic phase<br>(O)                         | Outer water phase<br>(W <sub>2</sub> ) |
|--|--|--|
| cold-water-fish gelatin<br>5-20 % w/v  | PCL in DCM<br>(16-30%, w/v)                  | PVA 1% w/v                             |
| water                                  | PCL in DCM<br>(16-30%, w/v)<br>PGPR 2-4% w/v | PVA 1% w/v                             |
| cold-water-fish gelatin<br>5-20 % w/v  | PLGA (10-30%, w/v)                           | PVA 1% w/v                             |

## 2.2. W/O/W emulsion preparation: membrane emulsification equipment

W<sub>1</sub>/O/W<sub>2</sub> emulsion was prepared by a two-step emulsification procedure. Firstly, a primary W/O emulsion containing 10% of aqueous phase and different concentration of polymer was emulsified using a mechanical homogenizer (Ultra-Turrax®, model T10, IKA Works, USA) for 3 minutes at 30000 rpm. This parameters guarantees small, very well dispersed water droplets in the polymer matrix. A small size is important to avoid inner droplets disruption during the secondary emulsification. The primary emulsion was subsequently used as dispersed phase for the preparation of the double W/O/W emulsion using the Dispersion Cell (Micropore Technologies Ltd., Leicestershire, UK). Micro-sieve flat sheet stainless steel membrane with 10  $\mu$ m circular pore size distributed in a ringed area of 1.85 cm<sup>2</sup> and a porosity of 0.19% was used for the preparation of the double emulsion. Before each experiment the membrane was pre-wetted with the continuous phase by sonication in an ultrasonic bath for 1 min to remove air from the pores and fill them with the continuous phase. After each experiment, the membrane was cleaned in an ultrasonic bath for 1 min in dichloromethane to remove residual polymer on its surface and inside the pores. Subsequently, it was rinsed with a solution of sodium hydroxide (4 M) and distilled water in an ultrasonic bath for 1 min.

### 2.3. Droplet size modeling

There are several forces acting on a growing droplet at the opening pore, the most important in the dynamic ME are the capillary force,  $F_{ca}$ , and the drag force,  $F_d$  (Figure 1.5).

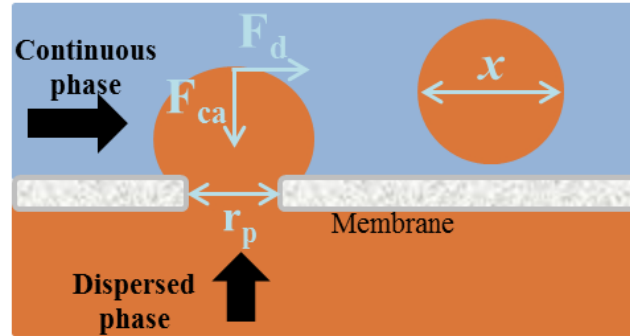


Figure 1.5 Schematic representation of the capillary force and drag force acting on a growing droplet

The capillary force ( $F_{ca}$ ) is the force that retains the drop at the pore opening, and it is a function of the interfacial tension [12].

$$F_{ca} = 2\pi\gamma r_p \quad (1)$$

where  $\gamma$  is the interfacial tension and  $r_p$  is the pore radius. The drag force ( $F_d$ ) is a detaching force and it is correlated with the shear stress produced by the rotation of the stirrer as reported in Equation 2 [12].

$$F_d = 18\pi\tau x\sqrt{x^2 - r_p^2} \quad (2)$$

where  $r_p$  is the pore radius,  $\tau$  is the shear stress and  $x$  is the droplet diameter. The produced droplets diameter ( $x$ ) can be predicted from a force balance of the drag force and the capillary force acting on a deformed droplet growing at the pore during the emulsification process [12-13]

$$x = \frac{\sqrt{18\tau^2 r_p^2 + 2\sqrt{81\tau^4 r_p^4 + 4r_p^2 \tau^2 \gamma^2}}}{3\tau} \quad (3)$$

The shear stress ( $\tau$ )[Pa] at the surface of the membrane depends on the angular velocity ( $\omega$ ) [ $s^{-1}$ ] of the stirrer, which can be regulated by selecting the appropriate voltage via a voltage regulator. The shear over the whole membrane area can be calculated with the following equation [13]

$$\tau_{max} = 0.825\mu_c \omega r_{trans} \frac{1}{\delta} \quad \text{for } r < r_{trans} \quad (4)$$



$$\tau = 0.825\eta\omega r_{trans} \left(\frac{r_{trans}}{r}\right)^{0.6} \frac{1}{\delta} \quad \text{for } r > r_{trans} \quad (5)$$

where  $\mu_c$  [Pa s] is the continuous phase viscosity,  $r_{trans}$  is the transitional radius and  $\delta$  is the boundary layer thickness given from the Landau-Lifshitz equation:

$$\delta = \sqrt{\mu/\omega\rho} \quad (6)$$

For the Dispersion cell the shear stress is not uniformly distributed over the membrane surface and it can be assumed that the maximal shear ( $\tau_{max}$ ) is reached at distance  $r_{trans}$  from the center of the membrane;  $r_{trans}$  is the transitional radius in which the rotation changed from a free vortex to a forced vortex, and can be calculated using Equation 7 [12]:

$$r_{trans} = \frac{D}{2} 1.23 \left(0.57 + 0.35 \frac{D}{T}\right) \left(\frac{b_h}{T}\right)^{0.036} n_b^{0.0116} \frac{Re}{1000+1.43Re} \quad (7)$$

where  $b_h$  is the blade height,  $T$  is the cylinder width,  $D$  is the stirrer width, and  $n_b$  is the number of blades.  $Re$  is the Reynolds Number and it is defined as  $Re = \rho\omega D^2 / 2\pi\eta$ , where  $\rho$  is the continuous phase density and  $\eta$  is the continuous phase viscosity.

#### 2.4. Microparticle preparation

Double W/O/W emulsion/solvent diffusion process was used for the production of the matrix particles. It consists in the addition of the double emulsion into a known volume of fresh aqueous phase with a stabilizer under gentle stirring to induce the diffusion of the solvent from the droplets into the external phase. This leads to the deposition of the polymer around the droplets and a consequent formation of a solid matrix. The resulting samples were decanted in a first step and subsequently recovered by filtration with a vacuum flask. Afterwards, particles were washed 3 times with deionized water and freeze dried. Since the solubility of dichloromethane in water is known (2%, w/v), the theoretic minimum volume of water required to ensure the diffusion of solvent contained in the dispersed phase ( $V_{theoretic}$ ) was calculated. Considering the percentage of the dispersed phase used for emulsion preparation (6 % v/v), the polymer concentration (16-30% w/v) and the percentage of the inner aqueous phase (10% v/v), the volume of DCM was in the range of 4,18 ml and 4,75 ml. The solidification of the particles was carried out using a volume of water 3 times the theoretic volume in order to have a fast solidification of the polymer matrix [14].

#### 2.5. Particle characterization

Oil droplet of simple O/W and double W/O/W emulsion were analyzed using an image analysis system running Scion Image software. Particle size and size distribution of

solidified particle were measured using laser diffraction (Mastersizer 2000, Malvern Instruments, UK). The mean particle size was expressed as the volume median diameter  $D(v, 0.5)$  and the uniformity as span number (see Appendix 1 for the calculation). Three samples were analyzed for each experiment and the reported results are the average of three different experiments.

### 3. Results and discussion

#### 3.1 Influence of process parameters on simple particle production: dispersed injection flux and shear stress

The effect of shear stress and injection flux on particle size and uniformity was evaluated for the production of simple O/W emulsions. This effect was studied using two different polymer solutions, containing PCL or PLGA at two different concentrations corresponding to the highest (30%,wt) and the lowest (16% wt of PCL and 10% wt of PLGA) concentration used for the preparation of the particles. The effect of the injection flux on oil droplet size, particle size and size distribution is reported in Figure 2.5 The effect of this parameter was evaluated keeping constant the shear stress at 8 Pa.

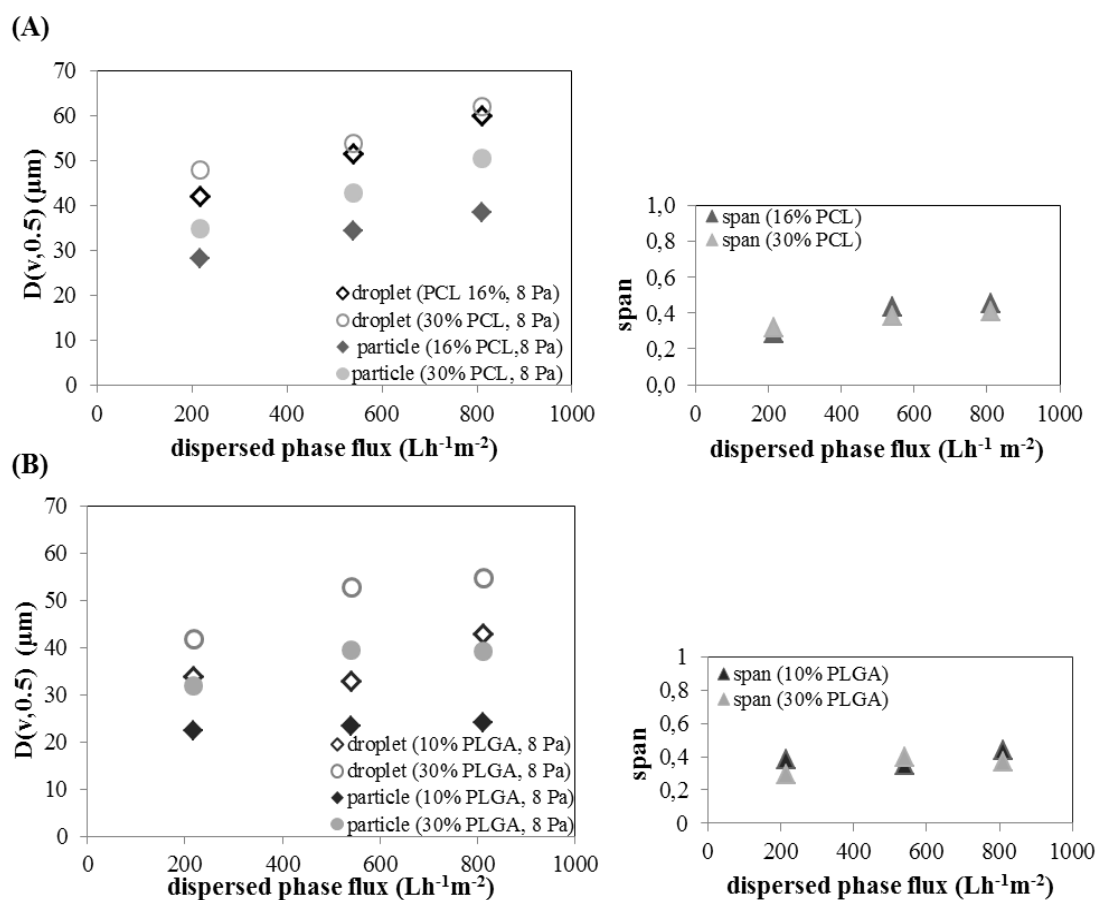


Figure 2.5 Effect of injection flux on particle and droplet size and size distribution of O/W emulsion and solid particles containing: A) PCL (16 and 30% ) in the dispersed phase; B) PLGA ( 10 and 30% ) in the dispersed phase

An increase of particle size from 28  $\mu\text{m}$  to 38  $\mu\text{m}$  and from 35  $\mu\text{m}$  to 50  $\mu\text{m}$  was observed when the dispersed phase flux was increased in a range between 220  $\text{Lh}^{-1}\text{m}^{-2}$  and 810  $\text{Lh}^{-1}\text{m}^{-2}$  using a dispersed phase with 16% and 30% of PCL respectively (Figure 2.5,A). A good uniformity in a range between 0.30 and 0.45 was maintained in the same range of flux. The mean size of PLGA particles produced in the same range of flux showed a slight increase in a range of 32  $\mu\text{m}$  and 39  $\mu\text{m}$  when 30% of PLGA was used in the dispersed phase (Figure 2.5,B). No significant variation was observed when 10% of PLGA was used and particle with a mean size of 23  $\mu\text{m}$  were produced (B). A good uniformity of the particles in a range between 0.30 and 0.39 was maintained in the same range of flux. The increase of the dispersed phase flux is correlated with a faster increase of droplet growth at the pore level resulting in larger droplet before the detachment. In addition, when the drop grows faster the interface cannot be stabilized fast enough by adsorbed emulsifier molecules, so the interfacial tension decreases slowly and the droplet grows to a larger diameter before it detaches from the pore [15]. The different effect of the injection flux on PCL and PLGA particle size can be explained considering the chemical structure of the polymers. PLGA is characterized by the presence of more polar groups (carbonyl groups and carboxylic end groups) that may interact at the water/oil interface resulting in an improvement of the stability of the system. In this way the faster growth of the droplet is negligible compared to the interface stabilization. Particle shrinkage was also observed for both the particles produced with PLGA and PCL. Quite similar shrinkage of 34% and 40% was measured for the particles prepared with 16% and 10% of PCL and PLGA respectively, while a lower shrinkage of 22% and 26% was observed for the particles prepared with 30% of polymer concentration. The particle reduction is a consequence of the removal of the solvent through the droplets in the solidification step and it is proportional with the amount of solvent within the droplet.

In Figure 3.5 is reported the effect of shear stress on particle size and size distribution of oil droplets and solidified particles produced keeping constant the injection flux at 216  $\text{Lh}^{-1}\text{m}^{-2}$ . The shear stress was increased by increasing the speed rotation of the paddle stirrer in a range of 420 rpm and 1550 rpm.

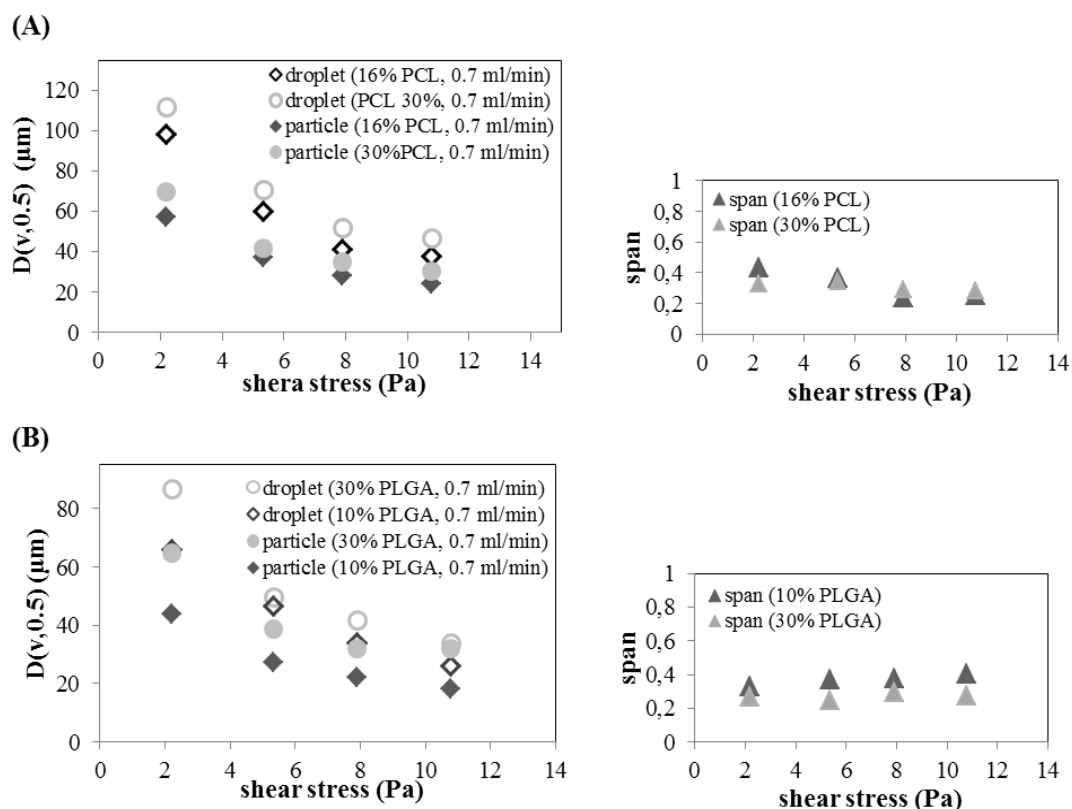


Figure 3.5 Effect of the shear stress on particle and droplets size and size distribution of O/W emulsion and solid particles containing: A) PCL (16 and 30%) in the dispersed phase; B) PLGA (10 and 30%) in the dispersed phase

A decrease of droplet size in a range of 112  $\mu\text{m}$  and 40  $\mu\text{m}$  (which corresponds to the production of solidified PCL particles in a range of 70  $\mu\text{m}$  and 25  $\mu\text{m}$ ) was observed with the increase of the shear stress in a range of 2 Pa and 11 Pa (A), keeping a good uniformity with a span in a range between 0.38 and 0.30 when the lowest and the highest shear stress were applied. Moreover, the size distribution of PCL particle was not affected by polymer concentration. PLGA droplet size reduced from 90  $\mu\text{m}$  to 25  $\mu\text{m}$  (which corresponds to solidified particles with a mean size between 65  $\mu\text{m}$  and 18  $\mu\text{m}$ ) in the same range of shear stress (B). An improvement of particle size distribution from 0.37 ( $\pm 0.01$ ) to 0.27 ( $\pm 0.01$ ) was observed when PLGA concentration was increased from 10% to 30%. The decrease of droplet size is correlated with an increase of the drag force acting on the droplets that were detached sooner. This effect is more significant when shear stress lower than 6 Pa is applied while the median drop size is virtually independent on the drag force at shear stress higher than 6 and droplets almost 4 and 2 times the pore size of the membrane could be produced when PCL and PLGA polymer solution were used respectively.

The decrease of droplet size is in good accordance with the predicted model (Equation 3) reported in Figure 4.5 for both kind of formulations. The droplet size produced with PCL in the organic phase fits better at lowest shear stress while the droplet size produced with PLGA in the organic phase fits better at highest shear stress.

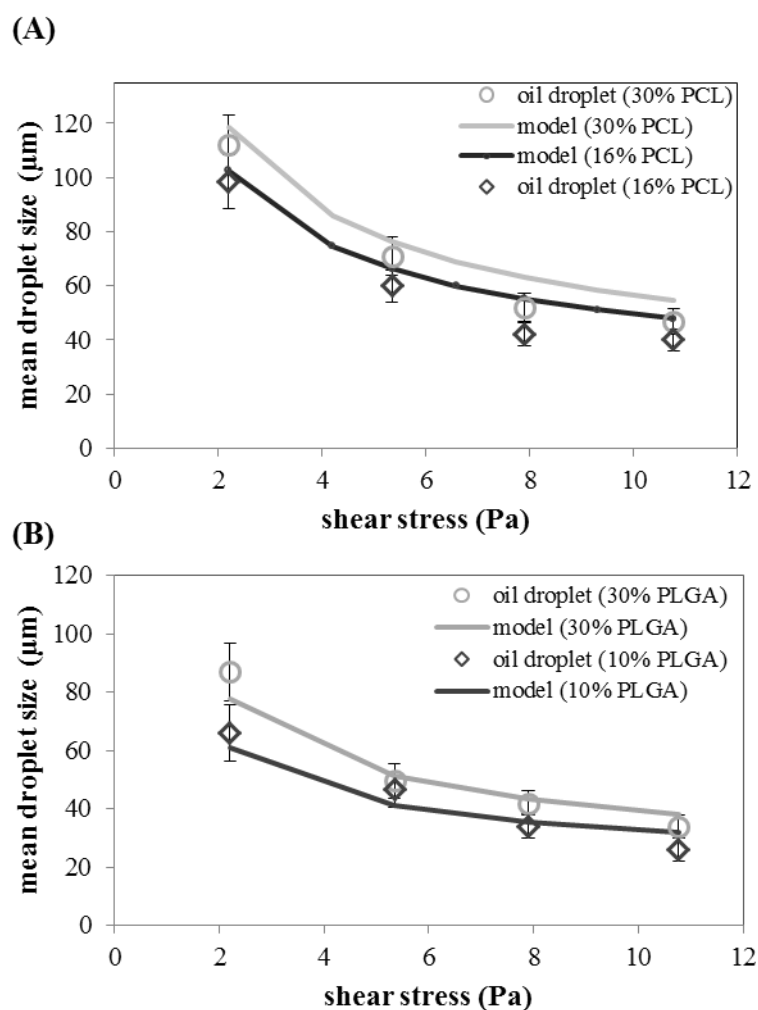


Figure 4.5 Droplet size and the predicted model against the shear stress: A) PCL (16 and 30%) in the dispersed phase; B) PLGA (10 and 30%) in the dispersed phase

The model can be influenced by the physical properties of the phases: density and viscosity of the continuous phase and the interfacial tension. The viscosity was assumed equal to the pure water although the presence of 1% of PVA and DCM did not affect significantly the value. The difference in density between the phases that affects the buoyancy force is negligible because of the presence of high agitation and small diameter. Therefore, the empirical determination of the interfacial tension is an important parameter that can affect the model. This parameter was measured using the Du Noüy ring method (see Appendix 1). During the measurement, DCM in the water phase can evaporate at air/water interface and fresh DCM can diffuse from the oil into the water phase affecting the measurements. This can explain the high standard deviation of the measurements of the interfacial tension of the system organic/water phase reported in Table 2.5. The experimental error of the measurements of the interfacial tension influenced also the fitting of the predicted droplet size of the model with the experimental data.

Table 2.5 Effect of polymer kind and polymer concentration on the interfacial tension at organic/water interface

| Organic phase<br>(polymer in DCM), % | Water phase<br>(saturated with DCM) | $\gamma$<br>(mN/m) |
|--------------------------------------|-------------------------------------|--------------------|
| 5 (PCL)                              | 1% PVA                              | 2.5±0.5            |
| 16 (PCL)                             | 1% PVA                              | 3.4±0.3            |
| 20 (PCL)                             | 1% PVA                              | 3.9±0.2            |
| 30 (PCL)                             | 1% PVA                              | 4.2±0.3            |
| 10 (PLGA)                            | 1% PVA                              | 0.9±0.2            |
| 30(PLGA)                             | 1% PVA                              | 1.5±0.1            |

The increase of polymer concentration in the organic phase produced a slight increase of the interfacial tension for both kind of polymer as reported in the Table 2.5. This increase can be probably due to an increase of the hydrophobicity of the organic phase which is less “wetted” by the aqueous phase when the amount of polymer at the interface was increased. The lower value of interfacial tension for the system containing PLGA in the organic phase can be correlated with the chemical structure of the polymer characterized by the presence of functional groups (more polar carbonyl groups and carboxyl groups) that adsorbs at water/oil interface resulting in an improvement of the stability of the interface. In membrane emulsification, a consequence of the increase of the interfacial tension is the increase of droplet size as reported in Figure 4.5. This is because the higher interfacial tension keeps the droplet adhesion at the edge of the pore retarding the detachment.

### 3.2. Influence of the chemical composition on the stability of the primary W/O emulsion

The stability of the primary W/O emulsion is of great importance to improve the encapsulation of the inner aqueous droplet into the double emulsion. The latter is thermodynamically unstable and the inner aqueous phase can separate easily resulting in lower encapsulation. PCL is not a good stabilizer as demonstrated by the high value of interfacial tension between water and the polymer solution ( $20 \pm 3$  mN/m) reported in Figure 5.5. Therefore, it is necessary to improve the stability of the system reducing the interfacial tension in order to retard the phase separation between the inner water phase and the organic phase. Phase separation could be retarded by the addition of an emulsifier in the organic phase or a stabilizer in the inner aqueous phase. Two oil soluble emulsifiers (PGPR and Abil EM-90) and a water soluble stabilizer (cold-water fish gelatin) were individually tested for the preparation of the primary W/O emulsion containing different concentration of PCL in the organic phase. The formulations used in this study are reported in Table 3.5.



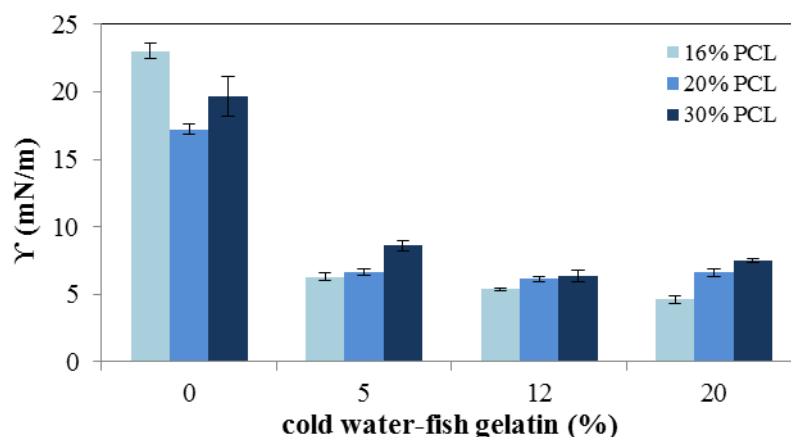


Figure 5.5 Influence of cold water-fish gelatin on the interfacial tension at water/oil interface containing PCL in the organic phase

In Figure 6.5 is reported the interfacial tension at water/oil interface in presence of different concentration of PGPR, Abil EM-90 and PCL. PGPR is a poly-glycerol ester of fatty acid widely used in food industry as oil soluble emulsifier and Abil EM 90 is a non ionic silicon emulsifier especially used in the cosmetic field. It is basically an hydrophilic modified silicone polymer with high flexibility that allow to achieve an orientation at the interface. The addition of Abil EM-90 in the organic phase did not improve significantly the stability of the primary emulsion as demonstrated by a reduction of the interfacial tension of just 20%, no matter what concentration of polymer was used. On the contrary, the addition of PGPR allowed a reduction of the interfacial tension of 76%. Moreover, the interfacial tension decreased from 6.2 ( $\pm 0.3$  mN/m) to 4.7 ( $\pm 0.2$  mN/m) with the increase of PGPR concentration up to 2%.

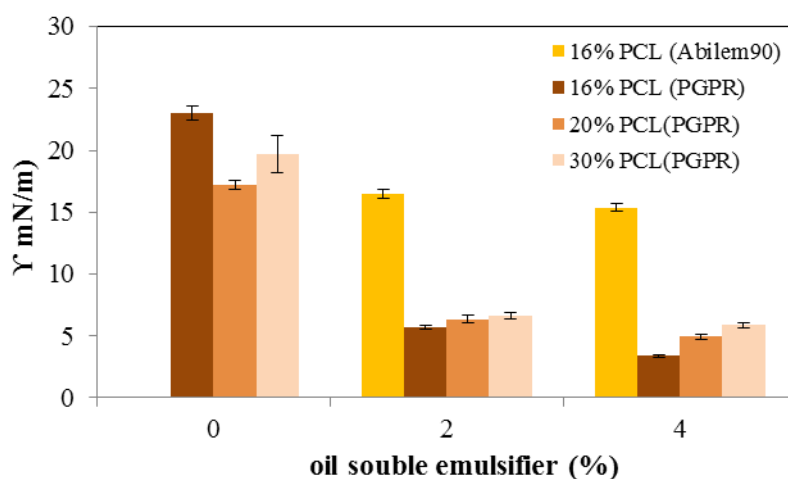


Figure 6.5 Influence of PGPR and Abil em-90 on the interfacial tension at water/oil interface containing PCL in the organic phase

PGPR is a powerful emulsifier for the preparation of stable W/O emulsion thanks to the excellent water-binding capacity of the long hydrophilic poly-glycerol chains. It is also

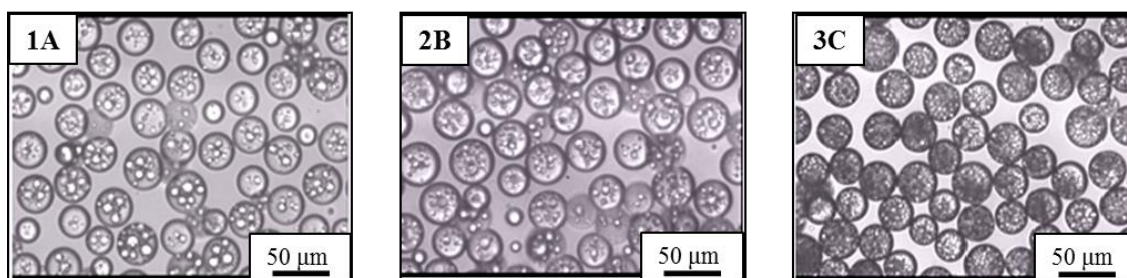


characterized by a lower HLB value compared to ABIL em-90 and this is correlated with a higher compatibility of the emulsifier with the oil phase.

### 3.3. Influence of the chemical composition on the stability of the double W/O/W emulsion

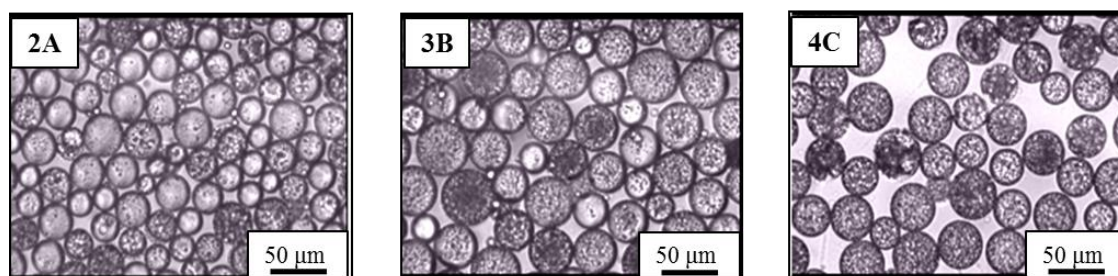
Multiple emulsion is a quite complex and delicate system that can easily destabilize. In this study, the influence of the chemical composition on the stability of the double emulsion was evaluated by optical microscopy observation of the emulsion droplets right after the emulsification process. In particular it was evaluated the influence of the polymer concentration (PCL) and the kind of stabilizer (fish gelatin and PGPR) used for the preparation of the primary W/O emulsion. In figure 7.5 are reported the photographs of double emulsions produced with different concentration of PCL and different stabilizer (fish gelatin or PGPR).

#### COLD WATER-FISH GELATIN



$W_1$ : 5% fish gelatin;  $O$ : PCL in DCM;  $W_2$ : 1% PVA

#### PGPR



$W_1$ : pure water;  $O$ : 4% PGPR with PCL in DCM;  $W_2$ : 1% PVA

Figure 7.5 Photographs of double  $W_1/O/W_2$  emulsion with different concentration of polymer in the organic phase: A) 16% PCL in DCM; B) 20% PCL in DCM; C) 30% PCL in DCM

The concentration of PCL in the organic phase was progressively increased keeping constant the concentration of fish gelatin in the inner aqueous phase or the concentration of PGPR in the organic phase. In the photographs of the emulsions produced with fish gelatin as stabilizer and with 16 % and 20% of PCL (1A, 2B) coalescence of the inner aqueous droplets was observed, while concentrated small droplets of inner aqueous phase were observed when 30% of PCL was used in the organic phase (3C). Gelatin

demonstrated to reduce the interfacial tension at water/oil interface, but it is also known to be a weaker emulsifier, thus destabilization of the system can occur if low concentration of polymer are used in the continuous phase. In the photographs of the double emulsion produced with PGPR as stabilizer coalescence was not observed and an increase of the encapsulation of the inner aqueous droplets was achieved with the increase of polymer concentration (2A, 3B, 4C). In this case the partial loss of the inner aqueous phase observed when low concentration of PCL is dissolved in the organic phase (2A) can be correlated with a transfer of some internal dispersed phase to the external continuous phase. The oil phase of a W/O/W emulsion is a sort of liquid 'membrane' which separates the internal and external aqueous phases. The increase of polymer concentration increases the viscosity of the organic phase where the aqueous droplets are dispersed reducing the possibility of coalescence of the internal phase or the mixing with the external aqueous phase [18].

#### *3.4. Influence of the chemical composition of the double emulsion on particle size and particle shape of PCL matrix particles*

The effect of the volume of water used for the solvent diffusion on the solidification rate of the polymer and the shape of simple PCL particles was already discussed in chapter 4. In this paragraph the influence of the formulation of the double emulsion on particle shape and size will be discussed for the preparation of PCL matrix particles. In Fig. 8.5 is reported the effect of the kind of stabilizer and the concentration of polymer on particle size and uniformity of the double emulsion and solid particles, keeping constant the process parameters at injection flux of  $216 \text{ Lh}^{-1}\text{m}^{-2}$  and shear stress of 11 Pa. Solidified particles with a mean size in the range of 21  $\mu\text{m}$  and 30  $\mu\text{m}$  (corresponding to droplet size in a range of 32  $\mu\text{m}$  and 42  $\mu\text{m}$ ) were obtained with the increase of PCL concentration from 16% to 30%. This effect was also observed previously for the production of simple particles from O/W emulsion.

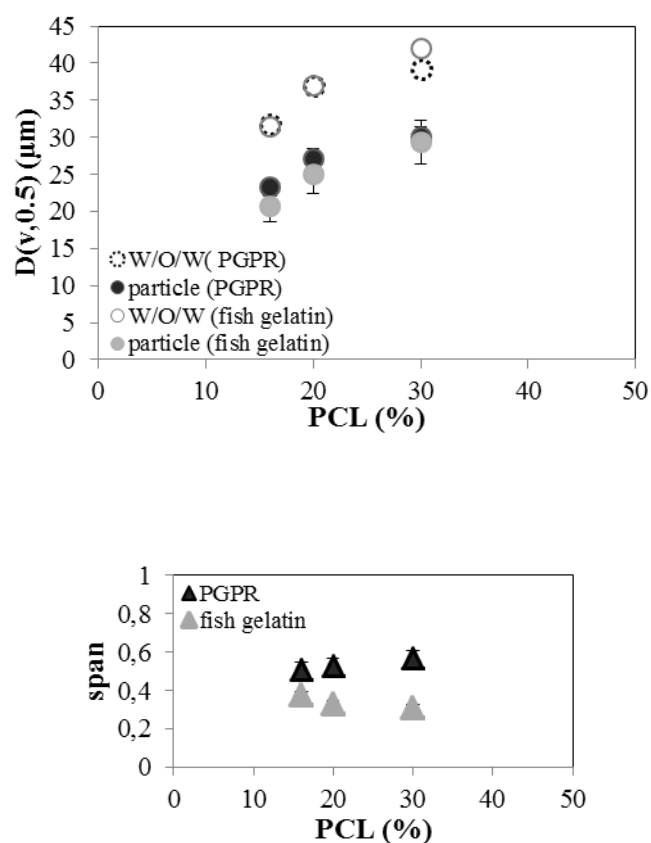


Figure 8.5 Particle size and size distribution of W/O/W emulsion and matrix particles produced with different concentration of PCL (16-30%) and different stabilizer (5% fish gelatin or 4% of PGPR)

A shrinkage of the droplet size of about 30% and 26% was also measured for the matrix particles produced in the same range of PCL concentration. The particle reduction is slightly lower compared to the simple particles and this can be due to the presence of the inner aqueous phase entrapped in the polymeric matrix. The kind of stabilizer of the double emulsion did not influence significantly the particle size while it affected the size distribution of solidified particles. More uniform particles with a span value of  $0.32 \pm 0.03$  were produced when fish gelatin was used as stabilizer in the inner aqueous phase whereas particles with a span value of  $0.53 \pm 0.03$  were produced when PGPR was used as stabilizer in the organic phase. Since the solidification of the droplets was carried out in water, the poly-glycerol chains of PGPR can be exposed into the water phase at the oil/external aqueous interface promoting the transport of water between the outer and inner aqueous phase of the droplets with a consequent formation of particles less uniform and with irregular shape as showed in Figure 9.5 (A,B,C). Some particles lost their integrity as highlighted in the red circles in the photographs (A,B,C). On the contrary, particles produced with fish gelatin in the inner aqueous phase preserved the integrity of the initial droplet, resulting in the production of particles with a more uniform shape as showed in Figure 9.5 (D,E,F). In this case the spherical shape of the initial droplets was preserved better when the polymer concentration was increased. The particles produced with 16% of PCL are characterized by an elongated shape (D) while the particles produced with 30% of PCL have a better spherical shape (F). This can be

due to the formation of a more rigid and thick matrix structure in the solidification step when higher amount of polymer was dissolved in the organic phase. We can assume that the particles produced from W/O/W emulsion are associated with the formation of a multicore-internal structure due to the dispersion of the aqueous phase in the polymer solution. Moreover, when the solidification of the polymer within the droplets is fast the coalescence of the internal aqueous phase can be avoided resulting in a porous internal structure of the particles as reported in literature [19,20].

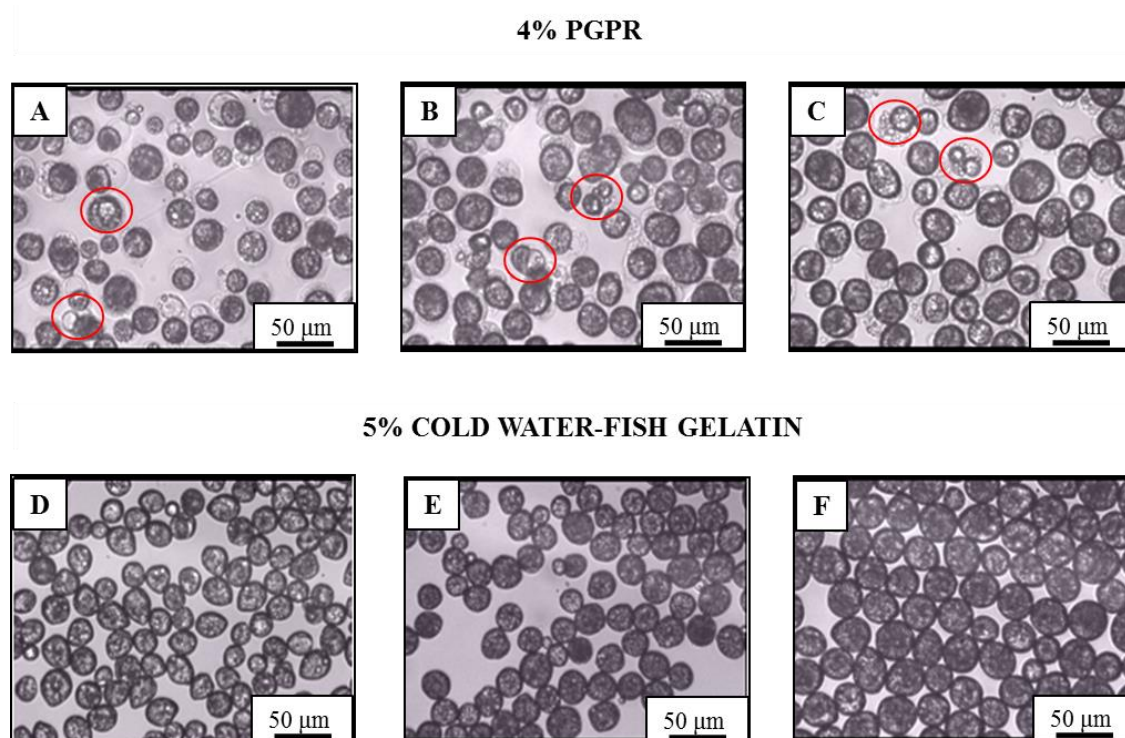


Figure 9.5 Photographs of matrix particles produced with different concentration of polymer and different stabilizer. A-B-C (4% PGPR), 16-20-30% of PCL in DCM; D-E-F (5% fish gelatin):16-20-30% of PCL in DCM. Solidification conditions:  $V_{sd}=3V_{th}$  and SDS as stabilizer

### 3.5. Effect of the polymer concentration on particle size and size distribution of PLGA matrix particles

The preparation of PLGA particles was carried out using fish gelatin (5%) as stabilizer and the same solidification conditions ( $V_{sd}=3V_{th}$ ) used for the preparation of PCL particles. In Figure 10.5 is reported the influence of the polymer concentration on particle size and size distribution of droplet size and solidified particles, keeping constant the process parameters at injection flux of  $216 \text{ Lh}^{-1}\text{m}^{-2}$  and shear stress of 11 Pa. An increase of polymer concentration is correlated with an increase of particle size as previously discussed. Particles in a range of  $22 \mu\text{m}$  and  $32 \mu\text{m}$  (which corresponds to droplet size in a range of  $34 \mu\text{m}$  and  $42 \mu\text{m}$ ) were produced with an increase of PLGA concentration from 10 % to 30%.

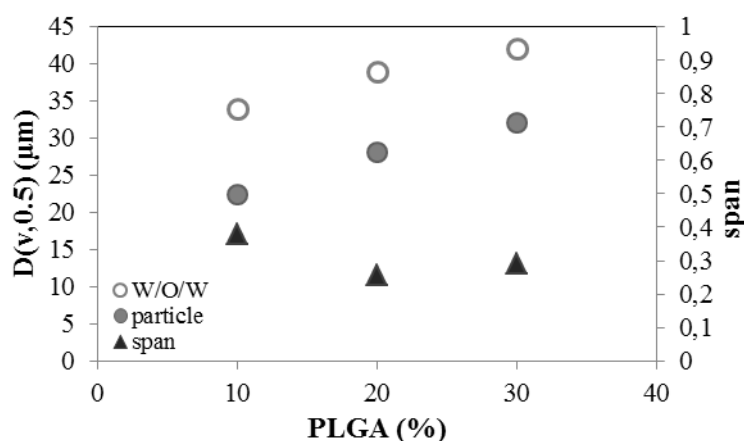


Figure 10.5 Particle size and size distribution of W/O/W emulsion droplets and matrix particles produced with different concentration of PLGA (10-30%) and 5% of fish gelatin in the inner aqueous phase.

A shrinkage of the solid particles compared with the droplet size was measured corresponding to 34% and 24% when the lowest and the highest concentration of PLGA was used respectively. The size distribution of the particles slightly reduced from 0.38 to 0.29 with the increase of polymer concentration. The particles preserved the spherical shape of the initial oil droplet as showed in the photographs in Figure 11.5.

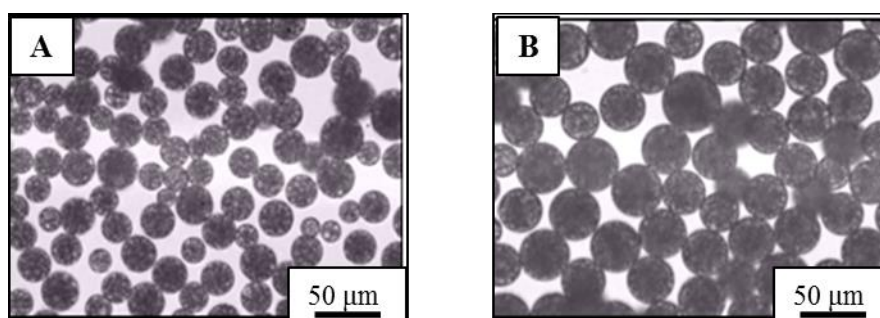


Figure 11.5 Photographs of matrix particles produced with fish gelatin and PLGA 10% (A) and 30% (B). Solidification conditions:  $V_{sd} = 3V_{th}$  and PVA as stabilizer

Aggregation of the particles was observed during the solidification when SDS (2%) was used as stabilizer in the aqueous phase, probably due to the formation of polymer-surfactant complex onto the polar side groups of the polymer chain [19]. For this reason, PVA was used as stabilizer in the water phase for the solvent diffusion process and aggregation was not observed.

#### 4. Conclusion

Highly uniform multi-core matrix particles between 18  $\mu\text{m}$  and 70  $\mu\text{m}$  were successfully produced by membrane emulsification/solvent diffusion process. The use of membrane emulsification allowed the precise control of droplet size and uniformity of the double emulsion. The stability of the primary W/O emulsion was improved using

fish gelatin as inner aqueous phase or PGPR in the organic phase as demonstrated by the reduction of the interfacial tension of 70% and 76% respectively. Quite stable double W/O/W emulsions were produced combining the stabilizer property of PGPR or fish gelatin with high concentration of polymer in the organic phase (30%). The fast solidification of the polymer matrix in the post emulsification step allowed to preserve the uniformity of the particles and the shape of the initial oil droplet when fish gelatin was used as stabilizer in the inner aqueous phase. A shrinkage of the particle in a range between 36% and 24% was observed when the lowest (10% and 16%) and the highest (30%) polymer concentration was used respectively. This shrinkage is a consequence of the solvent removal from the droplet during the solidification of the particles. The multi-core matrix particles produced in this work are characterized by an hydrophobic matrix material and hydrophilic core material, therefore they can be potentially used for the simultaneous encapsulation of water soluble and oil soluble compounds.

### *References*

1. Benita S. Microencapsulation. Methods and Industrial Application. CRC 2005.
2. Zuidam NJ, Shimoni E. Overview of Microencapsulates for Use in Food Products or Processes and Methods to Make Them. New York. 2010;3–30.
3. Jyothi NVN, Prasanna PM, Sakarkar SN, Prabha KS, Ramaiah PS, Srawan GY. Microencapsulation techniques, factors influencing encapsulation efficiency. *J Microencapsul.* 2010;27(3):187–97.
4. Nair LS, Laurencin CT. Biodegradable polymers as biomaterials. *Prog Polym Sci.* 2007;32(8-9):762–98.
5. Liu R, Huang S-S, Wan Y-H, Ma G-H, Su Z-G. Preparation of insulin-loaded PLA/PLGA microcapsules by a novel membrane emulsification method and its release in vitro. *Colloids Surf B Biointerfaces.* 2006;51(1):30–8.
6. Gasparini G, Kosvintsev SR, Stillwell MT, Holdich RG. Preparation and characterization of PLGA particles for subcutaneous controlled drug release by membrane emulsification. *Colloids Surf B Biointerfaces.* 2008 ;61(2):199–207.
7. Liu R, Huang S-S, Wan Y-H, Ma G-H, Su Z-G. Preparation of insulin-loaded PLA/PLGA microcapsules by a novel membrane emulsification method and its release in vitro. *Colloids Surf B Biointerfaces.* 2006;51(1):30–8.
8. Ito F, Honnami H, Kawakami H, Kanamura K, Makino K. Preparation and properties of PLGA microspheres containing hydrophilic drugs by the SPG (shirasu porous glass) membrane emulsification technique. *Colloids Surf B Biointerfaces.* 2008;67(1):20–5.

9. Ito F, Fujimori H, Honnami H, Kawakami H, Kanamura K, Makino K. Study of types and mixture ratio of organic solvent used to dissolve polymers for preparation of drug-containing PLGA microspheres. *Eur Polym J*. 2009;45(3):658–67.
10. Ito F, Makino K. Preparation and properties of monodispersed rifampicin-loaded poly(lactide-co-glycolide) microspheres. *Colloids Surf B Biointerfaces*. 2004;39(1-2):17–21.
11. Li M, Rouaud O, Poncelet D. Microencapsulation by solvent evaporation: state of the art for process engineering approaches. *Int J Pharm*. 2008;363(1-2):26–39.
12. Kosvintsev SR, Gasparini G, Holdich RG, Cumming IW, Stillwell MT. Liquid - Liquid Membrane Dispersion in a Stirred Cell with and without Controlled Shear. *Ind Eng Chem Res*. 2005;9323–30.
13. Stillwell MT, Holdich RG, Kosvintsev SR, Gasparini G, Cumming IW. Stirred Cell Membrane Emulsification and Factors Influencing Dispersion Drop Size and Uniformity. *Ind Eng Chem Res*. 2007;46(3):965–72.
14. Imbrogno A, Piacentini E, Giorno L. Preparation of uniform poly-caprolactone Microparticles by membrane emulsification/ solvent diffusion process. *J Memb Sci*. 2014; 467: 262–268
15. Schro V. Production of emulsions using microporous, ceramic membranes. *Colloids Surfaces A Physicochem Eng Asp*. 1999;152:103–9.
16. Surh J, Decker E, McClements D. Properties and stability of oil-in-water emulsions stabilized by fish gelatin. *Food Hydrocoll*. 2006;20(5):596–606.
17. Karim a. a., Bhat R. Fish gelatin: properties, challenges, and prospects as an alternative to mammalian gelatins. *Food Hydrocoll*. 2009;23(3):563–76.
18. Alex R, Bodmeier R. Encapsulation of water-soluble drugs by a modified solvent evaporation method. I. Effect of process and formulation variables on drug entrapment. *J Microencapsul*. 1990;7(3):347–55.
19. Yang YY, Chung TS, Ng NP. Morphology, drug distribution, and in vitro release profiles of biodegradable polymeric microspheres containing protein fabricated by double-emulsion solvent extraction/evaporation method. *Biomaterials*. 2001;22(3):231–41.
20. Schugens C, Laruelle N, Nihant N, Grandfils C, Jkrome R, Teyssi P. Effect of the emulsion stability on the morphology and porosity of semicrystalline poly-lactide

microparticles prepared by w / o / w double emulsion-evaporation. J Control Release. 1994;32(94):161–76.

21. Jones MN. The interaction of sodium dodecyl sulfate with polyethylene oxide. J Colloid Interface Sci. 1967;23(1):36–42.



# CHAPTER 6

## **Pulsed back-and-forward membrane emulsification for the production of micro and nanoparticles for pharmaceutical application**

### **1. Introduction**

Micro and nanoparticles are defined as particulate dispersions or solid particles with a size in the range of 1-1000  $\mu\text{m}$  and 10-1000 nm, respectively. In recent years, micro-nanoparticles have been used as potential drug delivery devices because of their unique advantages including: i) the manipulation of particle size and surface characteristics of particles to achieve drug targeting, ii) the control and sustain release of drug at the target site to achieve an increase in drug therapeutic efficacy and reduction in side effects, iii) the modulation of controlled release and the characteristics of particle degradation by the choice of matrix constituents, iv) the use for various routes of administration including oral, nasal, parenteral, intra-ocular etc. [1]. The drug can be dissolved, entrapped, encapsulated or attached to the particle matrix. For specific therapeutic interests, particles may be administered through different routes. An accurate control of particle size is especially required for parenteral administration. In this case, the size of particles distributed into the bloodstream must be significantly smaller than 5  $\mu\text{m}$ , because the smallest capillaries in the body are 5–6  $\mu\text{m}$  in diameter and the injection of bigger particles can cause embolism [2].

Despite the great potentials of particulate systems, further advances are necessary in order to turn the concept of target particles technology into a realistic practical application as advanced drug delivery system. Actually, most of the methods used for the preparation of micro and nanoparticles include two main steps. The preparation of an emulsified system occurred in the first step, whereas the solidified particles were formed during the second step of the process. The first step is crucial to design particles with controlled size. In the post-emulsification step, the solidified particles can be obtained by the precipitation of preformed polymer within the droplet or by polymerization of monomer contained within the droplet. The precipitation of the polymer with the concomitant formation of two immiscible phases (a polymer rich phase and a polymer poor phase) is achieved after a perturbation of the equilibrium of the system. The latter can be carried out by : i) addition of salt (salting out) in the polymer solution in order to induce a desolvation of the polymer that precipitates; ii) variation of pH in the case of polymer solution that has a water solubility pH dependent (polymer gelation); iii) addition of a third component (non solvent) to induce the demixing of the polymer solution (solvent diffusion); iiiii) evaporation of volatile solvent from the organic phase with the precipitation of the polymer within the droplet (solvent evaporation). The preparation of particles by polymerization method involved the activation of the initiator within the droplets or in alternative the initiator can be

added into the emulsion [3,4]. Simple and reproducible techniques, suitable for large scale production are important requirements for the industrial applicability of a particle preparation methodology. Moreover, the development of a technique that allows the incorporation of biomolecules without affecting their activity is of crucial importance in order to preserve their bioactivity [5]. During the last decade, progresses were mainly focused on the improvement of existing methods thanks to the innovation of the emulsification methods. Particulate systems such as spheres, beads, capsules have been prepared in a micron range [6] by using membrane emulsification (ME) technology, whereas few works are reported for the preparation of particles in submicron range [7-11].

Cross-flow ME and premix ME are the membrane-based processes generally used for particles preparation at large scale, however some disadvantages still limit their applicability. Two important factors responsible of particles damage or breakage when using shear sensitive materials are the mechanical stress generated by the continuous recirculation of the emulsions along the circuit and the pump in cross-flow ME and the repeated passage of the emulsion through the membrane in premix ME [12-14]. In this work, we investigated the preparation of micro and nano polymeric particles by using pulsed back-and-forward membrane emulsification [15] for application in pharmaceutical field. Pulsed back-and-forward ME is particularly attractive for the production of fragile particulate products because its configuration offers the possibility to produce uniform emulsions by applying lower shear conditions compared to the other conventional ME suitable for industrial application, such as cross-flow ME. In this way no damage of the formed droplets occurred during the emulsification process because the breakage or coalescence of the droplets (due to the recirculation of the emulsion in the pump and along the circuit for long time) were eliminated. The above mentioned technology was used for the preparation of uniform polycaprolactone (PCL) micro and nanoparticles suitable for parenteral administration. The fluid-dynamic conditions suitable for controlled particle production were studied and the production of particles with target size was achieved by selecting an appropriate pore size of the membrane (1  $\mu\text{m}$  and 0.1  $\mu\text{m}$ ). The solidification step was carried out by the solvent diffusion process that offers the advantage of a fast solidification of the polymer, better control of particle size and particle morphology respect to other techniques.

## **2. Experimental section**

### *2.1. Chemicals*

A polymer solution of polycaprolactone (PCL, 16% w/v, Sigma-Aldrich, Mw 14 kDa) in dichloromethane (DCM, Sigma-Aldrich) was used as dispersed phase for the preparation of oil-in-water emulsion (O/W) and subsequently particles. An aqueous phase containing Sodium Dodecyl Sulphate (SDS 2% w/v, Sigma Aldrich) was used as continuous phase for the preparation of the emulsions and as dilution medium for the preparation of particles by solvent diffusion process. The continuous phase was

saturated with DCM in order to avoid its diffusion during the emulsification step. Ultrapure water (USF Elsa, model Purelab Classic PL5221) with a resistivity of 18.2 M $\Omega$ .cm was used for the preparation of the aqueous phase and for the cleaning of the membrane.

## 2.2. O/W emulsion preparation: membrane emulsification equipment

Shirasu Porous Glass (SPG, Miyazaki, Japan) hydrophilic tubular membranes with a pore size of 1  $\mu\text{m}$  and 0.1  $\mu\text{m}$  distributed in a membrane area of 31.3  $\text{cm}^2$  and with a porosity of 50-60% were used for the preparation of the emulsions. The pulsed back-and-forward membrane emulsification plant is illustrated in Figure 1.6.

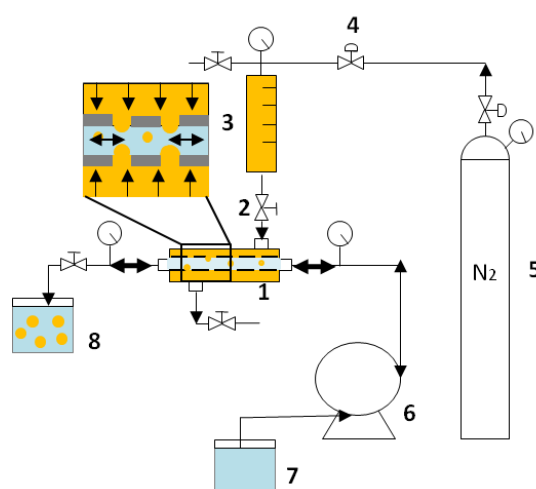


Figure 1.6 Pulsed back and forward membrane emulsification system. 1: membrane module; 2: purge valve; 3: dispersed phase graduated tank; 4: pressure regulator; 5: nitrogen gas cylinder; 6: peristaltic pump; 7: continuous phase tank; 8: emulsion tank

The dispersed phase (under gas pressure) was forced to pass through the pores of the membrane. The transmembrane pressure,  $\Delta P_{tm}$ , was calculated as the difference between the pressure of the dispersed phase,  $P_d$ , and the mean pressure of the continuous phase as reported in Chapter 1 (Equation 8).

The dispersed phase flux ( $J_d$ ) [ $\text{L h}^{-1}\text{m}^{-2}$ ] was calculated as follows:

$$J_d = \frac{Q_d}{A} \quad (1)$$

where  $Q_d$  [ $\text{L h}^{-1}$ ] is the dispersed phase flow rate and  $A$  [ $\text{m}^2$ ] is the membrane area. The effect of the transmembrane pressure was studied in the range of 40 kPa and 240 kPa using the membrane with 1  $\mu\text{m}$  pore size. A constant transmembrane pressure of 500 kPa was used for the production of the emulsion using the membrane with 0.1  $\mu\text{m}$  pore size.

The continuous phase was injected using a programmable peristaltic pump (Digi-Staltic double-Y Masterflex pump micropump, model GJ-N23.JF1SAB1) with a reverse flow direction function to produce a pulsed cyclic flow of the continuous phase tangentially to the membrane surface. The shear stress ( $\tau_{max}$ )[Pa] at the membrane surface depends on the frequency ( $f$ ) [Hz] and the amplitude ( $a$ )[m] of the continuous phase flow. They can be regulated by varying the flow rate of the pump ( $Q_c$ ) [ $m^3 s^{-1}$ ] and the volume of the continuous phase pumped back and forward within the membrane lumen ( $V_c$ )[ $m^3$ ]. They were calculated according to the following equations [15,16]:

$$f = \frac{2Q_c}{V_c} \quad (2)$$

$$a = \frac{4V_c}{\pi d_h^2} \quad (3)$$

$$\tau_{max} = 2a(\pi f)^{1.5}(\mu_c \rho_c)^{0.5} \quad (4)$$

where  $d_h$  [m] was the hydraulic diameter of the membrane,  $\mu_c$  [Pa s] was the continuous phase viscosity and  $\rho_c$  [ $kg m^{-3}$ ] the continuous phase density. The effect of amplitude and frequency was investigated in the range 4.7 cm to 9.4 cm and 2.5 Hz to 4.2 Hz, respectively, using the membrane with 1  $\mu m$  pore size. The membrane with 0.1  $\mu m$  pore size was used at a constant amplitude and frequency of 9.4 cm and 2.5 Hz. In Table 1.6 are reported the experimental conditions used to control the shear stress of the continuous phase.

Table 1.6 Experimental conditions used to increase the shear stress by increasing the amplitude or the frequency of pulsation of the continuous phase

| $Q_c$ [L/h] | $a$ [ $10^{-2}m$ ] | $f$ (Hz) | $\tau$ (Pa) | $J_d$ [ $L h^{-1}m^{-2}$ ] |
|-------------|--------------------|----------|-------------|----------------------------|
| 51          | 4.7                | 2.5      | 2.1         | 2.2                        |
| 72          | 4.7                | 3.6      | 3.5         | 2.2                        |
| 78          | 4.7                | 3.9      | 4.1         | 2.2                        |
| 102         | 9.4                | 2.5      | 4.1         | 2.2                        |

The volume % of the dispersed phase obtained for each experiment respect to the continuous phase volume was 20%. Before each experiment, the membrane was pre-wetted with the continuous phase by sonication in an ultrasonic bath for 10 min to remove the air from the pores and fill them with the continuous phase. After each experiment, the membrane was cleaned in an ultrasonic bath in dichloromethane for 10 min, in order to remove the excess of the polymer from the membrane surface and inside the pores. Subsequently, the membrane was rinsed with isopropanol and water until a clear solution was obtained and with distilled water until water was clear. SPG water permeability was totally recovered by using the cleaning procedure described.

### *2.3. Particle preparation*

The resulting oil droplets were solidified by emulsion/ solvent diffusion process discussed in more details in Chapter 4. In this study, the volume of water used to promote the solvent diffusion ( $V_{sd}$ ) was 3 times the theoretic volume ( $V_{theoretic}$ ) in order to have a fast solidification of the polymer within the droplets. Microparticles were recovered by centrifugation at 6000 rpm for 5 minutes and washed three times with distilled water. Nanoparticles were recovered on a filter membrane with a pore diameter of 0.1  $\mu\text{m}$  (Anodisc Whatman Ltd.) and washed with distilled water. Particles were dried in a stove at 40 °C over-night.

### *2.4. Particles characterization: size, morphology and surface charge*

O/W emulsions and solidified microparticle and nanoparticle size and size distribution were measured by using Zetasizer NanoZS and Mastersizer 2000. The mean particle size measured by Zetasizer is expressed as Z- average and particle size distribution is expressed as polydispersion index (PDI). The mean particle size measured by Mastersizer is expressed as D[3,2] and D[4,3]. Size distribution of microparticles measured by Mastersizer is expressed as a Span number (see Appendix 1 for the calculation). The morphology of the particles was observed by Scanning Electron Microscopy (SEM Zeiss EVO MA and LS Series). Dried samples were sprinkled on a double-sided adhesive tape attached to an aluminum stub and coated with chrome. The surface zeta potential of microparticles was determined using Zetasizer NanoZS.

## **3. Results and discussion**

### *3.1. Effect of dispersed phase flux on particle size and size distribution*

The effect of dispersed phase flux on particle size and size distribution of solidified particles was studied using the membrane with 1  $\mu\text{m}$  pore size and the results are reported in Figure 2.6. The flux was progressively increased by increasing the transmembrane pressure while keeping constant the shear stress at a value of 2.1 Pa.

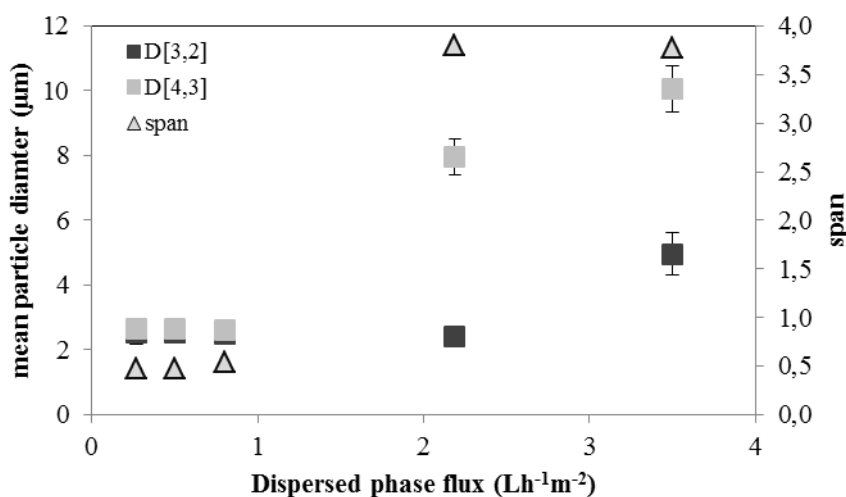


Figure 2.6 Effect of the dispersed phase flux on particle size and size distribution of microparticles prepared with SPG membrane with 1  $\mu\text{m}$  pore size and a shear stress of 2.1 Pa

Uniform particles with mean size of 2.4 ( $\pm 0.2$ )  $\mu\text{m}$  and size distribution of 0.49 ( $\pm 0.02$ ) were obtained when the flux was maintained below 0.9  $\text{L h}^{-1}\text{m}^{-2}$ . The formation of large particles was observed when the flux was further increased above 0.9  $\text{L h}^{-1}\text{m}^{-2}$ . This effect was more significant considering D[4,3] which is more sensitive to the presence of large particles. D[4,3] was 8  $\mu\text{m}$  and 10  $\mu\text{m}$  when the dispersed phase flux was 2.2 and 3.8  $\text{L h}^{-1}\text{m}^{-2}$ , respectively. Also the widening of size distribution at 3.8 was observed in the same range of dispersed phase flux. The transition from uniform size distribution to polydisperse size distribution with the increase of the dispersed phase flux can be interpreted in terms of the transition from “dripping” to “jetting” mechanisms of drop detachment [17]. The increase of dispersed phase flux is related not only to an increase of the flow rate through the separate pores, but mostly to the activation of additional pores, determining coalescence of droplets during their growth at two neighboring pores of the membrane.

### 3.2. Effect of the shear stress on particle size and size distribution

The effect of shear stress on particle size and size distribution was studied at a constant dispersed phase flux of 2.2  $\text{L h}^{-1}\text{m}^{-2}$ . In this process the shear stress is a function of the frequency and the amplitude of the pulsation along the lumen side of the membrane and an increase of these two parameters results in an increase of the shear stress. In this study the shear stress was increased in a range between 2.1 and 4.1 Pa either by increasing the frequency in a range between 2.5 and 3.9 Hz (keeping low the amplitude at a value of  $4.7 \cdot 10^{-2}$  m) or by increasing the amplitude in a range between 4.7 and 9.4  $10^{-2}$  m (keeping low the frequency at a value of 2.5 Hz). In Figure 3.6 is reported Malvern Mastersizer size distribution of particles prepared with a shear stress in a range between 2.1 and 4.1 Pa.

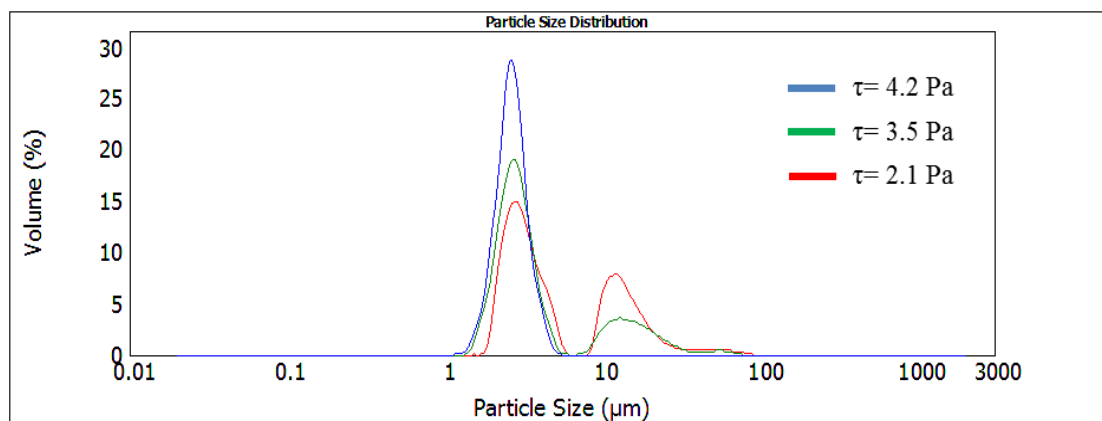


Figure 3.6 Malvern Mastersizer particle size distribution of microparticles prepared at different value of shear stress and constant dispersed phase flux ( $2.2 \text{ L h}^{-1}\text{m}^{-2}$ ).

A polydispersed size distribution was obtained when the minimum shear stress was applied. The presence of a secondary peak of large particles ( $\tau = 2.1 \text{ Pa}$ ) with a mean size of  $13 \mu\text{m}$  was observed. The formation of large particles at lower shear stress is correlated with the coalescence of the droplets at the pore level before the detachment in the continuous phase. When the shear stress was increased from 2.1 to 3.5 Pa the volume % of the secondary peak corresponding to the larger particles was decreased. At the maximum shear stress (4.1 Pa) particles with monodispersed size distribution was produced and one peak, corresponding to a mean particle size of  $2.4 \mu\text{m}$  was obtained. The higher the shear, the lower was the particle size as a consequence of the fast detachment of the growing droplets from the pore level. Shear force is required to detach sooner the droplets from the pore opening in order to obtain a good control of particle uniformity.

The effect of shear stress on particle size and size distribution is strictly correlated with the dispersed phase flux used during the emulsification process. In Figure 4.6 is reported the effect of shear stress on particle size and size distribution when it is associated with lower and higher dispersed phase flux ( $0.9 \text{ L h}^{-1}\text{m}^{-2}$  and  $2.2 \text{ L h}^{-1}\text{m}^{-2}$ ). Particle size and size distribution were significantly larger at higher dispersed phase flux and lower shear stress, as a consequence of the slow detachment of the droplets in the continuous phase respect to their fast grow at the membrane pore level.

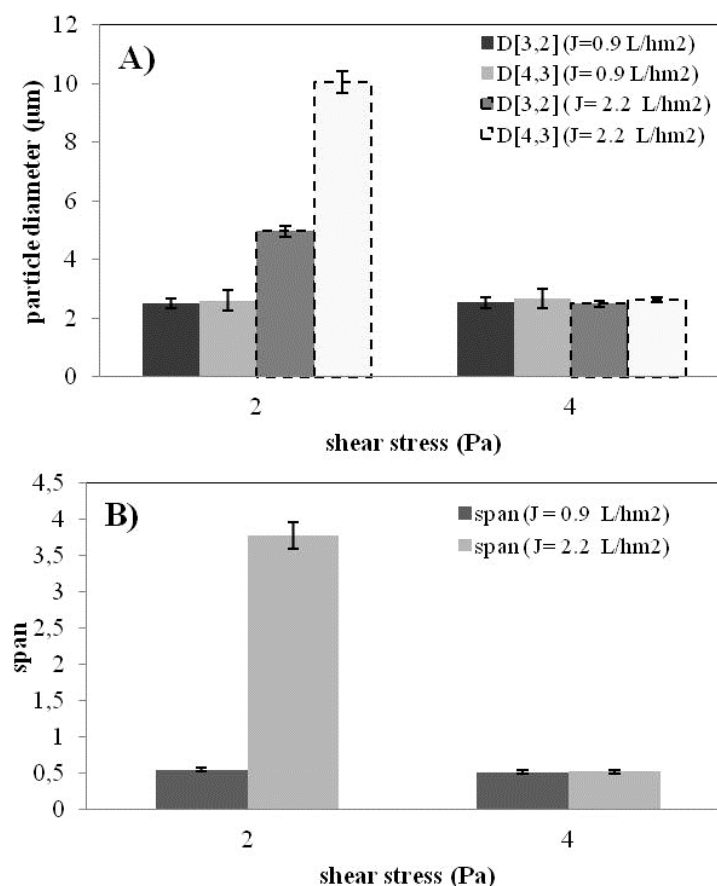


Figure 4.6 Effect of shear stress on: **A)** particle size and **B)** size distribution at lower ( $0.9 \text{ L h}^{-1} \text{ m}^{-2}$ ) and higher ( $2.2 \text{ L h}^{-1} \text{ m}^{-2}$ ) dispersed phase flux.

### 3.3. Effect of the membrane pore size: particle size from micro to nanoscale

The most important application of membrane emulsification is for the production of emulsions with monodispersed droplets and target size. The droplet size is correlated with the pore size of the membrane by a linear relationship and the shift from micro to nano scale was carried out by changing the pore size of the membrane. The fluid-dynamic conditions used for the preparation of the emulsions were  $\tau = 4.1 \text{ Pa}$  and  $J_d = 0.9 \text{ L h}^{-1} \text{ m}^{-2}$  for both type of membranes.

There are few works in literature about the preparation of nanoparticles by membrane emulsification suitable for pharmaceutical applications and in most cases the cross flow method operation has been used.

In these cases the axial velocity required to produce monodispersed nanoparticles was in the range between  $1$  and  $4.5 \text{ m s}^{-1}$  that is related with a shear stress in the range between  $1.3$  e  $6 \text{ Pa}$  [7,10,11]. The use of low shear conditions is especially required for the preparation of formulations containing labile molecules (such as bioactive compounds) in order to prevent their degradation. In this study, uniform nanoparticles could be obtained by using pulsed back-and-forward cross-flow batch membrane emulsification with an axial velocity of  $0.5 \text{ m s}^{-1}$  that corresponded to a shear stress of  $4.1 \text{ Pa}$ . The axial velocity used is about 10 times lower than the maximum values



reported in literature. Data indicated that pulsed back-and-forward cross-flow batch membrane emulsification allowed a precise control of the uniform nanoparticle production in milder operating conditions.

In Figure 5.6 is reported the effect of membrane pore size on the particle size of emulsions droplets (reported as Z-average) and solidified particles.

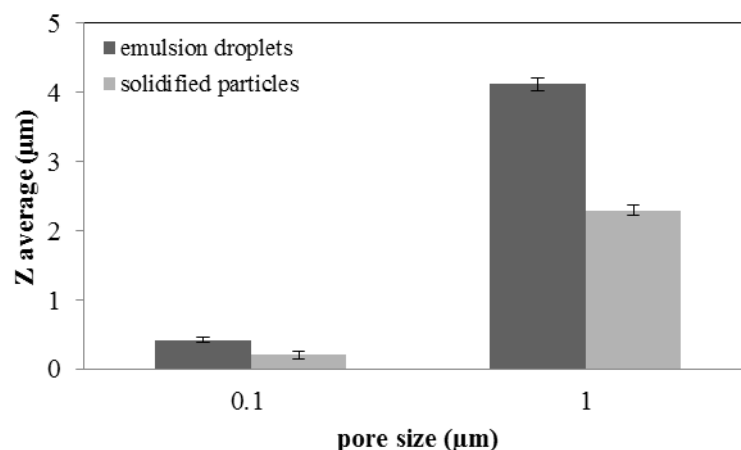


Figure 5.6 Effect of membrane pore size on Z-average of emulsion droplets and solidified particles measured by Zetasizer NanoZS

The mean emulsion droplets size was  $0.425 (\pm 0.03) \mu\text{m}$  and  $4.12 (\pm 0.2) \mu\text{m}$  when the membrane pore size was 0.1 and 1  $\mu\text{m}$ , respectively. The mean solidified particles size was  $0.21 (\pm 0.01) \mu\text{m}$  and  $2.35 (\pm 0.14) \mu\text{m}$  when the membrane pore size was 0.1 and 1  $\mu\text{m}$ , respectively. The droplet size and the solidified particle size were 4 and 2 times the pore size of the membrane, respectively. The linear relationship existing between emulsion droplets and membrane pore size was maintained also after the solidification step when the particle size was decreased as a consequence of the solvent removal. A shrinkage of the emulsion droplets was also observed as a consequence of the removal of the solvent through the droplets in the post-emulsification step. The measured shrinkage factor for nanoparticles produced by using the membrane with a pore size of 0.1  $\mu\text{m}$  was 1.7.

The range of particle size obtained in the present work is suitable for parenteral administration. Intravenous, subcutaneous or intramuscular injections are associated with a rapid drug absorption and they are the most common and efficient administration routes for the delivery of active drug substances with poor bio-availability. Moreover, they also offer the advantage to avoid the biotransformation of drugs in the liver by “first pass metabolism” and they are the most preferred routes of administration in the case of emergency.

#### 3.4. From emulsion droplets to solidified PCL particles

The production of solidified particles was carried out by inducing the diffusion of the solvent from the droplets into the external phase with a consequent polymer accumulation and solidification at water droplet interface. The removal of the solvent

decreased the volume of each droplet by a shrinkage factor ( $\alpha$ ) given by the chemical composition of the organic phase. This factor is defined as the ratio between the diameter of the emulsion droplet ( $d_d$ ) and the diameter of the solidified particle ( $d_s$ ) [18]. Knowing the initial polymer concentration (16% w/v) and the volume of dispersed phase emulsified (4 ml), it is possible to predict the mean size of the solidified particles by calculating a theoretical shrinkage factor ( $\alpha$ ) expressed as:

$$\alpha = \frac{d_d}{d_s} = \left( \frac{V_p + V_s}{V_p} \right)^{1/3} \quad (5)$$

where  $V_p$  is the volume of polymer and  $V_s$  is the volume of the solvent. The predicted theoretical shrinkage factor (calculated considering the chemical composition of the dispersed phase) corresponds to 1.9.

In the emulsification step, oil droplets with a mean size of 4.12 ( $\pm$  0.4)  $\mu\text{m}$  were prepared by using the membrane with a pore size of 1  $\mu\text{m}$  and at the optimized fluid-dynamic conditions ( $\tau = 4.2$  Pa;  $J_d = 2.2$  L h<sup>-1</sup>m<sup>-2</sup>) while, after solvent removal, the solidified particles had a mean size of 2.35 ( $\pm$  0.14)  $\mu\text{m}$ . The measured shrinkage factor calculated considering the ratio between the initial and the final particle size was 2.0 that was very close to the predicted theoretical shrinkage factor.

The size distribution of emulsion droplets and solidified particles were a span value of 0.49 ( $\pm$  0.02) and a PDI of 0.06 ( $\pm$  0.01), respectively. Data demonstrated that the solidified particles preserved the uniformity of the initial emulsion, therefore coalescence of droplets did not occur during the solidification step and the control of particle size and size distribution is achieved during the emulsification step.

### 3.5. Particles Morphology

As previously reported in Chapter 4, the volume of water used for the solvent diffusion influenced the solidification rate of the polymer within the droplets and consequently the shape of the solidified particles. Micro and nanoparticles preserved the spherical shape of the initial oil droplets as showed in the SEM pictures in Figure 6.6 (A-D). This is because the experimental conditions used for the solidification of oil droplets allowed a fast solvent removal in order to preserve the integrity and the shape of the single droplet ( $V_{sd} = 3 V_{\text{theoretic}}$ ). Solidified particles are characterized by a dense and slightly rough surface with no apparent pores (Figure 6.6 B). The slight roughness of the particle could be advantageous to improve the water absorption on the surface, that is the main factor influencing the hydrolytic degradation pathway of aliphatic polyesters. The rate of water intrusion into the polymer bulk determines the hydrolytic cleavage of the polymer backbone in oligomers or monomers [19].

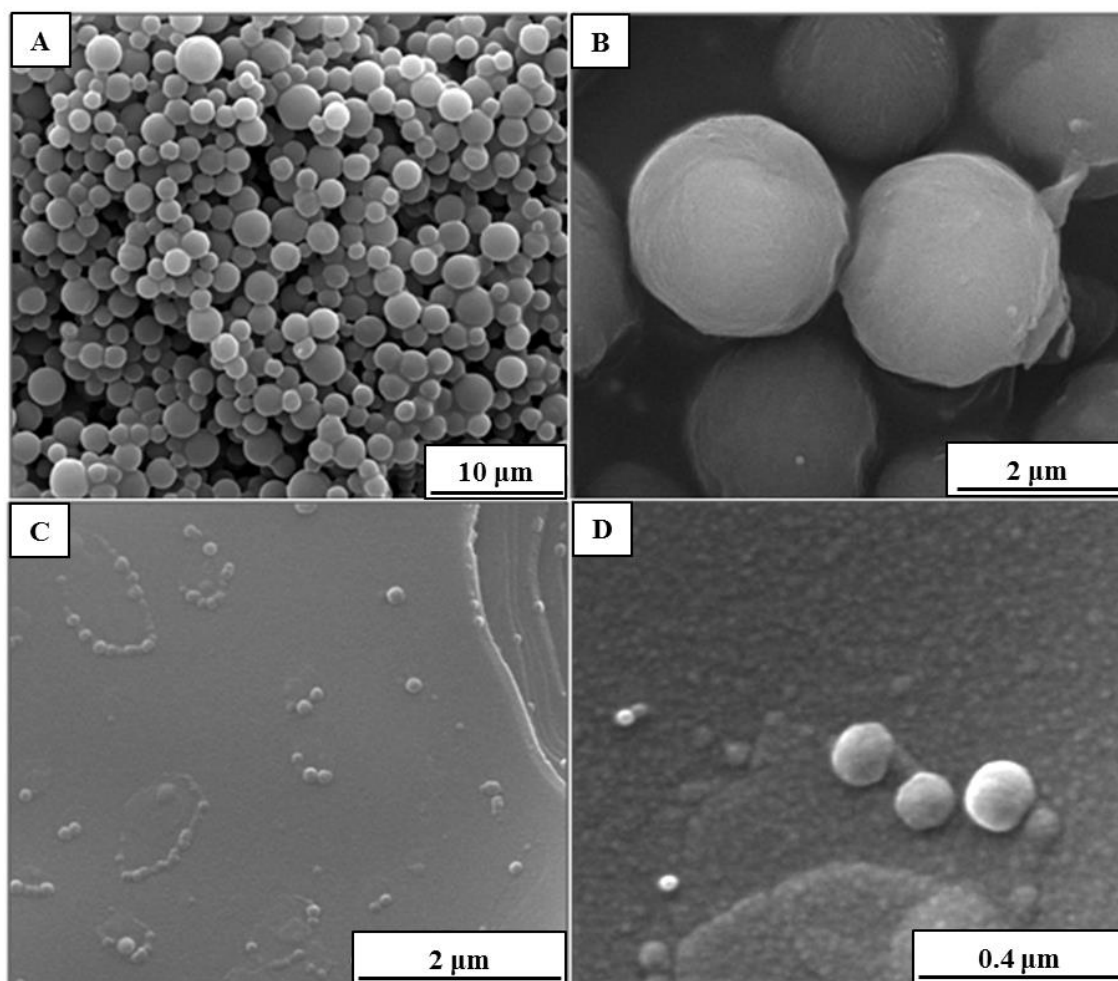


Figure 6.6 SEM pictures of polycaprolactone micro and nanoparticles prepared by pulsed back and forward membrane emulsification. **A-B**: microparticles prepared with SPG membrane with 1  $\mu\text{m}$  pore size; **C-D**: nanoparticles prepared with SPG membrane with 0.1  $\mu\text{m}$  pore size.

### 3.6. Particles stability

Solidified particles were also characterized in terms of surface charge by measuring zeta potential in order to evaluate the physical stability of the suspension that is associated with particle aggregation. For pharmaceutical use, a suspension must have a minimal tendency to agglomerate, which could lead to the formation of big aggregates that rapidly sediment. The zeta potential of a suspension is governed by both the stabilizer and the material of the particles. A minimum value of  $\pm 30$  mV is required to obtain a suspension with good physical stability [20]. A negative zeta potential of  $-41 (\pm 3)$  mV was obtained at pH (6.8-7) predicting a good stability of the suspension at physiological conditions due to the high-energy barrier between the particles. The presence of anionic sulphate groups exposed at solid/water interface by the emulsifier (SDS) can be responsible of the negative surface charge of the particles along with the presence of low polar carbonyl groups with a partly negative oxygen exposed by the polymeric chains into the water phase.

#### 4. Conclusions

Pulsed back-and-forward cross-flow batch membrane emulsification was successfully applied for the preparation of micro and nano polymeric particles in a size range between  $2.35 (\pm 0.14) \mu\text{m}$  and  $0.21 (\pm 0.01) \mu\text{m}$  suitable for injectable administration. The production of particles with target size was achieved by using membrane with different pore size ( $1 \mu\text{m}$  and  $0.1 \mu\text{m}$ ) and optimized fluid-dynamic conditions. The spherical shape and the uniformity of the particles could be easily controlled in the post emulsification step because of a fast solidification of the polymer within the droplet.

The particle suspension revealed also a good physical stability with a negative surface zeta potential of  $-41 (\pm 3) \text{mV}$  resulting in high-energy barrier between particles without the formation of aggregates. Therefore it can be potentially used as drug carrier for the encapsulation of hydrophobic compounds.

Data indicates that pulsed back-and-forward cross-flow batch membrane emulsification allows the control of the production of nanoparticles with tuned structural properties at low shear conditions. This process can offer great potentials to convert poorly soluble, poorly absorbed and labile biologically active substance into promising deliverable drugs. The method introduces advances in particles production engineering in order to turn the concept of nanoparticle technology into a realistic practical application as the next generation of drug delivery system.

#### References

1. Woodruff MA., Hutmacher DW. The return of a forgotten polymer: Polycaprolactone in the 21st century. *Prog. Polym. Sci.* 2010; 35: 1217-1256
2. Wong, J., Brugger A., Khare A., Chaubal M., Papadopoulos P., Rabinow B., Ning J. Suspensions for intravenous (IV) injection: a review of development, preclinical and clinical aspects. *Adv. Drug Deliv. Rev.* 2008;60(8): 939-954
3. Vauthier C., Bouchemal K. Methods for the preparation and manufacture of polymeric nanoparticles. *Pharm. Res.* 2009;26(5): 1025-1058
4. Freiberg S., Zhu, XX. Polymer microspheres for controlled drug release. *Int. J. Pharm. Sci.* 2004;282(1): 1-18.
5. Pinto Reis C., Neufeld RJ., Ribeiro AJ., Veiga F. Nanoencapsulation I. Methods for preparation of drug-loaded polymeric nanoparticles. *Nanomed: Nanotechnol, Bio. Med.* 2006;2(1): 8-21
6. Vladislavljević GT., Williams RA. Recent developments in manufacturing emulsions and particulate products using membranes. *Adv Colloid Interface Sci.* 2005;113(1): 1-20

7. Charcosset, C., Fessi H. Preparation of nanoparticles with a membrane contactor. *J Membr Sci.* 2005;266(1): 115-120
8. Lv PP., Wei W., Gong, FL., Zhang YL., Zhao, HY., Lei, JD., Ma, GH. Preparation of uniformly sized chitosan nanospheres by a premix membrane emulsification technique. *Ind Eng Chem Res.*2009;48(19): 8819-8828
9. Wei Q., Wei W., Lai B., Wang LY., Wang, YX., Su ZG., Ma, GH. Uniform-sized PLA nanoparticles: Preparation by premix membrane emulsification. *Inter J Pharm*,2008;359(1): 294-297
10. Charcosset, C., El-Harati, A., Fessi, H. Preparation of solid lipid nanoparticles using a membrane contactor. *J Control Release.*2005;108(1): 112-120
11. Sheibat-Othman, N., Burne, T., Charcosset, C., Fessi, H. Preparation of pH-sensitive particles by membrane contactor. *Coll Surf A: Physicochem Eng Aspects.* 2008;315(1): 13-22
12. Piacentini E., Drioli E., Giorno L. Membrane emulsification technology: Twenty-five years of inventions and research through patent survey. *J Membr Sci.* 2014;468:410–422
13. Vladisavljević, GT., Kobayashi, I., Nakajima, M. Production of uniform droplets using membrane, microchannel and microfluidic emulsification devices. *Microfluid. Nanofluid.* 2012;13(1): 151-178
14. Nazir, A., Schroën, K., Boom, R. Premix emulsification: A review. *J Membr Sci.* 2010;362(1): 1-11
15. Piacentini E., Drioli E., Giorno L. Pulsed back-and-forward cross-flow batch membrane emulsification with high productivity to obtain highly uniform and concentrate emulsions, *J Membr Sci.*2014; 453: 119–125
16. Holdich, RG., Dragosavac MM., Vladisavljević GT., Piacentini, E. Continuous membrane emulsification with pulsed (oscillatory) flow. *Ind Eng Chem Res.*,2012;52(1): 507-515
17. Christov NC., Danov KD., Kralchevsky PA. The Drop Size in Membrane Emulsification Determined from the Balance of Capillary and Hydrodynamic Forces, *Langmuir.* 2008;24: 1397-1410
18. Rosca, ID., Watari, F., Uo, M. Microparticle formation and its mechanism in single and double emulsion solvent evaporation. *J Control Release.*2004;99(2): 271-280

19. Lam CX., Hutmacher DW., Schantz, JT., Woodruff, MA., Teoh, SH. Evaluation of polycaprolactone scaffold degradation for 6 months in vitro and in vivo. *J Biomed. Mater Res. part A.* 2009;90(3): 906-919
20. Patravale VB., Kulkarni RM. Nanosuspensions: a promising drug delivery strategy. *J Pharm Pharmacol.* 2004;56(7): 827-840

# CHAPTER 7

## **Study of micro-sieve stainless steel membrane in torsional motion for large scale production of simple O/W and double W/O/W emulsion**

### **1. Introduction**

In this last twenty five years, the process of membrane emulsification (ME) has been demonstrated to offer numerous benefits over conventional emulsification techniques. Advantages such as lower applied shear, less energy consumption, good process repeatability and a significant level of control over droplet size are widely reported in literature [1–4]. About 66% of patents have been issued in the last 11 years demonstrating the increasing interest towards this new emulsification technique [1]. However, there are still some limitations on the membrane emulsification process to advance at an industrial level. In particular the low productivity (which is often related to low dispersed phase flux and long production time) may hinder the industrial application. Some solutions to overcome this issue were introduced, such as premix emulsification. However, the fouling of the membrane can occur during pre-mix operation and the frequent membrane cleaning requirements may undermine the production rate from an industrial perspective [1,2]. The use of high-throughput membrane that are suitable for membrane emulsification within an industrial setting can be a promising strategy to overcome the existing flux limitations. Micrometer pore sized sieve type membranes are increasingly being used in ME because they can afford much higher transmembrane flux than Shirasu Porous Glass membrane, or ceramic membranes. Micro-sieve membranes are ultrathin foils with rectilinear pores and low internal pore area, and are less prone to fouling by emulsion ingredients than the highly tortuous SPG membranes, as the sieve type of membrane does not have any internal surface, or structure, on which the fouling can occur [5]. Another issue of the membrane emulsification process currently used for industrial application (such as cross-flow ME) is the breakage of the emulsion or damage of shear sensitive material due to the recirculation along the circuit. Therefore, it is quite important to maintain low shear conditions in the bulk of the product stream in order to prevent breakage of shear sensitive material, although shear stress at the membrane surface can be quite significant. Alternative methods of keeping low shear away from the membrane surface are based on the movement of the membrane to generate the shear stress required for the droplet detachment. The set-ups associated with this approach are either the rotating [6,7] or the vibrating [8,9] membrane emulsification systems. Recently another approach consisting in the generation of the shear stress by a pulsed flow of the continuous phase along the membrane surface was also proposed for the production of fragile products or large droplets at lower shear conditions [10,11]. In this work, we investigated the production of simple O/W and double W/O/W emulsion at high

throughput and low shear condition using the torsional membrane emulsification, a recently introduced membrane emulsification process in which a micro-sieve stainless steel membrane in tubular configuration is used. The advantages properties of micro-sieves combined with the mechanical strength and chemical resistance of stainless steel allows to achieve potentially high flux suitable for an industrial setting preserving at the same time the uniformity of the particles. The generation of the shear stress on the membrane surface by the torsional motion of the membrane guarantees low shear conditions in the bulk of the product stream and the flowing of the continuous phase inside the module was applied only to recover the emulsion at the outlet side of the system and not to assist the droplet generation. In this way, high dispersed to continuous phase ratio can be produced in a single pass of the continuous phase, without the necessity of high shear within the fluid which may damage shear sensitive components, such as polymer solution or bioactive compounds. The configuration of the system allows also to operate in continuous mode so it is suitable to be applied in an integrated system for the production of particles at large scale. The influence of process parameters (dispersed phase flux, frequency and amplitude of the torsion) on particle size and size distribution was evaluated at the emulsification step keeping the same chemical composition used for the preparation of the emulsion at batch scale (Dispersion Cell). The removal of the solvent by the diffusion process can be potentially carried out continuously by mixing the emulsion collected from the outlet side of the membrane module with known volume of water to achieve fast solidification of the polymer within the droplets.

## 2. Experimental section

### 2.1. Chemicals

A polymer solution of poly-caprolactone (PCL, Sigma-Aldrich, Mw 14KDa, 30% wt/v) in dichloromethane (DCM, Sigma-Aldrich) was used as dispersed phase for the preparation of O/W emulsions and as organic phase (O) of the double W/O/W emulsion. In the latter case cold water-fish gelatin (MW 60 kDa, 5% wt/v) was used as stabilizer in the inner ( $W_1$ ) aqueous phase of the double emulsion ( $\phi_{wo}=0.1$ ) and Cu(II) in the form of copper sulphate (Fisher Scientific, MW 65 g/mol, 2000 ppm) was used as hydrophilic drug model. Poly-vinyl alcohol (PVA, MW 13-23kDa, 1% wt/v) was used as emulsifier for the preparation of simple O/W and double W/O/W emulsion. All the aqueous solutions were prepared using ultrapure water with a resistivity of 18.2 M $\Omega$ ·cm. Sodium hydroxide (NaOH, Fisher Scientific, 4M) was used for the cleaning of the membrane.

### 2.2. Membrane emulsification equipment

Simple O/W and double W/O/W emulsion were produced using a torsional membrane system with tubular micrometer pore sized sieve type stainless steel membrane. The pore size of the membrane was 15  $\mu$ m distributed in a membrane area of 52 cm<sup>2</sup> and



with a porosity of 0.44 %. The membrane as well as the torsional system were supplied by Micropore Technologies Ltd. (UK). A schematic representation of the system is illustrated in Figure 1.7. The dispersed phase was injected with the syringe pump radially through the porous membrane wall and forms droplets moving into the continuous phase. The dispersed phase flux ( $J_d$ ) [ $L h^{-1} m^{-2}$ ] was calculated as the ratio of the flow rate of the syringe pump to the membrane area.

### Torsional movement

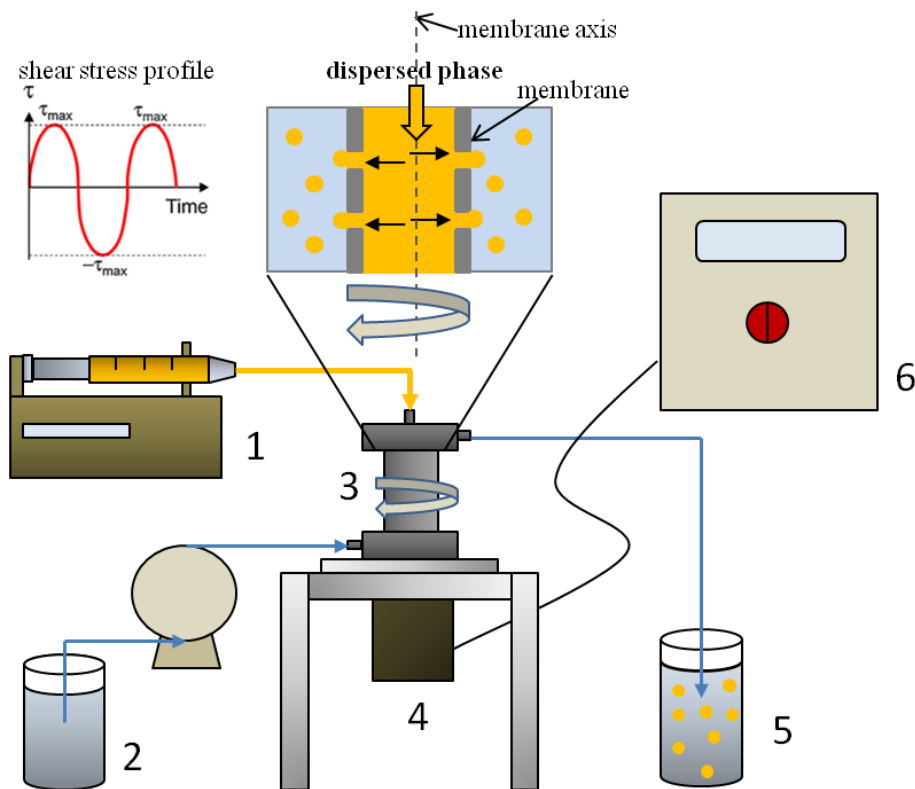


Figure 1.7 Torsional system equipment scheme. 1-syringe pump containing the dispersed phase; 2- continuous phase tank; 3- membrane module; 4- servo motor; 5- emulsion tank; 6- control panel

The continuous phase is slowly pumped with a peristaltic pump upwards into the annulus between the stationary vessel and the membrane tube and the emulsion is collected from the top of the vessel. The shear stress is generated by twisting the membrane rather than by flowing the continuous phase, since the cross-flow velocity is negligible. The percentage of dispersed phase emulsified (%DP) is given by the ratio dispersed phase flow rate ( $Q_{dp}$ ) to continuous phase flow rate ( $Q_{cp}$ ):

$$\% DP = (Q_{dp}/Q_{cp}) * 100 \quad (1)$$

The torsion of the membrane is generated by a servo motor fitted with the membrane. The amplitude and frequency of the torsion can be regulated using a digital control

panel. The torsion of the membrane used in this work was applied in a sinusoidal way, therefore the maximum shear occurs twice per cycle.

Before each experiment the membrane was pre-wetted with the continuous phase by sonication in an ultrasonic bath for 30 sec to remove air from the pores and fill them with the continuous phase. After each experiment, the membrane was immersed in dichloromethane for 1 hour and sonicated for few seconds several times in order to remove residual polymer inside the pores and the internal cavity of the membrane. Subsequently, it was rinsed with warm water several times and it was immersed in a solution of sodium hydroxide (4 M) for 1 hour and sonicated for few seconds several times. After this the membrane was rinsed with deionized water several times until water was clear.

### 2.3. Droplet size modelling

The produced droplets diameter ( $x$ ) can be predicted from a force balance reported in more details in Chapter 5 [12,13] and in Equation 2:

$$x = \frac{\sqrt{18\tau^2 r_p^2 + 2\sqrt{81\tau^4 r_p^4 + 4r_p^2 \tau^2 \gamma^2}}}{3\tau} \quad (2)$$

where  $r_p$  [m] is the pore radius,  $\tau$  [Pa] is the shear stress and  $\gamma$  [mNm<sup>-1</sup>] is the interfacial tension. The latter was measured experimentally by using the Du Noüy ring method (see Appendix 1) and it was 4.2 ( $\pm 0.3$ ) mNm<sup>-1</sup> and 3.9 ( $\pm 0.3$ ) mNm<sup>-1</sup> for simple O/W and double W/O/W emulsion respectively. The shear stress ( $\tau_{max}$ )[Pa] depends on the frequency ( $f$ ) [Hz] and the amplitude ( $a$ )[m] of the torsional movement of the membrane and it was calculated using Equation 3 [10]:

$$\tau_{max} = 2a(\pi f)^{1.5}(\mu_c \rho_c)^{0.5} \quad (3)$$

where  $\mu_c$  [Pa s] was the continuous phase viscosity and  $\rho_c$  [kg m<sup>-3</sup>] the continuous phase density. In Table 1.7 are reported the experimental conditions used to control the shear stress on the membrane surface. The effect of amplitude and frequency was investigated in the range between 1 mm to 3.5 mm and 15 Hz to 50 Hz corresponding to a shear stress in a range of 1 Pa to 5.9 Pa

Table 1.7 Amplitude and frequency used to control the shear stress in the torsional system

| $a$ [ $10^{-3}$ m] | $f$ [Hz] | $\tau_{\max}$ [Pa] |
|--------------------|----------|--------------------|
| 1.5                | 15       | 1                  |
| 1                  | 25       | 1.4                |
| 1.5                | 30       | 2.7                |
| 2                  | 25       | 2.8                |
| 3                  | 25       | 4.2                |
| 3.5                | 25       | 4.9                |
| 1.5                | 45       | 5.0                |
| 1.5                | 50       | 5.9                |

#### 2.4. Microparticle preparation

Emulsion/solvent diffusion process was employed for the production of simple and multi-core matrix particles. The method was discussed in more details in Chapter 4 and 5. In this study, the emulsion was collected from the top of the vessel and it was calculated the theoretic volume of water for the solvent diffusion process taking into account the percentage of the dispersed phase emulsified in one minute. Thus, the emulsion was diluted in a volume of water 3 times the theoretic volume in order to have a fast solidification of the polymer. The torsional emulsification system allowed a continuous production of the emulsion, therefore the production of solidified particles can be potentially carried out continuously.

#### 2.5. Particle characterization

O/W emulsions and solidified particles were observed by optical microscopy. Oil droplet size was analyzed using an image analysis system running Scion Image software. Particle size and size distribution were measured by laser diffraction (Mastersizer 2000, Malvern Instruments, UK) in deionized water with an emulsifier to avoid their aggregation. The mean particle size was expressed as the surface weighted mean diameter (or Sauter diameter),  $D[3,2]$  and as the volume weighted mean diameter, (or De Brouckere diameter),  $D[4,3]$ . Droplet size distribution was expressed as a Span number. Three samples were analyzed for each experiment and the reported results are the average of three different experiments.

#### 2.6. Encapsulation efficiency of copper into the double W/O/W emulsion

According to the study of Vladisavljevic et al [9], the encapsulation efficiency (EE%) of the double emulsion was calculated as the ratio between the mass of Cu(II) entrapped in the double emulsion ( $M_0$ ) immediately after the emulsification process ( $t=0$ ) and the total mass of Cu(II) added into the inner water phase ( $M_i$ ):

$$EE = \frac{M_i - M_0}{M_i} \quad (3)$$

The mass of Cu(II) added into the inner water phase is given by Equation 4:

$$M_i = C_i \phi_{wo} \phi_{wow} V_{wow} \quad (4)$$

where  $C_i$  is the initial concentration of Cu(II) in the inner water phase,  $V_{wow}$  is the volume of double W/O/W emulsion produced,  $\phi_{wo}$  is the volume fraction of the inner aqueous phase emulsified in the primary W/O emulsion and  $\phi_{wow}$  is the volume fraction of the primary W/O emulsion emulsified in the double W/O/W emulsion. The mass of Cu(II) released at  $t = 0$  is given by Equation 5:

$$M_0 = C_0 V_{wow} (1 - \phi_{wow}) \quad (5)$$

where  $C_0$  is the concentration of Cu(II) in the outer water phase at  $t = 0$  measured experimentally. The substitution of Equation 4 and 5 into Equation 3 gives:

$$EE = 1 - \frac{C_0 (1 - \phi_{wow})}{C_i \phi_{wow} \phi_{wo}} \quad (6)$$

In this study  $C_i$  was 2000 ppm,  $\phi_{wo}$  was 0.1 and  $\phi_{wow}$  is 0.35.

### 3. Results and discussion

#### 3.1. Influence of the frequency and amplitude of the torsion on simple O/W emulsion and solid particle size and size distribution

In the torsional membrane emulsification the shear stress can be adjusted by varying two parameters, the frequency and the amplitude of the membrane torsion. The particle size is not determined by individual values of frequency or amplitude but a combination of both values influenced the shear stress on the membrane surface. In general the higher amplitude must be offset by the lower frequency and vice versa. In Figure 2.7 (A) is reported the droplet size and the solid particle size and size distribution as a function of the frequency of the membrane torsion keeping low the amplitude at 3 mm and in Figure 2.7 (B) is reported the droplet and the mean particle size and size distribution as a function of the amplitude keeping low the frequency at 25 Hz. Two different injection flow rates of the dispersed phase (1 and 4 ml/min) were used to evaluate the effects of these parameters. At low injection flow rate (1 ml/min) a reduction of the mean particle size from 75  $\mu\text{m}$  to 38  $\mu\text{m}$  was observed with the increase of the frequency in a range of 15 Hz and 50 Hz, corresponding to shear stress in a range of 1 Pa and 5.9 Pa. The increase of the amplitude in a range of 1 mm to 3.5 mm

produced an increase of shear stress in a range of 1.4 Pa to 4.9 Pa with a consequent particle reduction in a range of 63  $\mu\text{m}$  and 43  $\mu\text{m}$ . The shear force is directly correlated with the frequency and the amplitude of the torsion, therefore the decrease of particle size is a consequence of the increase of the shear stress acting on the membrane surface.

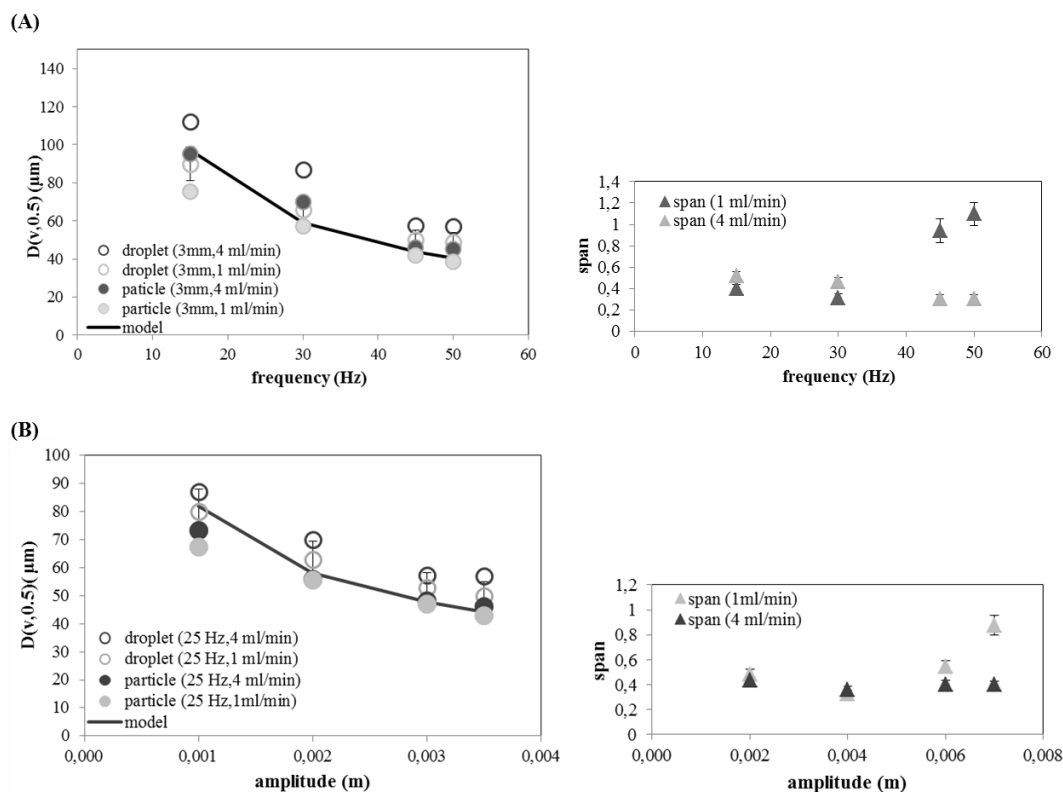


Figure 2.7 Oil droplet and solid particle size and size distribution as a function of frequency (15-50 Hz,  $a = 1.5\text{mm}$ ) and amplitude (1-3.5 mm,  $f = 25$  Hz);  $Q_{dp} = 1 \text{ mlmin}^{-1}$ ;  $4 \text{ mlmin}^{-1}$

The droplet size produced at low flow rate ( $1 \text{ mlmin}^{-1}$ ) are closer to the predicted values of the model while larger droplet size are produced at high flow rate compared with the model ( $4 \text{ mlmin}^{-1}$ ). The increase of the flow rate is correlated with an increase of the dispersed phase flux and the model did not consider the contribution of this parameter to the formed droplet size [14]. However, a widening of size distribution was observed when the dispersed phase was injected at low flow rate and high shear stress. Indeed, size distribution increased from 0.48 to 0.89 when highest amplitude (3-3.5 mm) was applied and a polydispersed emulsion with a span value of 1.1 was produced using the highest frequency (45-50 Hz). In Figure 3.7 (photograph C) the emulsion produced at frequency of 50 Hz and low injection flow rate of the dispersed phase ( $1 \text{ ml/min}$ ) appears to be bimodal and small droplets with a mean size of  $12 \mu\text{m}$  were formed together with larger droplets. Since the dispersed phase was injected at low flow rate and the membrane did not have tortuous pore channel, the pressure generated by the flowing of the continuous phase inside the module can promote a passage of the continuous phase into the side of the membrane where the dispersed phase is present. A consequence is the partial mixing of the phases at the pore level during the membrane movement generating small droplets. This phenomena was observed also by Holdich et

al. for the production of emulsion with pulsed flow of the continuous phase [10]. Increasing the flow rate of the dispersed phase at 4 ml/min the mixing of the phases was avoided and uniform particles with a span value in a range of 0.30 and 0.39 were produced at the highest frequency (45-50 Hz) or amplitude (3-3.5 mm) respectively. In this conditions, a controlled particle reduction from 95  $\mu\text{m}$  to 45  $\mu\text{m}$  was achieved in a range of shear stress of 1 Pa and 5.9 Pa. At shear stress up than 5 Pa (which corresponds to frequency up than 45 Hz or amplitude of 3.5 mm) the particle size remained constant at 45 ( $\pm 1$ )  $\mu\text{m}$ , which is 3 times the pore size of the membrane. The same relationship between pore size and particle size was obtained in a range of shear stress quite similar (up than 6 Pa) using the Dispersion Cell at batch scale.

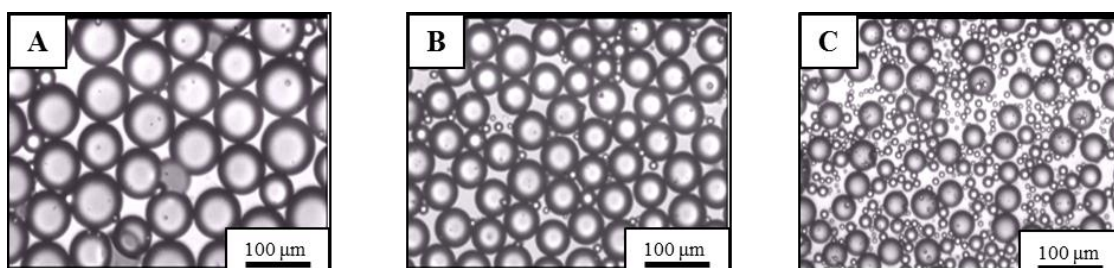


Figure 3.7 Photographs of O/W emulsion produced with  $a= 1.5$  mm,  $Q_{dp}= 1$  mlmin<sup>-1</sup> and  $f=15$  Hz (A), 30 Hz(B) and 50 Hz (C)

### *3.2. Influence of the frequency and amplitude of the torsion on double W/O/W emulsion and solid particle size and size distribution*

The influence of the frequency and the amplitude of the membrane torsion was evaluated in the same range used for the production of simple emulsion and particles. In Figure 4.7 are reported the mean droplet and particle size and the size distribution as a function of frequency and amplitude keeping constant the injection flow rate at 4 ml/min. A controlled reduction of particle size from 76  $\mu\text{m}$  to 46  $\mu\text{m}$  was achieved either when the frequency or the amplitude were increased because of an increase of the shear stress in a range of 1 Pa and 5.9 Pa. Slight reduction of span value from 0.46 to 0.28 ( $\pm 0.02$ ) was achieved with the increase of the frequency whereas the increase of the amplitude did not influence significantly the uniformity of the particles that was almost constant at 0.34 ( $\pm 0.02$ ).

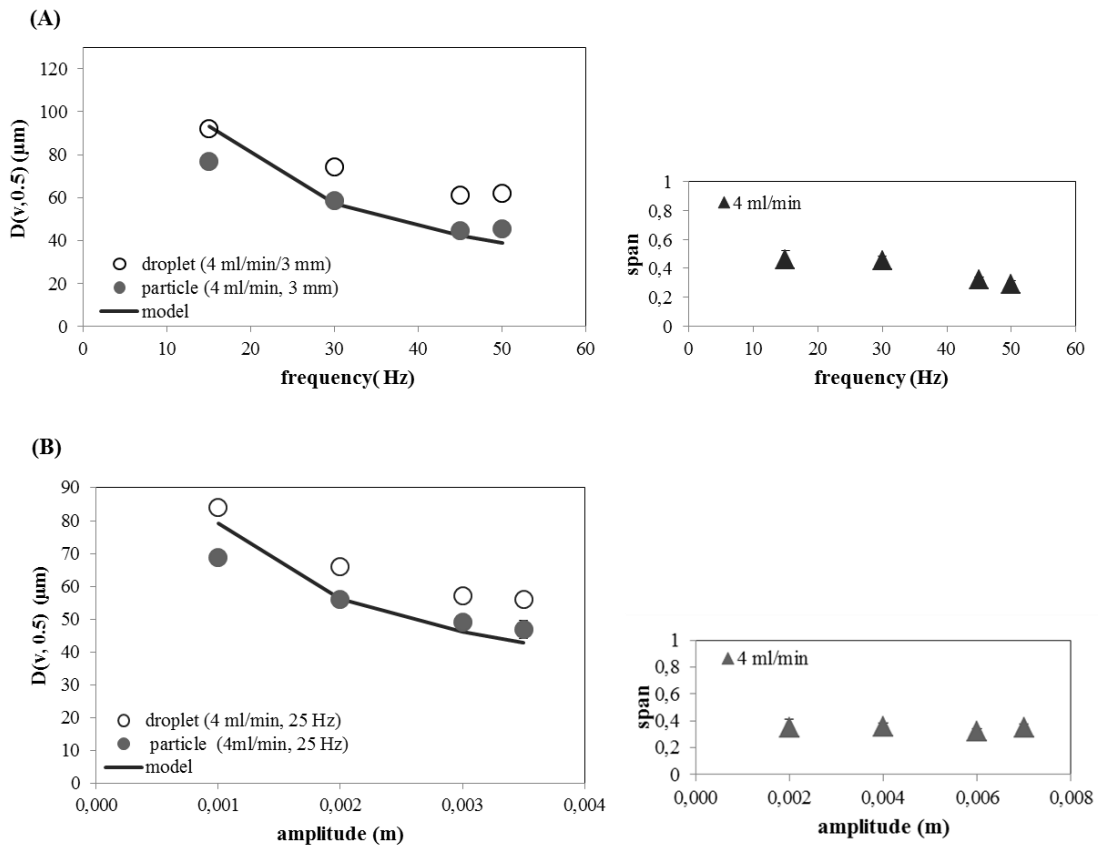


Figure 4.7 Droplet size of W/O/W emulsion and solid particle size and size distribution as a function of frequency (15-50 Hz,  $a = 1.5$  mm) and amplitude (1-3.5 mm,  $f = 25$  Hz);  $Q_{dp} = 4$  mlmin<sup>-1</sup>

### 3.3. Influence of dispersed phase injection flux on emulsion (O/W and W/O/W) and particle production

In Table 2.7 are reported the experimental conditions used to study the effect of the dispersed phase flux on particle size and size distribution of simple and double emulsion and solid particles. The injection flux was increased in a range of 23 Lh<sup>-1</sup>m<sup>-2</sup> to 288 Lh<sup>-1</sup>m<sup>-2</sup> increasing the flow rate of the syringe pump in a range of 2 ml min<sup>-1</sup> to 25 ml min<sup>-1</sup>. The shear stress and the flow rate of the continuous phase were constant at 5 Pa (45 Hz, 3 mm) and 53 ml min<sup>-1</sup> respectively.

Table 2.7 Effect of dispersed phase flux on mean droplet size, solid particle size and size distribution and experimental conditions

| O/W emulsion and solid particle |                     |              |   |             |                                 |                                 |            |
|---------------------------------|---------------------|--------------|---|-------------|---------------------------------|---------------------------------|------------|
| Droplet size [µm]               | D(v, 0.5) ±1.3 [µm] | Span (±0.03) | $J_{dp}$ [Lh <sup>-1</sup> m <sup>2</sup> ] | $\tau$ [Pa] | $Q_{dp}$ [mlmin <sup>-1</sup> ] | $Q_{cp}$ [mlmin <sup>-1</sup> ] | % DP (v/v) |
| 57                              | 44.8                | 0.31         | 23  | 5           | 2                               | 53                              | 3.8        |

| 57.4                              | 44.6                                  | 0.30                | 46                                      | 5           | 4                                | 53                               | 7.6        |
|-----------------------------------|---------------------------------------|---------------------|---|-------------|----------------------------------|----------------------------------|------------|
| 57.4                              | 46.9                                  | 0.28                | 125                                     | 5           | 10.8                             | 53                               | 20.6       |
| 66.5                              | 57.9                                  | 0.37                | 192                                     | 5           | 16.7                             | 53                               | 31.7       |
| 76                                | 60.8                                  | 0.40                | 288                                     | 5           | 25                               | 53                               | 47.5       |
| W/O/W emulsion and solid particle |                                       |                     |   |             |                                  |                                  |            |
| Droplet size [ $\mu\text{m}$ ]    | D(v, 0.5) $\pm 1.3$ [ $\mu\text{m}$ ] | Span [ $\pm 0.03$ ] | $J_{dp}$ [ $\text{Lh}^{-1}\text{m}^2$ ] | $\tau$ [Pa] | $Q_{dp}$ [ $\text{mlmin}^{-1}$ ] | $Q_{cp}$ [ $\text{mlmin}^{-1}$ ] | % DP (v/v) |
| 54                                | 44.6                                  | 0.35                | 23                                      | 5           | 2                                | 53                               | 3.8        |
| 61                                | 44.4                                  | 0.32                | 46                                      | 5           | 4                                | 53                               | 7.6        |
| 60                                | 48.6                                  | 0.34                | 125                                     | 5           | 10.8                             | 53                               | 20.6       |
| 59                                | 48.5                                  | 0.36                | 192                                     | 5           | 16.7                             | 53                               | 31.7       |
| 60                                | 46.9                                  | 0.31                | 216                                     | 5           | 18.3                             | 53                               | 35         |

The increase of the injection flux produced a slight increase of droplet size of O/W emulsion from 57  $\mu\text{m}$  to 76  $\mu\text{m}$  (which corresponds to an increase of solid particle size from 44.8  $\mu\text{m}$  to 60.8  $\mu\text{m}$ ). Quite uniform oil droplets were produced as showed in the photographs in Figure 5.7 (A-D) and span slightly increased from 0.30 to 0.4 in the same range of flux. Uniform droplets of double W/O/W emulsion with a mean size of 59  $\mu\text{m}$  (which corresponds to solid particles with a mean size of 47  $\mu\text{m}$ ) were produced in a range of flux between 23  $\text{Lh}^{-1}\text{m}^2$  and 216  $\text{Lh}^{-1}\text{m}^2$ . The uniformity of the particles was maintained constant with a span value in a range of 0.31 to 0.36 as showed in the photographs in Figure 5.7 (1A-1D). In membrane emulsification, the droplet formation and breakup process can be correlated with a dripping or jetting regime depending on the relative strength of different forces acting on the process. Results demonstrated that the “dripping” regime was dominant for the range of flux studied. In this regime, the drag force imparted by the torsional movement of the membrane and the surface tension force are the dominant forces affecting the droplet size. Therefore, the inertial contribution from the dispersed phase flux was negligible to the droplet size [15].

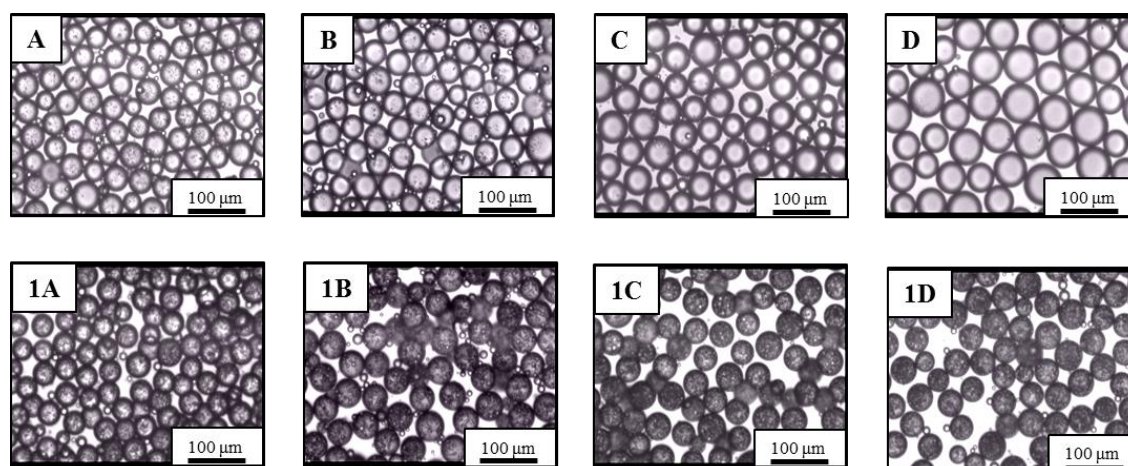


Figure 5.7 Photographs of O/W emulsion (A-D) and W/O/W emulsion (1A-4D) produced at



constant shear stress of 5 Pa (45 Hz, 1.5 mm) and different injection flux: A-23 Lh<sup>-1</sup>m<sup>-2</sup>; B-125 Lh<sup>-1</sup>m<sup>-2</sup>; C-288 Lh<sup>-1</sup>m<sup>-2</sup>; 1D-216 Lh<sup>-1</sup>m<sup>-2</sup>.

In this study, the use of micrometer pore sized sieve type membrane allowed the achievement of a controlled particle production in a wide range of flux thanks to the low porosity (0.44%) compared to SPG membrane (50-60%) and very low pressure drop required to inject the dispersed phase through the pores. The latter is due to the lack of tortuous pore channel compared with the structure of SPG or ceramic membranes. Another important aspect of this process is the possibility to produce very highly concentrated emulsion per unit time without the recirculation of the continuous phase along the circuit. The maximum concentration achieved in this study was almost 50% v/v per unit time (which means for a single pass of the continuous phase) keeping a good uniformity with a span of 0.4. This is a great challenge for the production of particles at industrial level because it is possible to achieve high productivity in shorter time and without the damage of fragile products that usually occurred in the cross-flow ME during the pump circulation.

### 3.4. From batch-scale to large scale production by torsional membrane emulsification

The possibility to produce particle with tailored size and uniformity by simple and reproducible techniques suitable for large scale production are important requirements to take into account in designing a microencapsulation process. The Dispersion Cell is suitable to work at batch scale but cannot be easily scale-up, therefore the torsional membrane emulsification was used to shift the preparation of simple O/W and double W/O/W emulsions from batch scale to large scale production. In Table 3.7 is reported a comparison of the process parameters (fluid-dynamic parameter and membrane parameters), the product achieved in terms of percentage of dispersed phase emulsified per unit time, size and uniformity of solidified particles at batch scale and large scale.

Table 3.7 Comparison of process and membrane parameters, particle size, uniformity and encapsulation efficiency achieved at bath scale and large scale production. DP-dispersed phase emulsified; MC-membrane configuration; MA-membrane area

| Batch-scale production (by Dispersion Cell) |  |           |  |                            |           |                  |                 |                                   |
|---|--|-----------|--|----------------------------|-----------|------------------|-----------------|-----------------------------------|
| Particle                                    | J <sub>dp</sub><br>[Lh <sup>-1</sup> m <sup>-2</sup> ] | τ<br>[Pa] | M.C.   | M.A.<br>[cm <sup>2</sup> ] | DP<br>(%) | D(v,0.5)<br>[μm] | span            | EE <sub>wow</sub><br>(%)<br>C(II) |
| simple                                      | 216  | >6        | Flat-sheet<br>stainless<br>steel pore<br>size:10μm | 1.85                       | 6         | 30.5<br>(±0.7)   | 0.30<br>(±0.03) | /                                 |
| Multi-<br>core<br>matrix<br>particle        | 216  | >6        | Flat-sheet<br>stainless<br>steel pore<br>size:10μm | 1.85                       | 6         | 29.3<br>(±0.8)   | 0.32<br>(±0.03) | 97 (±1)                           |

| Large- scale production (by Torsional membrane emulsification) |   |                |   |                            |                           |                        |                           |                                   |
|--|---|----------------|---|----------------------------|---------------------------|------------------------|---------------------------|-----------------------------------|
| Particle   | $J_{dp}$<br>[Lh <sup>-1</sup> m <sup>-2</sup> ] | $\tau$<br>[Pa] | M.C.  | M.A.<br>[cm <sup>2</sup> ] | DP<br>(%)                 | D(v,0.5)<br>[ $\mu$ m] | span                      | EE <sub>wow</sub><br>(%)<br>C(II) |
| simple   | 216   | >5             | Tubular<br>stainless<br>steel<br>Pore size:<br>15 $\mu$ m | 52                         | 35<br>per<br>unit<br>time | 59.3<br>( $\pm$ 1.3)   | 0.38<br>( $\pm$ 0.0<br>3) | /                                 |
| Multi-<br>core<br>matrix<br>particle                           | 216   | >5             | Tubular<br>stainless<br>steel<br>Pore size:<br>15 $\mu$ m | 52                         | 35<br>per<br>unit<br>time | 46<br>( $\pm$ 1)       | 0.31<br>( $\pm$ 0.0<br>2) | 98.5<br>( $\pm$ 1.1)              |

Highly uniform simple and micro-structured particles were produced at batch scale using a dispersed phase flux ( $J_{dp}$ ) of 216 Lh<sup>-1</sup>m<sup>-2</sup> and for shear stress up than 6 the particle size was 3 times the pore size of the membrane. Emulsions with a maximum content of dispersed phase of 6 % (v/v) were produced. The shift to higher throughput was carried out increasing the membrane area of almost 30 times, using membrane with tubular configuration (thus it is possible to further increase the membrane area adding more membranes in a device) and working in continuous mode. In this way, the droplet size can be controlled without interrupting the process and replacing the membrane and high dispersed phase concentration can be achieved per unit time controlling the ratio between the flow rate of the flowing continuous phase and the injection flow rate of the dispersed phase. In this study, emulsions with a content of dispersed phase of 35% were produced per unit time using the same dispersed phase flux of the batch scale process ( $J_{dp}$ =216 Lh<sup>-1</sup>m<sup>-2</sup>). The maximum content of dispersed phase achieved with this system was 47 % v/v increasing the injection flow rate of the dispersed phase ( $J_{dp}$ =288 Lh<sup>-1</sup>m<sup>-2</sup>) as reported in the previous paragraph. This means the production of 3.2 liter per hour of uniform emulsions with a content of dispersed phase in a range of 35 and 47 % in volume keeping the same fluid-dynamic conditions optimized at batch scale ( $J_{dp}$ =216 Lh<sup>-1</sup>m<sup>-2</sup>;  $\tau$ =5 Pa). Uniform simple and micro-structured particles with a mean size 3 times the pore size of the membrane were produced by torsional membrane emulsification keeping the same fluid-dynamic conditions optimized at batch scale ( $J_{dp}$  =216 Lh<sup>-1</sup>m<sup>-2</sup>;  $\tau$  > 6 Pa). The great advantage of the use of membrane based process to produce emulsion is the possibility to easily scale-up the process once optimized the chemical and process parameters at batch scale by increasing the membrane area without affecting the uniformity of the emulsion.

The encapsulation efficiency of copper into the double emulsion produced at the optimized fluid-dynamic conditions ( $J_{dp}$  =216 Lh<sup>-1</sup>m<sup>-2</sup>;  $\tau$ = 5 Pa) by the torsional membrane emulsification was 98.5 ( $\pm$ 1.1)%. This result is quite similar to the encapsulation achieved at batch scale using the Dispersion Cell (97%). This means that the breakage or damage of the double emulsion did not occur in the torsional system thanks to the absence of additional shear related to the circulation of the emulsion in the pump and the circuit. This demonstrated the great potential of this system for the

production of pharmaceutical products in which the bioactive compounds can be easily degraded by high shear conditions.

#### 4. Conclusions

The shift from batch scale to large scale production of simple O/W and double W/O/W emulsion was successfully achieved by using torsional membrane emulsification. The use of this system allowed the production of highly concentrated emulsions with a content of dispersed phase up than 35% (v/v) in a single pass of the continuous phase keeping the uniformity of the particles and a dispersed phase flux in a range of 216 and 288 Lh<sup>-1</sup>m<sup>-2</sup>. Simple particle in a range of 95 μm and 45 μm and multi-core matrix particles in range of 76 μm and 46 μm were produced at a shear stress in a range of 1 Pa and 5.9 Pa. The possibility to generate the shear stress without the recirculation of the emulsion along the circuit and the pump allowed to preserve the integrity of fragile products such as double W/O/W emulsion as demonstrated by the quite high encapsulation efficiency of copper of 98.5%. This demonstrated the great potential of this system for the production of drug delivery system in which the bioactive compounds can be easily degraded by high shear conditions. Another potential advantage of this process for an industrial outlook is the possibility to be applied in an integrated system in which a reactor downstream the emulsification step is used for the formation of the polymeric particles by the solvent diffusion process. In this way a controlled production of uniform solidified particles could be achieved continuously with high throughput.

#### References

1. Piacentini E, Drioli E, Giorno L. Membrane emulsification technology: Twenty-five years of inventions and research through patent survey. *J Memb Sci.* 2014;468:410–22.
2. Spyropoulos F, Lloyd DM, Hancocks RD, Pawlik AK. Advances in membrane emulsification. Part B: recent developments in modelling and scale-up approaches. *J Sci Food Agric.* 2014;94(4):628–38.
3. Joscelyne SM, Trägårdh G. Membrane emulsification — a literature review. *J Memb Sci.* 2000;169:107–17.
4. Vladislavljević GT, Williams R a. Recent developments in manufacturing emulsions and particulate products using membranes. *Adv Colloid Interface Sci.* 2005;113(1):1–20.
5. Vladislavljević GT, Kobayashi I, Nakajima M. Production of uniform droplets using membrane, microchannel and microfluidic emulsification devices. *Microfluid Nanofluidics.* 2012;13(1):151–78.

6. Vladisavljević GT, Williams R a. Manufacture of large uniform droplets using rotating membrane emulsification. *J Colloid Interface Sci.* 2006;299(1):396–402.
7. Yuan Q, Aryanti N, Hou R, Williams R a. Performance of slotted pores in particle manufacture using rotating membrane emulsification. *Particuology.* 2009;7(2):114–20.
8. Holdich RG, Dragosavac MM, Vladisavljevic GT. Membrane Emulsification with Oscillating and Stationary Membranes. *Ind Eng Chem Res.* 2010;3810–7.
9. Vladisavljevic GT, Wang B, Dragosavac MM, Holdich RG. Production of food-grade multiple emulsions with high encapsulation yield using oscillating membrane emulsification. *Colloids Surfaces A Physicochem Eng Asp.* 2014;458:78–84.
10. Holdich RG, Dragosavac MM, Vladisavljevic GT, Piacentini E. Continuous Membrane Emulsification with Pulsed ( Oscillatory ) Flow. *Ind Eng Chem Res.* 2013;52:507–15.
11. Piacentini E, Drioli E, Giorno L. Pulsed back-and-forward cross-flow batch membrane emulsification with high productivity to obtain highly uniform and concentrate emulsions. *J Memb Sci.* 2014;453:119–25.
12. Kosvintsev SR, Gasparini G, Holdich RG, Cumming IW, Stillwell MT. Liquid - Liquid Membrane Dispersion in a Stirred Cell with and without Controlled Shear. *Ind Eng Chem Res.* 2005;9323–30.
13. Stillwell MT, Holdich RG, Kosvintsev SR, Gasparini G, Cumming IW. Stirred Cell Membrane Emulsification and Factors Influencing Dispersion Drop Size and Uniformity. *Ind Eng Chem Res.* 2007;46(3):965–72.
14. Dragosavac MM, Sovilj MN, Kosvintsev SR, Holdich RG, Vladisavljević GT. Controlled production of oil-in-water emulsions containing unrefined pumpkin seed oil using stirred cell membrane emulsification. *J Memb Sci.* 2008;322(1):178–88.
15. Pathak M. Numerical simulation of membrane emulsification: Effect of flow properties in the transition from dripping to jetting. *J Memb Sci.* 2011;382(1-2):166–76.

# CHAPTER 8

## **Micro-structured particles for the encapsulation of hydrophilic and hydrophobic compounds: influence of process and chemical parameters**

### **1. Introduction**

Microencapsulation is an extensively used technique to encapsulate food compounds, cosmetics, drugs, protein, cells etc. In the pharmaceutical industry, the microencapsulation of drug allowed: 1) to improve its stability, 2) to protect it from environmental conditions, 3) to reduce side effects or mask unpleasant taste, 4) to reduce dosing frequency and total dosing amount, 5) to obtain a better pharmacological activity and controlled release [1]. So far, most of promising therapeutic substances have been limited in clinical practice because of their restrictive physico-chemical properties, which have required frequent administration. These substances may become more widely used in a clinical setting if appropriate microencapsulation techniques can be designed to overcome their intrinsic inconveniences. Some cases, the poor efficacy of drugs can be attributed also to a drug-mitigating response of the biological system. In this case drugs designed to act against an individual target cannot combat complex diseases such as cancer, or diseases which affect multiple tissue or cell types such as diabetes, immune-inflammatory disorders, bacterial and viral infections [2]. The limitations of many monotherapies can be overcome by attacking the disease on multiple fronts because the biological system is less able to adaptive resistance for the action of two or more drugs simultaneously. Indeed, multi-target approach is the novel strategy especially for the treatment of cancer. The process of oncogenesis is known to be multigenic and the targeting of the key node or pathway essential for cancer cell survival or resistance can suppress cancers more efficiently [3]. Co-administration of two or more drugs in clinical practice is a common strategy for the improvement of the therapeutic efficacy, because it offers the possibility to overcome the drug resistance and takes the advantage of the synergistic effect of drugs. However, the combined drugs are usually taken separately and have poor distribution and absorption in the body. The ability to include the various drugs in a single carrier allows to overcome this problem by minimizing the side effects and reduce the frequency of administration [4]. Some example of carrier at micro and nano scale, such as liposomes, micelles, polymer-drug conjugates and core-shell particles have been developed for co-delivery of multiple drugs [5–8]. However, to date, combining drugs into a single carrier is still a challenge for encapsulation technologies and very few studies have reported the simultaneous encapsulation and delivery of hydrophilic and hydrophobic compounds. Compared with nanocarrier, microcarrier can encapsulate easier bio-macromolecular drugs (such as protein or nucleic acid) and more small molecular drugs due to the bigger volume [8].

In this study, multi-core matrix particles with an hydrophobic matrix material entrapping an aqueous core were tested for the simultaneous encapsulation of hydrophilic and hydrophobic compounds. Copper ions and  $\alpha$ -tocopherol were used as hydrophilic and hydrophobic drug models and they were encapsulated in the core and polymer matrix of the particles. The particles were obtained from the W/O/W double emulsion-solvent diffusion process discussed in Chapter 5. The use of membrane based process in the emulsification step allowed to produce uniform droplets under gentle process conditions compared to the conventional methods leading to high encapsulation efficiencies of the molecules. The influence of chemical and process parameters on particle morphology and encapsulation efficiency were studied in the post emulsification step.

## 2. Experimental section

### 2.1. Chemicals

Cu(II) in the form of copper sulphate (Fisher Scientific, MW 65 g/mol, 2000 ppm) was used as hydrophilic drug model entrapped in the core material of the particles.  $\alpha$ -tocopherol or vitamin E (Sigma Aldrich, MW 430.71 g/mol, 5000 ppm) was used as hydrophobic drug model entrapped in the polymer matrix of the particles. Dichloromethane (DCM, supplied from Sigma-Aldrich) was used as organic solvent for the disruption of the particles. Ethanol (supplied from Sigma-Aldrich) was used for the dissolution of  $\alpha$ -tocopherol and for the extraction from the solid particles. All the aqueous solutions were prepared using ultrapure water with a resistivity of 18.2 M $\Omega$ ·cm.

### 2.2. Multi-core matrix particle preparation

W/O/W double emulsion/solvent diffusion method was used for the production of the multi-core matrix particles and this part of the work is discussed in more details in Chapter 5.

### 2.3. Copper extraction, encapsulation efficiency and drug loading

The encapsulation of copper ions was investigated immediately after the emulsification process and by extraction method after particle disruption. According to the study of Vladislavljevic et al. [8], the encapsulation efficiency ( $EE\%$ ) of the double emulsion was calculated as reported in Equation 1. The calculation of the equation is discussed in more details in the experimental section of Chapter 7.

$$EE = 1 - \frac{C_0}{C_i} \frac{1 - \phi_{wow}}{\phi_{wow} \phi_{wo}} \quad (1)$$

In this study  $C_i$  was 2000 ppm,  $\phi_{wo}$  was changed in the range between 0.1 and 0.3 and  $\phi_{wow}$  is 0.06. The maximum concentration of Cu(II) in the double emulsion corresponding to infinitely long release time ( $C_\infty$ ) was in the range between 12.76 ppm and 38.3 ppm.  $C_\infty$  was calculated from Equation 1 as  $C_0$  value for  $EE=0$ .

The encapsulation efficiency of the particles was determined by an extraction method of copper after particle disruption. In this case, 100 mg of powder was dissolved in 4 ml of DCM using ultrasounds for few seconds. Afterwards, 6 ml of water was added in the organic phase and the mixture was stirred gently over-night in order to extract the copper ions into the aqueous phase. The sample was centrifuged at 3000 rpm for 10 minutes in order to have a complete separation of the phases and the concentration of copper ions in the aqueous phase was determined by Atomic Adsorption Spectroscopy (AAS, SpectrAA 55B, Varian). It allows a precise measurement of a specific element at very small concentration. The operating parameters used and the calibration curve are reported in the Appendix 1 of the thesis.

The encapsulation efficiency ( $EE\%$ ) was calculated as the ratio between the mass of copper measured by AAS to the mass of copper added (Equation 2). The latter was calculated taking into account the maximum concentration of Cu(II) in the double emulsion right after the emulsification process ( $C_\infty$ ).

$$EE \text{ (copper ions)}\% = \frac{\text{mass Cu(II)extracted (g)}}{\text{mass Cu(II)added (g)}} * 100 \quad (2)$$

The drug loading ( $DL\%$ ) was calculated as the ratio of the drug encapsulated to the total mass of powder:

$$DL(\%) = \frac{\text{mass of drug extracted (g)}}{\text{mass of powder (g)}} * 100 \quad (3)$$

#### 2.4. Vitamin extraction and encapsulation efficiency

For the extraction of  $\alpha$ -tocopherol, 60 mg of powder was dissolved in 4 ml of DCM using ultrasounds for few seconds. The extraction of  $\alpha$ -tocopherol was performed by adding a known volume of ethanol in DCM after particle disruption. Afterwards, since DCM has a very low boiling point (40° C) compared to ethanol (80° C), it was easily removed by evaporation under a fume cupboard with a consequent precipitation of the polymer. The organic suspension was centrifuged at 3000 rpm for 10 minutes and the vitamin content in the supernatant was analyzed by UV/VIS spectroscopy ( $\lambda=285$  nm). The calibration curve is reported in the Appendix 1 of the thesis. The experiment was performed in triplicate and the encapsulation efficiency was calculated using the ratio of the mass of  $\alpha$ -tocopherol determined analytically to the mass of  $\alpha$ -tocopherol added, as shown in Equation 4:

$$EE \text{ (}\alpha\text{-tocopherol)}\% = \frac{\text{mass extracted (g)}}{\text{mass added (g)}} * 100 \quad (4)$$

### 2.5. Particle morphology

The morphology of the particles was observed by Scanning Electron Microscopy (SEM). Dried samples were sprinkled on a double-sided adhesive tape attached to an aluminum stub and metal coated.

## 3. Results and discussion

There are three main factors that can affect the drug encapsulation efficiency during the emulsification and solidification of the double emulsion: i) coalescence between internal and external water phase, ii) coalescence or break-up of double emulsion droplets, iii) diffusion of drug from the inner to the outer aqueous phase through the oil phase. All these factors are correlated with leakage of the hydrophilic drug into the external aqueous phase. The chemical composition of the double emulsion and the process parameters of the solidification step affects the encapsulation efficiency by controlling these mechanisms.

### 3.1. Influence of the chemical composition on particle morphology and encapsulation efficiency

Two different formulations (F1 and F2) were used to study the influence of the composition of the double W/O/W emulsion on the encapsulation efficiency. In Figure 1.8 is reported the encapsulation efficiency of Cu(II) in the double emulsion and in the solidified particles and the chemical composition of the formulations.

|            |  |
|------------|--|
| <b>F 1</b> | $W_1$ -5 % of fish gelatin; $O$ - 30% of PCL in DCM; $W_2$ -PVA 1%               |
| <b>F 2</b> | $W_1$ -ultrapure water; $O$ - 30% of PCL and 4% of PGPR in DCM;<br>$W_2$ -PVA 1% |



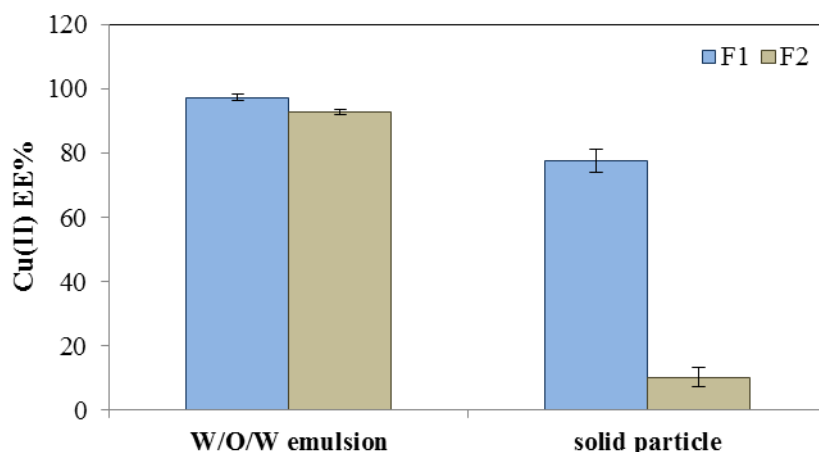


Figure 1.8 Encapsulation efficiency of Cu(II) of the double emulsion and solidified particles produced with 30% of PCL and fish gelatin (F1), PGPR (F2)

The kind of stabilizer used for the preparation of the double emulsion did not influence significantly the encapsulation of copper right after the emulsification process and it was quite constant in a range of 97.4 ( $\pm 0.8$ ) % and 92.7 ( $\pm 0.5$ ) % for the formulation containing fish gelatin and PGPR respectively. This is in good agreement with data collected for the stability of the primary emulsion reported in chapter 5.

On the contrary, the kind of stabilizer affected the encapsulation efficiency of the solidified particles: 77.5 ( $\pm 3.6$ ) % of copper was extracted from the particles produced with fish gelatin as stabilizer while 10 ( $\pm 3$ ) % of copper was extracted from the particles produced with PGPR as stabilizer. The particles were solidified in excess of water ( $V_{sd}=2.5V_{th}$ ) in order to have a fast solidification of the polymer at the interface. The measured encapsulation efficiencies can be explained with the analysis of particle morphology. In Figure 2.8 are reported SEM pictures of particles produced with different kind of stabilizer in the double emulsion.

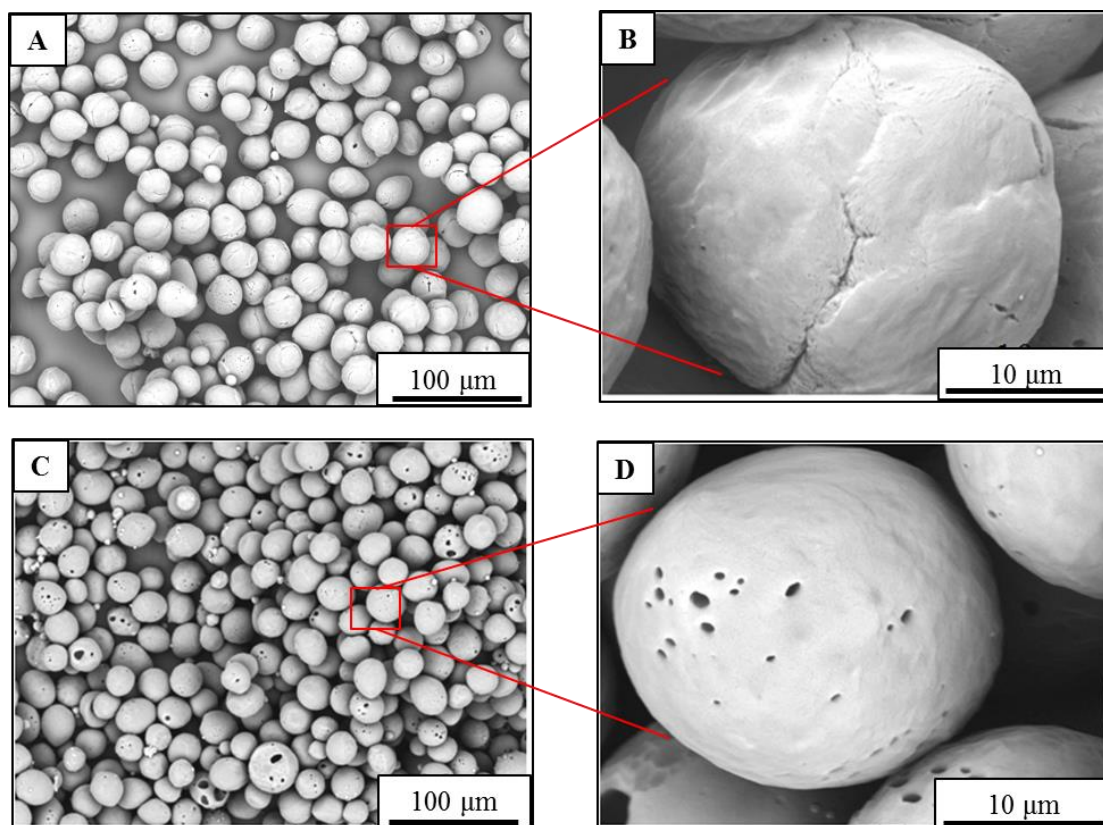


Figure 2.8 SEM photographs of multi-core matrix particles containing: 5% of fish gelatin (A and B), 4% of PGPR (C and D)

Matrix particles containing fish gelatin in the core material are characterized by a spherical shape and a slightly rough surface with some cracks probably due to the shrinkage of the particle when the solvent diffused out of the droplet (photographs A-B). No pores appeared on the surface, thus the structural integrity of the particles was preserved in the solidification step leading to the encapsulation of the hydrophilic molecule within the particle. On the contrary, most of the particles produced with PGPR as emulsifier in the organic phase are characterized by the presence of big holes and pores on the surface (photograph C-D). During the solidification of the particles the poly-glycerol chains of PGPR can be exposed into the water phase at the oil/external aqueous interface promoting the absorption and transport of water between the outer and inner aqueous phase leading to the formation of channels or pores in the matrix. The porous structure is related with a loss of the inner aqueous phase resulting in low encapsulation efficiency of the hydrophilic molecule. The encapsulation efficiency of  $\alpha$ -tocopherol was not affected by the chemical composition of the double emulsion and quite similar encapsulation of  $93 (\pm 6.7)\%$  and  $99 (\pm 1)\%$  was measured for the particle containing fish gelatin and PGPR respectively. This is an expected result considering that  $\alpha$ -tocopherol is a molecule not soluble in water, so it was entrapped in the hydrophobic polymer matrix during the solidification step and the loss into the water phase was negligible.

### 3.2. Influence of the volume of dilution medium and the kind of stabilizer used in the solidification step

The solidification of the particles was carried out using the solvent diffusion process already discussed in Chapter 4 and 5 for the preparation of simple and multi-core particles. In this process the formation of solidified particles is correlated with the solvent removal from the drop that causes the polymer accumulation and solidification at droplet interface forming a polymeric crust. The encapsulation efficiency of hydrophilic molecules is strongly affected by the solidification rate of the polymeric matrix. In this process, changing the volume of water ( $V_{sd}$ ) respect to the theoretic volume ( $V_{th}$ ) is possible to control the solidification rate of the droplets and the morphology of solidified particles. In this study the particles were produced from a double W/O/W emulsion containing 30% of polymer in the organic phase and 5% of fish gelatin in the inner aqueous phase. The primary W/O emulsion contained 10% (v/v) of aqueous phase and double W/O/W emulsion with 6% of dispersed phase (W/O) was produced. In Table 1.8 are reported the experimental conditions used for the solidification of the particles.

Table 1.8 Experimental conditions to carry out the solvent diffusion process at increased  $V_{sd}/V_{theoretic}$  ratio and the effect on the solidification time of the droplets

| $V_{sd}$ (L) | $V_{sd}/V_{theoretic}$ | Droplet solidification time |
|--------------|------------------------|-----------------------------|
| 0.3          | 1                      | 1 hour                      |
| 0.75         | 2.5                    | 10 minutes                  |
| 1.5          | 5                      | instantaneous               |
| 2.4          | 8                      | instantaneous               |

Results demonstrated that increasing the volume of water available for the solvent diffusion compared to the theoretic volume allowed a reduction of the solidification time of the polymer within the droplet because of a faster diffusion of the solvent through the droplet. An instantaneous solidification of the droplets was observed when the volume of water used was in high excess, 5 and 8 times the theoretic volume. This aspect is of great importance when a drug soluble in water is encapsulated because the rapid formation of the polymeric crust reduced the drug diffusion before the particle solidification. In Figure 3.8 is reported the encapsulation efficiency of  $\alpha$ -tocopherol and Cu(II) of the particles solidified in different volume of water and with different kind of stabilizer in the dilution medium. Two water soluble stabilizers (1% SDS and 1% PVA) were used in the water phase for the solidification to study the influence on the encapsulation efficiency of the particles. SDS is an anionic emulsifier with a MW of 288 Da and PVA is a polymeric non-ionic stabilizer with a MW of 13-23 kDa. The encapsulation efficiency of  $\alpha$ -tocopherol was not affected by the volume of water used for the solvent diffusion and is quite constant at 93 ( $\pm$  6.7)% with a drug loading of 1.5 ( $\pm$  0.2)%. On the contrary, an increase of the encapsulation efficiency of copper from 29.6 ( $\pm$  5.3) % to 95 ( $\pm$  4)% and an increase of the drug loading from 1.3 ( $\pm$  0.3)% to 4.4 ( $\pm$

0.2)% was observed when the volume of water was increased from 1 to 8 times the theoretic volume and SDS was used as stabilizer in the aqueous phase.

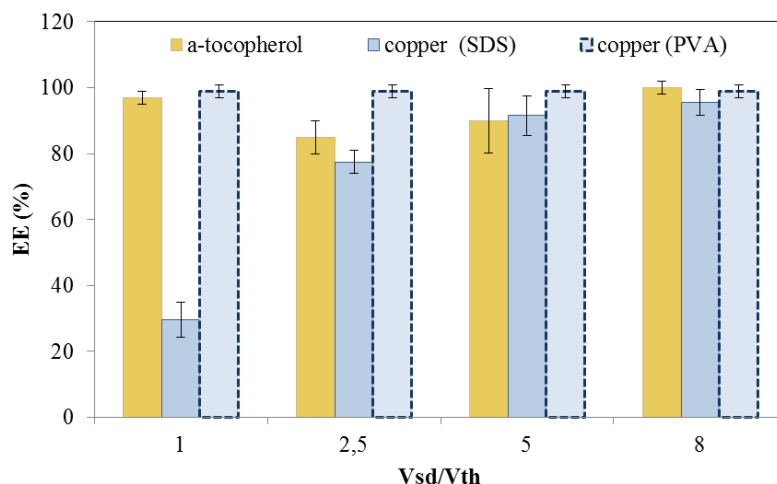


Figure 3.8 Encapsulation efficiency of Cu(II) and  $\alpha$ -tocopherol of multi-core matrix particles solidified in different volume of water and with different stabilizer

The different encapsulation efficiency of the particles solidified in different volume of water was in accordance with the particle morphology analyzed by SEM and illustrated in Figure 4.8. Particles with a porous structure were produced when the lowest volume of water ( $V_{sd}/V_{th}=1$ ) was used for the solidification. This is a consequence of the diffusion of water between the outer and inner aqueous phase which can occur when the organic phase was in a semi-solid state for long time (photograph A). In this case, the slow solidification of the polymer matrix is responsible for the loss of the inner aqueous phase resulting in low encapsulation efficiency [9]. The increase of the volume of water ( $V_{sd}/V_{th}=2.5$ ) allowed to reduce the solidification time of the polymer and the formation of pores and holes was avoided. However, some cracks and a slight roughness were observed on the surface of the particles (photograph B). When the solidification was moderately fast, water did not flow in the organic phase substantially and the polymer matrix was dense. However, the slow formation of a polymeric crust at water/droplet interface resulted in the formation of an irregular surface of the particle. A further increase of the volume of water ( $V_{sd}/V_{th}=5$  and 8) allowed the production of particles with dense and smooth surface because of an instantaneous solidification of the polymer at the interface that allowed to preserve the integrity of the particle and keep the inner aqueous phase within the particles (photographs C-D).

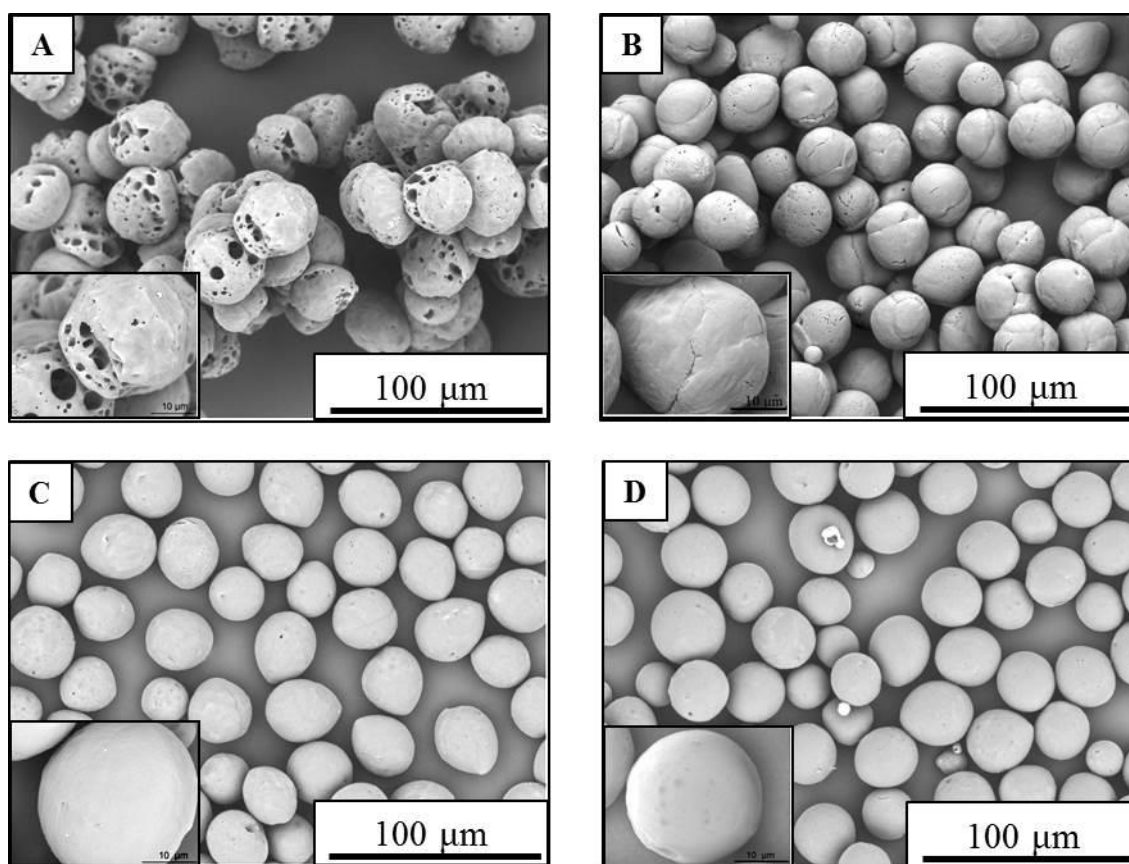


Figure 4.8 SEM photographs of PCL matrix particles produced with different ratio between the volume used ( $V_{sd}$ ) and the theoretic volume ( $V_{th}$ ) and SDS 2% as stabilizer. A)  $V_{sd}/V_{th}=1$ ; B)  $V_{sd}/V_{th}=2.5$ ; C)  $V_{sd}/V_{th}=5$ ; D)  $V_{sd}/V_{th}=8$

The use of PVA as stabilizer in the aqueous phase allowed to achieve an encapsulation efficiency of copper of almost 100% independently from the volume of water used for the solidification of the particles (Figure 3.8). PVA is a viscosity-enhancing stabilizer and a polymer colloid compared to SDS. Thus, the adsorbed layer of the polymeric stabilizer at the droplet/ water interface can slow down the diffusion of water between the external and inner aqueous phase through the polymer film, when the solidification of the polymer matrix was carried out in low volume of external aqueous phase ( $V_{sd}/V_{th}=1$ ). Bodmeier et al. [10] and Yang et al. [11] observed an increase of the encapsulation efficiency of hydrophilic molecule with the increase of PVA concentration in the aqueous phase which is in agreement with ours result. The analysis of particle morphology (Figure 5.8, A-C) confirmed that the presence of PVA in the external aqueous phase allowed to avoid the transfer of water between the inner and outer aqueous phase due to the formation of an adsorbed layer around the droplets. Indeed, the particles are characterized by a quite dense polymer matrix without porous surface independently from the volume of aqueous phase used for the solidification. The use of polymeric stabilizer for the solidification of the particles can be advantageous because it allowed to preserve the shape and uniformity of the particles and to achieve high encapsulation efficiency of the hydrophilic molecule using lower volume of water.

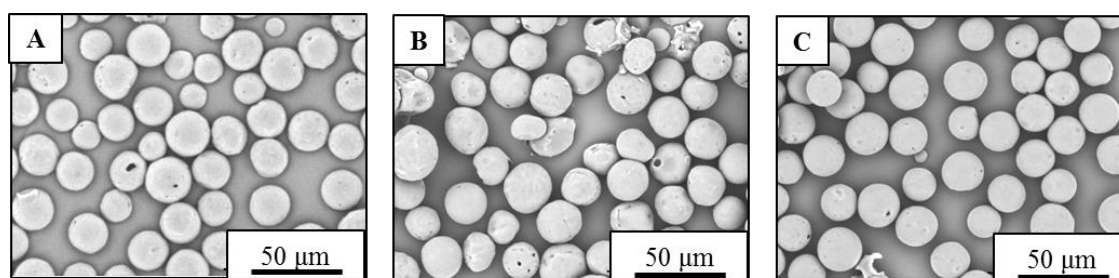


Figure 5.8 SEM photographs of PCL matrix particles produced with different ratio between the volume used ( $V_{sd}$ ) and the theoretic volume ( $V_{th}$ ) and PVA 1% as stabilizer. A)  $V_{sd}/V_{th}=1$ ; B)  $V_{sd}/V_{th}=2.5$ ; C)  $V_{sd}/V_{th}=5$

### 3.3. Influence of the inner aqueous phase volume fraction ( $W_1$ ) on the encapsulation efficiency

The influence of the volume fraction of the inner aqueous phase ( $\phi_{wo}$ ) was evaluated increasing this parameter from 0.1 to 0.3 keeping the same volume of organic phase at 15 ml. In Table 2.8 are reported the chemical composition of the emulsions used for the preparation of the particles, the encapsulation efficiency of copper ions and  $\alpha$ -tocopherol and the drug loading. The solidification of the particles was carried out using a volume of water 5 times the theoretic volume in order to have a fast solidification of the polymer.

Table 2.8 Experimental conditions, encapsulation efficiency (EE) and drug loading (DL) of solid particles produced at different volume fraction of  $W_1$  ( $\Phi_{wo}$ ). FG-fish gelatin; PCL-polycaprolactone; PVA-poly-vinyl alcol; Vsd-Volume used; Vth- theoretic volume;  $\Phi$ -volume fraction; Th-teorethical

| $W_1$<br>(FG) | O<br>(PCL) | $W_2$<br>(PVA) | $\Phi_{wo}$ | $\Phi_{wow}$ | $V_{sd}/$<br>$V_{th}$ | EE(%)<br>Cu(II)       | EE<br>(%)<br>Vit E    | DL%                  |      |
|---------------|------------|----------------|-------------|--------------|-----------------------|-----------------------|-----------------------|----------------------|------|
|               |            |                |             |              |                       |                       |                       | Actual               | Th   |
| /             | 30%        | 1%             | 0           | 0.06         | 5                     | /                     | 99<br>( $\pm 1$ )     | /                    | /    |
| 5%            | 30%        | 1%             | 0.1         | 0.06         | 5                     | 95.5<br>( $\pm 4$ )   | 99<br>( $\pm 1$ )     | 4.4<br>( $\pm 0.2$ ) | 4.4  |
| 5%            | 30%        | 1%             | 0.15        | 0.06         | 5                     | 65.32<br>( $\pm 1$ )  | 95.8<br>( $\pm 5.9$ ) | 4.3<br>( $\pm 0.2$ ) | 7    |
| 5%            | 30%        | 1%             | 0.3         | 0.06         | 5                     | 31.9<br>( $\pm 5.9$ ) | 99<br>( $\pm 1$ )     | 4.2<br>( $\pm 0.2$ ) | 11.7 |

The comparison of the encapsulation efficiency of  $\alpha$ -tocopherol in simple particle produced from an O/W emulsion ( $\phi_{wo}=0$ ) and multi-core matrix particles ( $\phi_{wo}=0.1-0.3$ ) revealed that it was not affected by the change of the particle structure. The encapsulation efficiency of copper into the double emulsion was slightly reduced from 97.4 ( $\pm 0.8$ ) % to 93.4 ( $\pm 0.2$ ) % when the volume fraction of the inner aqueous phase

( $\phi_{wo}$ ) was increased from 0.1 to 0.3. Since more aqueous phase is added into the same volume of organic phase, droplet of double emulsion with a thinner organic film between the inner and outer aqueous phase are produced and some diffusion of copper can easily occurred during the emulsification process. In the solidification step, a reduction of the encapsulation efficiency from 95 ( $\pm 4$ )% to 31.9 ( $\pm 5.9$ )% was observed with the increase of volume fraction. The latter produced an increase of the theoretical drug loading from 4.4% to 11.7 % because the total amount of the inner aqueous phase into the same volume of organic phase was increased. However, the actual drug loading decreased compared to the theoretical value and was almost constant in a range between 4 ( $\pm 0.3$ ) % and 4.5 ( $\pm 0.1$ ) %. Two mechanisms can be correlated with the reduction of encapsulation efficiency and the actual drug loading when the volume fraction of the inner water phase is increased. The first is the increase of the concentration gradient of the encapsulated copper ions that is the drag force to induce the diffusion of ions into the external aqueous phase [12]. The second mechanism is the contact between the internal and external aqueous phase and the coming out of the hydrophilic drug can occurred easily during the solidification step [12]. The last mechanism seems to be the main responsible of the low encapsulation efficiency of the particles produced with a volume fraction of 0.3 as demonstrated by the analysis of the particle morphology illustrated in Figure 6.8 (photograph C). The particle are characterized by the presence of holes and porous skin which are a consequence of the diffusion of water through the polymeric film during the solidification step. Particles containing a volume fraction of 0.15 (photograph B) are characterized by a quite dense structure of the polymer matrix without a significance presence of pores and holes and the morphology was quite similar to the particles produced with the volume fraction of 0.10 (photograph A). Thus, the lower encapsulation efficiency was not due to the loss of inner aqueous phase but can be correlated mainly with the diffusion of copper ions as previously described.

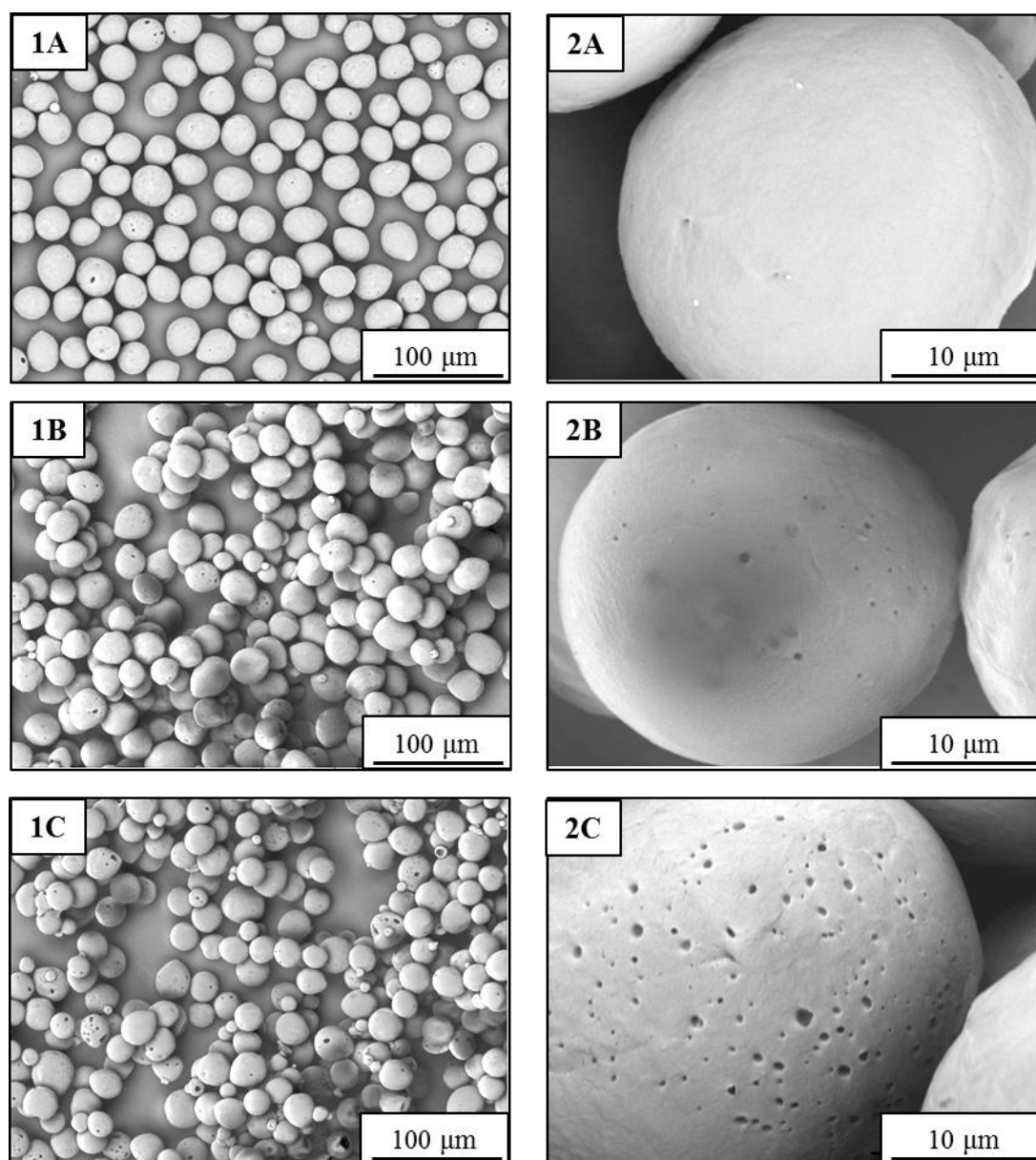


Figure 6.8 SEM photographs of PCL multi-core matrix particles produced with different volume fraction of inner aqueous phase ( $\phi_{wo}$ ). A (1-2):  $\phi_{wo}=0.1$ ; B(1-2):  $\phi_{wo}=0.15$ ; C(1-2):  $\phi_{wo}=0.3$ . Solidification conditions:  $V_{sd}/V_{th}=5$  and 2% SDS.

### 3.4. Comparison between PLGA and PCL for the encapsulation of hydrophilic molecules

PLGA is the most popular biodegradable polymers used for the preparation of drug delivery systems. The main advantage of this polymer is the possibility to tune the physical properties controlling the ratio of lactic acid and glycolic acid to achieve a controlled degradation and so the release of the drug overtime [13]. In this study a comparison of the entrapment efficiency of copper between PCL and PLGA particles was carried out. PLGA (75:25) is composed of 75% of poly-lactic acid (PLA) and 25% of poly-glycolic acid (PGA). The latter shows highly crystalline structure and hydrophilic property compared to PLA. In Table 3.8 are reported the chemical



composition of the double emulsion used for the preparation of the particles, the solidification conditions, encapsulation efficiency and drug loading of copper in the solidified particles.

Table 3.8 Encapsulation efficiency (EE%) and drug loading (DL%) of copper into PLGA and PCL particles

| <b>W<sub>1</sub></b><br><b>(FG)</b> | <b>O</b> | <b>W<sub>2</sub></b><br><b>(PVA)</b> | $\phi_{wo}$ | $\phi_{wow}$ | $V_{sd}/V_{th}$<br><b>(1%<br/>PVA)</b> | <b>Particle<br/>size<br/>(<math>\mu\text{m}</math>)</b> | <b>EE(%<br/>Copper)</b> | <b>DL(%<br/>Copper)</b> |
|-------------------------------------|----------|--------------------------------------|-------------|--------------|--|---|-------------------------|-------------------------|
| 5%                                  | 30%      | 1%                                   | 0.1         | 0.06         | 5                                      | 28.8<br>( $\pm 0.5$ )                                   | 99 ( $\pm 1$ )          | 4.4 ( $\pm$<br>0.2)     |
|                                     | PCL      |                                      |             |              |  |   |                         |                         |
| 5%                                  | 30%      | 1%                                   | 0.1         | 0.06         | 5                                      | 32 ( $\pm 1$ )  | 76 ( $\pm 1$ )          | 3.4 ( $\pm$<br>0.1)     |
|                                     | PLGA     |                                      |             |              |  |   |                         |                         |

The encapsulation efficiency of copper is 99 % and 76% with a drug loading of 4.4 % and 3.4 % for PCL and PLGA particles respectively. SEM analysis (Figure 7.8) of the particles revealed a quite similar morphology characterized by a dense and spherical polymer matrix with a smooth and pore-free skin. This demonstrated that the different encapsulation of copper is not related to a loss of the aqueous phase during the solidification process. The chemical properties of the polymer structure can be considered another potential factor to influence the encapsulation efficiency of hydrophilic molecule. PLGA used in this work is composed of a low percentage of PGA with hydrophilic property. The presence of this low molecular weight hydrophilic fractions is responsible of water absorption in the polymeric matrix because of the interaction between the highly dipolar water molecules and polymer polar groups (carbonyl and carboxyl groups). This interaction resulted in a reduction of the glass transition temperature of PLGA with a consequent influence on the structure of the polymer matrix. This plasticizer effect of water influenced the micro-structured property of the polymer characterized by an increased molecular mobility of the chains [14]. This structural modification of the polymer at macromolecular level can be responsible of a partial diffusion of copper ions during the solidification process resulting in lower encapsulation efficiency. Copper ions are very small molecules so the diffusion into the aqueous phase can easily occurred in this condition. On the contrary, PCL is an hydrophobic polymer with a poor content of carbonyl groups so the adsorption and interaction with water molecules is negligible compared to PLGA. In this way small hydrophilic molecules could be efficiently entrapped into the polymer matrix achieving high encapsulation efficiency.

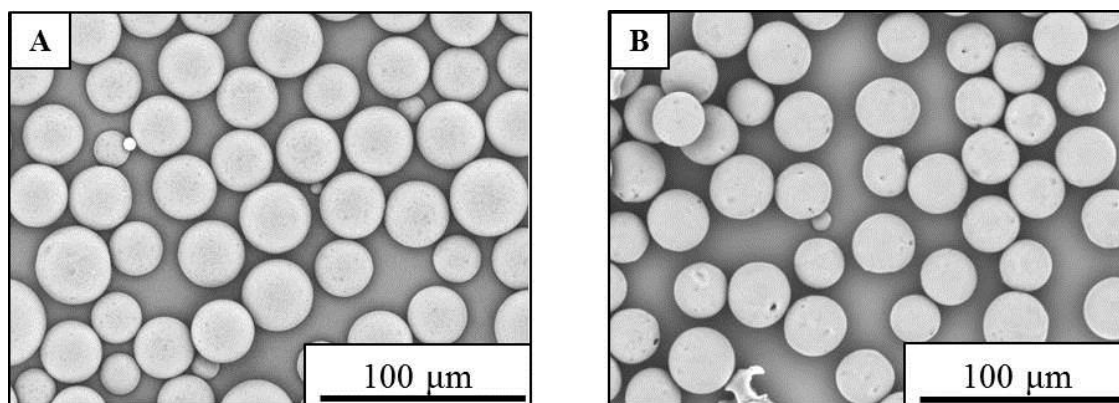


Figure 7.8. SEM photographs of: A) multi-core matrix particles with PLGA, 30%; B) multi-core matrix particles with PCL, 30%;

#### 4. Conclusion

A simultaneous encapsulation of hydrophilic and hydrophobic compounds of  $95 (\pm 4)\%$  and  $93 (\pm 6)\%$  was successfully achieved for multi-core matrix particles containing fish gelatin and poly-caprolactone and solidified with the solvent diffusion process. The volume of water used for the dilution of the emulsion and the kind of stabilizer are key parameters to control the particle morphology and the encapsulation efficiency of copper ions in this process. High encapsulation of hydrophilic copper ions in a range between 99% and 95% could be achieved either when a fast solidification of the polymeric matrix was carried out (using high excess of water) or when a polymeric stabilizer (such as PVA) is dissolved in the dilution medium. The high hydrophobicity of PCL allowed the achievement of higher entrapment of small copper ions during the solidification step compared to PLGA. The particles produced in this work could be potentially used as drug delivery system for multi-therapy and further studies regarding the increase of drug loading and the drug release over time could be interesting future works.

#### References

1. Huang H-J, Yuan W-K, Chen XD. Microencapsulation Based on Emulsification for Producing Pharmaceutical Products: A Literature Review. *Dev Chem Eng Miner Process*. 2008;14(3-4):515–44.
2. Zimmermann GR, Lehár J, Keith CT. Multi-target therapeutics: when the whole is greater than the sum of the parts. *Drug Discov Today*. 2007;12(1-2):34–42.
3. Reddy LH. Drug delivery to tumours: recent strategies. *J Pharm Pharmacol*. 2005;57(10):1231–42.

4. Wang B, Jiang W, Yan H, Zhang X, Yang L, Deng L, et al. Novel PEG-graft-PLA nanoparticles with the potential for encapsulation and controlled release of hydrophobic and hydrophilic medications in aqueous medium. *Int J Nanomedicine*. 2011;6:1443–51.
5. Hombreiro Pérez M, Zinutti C, Lamprecht A, Ubrich N, Astier A, Hoffman M, et al. The preparation and evaluation of poly(epsilon-caprolactone) microparticles containing both a lipophilic and a hydrophilic drug. *J Control Release*. 2000;65(3):429–38.
6. Windbergs M, Zhao Y, Heyman J, Weitz D a. Biodegradable core-shell carriers for simultaneous encapsulation of synergistic actives. *J Am Chem Soc*. 2013;135(21):7933–7.
7. Zhang H, Wang G, Yang H. Drug delivery systems for differential release in combination therapy. *Expert Opin Drug Deliv*. 2011;8(2):171–90.
8. Goran T Vladislavljevic, Wang B, Dragosavac MM, Holdich RG, Vladislavljevi GT. Production of food-grade multiple emulsions with high encapsulation yield using oscillating membrane emulsification. *Colloids Surfaces A Physicochem Eng Asp*. 2014;458:78–84.
9. Jyothi NVN, Prasanna PM, Sakarkar SN, Prabha KS, Ramaiah PS, Srawan GY. Microencapsulation techniques, factors influencing encapsulation efficiency. *J Microencapsul*. 2010;27(3):187–97.
10. Alex R, Bodmeier R. Encapsulation of water-soluble drugs by a modified solvent evaporation method. I. Effect of process and formulation variables on drug entrapment. *J Microencapsul*. 1990;7(3):347–55.
11. Yang YY, Chung TS, Ng NP. Morphology, drug distribution, and in vitro release profiles of biodegradable polymeric microspheres containing protein fabricated by double-emulsion solvent extraction/evaporation method. *Biomaterials*. 2001;22(3):231–41.
12. Liu R, Huang S-S, Wan Y-H, Ma G-H, Su Z-G. Preparation of insulin-loaded PLA/PLGA microcapsules by a novel membrane emulsification method and its release in vitro. *Colloids Surf B Biointerfaces*. 2006;51(1):30–8.
13. Makadia HK, Siegel SJ. Poly Lactic-co-Glycolic Acid (PLGA) as biodegradable controlled drug delivery carrier. *Polymers (Basel)*. 2011;3(3):1377–97.
14. Blasi P, D'Souza SS, Selmin F, DeLuca PP. Plasticizing effect of water on poly(lactide-co-glycolide). *J Control Release*. 2005;108(1):1–9.

## Overall Conclusions

The critical analysis of the literature allowed to identify the main limitations regarding the advancement of membrane emulsification at industrial level and several strategies have been investigated to improve the productivity of the process and the particle manufacturing for industrial outlook.

For what concerns the improvement of the productivity, membrane properties (such as wettability, porosity and pore structure) are of crucial importance to control the droplet size and the production rate of the emulsion. The tailored wettability property of the membrane between the lumen and the shell as well as the use of stainless steel micro-sieve membrane demonstrated to be successful to keep at the same time the controlled production of the emulsions and high dispersed phase flux. The results obtained give a contribution to promote the development of new membrane with specific structures and properties for the production of emulsions with high productivity.

Another important requirement for a particle-micro-manufacturing methodology is the possibility to make products at low shear conditions (to preserve the activity of the molecules encapsulated) keeping at the same time a precise control of particle size and uniformity. The combination of membrane emulsification and solvent diffusion process was investigated firstly at batch scale to identify the best conditions to produce particles with a controlled size and uniformity using two biodegradable polyesters suitable for pharmaceutical applications (PCL and PLGA). The use of microporous membrane allowed a simultaneous control of particle size and size distribution during the emulsification step. The control of the solidification of the polymer by the solvent diffusion rather than the evaporation of the solvent allowed to achieve a fast solidification of the polymer within the droplets keeping the morphology and the uniformity of the particles during the solidification step.

The production of particles by membrane emulsification/solvent diffusion process was subsequently investigated using recently introduced membrane emulsification processes suitable for large scale production and able to keep low shear condition in the bulk of the product stream (pulsed back-and-forward ME and torsional ME). Pulsed back-and-forward ME was investigated to shift from micro to nano scale particle production (particle size in a range of 2 $\mu\text{m}$  and 0.2 $\mu\text{m}$ ) using SPG membranes with appropriate pore size. The configuration of this system (in which the shear stress is generated by pulsating back-and-forward the continuous phase) allowed to achieve a controlled production of uniform emulsions using lower axial velocity than the values reported for the most commonly used cross-flow ME. This study introduces advances in the field of nanoparticle production technology and the process can be potentially used for the encapsulation of biomolecules.

The transition of the emulsion production from batch scale to large scale (in micron range) was achieved using micro-sieve stainless steel membrane in torsional motion. The advantages properties of the membrane allowed to keep a good control of particle uniformity at high dispersed phase flux. The generation of the shear stress by the

torsional motion of the membrane allowed to keep low shear conditions in the bulk of the product stream. Highly concentrated emulsion (> 40% v/v) were produced per unit time and in a continuous mode due to the configuration of the system. The potential advantage of this process for an industrial outlook is the possibility to be applied in an integrated system in which a reactor downstream the emulsification step is used for the production of the polymeric particles by the solvent diffusion process.

The micro-structured particles produced by membrane emulsification/solvent diffusion process were investigated for the simultaneous encapsulation of drugs. Few studies have been developed in the encapsulation of more drugs in a single carrier. The study carried out in this work permitted to identify the best operating and chemical conditions to achieve high encapsulation efficiency of hydrophilic as well as hydrophobic compounds. The particles produced in this work demonstrated to be good candidate for the simultaneous encapsulation of compounds and could be further investigated as drug delivery system for multi-therapy.

# APPENDIX 1

## A.I Malvern Mastersizer

Malvern Mastersizer was used for the characterization of the solid particles in terms of size and size distribution. The particles were suspended in water with an emulsifier to avoid their aggregation. The instrument is composed of three elements: i) *optical bench* in which the dispersed sample passes through and a laser beam illuminates the particles. A series of detectors then measures the intensity of light scattered by the particles within the sample; ii) *sample dispersion unit* which controls the sample dispersion and ensures that particles are delivered to the measurement area of the optical bench; iii) *instrument software* that controls the system during the measurement process and analyzes the scattering data to calculate particle size distribution. Malvern Mastersizer uses the technique of laser diffraction to measure the size of particles in a range of 0.02 to 2000  $\mu\text{m}$ . Laser diffraction measures particle size distributions by measuring the angular variation in intensity of light scattered as a laser beam passes through a dispersed particulate sample. Large particles scatter light at small angles relative to the laser beam and small particles scatter light at large angles. The angular scattering intensity data is then analyzed to calculate the size of the particles responsible to create the scattering pattern, using the Mie theory of light scattering. The latter calculates the particle size distribution, assuming a volume equivalent sphere model. Mie theory requires knowledge of the refractive index and absorbance of the sample being measured, along with the refractive index of the dispersant (generally water). A typical report of the measure showed a cumulative distribution curve defined by:

- $D(v, 0.5)$  is the size in microns at which 50% of the sample is smaller and 50% is larger;

-  $D(v, 0.1)$  is the size of particle below which 10% of the sample lies;

- $D(v, 0.9)$  gives a size of particle below which 90% of the sample lies;

The mean particle size is expressed as the surface weighted mean diameter (or Sauter diameter)  $D[3,2]$ , and as the volume weighted mean diameter, (or De Brouckere diameter)  $D[4,3]$  calculated as follows:

$$D[3,2] = \frac{\sum D_i^3 n_i}{\sum D_i^2 n_i} \quad (\text{A1})$$

$$D[4,3] = \frac{\sum D_i^4 n_i}{\sum D_i^3 n_i} \quad (\text{A2})$$

where  $D_i$  is particle diameter of class  $i$  and  $n_i$  is number of particles in class  $i$ . Droplet size distribution was expressed as *Span* number, calculated as follows:

$$Span = \frac{D[90] - D[10]}{D[50]} \quad (A3)$$

where  $D[x0]$  is the diameter corresponding to  $x_0$  vol.% on a relative cumulative droplet size curve.

### A.II Scion Image analysis

The software Scion Image was used to analyze the droplets dimensions of the W/O emulsions produced with the modified membrane, O/W and W/O/W emulsion produced with the stirrer Dispersion Cell and the torsional membrane emulsification. Since the instability of the oil droplets in the dispersant (for the presence of dichloromethane in the organic phase) it was not possible to measure the size of the droplets using Mastersizer. The emulsions were observed with the optical microscope (Zeiss, model Axiovert 25) equipped with a camera (JVC, model TK-C1481BEG). The images were acquired with Axiovision program and analyzed by using Scion Image software. The latter allows automatic counting and the measurement of the droplets in a selected area of the image and several random images were analyzed for each sample. A setting of the scale is necessary for the conversion of pixel to micron and it was performed measuring the corresponding pixel of 50 micron bar given with Axiovision. This procedure was performed for different magnification (10x-20x) and the corresponding conversions were measured: 1pixel=0.55  $\mu\text{m}$  (10x) and 1.14  $\mu\text{m}$  (20x). The diameter of each drops in the image was manually drawn and then the software converted automatically each diameter in micron. The resulting values were elaborated in Excel to calculate the mean diameter as  $D[3,2]$ ,  $D[4,3]$  and the size distribution as span using the Equation A1, A2, A3.

### A.III Zetasizer NanoZS

Zetasizer NanoZS was used to measure particle size and size distribution of the emulsions and solid micro and nanoparticles produced with the pulsed-back-and-forward ME. The instrument uses the technique of dynamic light scattering to measure the size of particles typically in a submicron range (0.6 nm to 6  $\mu\text{m}$ ). Dynamic light scattering (DLS) is a technique which measures Brownian motion of particles in suspension by illuminating the particles with a laser and analyzing the intensity fluctuations in scattered light. Brownian motions are correlated with the particle size: small particles move quickly and large particles move slowly. The fluctuation in scattering intensity depends on the speed of the Brownian motion and it is analyzed by a digital correlator which calculates a correlation function. Analysis of these intensity

fluctuations yields the velocity of the Brownian motion and hence the particle size using the Stokes-Einstein relationship:

$$d_H = \frac{KT}{3\pi\eta D} \quad (\text{A4})$$

where  $d_H$  is the hydrodynamic diameter,  $K$  is the Boltzmann's constant,  $\eta$  is the viscosity of the dispersant and  $D$  is the diffusion coefficient. The latter derived from the correlation function which is analyzed by cumulant analysis method. The standard report showed the intensity particle size distribution and the mean particle size is expressed as Z-average, which is the intensity weighted mean diameter derived from the cumulative analysis. Particle size distribution is expressed as polydispersion index (PDI), that is a dimensionless measure of the broadness of the size distribution calculated from the cumulant analysis. This is in the range between 0 and 1 and monodispersed sample showed a polydispersity below 0.1.

Zetasizer NanoZS was also used to measure the Zeta potential of solid particles in suspension. The charge or zeta potential of particles and molecules is determined by measuring their velocity while they are moving due to electrophoresis. The powder was dispersed in water with Tween 80 (1% v/v) as emulsifier at a pH of  $6.9 \pm 0.1$ . The suspension was displaced with a syringe into a capillary cells (Figure A.1) and an electric field is applied in order to induce the migration of charged particles or molecules towards an electrode (electrophoresis).

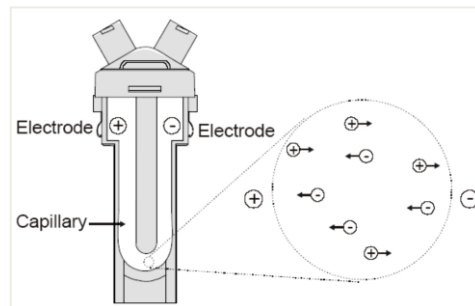


Figure A.1 Image of the capillary cells and electrophoresis of charged particle in presence of an electric field ([www.atascientific.com.au](http://www.atascientific.com.au))

The speed they move is proportional to the field strength and their zeta potential. The latter is correlated with the electrophoretic mobility ( $U_E$ ) of particles in Henry's equation:

$$U_E = \frac{2\varepsilon z F(Ka)}{3\eta} \quad (\text{A5})$$

where  $z$  is zeta potential,  $\varepsilon$  is the dielectric constant,  $\eta$  is the viscosity  $F(Ka)$  is Henry's function. The Zetasizer-Nano measures electrophoresis using the Doppler Effect in which a laser beam is passed through a sample undergoing electrophoresis and the



scattered light from the moving particles is frequency shifted. The mobility of the particles is measured with a technique called phase analysis light scattering (PALS).

#### A.IV Tensiometer- Du Noüy ring method

The interfacial tension measurements reported in this work were performed with the White Electric Instrument tensiometer (model DB2KS) using the Du Noüy ring method. In this method a platinum ring (Du Noüy ring) with defined geometrical dimensions is immersed inside the liquid with higher density (which is displaced at the bottom of a cylindrical glass vessel) and pulled out to the liquid with lower density (which is displaced on the top of glass vessel) by lowering the glass vessel until the detachment of the dense phase occurred and the interfacial tension is displayed. The interfacial tension is the maximum force ( $F$ ) required to pull the ring from the bottom liquid to the upper liquid. It can be expressed with the Equation A6:

$$F = 4\pi R\gamma\beta \quad (\text{A6})$$

where  $R$  is the ring radius,  $\gamma$  is the interfacial tension, and  $\beta$  the correlation factor.

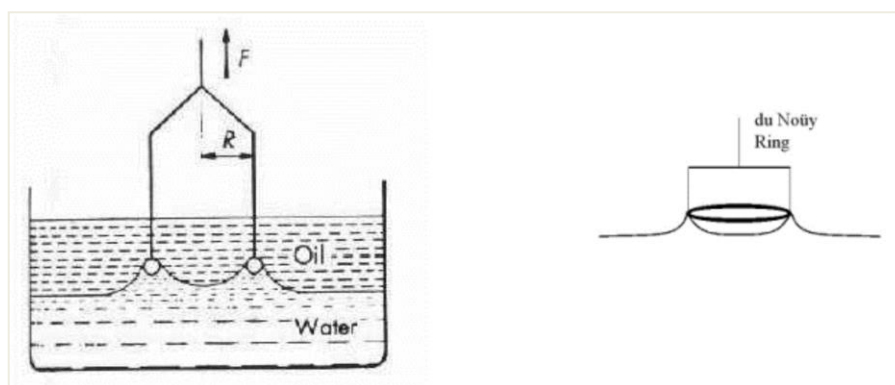


Figure A.2 Schematic representation of the Du Noüy ring method (<http://www.mastrad.com/tsd1.htm>)

#### A.V UV/Vis Spectrophotometer

UV/V spectroscopy (Lambda 35 and EZ201, Perkin Elmer) is commonly used in analytical chemistry for the quantitative determination of different analytes. In this thesis it was used for the quantification of protein (BSA and Lipase from *Candida Rugosa*) in combination with BCA test and for the quantification of  $\alpha$ -tocopherol extracted from the particles. The UV-Vis spectroscopy refers to absorption spectroscopy into the ultraviolet –visible spectra. The method is based on the capability of atoms to absorb and emit energy when they are excited in particular conditions. The energy absorbed at the excited state is emitted as a form of radiation when they return to their

ground state. The emission spectrum differs from each atomic species and the intensity of absorbed light is proportional to the concentration of the sample. The Lambert-Beer's law (Equation A7) states that the absorbance of a solution is directly proportional to the concentration of the absorbing species in the solution and the path length. Thus, for a fixed path length, UV/Vis spectroscopy can be used to determine the concentration of the absorber in a solution.

$$A = \log_{10}(I_0/I) = \epsilon cL \quad (\text{A7})$$

$A$  is the measured absorbance of the compound,  $I_0$  is the intensity of the incident light at a given wavelength,  $I$  is the transmitted intensity,  $L$  is the length of the chamber where the sample is put (path length),  $c$  is the concentration of the compound in the sample and  $\epsilon$  is a constant. A calibration curve (Figure A.3) was determined for  $\alpha$ -tocopherol dissolved in ethanol using  $\lambda=285\text{nm}$  and a range of concentration of  $0.01\text{-}0.4\text{ gL}^{-1}$ . The solutions were prepared by serial dilutions of a stock solution of  $5\text{ gL}^{-1}$ .

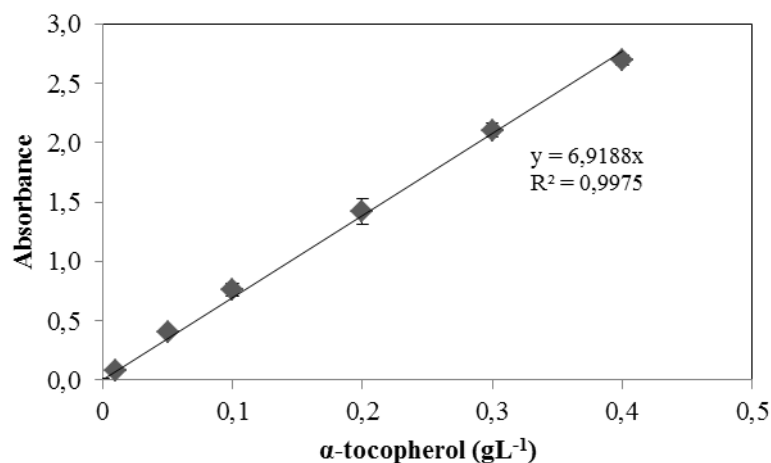


Figure A.3- Calibration curve of  $\alpha$ -tocopherol determined by UV/VIS spectrophotometer

#### A.VI BCA test

This test was used for the quantification of BSA and Lipase from *Candida Rugosa*. The principle of bicinchoninic acid (BCA) assay is based on the formation of a  $\text{Cu}^{2+}$ -protein complex under alkaline conditions, followed by reduction of  $\text{Cu}^{2+}$  to  $\text{Cu}^{1+}$ . This reduction occurred in presence of some aminoacids (cysteine, cystine, tryptophan, tyrosine) thus the amount of reduction is proportional to the protein amount. BCA forms a purple-blue complex with  $\text{Cu}^{1+}$  in alkaline condition. The color development is accelerated by incubation of the sample and the reagent at  $37\text{ }^\circ\text{C}$  for 30 minutes and it is subsequently quantified by UV/VIS spectrophotometer analysis ( $\lambda=562\text{ nm}$ ). The protein concentration is determined by comparison with a calibration curve obtained by quantification of BSA (Bovine Serum Albumin) protein standard solution. The angular

coefficient of the calibration curve is used to calculate the concentration of unknown protein samples. The calibration curve measured experimentally is reported in Figure A.4.

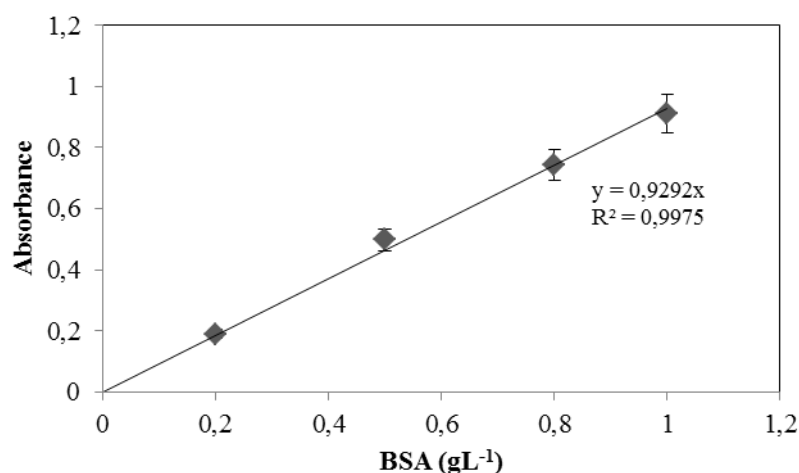


Figure A.4- Calibration curve of BSA determined by BCA assay and UV/VIS spectrophotometer

### A.VII Atomic Absorbance Spectrophotometer (AAS)

Atomic Absorption Spectrophotometer (Spectra AA 2000, Varian) was used for the determination of Copper, Cu(II), extracted from the particles and quantified in the continuous phase of the double emulsion. This is a technique based on the same principle of the “flame test” used in qualitative analysis. First the clear water solution containing metal ions is pumped in a chamber where they are subjected to an acetylene flame. The high temperature of the flame allowed a vaporization of the sample and the electrons of the metal ions are excited in order to shift to higher-energy orbital (excited state). The electrons naturally returned into their ground state and emission of energy occurred in the form of light at specific wavelength. The absorbed light is proportional to the concentration of the element in the flame and it can be measured with spectroscopy using the Lambert-Beer’s law (Equation A7). Since the theoretic concentration of copper into the double emulsion was in the range of 12.76 ppm and 38.3 ppm and taking into account that the extraction was performed using low amount of powder (100 mg) compared with the total amount, we expected to measure low concentration of copper. For this reason a calibration curve with standard solution of copper was measured setting the instrument at  $\lambda = 324.8$  nm which is recommended in the manual for a range of concentration of 0.03-10 ppm. The calibration curve (Figure A.5) was performed in a range of concentration of 0.5-3 ppm because it was the range that gave the best linear trend.

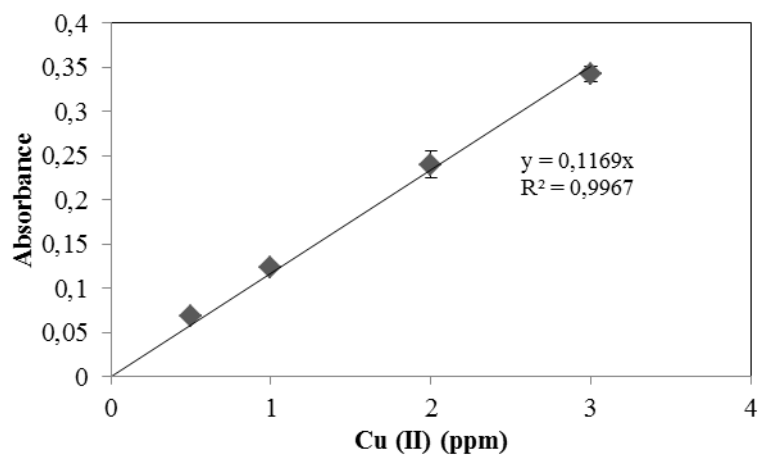


Figure A.5- Calibration of copper ions using SpectrAA in a range of concentration 0.5-3 ppm

## APPENDIX 2

### Award

Second EMS prize for the outstanding poster presentation on the 29th Summer School on Membranes (Essen, 2013) “Membrane Functionalized with Lipase for the Production of Water/Oil Emulsion by Membrane Emulsification” L. Giorno, **A. Imbrogno**, E. Piacentini

(Presenter: Alessandra Imbrogno)

Grant from Bioencapsulation Research Group for the participation to the conference "XXII International Conference on Bioencapsulation" (Bratislava, 2014)

### Education and training from 2011 to 2014

March-June 2012

Course on “Analysis and instrumentation data”, Prof. Di Maio, University of Calabria

March-April 2012

Course “Principles of chemical engineering”, Prof. Curcio, University of Calabria

Course “Introduction to Chemical Engineering”, Prof. Migliori, University of Calabria

May-June 2012

Course “Writing Technical English”, Prof. Broughton, University of Calabria

9-14 July, 2012

Participation to the Summer school on “Dense polymeric membranes fundamentals & applications: packaging, barriers & industrial separations”, Nancy (France)

11-12 September, 2012

Participation to the “ITM-CNR Seminar Days”, University of Calabria, Rende (CS)

January-March 2013

Attending of “Membrane course” at ITM-CNR, Rende (CS). Lecturers: Prof. E. Drioli, Dr. A. Figoli, Dr. Eng. Adele Brunetti, Dr. Eng. E. Curcio, Dr. Eng. G. Di Profio, Dr. Eng. G. Barbieri, Dr. Lidietta Giorno, Dr. L. De Bartolo, Dr. S. Morelli, Dr. Alfredo Cassano, Dr. E. Fontananova

22-26 July, 2013

Participation to the Summer School on “Membranes for liquid separations from an industrial and academic point of view”, Essen (Germany)

3 June 2013

Seminars “Research Valorization: fundraising, intellectual property, spin-off” organized by Scuola Pitagora in scienze ingegneristiche and Liason Office, Dott. P. Rossi, Dott.ssa A. Gallo, University of Calabria

7-16 October, 2013

Course on “Membrane materials based on polymers of intrinsic microporosity (PIMS) and Graphene” given by Prof. Peter Budd at Institute on Membrane Technology, ITM-CNR, Rende (CS)

10 October 2013

Seminar series for young researchers on “Membrane materials: challenges and opportunities”, ITM-CNR, Rende (CS). Lecturer: Prof. Peter Budd

30 October 2013

Participation to ITM-CNR seminar day on “Membrane operations and integrated membrane processes”, ITM-CNR, Rende (CS)

18-19 December, 2013

Participation to “Early-stage and Experienced Researchers Seminars”, ITM Seminar days series, University of Calabria, Rende (CS)

28 September-3 October 2014

Participation to the Summer School on “Innovative Membrane Systems”, Cetraro (Italy)

10 March- 29 August 2014

Study visit and research work at the Chemical Engineering Department of Loughborough University (UK) in collaboration with Prof. RG Holdich, Dr. MM Dragosavac and Dr. GT Vladislavljević.

The research focused on the preparation of W/O/W emulsion at batch scale for the encapsulation of water soluble compounds and scaling up of the process by the torsional membrane emulsification

### **Publications from 2011 to 2014**

#### *Articles in International Journals*

Piacentini, E., **Imbrogno, A.**, Drioli, E., Giorno, L. (2014). Membranes with tailored wettability properties for the generation of uniform emulsion droplets with high efficiency. *Journal of Membrane Science*, 459, 96-103.

**Imbrogno, A.**, Piacentini, E., Drioli, E.,Giorno, L. (2014) Preparation of uniform poly-caprolactone microparticles by membrane emulsification/solvent diffusion process. *Journal of Membrane Science*,467, 262–268

**Imbrogno, A.**, Piacentini, E., Drioli, E.,Giorno, L. (2014) Micro and nano poly-caprolactone particles preparation by pulsed back-and-forward cross-flow batch membrane emulsification for parenteral administration. *International Journal of Pharmaceutics*, 477, 344-350

**Imbrogno A.**, Piacentini E., Dragosavac M.M., Vladisavljević G.T., Holdich R.G., Giorno L. Poly-caprolactone multi-core matrix particles for the simultaneous encapsulation of hydrophilic and hydrophobic compounds by membrane emulsification/solvent diffusion process (under submission to *Colloids and Surfaces B: Biointerfaces*)

#### *Chapter in Book*

Piacentini E., **Imbrogno, A.**, Giorno, L. (2014) Nanostructured Sensing Emulsion Droplets and Particles: Properties and Formulation by Membrane Emulsification. *Smart Membranes and Sensors: Synthesis, Characterization, and Applications*. Chapter 13.367-398, Wiley.

#### *Contribution to Encyclopedia of Membranes*

**Imbrogno A.**, Piacentini E. Membrane emulsification in phase separation for microcapsules preparation, Springer (submitted)

#### **Proceedings**

##### *Oral Presentation*

**Imbrogno A.**, Piacentini E., Drioli E., Giorno L. “Preparation of Poly-caprolactone Microparticles by Membrane Emulsification/Solvent Diffusion Process”, *oral presentation*, Early-stage and Experienced Researchers Seminars, December 2013, University of Calabria (*Italy*)

**Imbrogno A.**, Piacentini E., Drioli E., Giorno L. “Preparation of Poly-caprolactone Particles for Pharmaceutical Applications by Membrane Emulsification”, ICOM 2014, OR-7-01054, July 2014, Suzhou (*China*)

**Imbrogno A.**, Piacentini E., Dragosavac MM, Giorno L. “Core-shell particles for the simultaneous encapsulation of hydrophilic and hydrophobic compounds produced by membrane emulsification”, XXII International Conference on Bioencapsulation, O3-5, September 2014, Bratislava (*Slovakia*)

*Poster presentation*

**Imbrogno A.**, Piacentini E., Giorno L. “Membrane Functionalized with Lipase for the Production of Water/Oil Emulsion by Membrane Emulsification”, 29th Summer School, *P17*, July 2013, Essen (*Germany*)

**Imbrogno A.**, Piacentini E., Drioli E., Giorno L. “From micro to nano scale particle production by pulsed back and forward membrane emulsification”, XXXI Summer School, *P50*, September-October 2014, Cetraro, (*Italy*)